LINEAGE RELATIONSHIP ANALYSIS OF LYMPHOID PROGENITOR SUBSETS IN THE BONE MARROW OF NAÏVE MICE AND DURING INFLAMMATION

REBECCA JANE LEYLAND

RESEARCH THESIS SUBMITTED FOR THE DEGREE OF DOCTOR OF PHILOSOPHY AT UNIVERSITY COLLEGE LONDON

SUPERVISOR: DR. ALEXANDRE J. POTOCNIK

DIVISION OF MOLECULAR IMMUNOLOGY

MRC NATIONAL INSTITUTE FOR MEDICAL RESEARCH

MILL HILL, LONDON

2011

I, Rebecca Jane Leyland, confirm that the work presented in this thesis is my own. Where information has been derived from other sources, I confirm that this has been indicated in the thesis. R J Leyland

ABSTRACT

During haematopoiesis multipotent stem cells generate all cellular components of the blood including lymphocytes. Despite great progress in the isolation of lineage restricted progenitors, the exact precursor-product relationship of these subsets remains poorly understood. In particular the exact branch point of T- and B-cell development in the bone marrow has not been unequivocally mapped. The aim of my project was to investigate the developmental relationship of various progenitor subsets in normal mice and during an acute inflammation.

In order to permanently identify all cells which emanated from early lymphoid compartments we generated a mouse model in which a Cre recombinase was inserted into the *Rag1* locus and functional Cre activity would result in activation of an eYFP reporter. Expression of the reporter was found in all T- and B-cells and in a significant subset of NK-cells and dendritic cells. Furthermore this model allowed the prospective isolation of an 'ELP analogue' and two subsets of CLPs on the basis of their reporter expression. Functional analysis of these subsets *in vivo* demonstrated comparable developmental properties with slightly different kinetics. Furthermore, *in vitro* analysis of isolated progenitors established that reporter-positive CLPs were significantly more advanced in their commitment to the B-cell lineage.

We extended our studies by investigating the impact of an acute systemic inflammation on the size and composition of early haemato-lymphoid subsets. Administration of LPS or heat-inactivated *E. coli* to mice *in vivo* resulted in a complete halt of bone marrow lymphopoiesis. In addition, a marked decrease in the number of myeloid progenitors accompanied by upregulation of Sca-1 on haematopoietic progenitors was observed. These inflammation-induced changes were found to be mainly caused by IFNγ and to a

lesser extend by TNFα, thus identifying these cytokines as key mediators for the infection-induced regulation of haematopoiesis.

ACKNOWLEDGEMENTS

I would primarily like to thank Dr. Alexandre Potocnik for the opportunity to work in his laboratory. During the last three and a half years, detailed discussions on haematopoietic development with Dr. Potocnik have enabled me to gain an in-depth understanding of the subject and has encouraged me to critically analyse experiments and the literature, which has certainly lead to the finalisation of this thesis and the results herein. In addition, Dr. Potocnik has provided me with scientific guidance and feedback which I am sure will be valuable in the next scientific position I undertake.

I would also like to thank Dr. Douglas Brown for introducing me to flow cytometry and cell sorting and Dr. Nikolai Belyaev for help carrying out molecular biology techniques. Both of the aforementioned post-docs have also contributed to scientific discussions with myself which has subsequently broadened my knowledge of immunology as a whole.

Ana-Isabel Garcia-Diaz has assisted me in both the preparation and analysis of infection experiments and I am very grateful for this. Judit Biro has provided sound advice, not exclusively related to science, and I am thankful for her company. I would also like to thank Dr. Dimitris Vasilakos and Dimitris Karamitros for general scientific advice.

CONTENTS

LIST OF FIGURES

LIST OF TABLES

ABBREVIATIONS

Arbp	acidic ribosomal protein
BCR	B-cell receptor
BM	bone marrow
BrdU	5-bromo-2'-deoxyuridine
CCR9	chemokine receptor 9
CD	cluster of differentiation
CDC	conventional dendritic cell
CDCP	common dendritic cell precursor
CFU-S	colony forming unit-spleen
CLP	common lymphoid progenitor
CMP	common myeloid progenitor
DC	dendritic cell
DN	double negative
DP	double positive
EBF	early B-cell factor
E. coli	escherichia coli
ELP	early lymphocyte progenitor
EpoR	erythropoietin receptor
ESC	embryonic stem cell
ETP	early thymic progenitor
EYFP	enhanced yellow fluorescent protein
FACS	fluorescent activated cell sorting
Flk-2	foetal liver kinase 2

GFP	green fluorescent protein
GM	granulocyte-macrophage
GM-CSF	granulocyte-macrophage colony stimulating factor
GMP	granulocyte-macrophage progenitor
HSC	haematopoietic stem cell
IC	intracellular
IFNγ	interferon gamma
IFNγR1	interferon gamma receptor 1
IL	interleukin
IL-7Rα	interleukin-7 receptor α
LIN	lineage
LMPP	lymphoid primed multipotent progenitor
LPS	lipopolysaccharide
LSK	lineage negative sca-1 positive c-kit high
LT-HSC	long term-haematopoietic stem cell
MCSF-R	macrophage colony stimulating factor receptor
MegE	megakaryocyte-erythocyte
MEP	megakaryocyte-erythrocyte progenitor
MHC	major histocompatibility complex
MPP	multipotent progenitor
NICD	notch intracellular domain
NK	natural killer
Pax5	paired box protein 5
PBS	phosphate buffered saline
PCR	polymerase chain reaction

PDC	plasmacytoid dendritic cell
Rag	recombinase activating gene
RBC	red blood cell
RFP	red fluorescent protein
R26R	Rosa26 locus reporter
Sca-1	stem cell antigen-1
SCF	stem cell factor
SLAM	signalling lymphocyte activation molecule
SP	single positive
ST-HSC	short term-haematopoietic stem cell
TCF-1	T-cell factor 1
TCR	T-cell receptor
TNFα	tumour necrosis factor α
TNFR1	tumour necrosis factor receptor 1
TSC	thymic seeding cell
VCAM	vascular cell adhesion molecule
VV	Vaccinia virus
WBC	white blood cell

CHAPTER 1

INTRODUCTION

1.1 The discovery of haematopoietic stem cells

The last fifty years of science have been critical to our understanding of embryonic and somatic development, owing to the discovery of pluripotent embryonic and multipotent adult stem cells. Defining characteristics of any stem cell are their ability to self-renew for several cell divisions (Verfaillie, 2002), the ability to generate at the single cell level differentiated progeny cells (Prockop, 1997) and the ability to functionally reconstitute a given tissue *in vivo*. Embryonic stem cells (ESCs), first obtained from mouse (Martin et al., 1981) and adult stem cells from various tissues have been shown to fulfill those criteria. It was found that ESCs from the inner cell mass of the blastocyst gave rise to cells from the three somatic germ layers; the ectoderm, the mesoderm and the endoderm (Martin, 1981; Thomson et al, 1998). The typical adult stem cell is considered multipotent as it can only give rise to differentiated cell types from the tissue of origin. For example, neural stem cells give rise to neurons, astrocytes and oligodendrocytes (Gage, 2000) whilst mesenchymal stem cells differentiate into fibroblasts, adipocytes, osteoblasts, chondrocytes and skeletal muscle cells (Prockop, 1997). However, the most well characterised adult stem cells are those which give rise to all components of the blood, namely haematopoietic stem cells (HSCs).

In 1961, Till and McCulloch demonstrated the existence of clonogenic bone marrow (BM) precursors that gave rise to multilineage haematopoietic colonies in the spleen. Such colonies, termed colony-forming unit spleen (CFU-S), were found to contain differentiated progeny of multiple blood lineages and a cellular subset of these colonies could re-establish CFU-S when transplanted into secondary hosts (Siminovitch et al., 1963). Based mainly on these results, further research to elucidate the identity of BM progenitor cells was undertaken and in later years monoclonal antibodies were produced which were able to bind to specific cell surface markers on haematopoietic cells, and

which has since allowed the identification of stem and progenitor cells. In addition, isolation and transplantation of BM progenitor populations has indicated the functional roles of these cell types. One of the most important findings from these studies has been that HSCs are able to differentiate at the single cell level into all mature blood elements and can functionally repopulate the haematopoietic system of a lethally irradiated mouse in a process named haematopoiesis (Williams et al., 1984).

1.2 The classical model of haematopoiesis

Haematopoiesis is the developmental process generating all mature blood cells which, under normal conditions, is compartmentalised in the BM of an adult organism. This process originates from a pluripotent cell population, the long-term haematopoietic stem cell (LT-HSC), which constitutes in mice ~ 0.005% of BM mononuclear cells. The phenotypic and functional characterisation of this cell population was carried out by isolation of lineage negative (LIN^-) Thy-1.1^{lo} Sca-1^{hi} cells, which were injected into lethally irradiated hosts and long term reconstitution was observed in all the lineages of the blood (Spangrude et al., 1988). This isolated population contained all functional LT-HSC activity and has subsequently allowed the prospective isolation of lineage-restricted progenitors downstream of HSCs (see Table 1), which can be grouped into various hierarchical developmental models. One of the most common models used in the literature to describe the developmental progression from a LT-HSC into a mature cell of the blood is the ‘classical’ hierarchical model (see Figure 1.1).

In the 'classical' model of haematopoiesis, LT-HSCs first differentiate into short term haematopoietic stem cells (ST-HSCs). All HSCs lack expression of lineage markers expressed by mature cell types, express the receptor tyrosine kinase c-kit and the GPI anchored protein Sca-1 and thus reside within the LIN^{-} c-kit^{hi} Sca-1^{+} (LSK) fraction of the BM. ST-HSCs differ from LT-HSCs by possessing only limited self-renewing capacity and are phenotypically different by expression of the CD34 cell surface marker. Recently, all LT-HSCs have been identified by LSK $CD150^{+}$ $CD48^{-}$ which is known as the 'SLAM' (Signaling Lymphocyte Activation Molecule) definition (Kiel et al., 2005). Kiel and colleagues reported that single LT-HSCs, identified by the SLAM definition, competitively reconstituted into irradiated mice gave rise to long-term reconstitution, whereas LT-HSCs isolated as LSK $Thy1^{lo}$ did not. Therefore, the SLAM definition provides a more simple and enhanced method to isolate a highly enriched population of LT-HSCs. This method would also be useful for the isolation and transplantation of pure LT-HSCs in order to fully repopulate cells of the blood in patients with immunological deficiencies. The next developmental step from ST-HSCs is the irreversible loss of self-renewal, producing a population named 'multipotent progenitors' (MPPs). Although this cell population also resides within the LSK compartment, these cells can be distinguished from ST-HSCs by low level expression of the tyrosine kinase receptor Flk-2 (foetal liver kinase 2; Adolffson et al., 2001). Expression of Flk-2 on haematopoietic progenitor cells has been shown to signify the stage in which cells lose long-term reconstitution potential (Zeigler et al., 1994) and develop down the lymphoid and myelo-erythroid lineages (Borge et al., 1999). According to the model by Akashi and colleagues (Akashi et al., 2000), MPPs then further differentiate along one of two pathways, the lymphoid or the myeloid-erythroid. It is thought that MPPs become irreversibly committed to one of these lineages,

eliminating the other lineage choice. In order to differentiate along these pathways, an MPP must first develop into one of two lineage restricted progenitors: a ‘common lymphoid progenitor’ (CLP)’ or a ‘common myeloid progenitor’ (CMP). The lymphoid pathway gives rise to B-, T- and NK-cells whilst the myeloid pathway produces monocytes, granulocytes, platelets and red blood cells (RBCs).

Figure 1.1

The 'classical' hierarchical model of haematopoiesis.

Adapted from Akashi et al., 2000.

In this hierarchical model of haematopoiesis, the generation of all blood lineages originates from self-renewing HSCs. LT-HSCs first give rise to ST-HSCs, losing some self-renewal activity. The next step in development is upregulation of Flk-2 on the cell surface, a population now known as MPPs. At this stage there is a strict bifurcation of the lymphoid and myelo-erythroid pathways. The CLP is thought to be the main progenitor giving rise to all mature lymphoid cells, whilst the CMP is the main myeloid progenitor which develops into a granulocyte-macrophage progenitor (GMP) or a megakaryocyte-erythroid progenitor (MEP), further differentiating into myelo-erythroid cells.

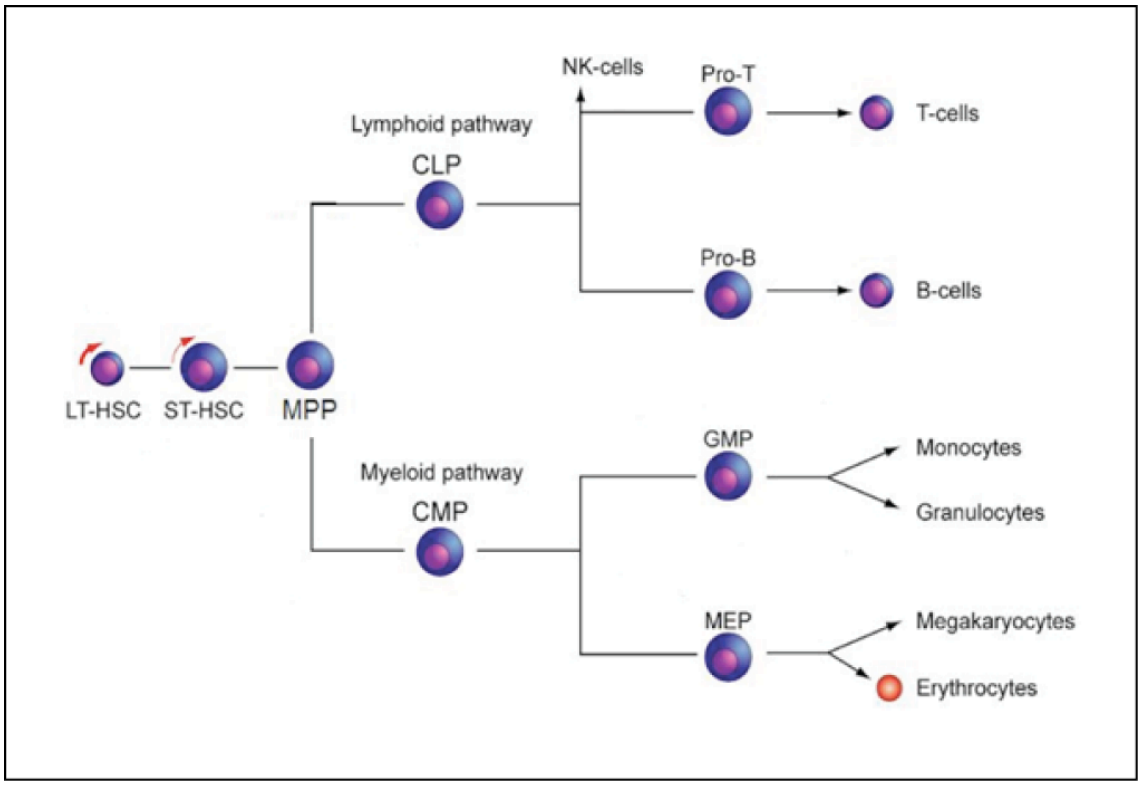
NK-cells
Pro-T
T-cells
Lymphoid pathway
CLP
Pro-B
B-cells
LT-HSC
ST-HSC
MPP
GMP
Monocytes
Myeloid pathway
Granulocytes
CMP
MEP
Megakaryocytes
Erythrocytes

1.3 Lineage-restricted progenitors of the lymphoid and myelo-erythroid pathways

According to the 'classical' hierarchical model of haematopoiesis (Figure 1.1), the first step in lineage restriction is thought to occur when a MPP commits to the lymphoid or myelo-erythroid lineage and in doing so, differentiates into a CLP or a CMP. Cellular requirements which distinguish a CLP from other BM progenitors include phenotypic isolation based specifically on IL-7Rα expression in the LIN^- compartment of the BM. In addition, the CLP is thought to possess restricted lymphoid potential by producing T-, B- and NK-cells, with no evidence of myeloid potential. This cell population was identified phenotypically by Kondo et al., (1997) and comprised ~0.02% of BM cells. In this study, LIN^- IL-7Rα^+ c-kit^{int} Sca-1^{int} cells were transferred into Ly5.1^+ mice and reconstitution of T and B donor-derived cells was evident in the blood. This lymphoid restricted developmental potential fulfilled the requirements of a CLP.

Another BM progenitor which was identified by phenotypic isolation was the CMP (Akashi et al., 2000). This cell population was defined as LIN^- Sca-1^- c-kit^{hi} $CD34^+$ FcγRII/III^{lo}, and was reported to give rise to all myeloid lineages *in vitro*. This myelo-erythroid restricted progenitor developed into either a MEP, characterised as LIN^- Sca-1^- c-kit^{hi} $CD34^-$ FcγRII/III^{lo} or a GMP, characterised as LIN^- Sca-1^- c-kit^{hi} $CD34^+$ FcγRII/III^+.

Based mainly on these findings, it was hypothesised that CLPs and CMPs were the sole progenitors orchestrating development down the lymphoid and myeloid lineages.

1.4 Early progenitors of lymphopoiesis

In the past ten years, the existence of intermediate progenitors between the ST-HSC and the CLP has created a more comprehensive view of lymphoid development. Adolfsson and co-workers (Adolfsson et al., 2005) reported heterogeneity of Flk-2 within the MPP compartment. Flk-2^{lo} MPPs exhibited megakaryocyte-erythrocyte (MegE), granulocyte-macrophage (GM) and lymphoid potentials, whereas Flk-2^{hi} MPPs lacked MegE potential. It was proposed that during the first lymphoid restriction step, MPPs lost their MegE potential, becoming 'lymphoid primed multipotent progenitors' (LMPPs) and gradually committing to the lymphoid lineage. However, this report was challenged by Forsberg and colleagues (Forsberg et al., 2006) who found that Flk-2^{+} LMPPs retained MegE potential *in vivo*. This group isolated Flk-2^{+} LMPPs from *β-actin*^{GFP} mice, transplanted the cells into wildtype mice and found the presence of GFP^{+} platelets in the blood. They therefore proposed that segregation of lymphoid and myelo-erythroid lineages occurred in the MPP population and that restriction to the lymphoid or myelo-erythroid pathways only occurred after development into either CLP or CMP progenitors. However, although GFP^{+} platelets were detected, the frequency of donor-derived cells which had developed into platelets was less than that of LT-HSC, ST-HSC and MPP populations, suggesting that as cells developed into LMPPs, they were losing MegE potential. In addition, this group also analysed LMPPs for putative erythroid potential by using CFU-S assays. They reported detectable CFU-S from LMPPs by day ten, although with a lower frequency than LT-HSCs, ST-HSCs or MPPs, consistent with the gradual loss of MegE potential in this population. Therefore, although minor MegE potential was detected in the LMPP population, the majority of LMPP cells appeared to be losing MegE potential.

Yoshida et al., (Yoshida et al., 2006) however reported supporting evidence for the loss of MegE potential in LMPPs by analysing a transgenic reporter mouse strain expressing GFP under control of the *Ikaros* promoter. They observed high expression of reporter activity in the LMPP, which was additionally found to possess GM and T-cell potential, but no MegE potential. Furthermore, it was reported that the Flk-2^{hi} MPP population lacked *Gata1* or *EpoR* (Erythropoietin receptor) expression at the transcriptional level, genes indicative for MegE development (Månsson et al., 2007). In addition, Arinobu and colleagues (Arinobu et al., 2007) reported that in *Gata1*^{GFP} mice, reporter expression could only be detected in LSK cells which were Flk-2^{-}, and was absent in LMPP cells. Therefore, due to these recent reports, it is generally accepted that MegE potential is lost in the LMPP population.

Another intermediate progenitor identified was the early lymphocyte progenitor (ELP). Igarashi and colleagues (Igarashi et al., 2002) utilised GFP expression to isolate ELPs in the LSK Flk-2^{+} $CD27^{+}$ GFP^{+} subset upon transcription and translation of the recombinase activating gene 1 (*Rag1*) locus. It was reported that after intravenous injection, ELPs could give rise to NK-, B- and T-cells. This cell population could also exhibit myeloid potential *in vitro*.

The discovery of these additional lymphoid progenitors introduced refined models of haematopoiesis (Figure 1.2), however the relationship between the LMPP, the ELP and the CLP populations remains unclear. In addition, although all populations have been shown to contain robust T-cell potential, the identity of the sole progenitor population which exits the BM, enters the circulation and seeds the thymus, giving rise to thymic seeding cells (TSCs) and subsequently early thymic progenitors (ETPs) is not known.

Table 1

Definitions of haematopoietic progenitor populations.

Table showing all haematopoietic progenitor populations, their abbreviations and the cell surface phenotype by which these cell populations can be identified.

All stem cells and lymphoid progenitors, except the CLP, reside in the LSK compartment of the BM. In the LSK fraction, LT-HSCs differ in their phenotype to ST-HSCs by lacking the expression of CD34. Both HSC subsets are negative for Flk-2 expression. As cells progress into the lymphoid compartment, Flk-2 expression appears on the surface of these cells (LMPPs) and *Rag1* upregulation can be observed during further lymphoid development (ELPs). The CLP expresses intermediate levels of both c-kit and Sca-1 and is defined strictly according to IL-7Rα expression.

Myelo-erythroid progenitors are defined according to FcγRII/III and CD34 expression and reside within the LIN^{-} c-kit^{hi} $Sca\text{-}1^{-}$ fraction of the BM.

Also included in this table is the common plasmacytoid and conventional dendritic cell progenitor (CDCP) which is believed to be the main progenitor giving rise to conventional (cDC) and plasmacytoid dendritic cells (pDC).

Cell population	Abbreviation	Phenotype
Long term haematopoietic stem cell	LT-HSC	LIN^- c-kit^{hi} Sca-1^+ Flk-2^- $CD34^-$
Short term haematopoietic stem cell	ST-HSC	LIN^- c-kit^{hi} Sca-1^+ Flk-2^- $CD34^+$
Lymphoid primed multipotent progenitor	LMPP	LIN^- c-kit^{hi} Sca-1^+ Flk-2^+ $CD34^+$
Early lymphocyte progenitor	ELP	LIN^- c-kit^{hi} Sca-1^+ Flk-2^+ $Rag1^{GFP+}$
Common lymphoid progenitor	CLP	LIN^- IL-7Rα^+ Flk-2^+ c-kit^{int} Sca-1^{int}
Common myeloid progenitor	CMP	LIN^- c-kit^{hi} Sca-1^- $CD34^+$ FcγRII/III^{lo}
Megakaryocyte-Erythroid progenitor	MEP	LIN^- c-kit^{hi} Sca-1^- $CD34^-$ FcγRII/III^{lo}
Granulocyte-Macrophage progenitor	GMP	LIN^- c-kit^{hi} Sca-1^- $CD34^+$ FcγRII/III$^+$
Common dendritic cell precursor	CDCP	LIN^- c-kit^{int} Flk-2^+ MCSF-R^+ IL-7Rα^-

Figure 1.2

Early lymphocyte development and thymic colonisation.

Adapted from Ye and Graf, 2007.

This model illustrates possible routes of T-cell development in relation to BM progenitors. Haematopoiesis begins in the LSK compartment of the BM with HSCs, which have the potential to develop into all cell types of the blood. In a first step, these cells become lymphoid-primed, losing MegE potential but retaining GM potential. These LMPPs are positive for Flk-2. It is believed that the LMPP population further develops into the ELP population, activating the *Rag1* locus, and that this population further differentiates into the CLP. However, the relationship between these three lymphoid progenitor pools remains unclear, as highlighted by the red circles and the red arrows between populations. As cells develop down the lymphoid pathway, GM potential is gradually lost. It is thought the main cell type giving rise to B-cells is the CLP, however it is not known which cell type is responsible for ETP generation. This model favours the ELP as the main thymic colonising population which first develops into a TSC before becoming an ETP. However, the model does not rule out the possibility that the LMPP or CLP populations contribute to the constant replenishment of the intrathymic progenitor pool.

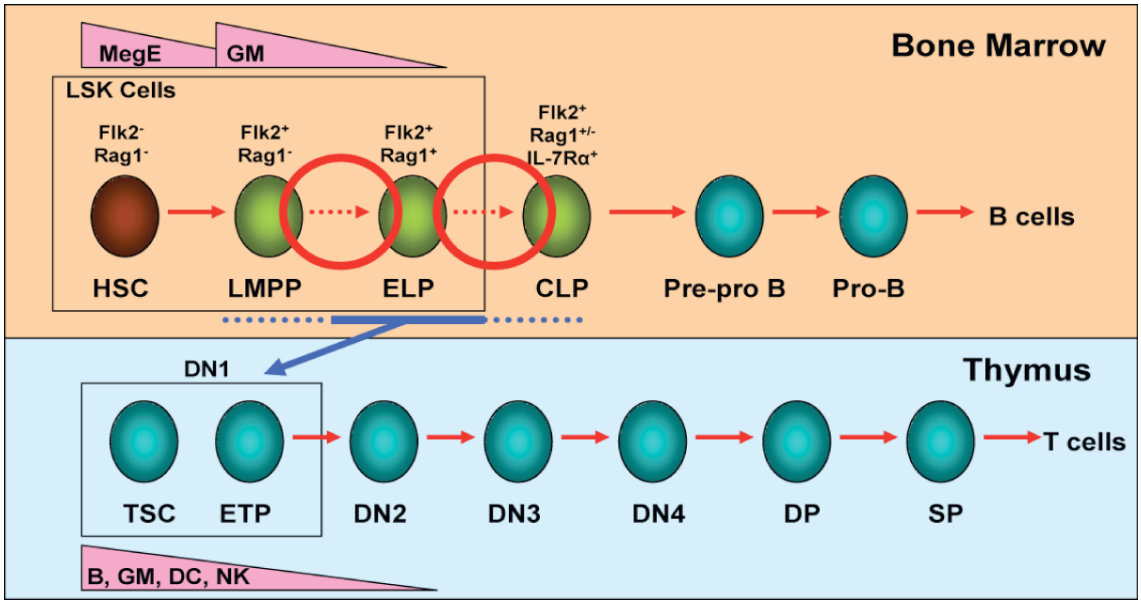
MegE
GM
Bone Marrow
LSK Cells
Flk2-
Rag1-
Flk2+
Rag1-
Flk2+
Rag1+
Flk2+
Rag1+/-
IL-7Rα+
HSC
LMPP
ELP
CLP
Pre-pro B
Pro-B
B cells
DN1
Thymus
TSC
ETP
DN2
DN3
DN4
DP
SP
T cells
B, GM, DC, NK

1.5 Cellular pathways of T-cell fate specification

The entry of BM-derived progenitors into the thymus is not a simple process. Foss et al., (Foss et al., 2001) reported that the murine thymus is not continually receptive to the import of haematopoietic progenitors and that there are specific refractory periods whereby progenitors are able to enter the thymus more efficiently. The first step in this process of thymic settling is the efficient migration and homing of BM progenitors to become part of the ETP pool.

Intrathymic T-cell development is initiated by the production of ETPs, which are defined by the phenotype LIN^{-} $CD44^{+}$ $CD25^{-}$ c-kit^{hi} (Godfrey et al., 1992). Development into a mature T-cell first entails the ETP progressing through double negative (DN) stages, characterised by the absence of CD4 and CD8 cell surface expression. These DN stages can be further subdivided by the expression of CD44 and CD25 antigens: DN1 is identified as LIN^{-} $CD44^{+}$ $CD25^{-}$ (encompassing the ETP), DN2 is LIN^{-} $CD44^{+}$ $CD25^{+}$, DN3 is LIN^{-} $CD44^{-}$ $CD25^{+}$ and DN4 is LIN^{-} $CD44^{-}$ $CD25^{-}$. Maturation proceeds into the double positive (DP) stage and finally results in differentiation into a committed CD4 single positive (SP) or CD8 SP T-cell (Figure 1.3).

Figure 1.3

Stages of T-cell development.

T-cell development begins once a BM-derived lymphoid progenitor has settled in the thymus and has become a TSC. These TSCs first develop into ETPs, which are part of the DN1 compartment and express high levels of c-kit on their cell surface. ETPs then progress through DN stages 1-4, finally becoming DP for both CD4 and CD8 antigens. In a final maturation step, a cell will finish its thymic development as either as CD4 SP or a CD8 SP cell.

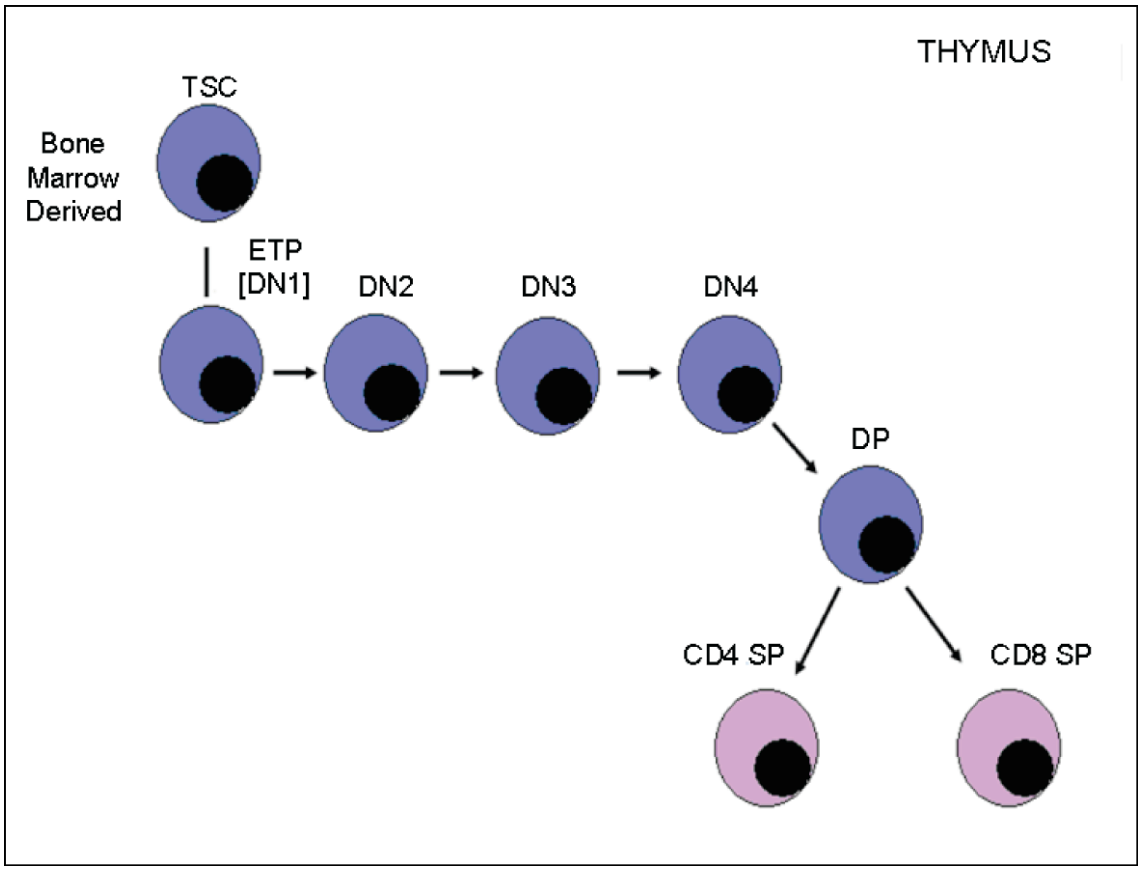
THYMUS
TSC
Bone
Marrow
Derived
ETP
[DN1]
DN2
DN3
DN4
DP
CD4 SP
CD8 SP

The definitive identity of the progenitors that leave the BM, enter the circulation and home to the thymus giving rise to the ETP population however still remains controversial. It is thought that only progenitors downstream of HSCs have the capacity to migrate to the thymus, as there is little evidence for self-renewing HSCs in this organ (Goldschneider et al., 1986). In addition, it was reported by Lai and Kondo (Lai and Kondo, 2006) that HSCs do not express the chemokine receptor CCR9 which is thought to be important for thymic homing.

Kondo and colleagues (Kondo et al., 1997) hypothesised that the CLP was the main cell type producing T-cells and more importantly the ETP. Moreover, Martin et al., (Martin et al., 2003) reported the identification of a CLP-2 population which was defined as c-kit$^-$ IL-7Rα^+ B220$^+$ CD19$^-$ and had the ability to produce T-cells. However, there has been sufficient evidence in the literature to suggest that CLPs may not be the main BM progenitors giving rise to ETPs in the thymus.

One report which clearly addressed this question was by Allman and colleagues (Allman et al., 2003). In order to investigate the relationship between CLPs and ETPs, this group compared CLPs to ETPs in respect to phenotypes, the kinetics from which they generated T-cells and the effect of a null mutation in *Ikaros*. They failed to detect IL-7Rα surface expression on ETPs, suggesting ETPs differed from IL-7Rα^+ CLPs. Additionally, they found that the cell surface expression of c-kit and Sca-1 on ETPs resembled the LSK fraction of the BM, supporting a model whereby cell populations such as LMPPs and ELPs are responsible for thymic homing. To assess the kinetics of development, CLPs and ETPs were injected intrathymically into allotype-matched recipients. In these experiments, the number of DP thymocytes in CLP inoculated mice declined between two and three weeks post transfer, whereas they peaked at three weeks in mice reconstituted with ETPs. Therefore, the authors suggested these cell populations

had different developmental properties. Moreover, in *Ikaros*-deficient mice, no CLPs or B-cells could be detected in the BM. In contrast, normal frequencies of ETPs were observed in the thymus of these animals, suggesting that B-cells may derive predominantly from CLPs, but the majority of ETPs developed via a CLP-independent pathway. Additional work from this group also showed that ETPs lack IL-7Rα mRNA expression at the population level. Therefore, the absence of IL-7Rα expression on ETPs may indicate colonisation by IL-7Rα^{-} precursors such as LMPPs or ELPs.

The hypothesis that CLPs should constitute the main source for thymic T-cell development clearly predicts the absence of myeloid potential in ETPs. However, there are some publications which have disagreed with this hypothesis. Wada et al., (Wada et al., 2008) showed that thymocytes at stages DN1-2 of thymopoiesis could develop into CD11b^{+} cells, showing macrophage-like appearance in histology. Similarly, Bell and Bhandoola, (2008) found that ETPs placed in short term cultures with Flk-2 ligand and interleukin-7 (IL-7) underwent expansion and expressed the myeloid lineage markers, CD11b, F4/80, Gr1 and MCSF-R. Furthermore, injected ETPs could give rise to myeloid cells. Taken together, these reports clearly demonstrate a robust myeloid potential in early intrathymic progenitors thereby further questioning the physiological role for the CLP as the main precursor entity of intrathymic T-cells. Additional evidence which promotes this assumption is the finding that CCR9 surface expression, which is thought to be important for thymic homing, was conveyed to be first acquired at the ELP stage (Heinzel et al., 2007). It seems conceivable that the ELP and earlier progenitors, such as the LMPP, may play a major role in providing TSCs.

Taking into account that there is considerable evidence for either LMPP or ELP populations being the main source of TSCs, a recent report has suggested that ETPs are derived from IL-7Rα expressing precursors (Schlenner et al., 2010). Despite the fact

that ETPs have been found to lack IL-7Rα mRNA expression (Allman et al., 2003), Schlenner and colleagues showed, by using *Il7rα*^{Cre}-driven fate mapping experiments, that approximately 85% of ETPs had a previous history of IL-7Rα expression. Therefore, this data suggests that ETPs are derived predominantly from IL-7Rα^{+} progenitors such as CLPs, and to a lesser extent LMPP and ELP populations, which express *Il7rα* transcripts. Therefore, it may be possible that all LMPP, ELP and CLP populations give rise to ETPs.

1.6 Cellular pathways of B-cell fate specification

In addition to identifying TSCs, the exact identity of BM-derived progenitors which give rise to B-cells is also not clear. The earliest progenitor cell type which is thought to be responsible for B-cell development is the CLP. B-cell development in the mouse BM can be characterised at all stages, from early progenitors to mature B-cells. Immediately after the CLP stage, B-lineage commitment can be first recognised by expression of B220 and AA4.1 antigens, labelling a population of pre-pro B-cells (Li et al., 1996). B-lineage cells cannot be recognised solely as $B220^+$, as NK-cell progenitors can also be found in this compartment (Rolink et al., 1996). However, clonal analysis of $B220^+$ $AA4.1^+$ pre-pro B-cells for B/macrophage potential has shown that only B-cells are produced (Allman et al., 1999). These pre-pro B-cells also express intermediate levels of c-kit and are positive for IL-7Rα expression. As B-cell development continues, cells begin to upregulate *Cd19*, the target gene of the transcription factor paired box protein 5 (Pax5), and the cells are then known as pro B-cells. During this stage of development, both alleles of the immunoglobulin heavy chain locus are D_HJ_H rearranged. Completion of a functional V_H-D_HJ_H rearrangement results in the expression of the pre B-cell receptor and the cells at this stage are then fully committed to the B-cell lineage, as transplantation of these cells into *Rag*-deficient hosts leads to long term reconstitution of mature B-cell populations (Rolink et al., 2000). In the final steps of B-cell development, cells express CD25 and IgM whilst downregulating c-kit and are defined as pre B and then immature B-cells. Upon entering the periphery, B-cells which survive undergo further differentiation to become fully mature B-cells that express IgD. Given the presented evidence, the developmental checkpoints of early B-cell development seem to be quite well established.

1.7 Transcription factors important for lymphoid specification

Another way to elucidate which cell pools contribute to T and B-cell development is the analysis of genes indicative or indispensable for lineage commitment. Differential expression of transcription factors is considered operational in directing cells towards a particular developmental fate. Of crucial importance for T-cell development in particular are *Notch1*, *Tcf1* and *Gata3*.

Notch comprises a family of highly conserved receptors, whose activation is induced by Delta and Jagged ligands, via cell-cell interactions (Artavanis-Tsakonas et al., 1999). Once activated, the Notch intracellular domain (NICD) is cleaved by γ-secretase, which leads to translocation of the NICD into the nucleus. Subsequently, the NICD associates with the transcription factor RBP-J, which initiates transcription of target genes such as the *hairy/enhancer of split (Hes)* and *Deltex*. Recent data suggests that Notch signalling and Hes-1 may play a critical role in promoting progression of T-cell development, including the choice of committing to the T-, rather than the B-cell lineage (Radtke et al., 1999). Radtke and colleagues utilised a mouse model whereby a loxP-flanked *Notch1* gene was inactivated by inducing Cre-recombinase under the control of the *mx1* promoter, thus allowing the inactivation of *Notch1* via type 1 interferon (Radtke et al., 1999). After *Notch1* inactivation, instead of T-cell generation, evidence for intrathymic B-cell generation was presented. This evidence suggests that Notch-1 is important in specifying progenitors in the thymus and may be further involved in the inhibition of B-cell development. In addition, it has been shown that *Notch1* mRNA is expressed in LMPPs, ELPs and CLPs, which is consistent with the presence of T-lineage potential in these populations (Rumfelt et al., 2006).

T-cell Factor-1 (TCF-1) is a T-cell specific nuclear binding protein. It is expressed in all thymocyte subpopulations, including the earliest DN1 stage, and has been regarded as the first definitive T-lineage marker (Verbeek et al., 1995). Mutation of TCF-1 results in the severe impairment of T-cell development during late DN cell stages, immediately following pre-TCR expression and ahead of TCRα gene expression (Verbeek et al., 1995).

One family of transcription factors which are clearly implicated in haematopoietic differentiation are members of the GATA family. The GATA-3 transcription factor is thought to be expressed at various levels in nearly every stage of lymphoid development, starting with HSCs, and is believed to drive cells specifically towards a T-cell fate. Evidence of this role was discovered by Ting and colleagues (Ting et al., 1996) who carried out experiments supporting a role for *Gata3* in early thymocyte development. A *Rag2*-null complementation system was utilised in conjunction with *Gata3*-null ESCs, to evaluate the role of *Gata3* in T-cell development. These cells contained normal B-cell numbers but there appeared to be no evidence of T-cell progenitors in the thymus.

Other members of this family are the GATA-1 and GATA-2 transcription factors. The GATA-1 transcription factor has a specific promoter which directs its expression in the erythroid, megakaryocytic, mast cell and eosinophil lineages (Burch, 2005). GATA-2 is expressed abundantly in HSCs and progenitor cells, but in the erythroid lineage, expression is thought to decrease with an opposing increase in GATA-1 expression (Ohneda et al., 2002). Determining the expression of GATA-1 and GATA-2 in haematopoietic tissues is likely to illustrate the myelo-erythroid potential and the lack of lymphoid potential in certain cell populations. Similarly, the expression of GATA-3 appears to indicate a commitment to the lymphoid lineage.

In contrast to T-cell specification, a completely different set of transcription factors are thought to be required for B-lineage specification. The most crucial of these have been reported to be Pax5, early B-cell factor (EBF) and the basic helix-loop-helix transcription factors.

The transcription factor Pax5 is exclusively expressed in the B-lymphoid lineage of the haematopoietic system and is crucial to the development of B-cells. It has been reported that in *Pax5*-deficient mice, V_H to D_HJ_H rearrangements are severely reduced at the pro B-cell stage (Nutt et al., 1997) and further differentiation along the B-lineage pathway is blocked (Nutt et al., 1999). However, this defect could be overcome by retroviral induction of *Pax5* (Nutt et al., 1999). Moreover *Pax5*-deficient progenitors from the BM efficiently develop into c-kit$^+$ B220$^+$ pre-pro B-cells in culture with stromal ST2 cells in the presence of IL-7 (Nutt et al., 1997). However, unexpectedly, if the IL-7 cytokine is substituted with alternate lineage cytokines such as GM-CSF, M-CSF or IL-2, these cells are able to differentiate into functional macrophages, granulocytes, DCs and NK-cells (Nutt et al., 1999). Hence, *Pax5*-deficient pre-pro B-cells appear to be uncommitted lymphoid progenitors harbouring a small amount of myeloid potential (Cobaleda et al., 2007). Together, these data identify Pax5 as the critical factor which directs developing cells down the B-lineage pathway.

The initiation of B-cell development also depends critically on the EBF transcription factor and the basic helix-loop-helix proteins encoded by the E box binding protein 2A (*E2A*) gene. In the absence of either transcription factors, B-cell development is attenuated at the pre-pro B-cell stage.

1.8 The effect of aging and gender on haematopoiesis

Aside from factors which can directly govern the fate of progenitor cells, other factors which can influence the kinetics of lymphoid development and the function of lymphoid progenitors are age and gender. The concept of aging during haematopoiesis has been widely investigated primarily in mature cells of the immune system. The aim of this research by many groups has been to understand why we age and the causes of it. The general consensus has been that as we age, the functions of the immune system decline. One example of this is that elderly people are more susceptible to infections such as influenza than younger individuals. Furthermore, investigations have been carried out which show that vaccinations are also less effective in the aged (McElhaney and Effros, 2009). Studies focusing on the innate immune system have been contradictory in the sense that some reports have shown an age-related decline in the number and function of neutrophils (Butcher et al, 2001), macrophages (Fietta et al., 1993) and NK-cells (Albright and Albright, 1983), whereas other studies have not observed these changes (Gomez et al., 2008). Therefore, the effect of aging within these compartments and on their respective progenitors still remains unclear. In contrast, studies on the adaptive immune system and aging have been rather fruitful. It has been very well established that thymic involution occurs with age and that the frequency and function of pre B-cells are markedly diminished in senescent mice (Stephan et al., 1996; Stephan et al., 1998). Examples of these defects include reduced antibody production by B-cells and reduced proliferation in response to antigen. However, studies on B-cell progenitors have not been as well characterised. One paper which partly addressed this was a study by Min et al., (2006) who reported age related defects in CLPs and pro B-cells. This group investigated the effects of aging using young (4-6 weeks) and old (18-20 months) mice by comparing the number of CLPs and pro B-cells. They found a significant

reduction in the number of cells as well as in the proliferative potential of these cells during aging and they attributed one of the reasons being loss of responsiveness to IL-7. Interestingly they found that the development of myeloid progenitors in old mice remained unchanged compared to young mice, indicating that lymphoid progenitors may be particularly susceptible to aging factors. However, to date studies into age-related changes in the functional competence of the LMPPs or ELPs have not been published.

There have however been numerous reports which suggest that HSCs are affected by aging. This has been very well demonstrated by isolating young and old HSCs from the same mouse strain and transplanting them into the same recipient (Harrison et al., 1983). Young mice exhibited a significantly higher repopulating efficiency than the older counterparts suggesting that there must have been an intrinsic factor such as aging which was negatively regulating the function of HSCs, as cells from both young and old mice were competing in the same environment. Taking into account the effect of aging in all haematopoietic populations, investigating lymphoid and myeloid progenitor numbers in relation to young and aged mice would further elucidate the effect of aging on haematopoietic progenitor composition.

Another factor which could influence haematopoietic progenitor composition and function is gender. There has been a variety of evidence suggesting that lymphopoiesis in the BM is limited by sex steroids and therefore gender may have profound effects on haematopoietic development. One observation which illustrates this concept is that in pregnant or oestrogen-treated mice there is a noticeable suppression of B-lymphopoiesis (Medina et al., 1993). During this study, B-cell subsets were compared between pregnant and non-pregnant mice and the number of pre B-cells was reduced by an average of five fold in pregnant mice. Furthermore, IL-7 responsive precursors declined

in number after injection of 1 mg 17-β estradiol indicating that B-cells and lymphoid progenitors are susceptible to regulation by oestrogen. This group also studied the number of myeloid progenitors and $CD11b^+$ cells by colony formation but found no significant differences. Furthermore, Kouro et al., (2001) isolated LIN^- c-kit^{hi} cells and placed them in stromal cell-free cultures containing only stem cell factor (SCF), Flk-2 ligand and IL-7. They found that with the inclusion of β-estradiol in the medium, the production of $CD19^+$ lymphocytes was almost completely prevented. These data indicate that early B-cell development is partially blocked by oestrogen treatment; whereas the myeloid compartment appears to be unresponsive to the effect of oestrogen, or is simply not affected by the hormone.

There have only been a limited number of studies which have addressed the effect of oestrogen on early lymphoid precursors. One study by Medina et al., (Medina et al., 2001) presented evidence that the LIN^- IL-$7R\alpha^+$ c-kit^{int} population, which would otherwise be representative of the CLP, was depleted in oestrogen treated animals. In addition, they utilised a competitive repopulation foetal thymic organ culture system to assess the potential of LIN^- c-kit^{hi} precursors for T-cell differentiation. Using cells isolated from oestrogen treated $Ly5.1^+$ mice and control $Ly5.2^+$ mice, they observed that upon mixtures of these cells, almost all of the progeny came from $Ly5.2^+$ mice. Therefore this study indicated that T- and B-cell progenitors may be affected by sex hormones. In order to further elucidate whether gender profoundly affects the number of BM and ETPs, a detailed comparative analysis would need to be carried out between male and female mice. In addition, there is a virtual absence of reports which have investigated the effects of aging in conjunction with gender in haematopoietic progenitor compartments.

1.9 Infection-induced changes of haematopoiesis

Another extrinsic factor which has been shown to influence the phenotype and function of haematopoietic progenitor populations is infection. There has been a significant amount of evidence suggesting that in conditions of stress, haematopoietic progenitor compartments are phenotypically and functionally altered. During steady state conditions, haematopoietic progenitor cells can be defined by particular cell surface markers which allows the isolation and functional assessment of these cells. However, surface expression of some of these antigens has been demonstrated to be significantly altered during acute infection or inflammation. One of the most notable changes appears in the LSK fraction of the BM which contains HSC and LMPP populations. Work in our lab using malaria as a model for an acute infection (Belyaev et al., 2010) has illustrated an expansion of the LSK compartment and a retraction in the frequency and number of LIN^{-} $Sca\text{-}1^{-}$ $c\text{-}kit^{hi}$ myeloid progenitors three days after infection. This was mainly due to the upregulation of Sca-1 on myeloid progenitors. Importantly, analysis of LT-HSCs during infection presented no change in the number of these cells, indicating that the upregulation of Sca-1 was not as a consequence of LT-HSC mobilisation and the need to generate differentiated progeny. Instead, the infected LSK fraction also appeared to express FcγRII/III, a marker of GM development and functional analysis of these cells produced myeloid progeny. Hence, a major proportion of LSK cells during infection or inflammation were lineage-restricted myeloid cells. The cytokine inducing the expression of Sca-1 on myeloid progenitors in malaria was IFNγ, as infection induced in *Ifngr1*-null mice showed no change in the expression of Sca-1 on myeloid progenitors compared to those observed during physiological conditions. These findings illustrate the plasticity of haematopoietic progenitors to alter their phenotype and function. Another study by Baldridge et al., (Baldridge et al., 2010)

reported alternate differences in haematopoietic progenitors during induction of a chronic *Mycobacterium avium* infection. This group reported a small mobilisation of LT-HSCs, accompanied by a decrease in the number of BM GMPs, CMPs and MEPs and an increase in the number of CLPs. These changes are more representative of a T-cell mediated response, rather than one of the innate immune system. However, both these reports clearly show that during a systemic infection, there are major phenotypic and functional differences in haematopoietic progenitor compartments.

One model of an acute bacterial septicaemia in which the haematopoietic response has not been fully examined is that of *Escherichia coli* (*E. coli*). So far, only one group have published data on the effect of *E. coli* on the LSK compartment of the BM. Zhang et al., (2008) injected *E. coli* intravenously (i.v.) into C57BL/6 mice and observed that 12 hours post infection, the number of LSK cells was increased seven fold. This compartment was further expanded to approximately ten fold after 24 hours. However, the infected LSK cells were not analysed for any other markers of the myeloid lineage and so the cause of LSK expansion could not be attributed directly to Sca-1 upregulation on myeloid cells. However, they did report a decrease in the number of LIN^- c-kit^{hi} $Sca\text{-}1^-$ cells during infection. In addition, they also measured the elevation in cytokines during *E. coli* infection and found GM-CSF, IL-6 and TNFα to have the highest increase compared to wildtype controls. TNFα, LPS and IFNγ were also sufficient to induce upregulation of Sca-1 on LIN^- c-kit^{hi} $Sca\text{-}1^-$ cells *in vitro,* however GM-CSF and IL-6 had minimal effect. Although these results provide an idea as to the mechanisms behind the alteration in haematopoietic progenitors, much further analysis is required in order to determine the exact nature of these observations, the effects in the periphery and the cytokines directly responsible for these changes.

Similar to *E. coli*, there have been few reports which have investigated the effects of lipopolysaccharide (LPS) on haematopoietic progenitor populations. One report which did provide some idea on how haematopoietic progenitors respond to LPS was by Nagai and colleagues (Nagai et al., 2006) who showed by flow cytometric analysis that TLR complexes could be found on haematopoietic progenitor cells. They reported that HSCs and CLPs expressed TLR4-MD complexes on their surface, the receptor by which LPS is recognised (Hoshino et al., 1999). In addition, LSK, LIN^- c-kit^{hi} $Sca\text{-}1^-$ and CLP cells also expressed TLR2 on their surface. Furthermore, when CLPs were isolated and placed in culture with added LPS, only $CD11b^+$ cells were produced, indicative of myeloid or DC populations. Therefore, in response to LPS, CLP cells appeared to give rise to cells of the myeloid lineage instead of the lymphoid lineage, indicating that there may be a high degree of plasticity within haematopoietic progenitor compartments in response to LPS. This effect was dependent on the TLR4 pathway, as CLPs did produce B-cells when isolated from *Myd88*-deficient mice. Therefore, although there is some evidence to suggest that haematopoietic progenitor cells can respond to LPS and gram negative bacteria, this has not been studied in depth. An *in vivo* model using LPS and/or *E. coli* could be further exploited to address the relative role for direct TLR-mediated signals as well as the action of pro-inflammatory cytokines on haematopoiesis.

1.10 Aims of study

One issue which many groups are still trying to understand is which BM-derived progenitors give rise to T- and B-cells. At this moment in time, there have been many publications which have questioned the role of the CLP as the main source of thymic progenitors. With the discovery of alternate lymphoid progenitor populations such as the LMPP and the ELP, research into the phenotype and developmental potential of these pools has indicated a more suitable role for these cells as thymic precursors. However, more elegant methods to monitor the development of these cells, for example utilising lineage tracing models, needs to be performed in order to fully establish the relationship between the LMPP, the ELP and the CLP populations and to determine which of these populations give rise to T- as well as B-cells. We aimed to assess the relationship between lymphoid progenitors; analyse their functional potential *in vivo* and *in vitro*; determine the expression of genes in these populations and ultimately dissect lymphoid developmental pathways utilising a novel lineage tracing reporter model, whereby the ELP population and all subsequent progeny were marked by enhanced yellow fluorescent protein (eYFP).

In addition, we also aimed to examine extrinsic factors which could influence the phenotype and composition of lymphoid progenitor compartments. It is clear from the literature that aging has a significant affect on the function of mature lymphoid cells; however this has not been fully investigated in early lymphoid progenitors. Similarly, there is little evidence of investigations into gender and haematopoiesis. Therefore, we aimed to combine the effects of both aging and gender and analyse the frequency and number of haematopoietic progenitor populations.

Another important factor which can exert profound effects on haematopoietic development is inflammation. There have been numerous publications which suggest an

alteration of phenotype and function in haematopoietic progenitor compartments upon infection. However, the effect of gram negative bacteria such as *E. coli* on the phenotype and composition of haematopoietic progenitors has been poorly investigated, as has the identification of key cytokines which are involved in phenotypic and functional changes. Therefore, by administering either LPS or *E. coli* into C57BL/6 and reporter mice, we aimed to further evaluate the effect of inflammation on haematopoiesis and identify the potential mechanism involved.

CHAPTER 2

MATERIALS AND METHODS

2.1 Mouse strains

C57BL/6 wildtype mice were bred and housed at the MRC National Institute for Medical Research (NIMR). The *B6.R26R*^{eYFP} strain was made by Srinivas et al., (2001) who inserted eYFP cDNA, preceded by a loxP-flanked stop sequence, into the constitutively active *Rosa26* locus. *B6.Rosa26*^{eYFP} mice, with ubiquitous expression of eYFP from the *Rosa26* locus, were generated by Belyaev and co-workers (Belyaev et al., 2010) by breeding *B6.R26R*^{eYFP} reporter mice with *PC3*^{Cre} mice. The *B6.R26R*^{eYFP} strain was also crossed to the *B6.vav1::iCre* strain (Georgiades et al, 2002), which was first active in the HSC compartment, the *B6.Rag1*^{Cre} strain (Esplin et al., 2009) which was expressed in early lymphoid development and the *B6.hCD2::iCre* strain (de Boer et al., 2003).

Recombinase activating gene 2-deficient (*Rag2*-null) mice on C57BL/6 background were generated by Shinkai et al., (1992). Mice deficient in both *Rag2* and the common cytokine receptor γ chain (*Rag2/Il2rg*-null) were created by Goldman and colleagues (Goldman et al., 1998). Mice lacking the interferon gamma receptor 1 (IFNγR1) were produced by Huang et al., (1993) and crossed to C57BL/6 mice to generate the *B6-Ifngr1*-null strain. Mice which were homozygous for a disrupted tumour necrosis factor receptor 1 (TNFR1) allele were created by Rothe et al., (1993). These mice were crossed to C57BL/6 mice for six generations to produce the *Tnfr1*-null (p55;N6) strain. All strains were bred and housed under specific pathogen free conditions at the MRC NIMR.

2.2 Isolation of progenitor subpopulations

2.2.1 Cell preparation

All organs were placed directly into Iscove's Modified Dulbecco's Medium (IMDM) buffer and mechanically processed to achieve single cell suspensions. BM was isolated by flushing the femur bones with IMDM and then passing through a 70 μm nylon mesh (BD Falcon). Spleens which were digested with 0.4 mg/ml collagenase (Liberase CI, Roche) were first perfused and then left to incubate at 37^{o}C for 20 minutes. Cell numbers were determined utilising 0.4% Trypan Blue solution (Sigma) and counted on a Neubauer chamber. Blood was isolated by cardiac puncture of lethally anesthetised mice (50 mg/kg Pentobarbitone, Animalcare Ltd.) with a heparin syringe (Heparin, Sigma-Aldrich).

2.2.2 Magnetic mediated depletion of cells

Enrichment of LIN^{-} cells was carried out firstly by incubation of single cell suspensions with Fc-receptor II/III antibody and then by using biotinylated antibodies against lineage antigens (see Table 2) which were incubated at 4^{o}C for 15 minutes in the dark. After washing with FACS (Fluorescence Activated Cell Sorting) buffer (PBS, 0.5% BSA, 2.5 mM EDTA), cells were labelled with streptavidin microbeads (Miltenyi Biotec) and passed though a cell separation column (Miltenyi Biotec), according to the manufacturer's instructions. The resulting eluant was referred to as LIN^{-} cells.

2.2.3 Analytical and preparative flow cytometry

All antibodies throughout this study were used at optimised dilutions and as given in Table 2.

For dead/live discrimination, 7-aminoactinomycin D (7AAD, 1:2000, Sigma) was added prior to analysis. Samples were analysed on a FACS Canto II flow cytometer (Becton Dickinson) or LSR II (Becton Dickinson). All flow cytometry data were analysed with Flowjo (Tree Star, Inc).

The sorting of cells for RNA preparation and transplantation was performed on a FACS Aria II (Becton Dickinson, UK). Cells were collected into either RNAse-free 1.5 ml tubes containing 600 µl Trisol (Helena Biosciences), supplemented with 6 µl polyacryl carrier (Helena Biosciences, UK), or FACS tubes filled with 5 ml sterile heat-inactivated FCS (Biosera, South America).

Table 2

Antibodies used throughout the study.

Table illustrating the antibodies used for defining lineage positive cells and antibodies used throughout the study to identify specific antigens. Columns illustrate the antigens recognised by the antibody, the fluorochrome with which the antibody is labelled and detected by flow cytometry, the isotype of the antibody, the manufacturer and the working dilution.

Antigen	Label	Isotype	Manufacturer	Dilution
Lineage				
CD11c	Biotin	Armenian Hamster IgG	eBioscience	1:200
Ter119	Biotin	Rat IgG2b	eBioscience	1:200
CD11b	Biotin	Rat IgG2b	eBioscience	1:200
CD3ε	Biotin	Armenian Hamster IgG	eBioscience	1:200
NK1.1	Biotin	Rat IgG2a	eBioscience	1:200
CD8α	Biotin	Rat IgG2a	eBioscience	1:200
B220	Biotin	Rat IgG2a	eBioscience	1:200
CD19	Biotin	Rat IgG2a	eBioscience	1:200
Gr1	Biotin	Rat IgG2b	eBioscience	1:200
Other antibodies				
7/4	PE	Rat IgG2a	AbD Serotec	1:200
B220	Pacific Blue	Rat IgG2a	eBioscience	1:200
B220	PE	Rat IgG2a	eBioscience	1:400
CD4	Pacific Blue	Rat IgG2a	eBioscience	1:200
CD8	PE-Cy7	Rat IgG2a	eBioscience	1:200
CD11b	Pacific Blue	Rat IgG2b	eBioscience	1:200
CD11c	APC-Cy7	Armenian Hamster IgG	eBioscience	1:200
CD19	APC	Rat IgG2a	Caltag	1:200
CD19	PE-Cy7	Rat IgG2a	eBioscience	1:200
CD34	APC	Rat IgG2a	eBioscience	1:50
CD48	APC	Armenian Hamster IgG	eBioscience	1:200
CD49b	PE	Rat IgM	eBioscience	1:400
CD71	PE	Mouse IgG1	eBioscience	1:800
CD150	PE-Cy7	Rat IgG2a	eBioscience	1:200
c-kit	APC-Cy7	Rat IgG2b	eBioscience	1:200
Flk-2	PE	Rat IgG2a	eBioscience	1:50
FcγRII/III	PE	Rat IgG2a	eBioscience	1:200
FcγRII/III	PE-Cy7	Rat IgG2a	eBioscience	1:200
Gr1	APC	Rat IgG2b	eBioscience	1:400
Gr1	APC-Cy7	Rat IgG2b	eBioscience	1:400
IgD	Biotin	Rat IgG2a	eBioscience	1:200
IgM	PE	Rat IgG2a	eBioscience	1:200
IL-7Rα	APC	Rat IgG2a	eBioscience	1:200
IL-7Rα	PE-Cy7	Rat IgG2a	eBioscience	1:200
Ly6C	APC	Rat IgG2a	eBioscience	1:500
M-CSF R	APC	Rat IgG2a	eBioscience	1:200
M-CSF R	PE	Rat IgG2a	eBioscience	1:200
MHC Class II	Biotin	Rat IgG2b	eBioscience	1:200
NK1.1	PE-Cy7	Mouse IgG2a	eBioscience	1:200
PDCA-1	APC	Rat IgG2b	eBioscience	1:200
Sca-1	Pacific Blue	Rat IgG2a	eBioscience	1:200
Streptavidin	Alexa Fluor 610	N/A	Invitrogen	1:2000
Streptavidin	Pacific Blue	N/A	Molecular Probes	1:200
Streptavidin	PE	N/A	Molecular Probes	1:2000
Streptavidin	PercP	N/A	Molecular Probes	1:200
TCRαβ	APC	Armenian Hamster IgG	eBioscience	1:400
TCRγδ	PE	Armenian Hamster IgG	eBioscience	1:200

2.3 RNA Extraction and Complementary DNA Synthesis

Cells were sorted into Trisol and homogenised for ten minutes by gentle inversion. In order to induce phase separation, 6 µl 1-bromo-3-chloropropane (BCP; Molecular Research Center, Inc.) was added to cells followed by centrifugation. The clear aqueous RNA layer was transferred into an RNAse free 1.5 ml eppendorf tube and precipitated with isopropanol (Fisher Scientific). RNA was washed repeatedly with 70% ethanol (Fisher Scientific). Finally, RNA was air dried and solubilised in Molecular Biology Grade water (Eppendorf) at a concentration of 500 cells/µl.

For one cDNA reaction (10,000 cells), 2 µl 500 µg/ml oligo dT (New England Biolabs) and 4 µl 10 mM dNTP (GE Healthcare) were added to the RNA. This mixture was heated to 65^{o}C for five minutes, followed by addition of 4 µl reaction buffer (Invitrogen), 2 µl 0.1 M DTT (Invitrogen) and 1 µl 40 U/µl ribonuclease inhibitor (Promega). 1 µl Superscript reverse transcriptase (Invitrogen) was added to the RNA and the reaction was left at 42^{o}C for 50 minutes. The reaction was inactivated by incubation at 70^{o}C for 15 minutes. The quality of the cDNA was tested by polymerase chain reaction (PCR) using HPRT primers.

2.4 Semi-quantitative Polymerase Chain Reaction and Agarose Gel Electrophoresis

PCRs were carried out in a final volume of 20 µl which was composed of 0.5 µM 5' HPRT Primer (See Table 3 for primer sequences), 0.5 µM 3' HPRT Primer, 0.4 µl 10 mM dNTPs, 2 µl 10X reaction buffer (Roche), 0.2 units Taq DNA polymerase (Roche), 50 ng cDNA and water. All PCR reactions were carried out using the PTC-200 Peltier Thermal Cycler (MJ Research) for 35 cycles. PCR products were analysed by agarose gel electrophoresis using a 1.5% gel, 6 x Orange G loading buffer and a current of

100V. Gels were visualised by emersion in ethidium bromide and observation on a UVP GelDoc-It TS Imaging System.

2.5 Quantitative Reverse Transcription Polymerase Chain Reaction

Quantitative reverse transcription polymerase chain reaction (qRT-PCR) was used to analyse gene expression in specific cell populations. Reactions were carried out in a total volume of 20 µl containing 1 µl Quantitect Custom Assay Primer mix (Qiagen), 1 µl Quantitect Custom Assay Probe (Qiagen), 10 µl Quantitect probe PCR mastermix (Qiagen) and 8 µl cDNA at a concentration of 125 cells/µl (see Table 3 for primer sequences). All reactions were carried out in triplicates for 45 cycles and covered with an adhesive film to prevent evaporation. QRT-PCR was carried out using a 7900HT fast Real-Time PCR System (Applied Biosystems) according to manufacturer's instructions. Data was analysed using the standard curve method (Applied Biosystems) and normalised according to levels of the housekeeping gene acidic ribosomal phosphoprotein (Arbp) as a standard.

Table 3

Primers used in semi-quantitative and qRT-PCR.

A) Primers used in semi-quantitative PCR. Primers were tested with total BM cDNA to determine their specificity.

B) Primer and Probe sequences used in qRT-PCR. Primer/probe sequences were designed manually by our lab using the Quantitect Assay software. Primers were tested with titrated total BM cDNA by generating a regression curve of threshold cycle (CT) versus $\log_{10}$ template dilution. Correlation co-efficients over 0.98 meant a good primer probe combination.

A

Gene	5' Sequence	3' Sequence
HPRT	GCTGGTGAAAAGGACCTCT	CACAGGACTAGAACACCTGGC

B

Gene	5' Sequence	Probe	3' Sequence
Arbp	TTTGACAACGGCAGCATT	CGACATCACAGAGCAGG	ACCCTCCAGAAAGCGAGA
GATA-1	GAAGCGAATGATTGTCAGCAAA	CAAACGACCACTACAAC	AGGCATTGCATACCGGATAC
GATA-2	CACAAGATGAATGGACAGAAC	CAGACGACAACCACCA	ATTGTGCAGCTTGTAGTAGAGG
GATA-3	TATCAAGCCCAAGCGAAG	AGACCACCACCACCAC	CATTAGCGTTCCTCCTCCAGA

2.6 *In vitro* culture of lymphoid progenitors

BM ELP, CLP eYFP$^-$ and CLP eYFP$^+$ populations were sorted into 5 ml sterile heat-inactivated FCS, then centrifuged and resuspended in IMDM. 10^3 ELP cells or 2 x 10^3 CLP eYFP$^-$ or CLP eYFP$^+$ cells were placed onto confluent GFP$^+$ OP9 stromal cells in six well plates, which had been irradiated with 3 Gray, and incubated at 37^{o}C with 7.5% CO_2. Cells were cultured with IMDM supplemented with 10% heat-inactivated FCS, L-glutamine, 10^{-4} M β-mercaptoethanol (Sigma) and IL-7 cytokine (1 ng/ml), Flk-2 ligand (5 ng/ml) and SCF (100 ng/ml), all purchased from Peprotech UK. Cultures were analysed at time points indicated by analytical flow cytometry.

2.7 *In vivo* transplantation assays

2 x 10^3 sorted CLP progenitor cells from 30 x B6/J CD45.1 mice were injected i.v. into *Rag2/Il2rg*-null mice which had been irradiated with 3 Gray, four to six hours prior to injection. Mice were analysed for CD45.1$^+$ donor-derived cells in BM, spleen and thymus at time points of two, three and four weeks post injection by flow cytometry. For analysis of other cell populations, 10^3 ELP progenitor cells or 2 x 10^3 CLP eYFP$^-$ or CLP eYFP$^+$ progenitor cells were injected into *Rag2*/*Il2rg*-null mice which had been irradiated with 3 Gray four to six hours prior to injection. Mice were analysed for eYFP$^+$ donor-derived cells in BM, spleen and thymus at indicated time points by flow cytometry.

2.8 Infection models

2.8.1 LPS-induced infection

LPS (Enzo Life Sciences), derived from *Salmonella minnesota* R595, induced inflammation was carried out on C57BL/6 mice, $Rag1^{wt/Cre}$ *x* $R26R^{wt/eYFP}$ mice, *Ifngr1*-null and *Tnfr1*-null (p55;N6) male and female mice aged six to ten weeks old. In order to measure the LPS-induced effect on body temperature and to identify each individual mouse, programmed temperature transponders (PLEXX) were inserted into the shoulder of each mouse according to the manufacturer's recommendations. Mice were then monitored for skin infection for at least 48 hours prior to LPS injection. To induce a sub-lethal inflammatory effect, 40 µg LPS or 40 µl double distilled endotoxin free water (Enzo Life Sciences) was injected intraperitoneally (i.p.) into each mouse at 8am on the day of the experiment. Temperature was measured at indicated time points using a DAS-7007S transponder reader (PLEXX). To measure the number of circulating granulocytes, lymphocytes, monocytes and RBCs, 5 µl blood from the tail of mice was collected at 3.5, 7, 12, 24 and 72 hour time points and added to 45 µl heparin and Krebs buffer (118 mM NaCl, 4.7 mM KCl, 1.2 mM KH_2PO_4, 1.2 mM $MgSO_4$, 4.2 mM $NaHCO_3$, 2 mM $CaCl_2$, 10 mM glucose, 200 mM sulphinpyrazone and 10 mM Hepes). Blood was analysed on a Vetscan HM2 Haematology System (Abaxis). In order to investigate the cytokine levels of LPS injected and non-injected mice, blood was taken by cardiac puncture of lethally anesthetised mice with a heparin covered syringe at 3.5, 7, 12, 24 and 72 hour time points. Blood was left at 4^oC overnight and then serum was isolated for analysis. To measure the levels of TNFα and IFNγ cytokines in the serum during LPS challenge, ELISA was carried out by Ana-Isabel Garcia-Diaz. For analysis of haematopoietic populations, BM and spleen were taken at 12, 24 and 72 hour time points.

In order to block TNFα, 675 µg anti-TNFα cytokine antibody (BioXcell) was injected i.p. into *Ifngr1*-null mice 24 hours prior to and immediately before LPS injection.

2.8.2 E. coli-induced infection

E. coli (strain DH10 B) containing a plasmid incorporating an ampicillin resistant gene was grown in L-Broth with 50 µg/µl ampicillin. The use of ampicillin selected for *E. coli* which had transformed the plasmid and also killed any additional bacteria which may have been growing in the media. The growth of *E. coli* was halted once the cells had reached the exponential phase, which was measured using a spectrophotometer at a wavelength of 600 nm. The total amount of *E. coli* was counted and calculated to be 4.48×10^{10} cells in 1 L. This was then transferred to a shaking water bath, which was set to a temperature of 56-58^{o}C, to induce pasteurisation. Cells were washed in distilled water and centrifuged, producing a pellet which weighed 2.64 g. The pellet was resuspended in 5 ml distilled water and left to lyophilise. Once the *E. coli* had dried, it was weighed again and resuspended in distilled water to give a concentration of 4.8×10^{9} cells/ml. Before injection into mice the *E. coli* solution was sonified.

The amount of *E. coli* which was equivalent to 40 µg LPS was calculated to be 1.5×10^{9} cells (Freudenberg et al., 1991). The equivalent volume was injected i.p. into C57BL/6 mice aged six to eight weeks old. To investigate the effect of a lower dose of *E. coli,* 3×10^{8} cells were also injected. These mice were also checked for temperature and changes in blood parameters. In addition, BM and splenic populations were analysed at the same time points as previous LPS experiments (see LPS-induced infection). To measure the levels of TNFα and IFNγ cytokines in the serum during *E. coli* infection, ELISA was carried out by Ana-Isabel Garcia-Diaz.

2.9 Statistical tests

Statistical significance was calculated using the Student's T-test with $p < 0.05$ (*) or $p < 0.01$ (**), indicating significance. Identical developmental populations from different individuals were subjected to a one-tailed test, with $p < 0.05$ considered to be significant.

CHAPTER 3

INVESTIGATION OF LYMPHOID PROGENITOR DEVELOPMENT UTILISING A NOVEL LINEAGE TRACING REPORTER

3.1 Introduction

The precise pathway by which lymphoid progenitors develop from multipotent stem cells into fully functional mature lymphocytes is still unknown. Whilst some groups argue that the CLP is the main lymphoid progenitor giving rise to T- as well as B-cells (Kondo et al., 1997, Karsunky et al., 2008), other reports favour a model whereby ETPs are derived from earlier progenitors such as LMPPs or ELPs (Benz and Bleul, 2005, Lai and Kondo, 2007). We aimed to investigate the source of thymic progenitors and further clarify the routes of lymphoid developmental pathways.

One experimental model which further dissected lymphoid development was the *Rag1*^{GFP} reporter mouse (Igarishi et al., 2002). This model allows isolation and functional analysis of an ELP population, however lineage mapping of ELP progeny *in situ* was limited due to non-continuous expression of GFP and rapid degradation of the fluorescence reporter with time. To overcome this limitation, we created a reporter model by inserting Cre recombinase into the *Rag1* locus (*Rag1*^{Cre}), thereby enabling eYFP expression from the *Rosa26* locus of *R26R*^{eYFP} reporter mice (Srinivas et al., 2001). We predicted that eYFP would permanently label cells which had passed via the ELP or any stage characterised by *Rag1* gene expression.

In addition to monitoring the onset and lineage specificity during lymphoid development by analysing eYFP expression in our reporter model, we also wanted to assess the effect of gender and age on lymphoid development. Lymphopoiesis has been shown to be depressed in pregnant (Medina et al., 1993) or oestrogen-treated mice (Medina et al., 2001) and abnormally elevated in ovariectomized female (Smithson et al., 1994) and castrated male mice (Wilson et al., 1995), indicating that steroid hormones play an important role in lymphoid development. Therefore, we wanted to compare the frequency and number of haematopoietic progenitor populations in male

and female mice. It has previously been reported that aging can also have a significant effect on lymphoid development. Involution of the thymus is one of the most prominent features of age-related changes and explains the diminished output of T-cells. In addition, B-cell generation is substantially reduced (reviewed by Linton and Dorshkind, 2004). It is generally thought that these changes are related to decreased output of lymphoid progenitor populations from the BM, and this was confirmed by Rossi and colleagues (Rossi et al., 2005) who reported a significant decrease in the frequency of LMPP and CLP populations in aged mice. This group also reported an increase in the frequency of LT-HSC and GMP populations, whilst ST-HSC, CMP and MEP populations remained unchanged. Taking into account the reports that age and gender can have inhibitory effects on haematopoiesis, we aimed to assess the effect of both age and gender simultaneously on the frequency and number of haematopoietic progenitor populations by analysing male and female mice of young and old age.

Other factors which are critical in lymphoid cell fate specification are the stepwise induction of genes (reviewed by Rothenberg and Taghon, 2005). Genes which are required for lymphoid development include *pTα, Gata3*, *Pax5, Il7rα and Ikzf3* (Aiolos). The expression of transcription factors in haematopoietic progenitor cells is thought to be crucial in promoting lymphoid development or by inhibiting the expression of other transcription factors required for the myelo-erythroid lineage. The transcription factor GATA-3 in particular is thought to be important for the specification of lymphoid progenitors into ETPs and is the only GATA family member expressed in T-cells (reviewed in Hosoya et al., 2010). A previous report by Hattori et al (1996) showed that in foetal thymic organ culture, the use of anti-sense oligonucleotides against *Gata3* in LIN^- c-kit^+ foetal thymocytes resulted in diminished T-cell development. In addition studies by Hendriks and colleagues (Hendriks et al., 1999) revealed that blastocysts

generated from *Gata3*-null embryonic stem cells could not contribute significantly towards intrathymic T-cell development. Both of these experiments suggest an important role for GATA-3 in T-cell fate specification.

Furthermore, genes which are thought to promote HSC development into the myelo-erythroid lineage include *Mpo* (myeloperoxidase), *Csf3r* (granulocyte-colony stimulating factor receptor; GCSF-R)*, Csfr1* (macrophage-colony stimulating factor receptor; MCSF-R*), Cebpα, Gata1, Gata2 and Epor* (erythropoietin receptor) as studied by Miyamoto and colleagues (2002). GATA-1 and GATA-2 are transcription factors involved predominantly in megakaryocyte and erythroid development (Zon et al., 1993; Harigae et al., 1998; Pevny et al., 1991) as well as in mast cell formation and differentiation (Tsai et al., 1997; Migliaccio et al., 2003) and inhibit the expression of PU.1, a transcription factor indistinguishable for GM or lymphoid development (Zhang et al., 1999; Nerlov et al., 2000, Dekoter et al., 2000). Therefore, the expression of *Gata1* and *Gata2* in haematopoietic cell populations can be used as readout for myelo-erythroid specification. Since members of the GATA family are expressed in both lymphoid (*Gata3*) and myelo-erythroid lineages (*Gata1/2*) and at specific stages of development, it was anticipated that analysing haematopoietic progenitor cells for their expression of *Gata1*, *2* and *3* would provide an indication as to which subsets would give rise to myeloid or lymphoid progeny, and most importantly ETPs.

3.2 Defining haematopoietic progenitors in the adult BM

One way to identify specific haematopoietic progenitor populations in the mouse BM is by utilising antibodies against selected surface markers of these cells. All haematopoietic progenitor populations are negative for the expression of mature lineage cell markers (LIN^-). The LT-HSC, ST-HSC and LMPP populations all reside within the LSK compartment and can be identified based on the expression of the receptor tyrosine kinase Flk-2 (CD135). All LT-HSCs and ST-HSCs can be defined as LSK Flk-2^- (Christensen and Weissman, 2001), whilst LMPPs can be defined as LSK Flk-2^+ (Adolfsson et al., 2001; Figure 3.1A). Taken together, the LT-HSC and ST-HSC populations consist of approximately 0.01% of the total BM, whereas LMPPs are approximately 0.05% of the total BM. For a more enriched population of LT-HSCs, the SLAM definition (Kiel et al., 2005) of LSK $CD48^-$ $CD150^+$ could be used (Figure 3.1B) which constitutes approximately 0.005% of mouse BM. LT-HSCs are also negative for the expression of CD34 on their cell surface, whereas ST-HSCs and LMPPs are positive and therefore ST-HSCs are defined as LSK $CD34^+$ Flk-2^- and LMPPs as LSK $CD34^+$ Flk-2^+ (Figure 3.1C). Throughout this study, LT-HSCs will be detected utilising the SLAM definition (Figure 3.1B), whilst ST-HSC and LMPP populations will be identified as LSK $CD34^+$ Flk-2^- and LSK $CD34^+$ Flk-2^+ (Figure 3.1C)

Similarly to stem cells and multipotent progenitors, myelo-erythroid progenitors also reside in the LIN^- compartment of the BM. However, these cells are found in LIN^- c-kit^+ Sca-1^- compartment (Figure 3.1D) and can be separated into three distinct subsets based on CD34 and FcγRII/III (CD16/32) expression (Akashi et al., 2000). The first progenitor population to arise in the myeloid compartment is the CMP which can be identified as $CD34^+$ FcγRII/III^- and which constitutes 0.2% of total BM cells. This cell population is then thought to further develop into GMP and MEP populations. The

GMP subset is defined as $CD34^{+}$ $Fc\gamma RII/III^{+}$ and constitutes 0.4% of total BM cells, and the MEP subset is defined as $CD34^{-}$ $Fc\gamma RII/III^{lo}$ and constitutes 0.1% of total BM cells (Figure 3.1D).

Another progenitor population which was recently described (Onai et al., 2007) is the CDCP. This cell population was isolated as LIN^{-} $c\text{-}kit^{int}$ $Flk\text{-}2^{+}$ $MCSF\text{-}R^{+}$ (Figure 3.2). The CDCP has been reported to derive from macrophage/DC progenitors in the BM (reviewed by Geissman et al., 2010) and is able to differentiate into cDCs and pDCs *in vitro* and *in vivo*. The CDCP population is the believed to represent the main DC progenitor and we will use this definition throughout the study.

Figure 3.1

Phenotypic definition of stem and progenitor subsets in lineage depleted adult BM cells.

A Representative FACS plot illustrating the definitions of HSC and LMPP populations in lineage depleted BM. Populations were isolated as LSK and further characterised as Flk-2^{-} (all stem cell activity) or Flk-2^{+} (LMPPs). Relative frequencies of each gated population are given in the respective figure.

B Representative FACS plot illustrating the HSC 'SLAM' definition for specifically identifying LT-HSCs in lineage depleted BM. The HSC SLAM definition allows the identification of LT-HSCs cells as LSK CD48^{-} CD150^{+}.

C Representative FACS plot illustrating a more specific definition for the identification of ST-HSC and LMPP populations in lineage depleted BM. ST-HSC cells can be distinguished as LSK CD34^{+} Flk-2^{-}. The LMPP population however is LSK CD34^{+} Flk-2^{+}.

D Representative FACS plot illustrating the identification of myelo-erythroid progenitors. CMP, GMP and MEP cells are separated into three populations by cell surface expression of CD34 and FcγRII/III. Gates were positioned according to positive and negative control populations.

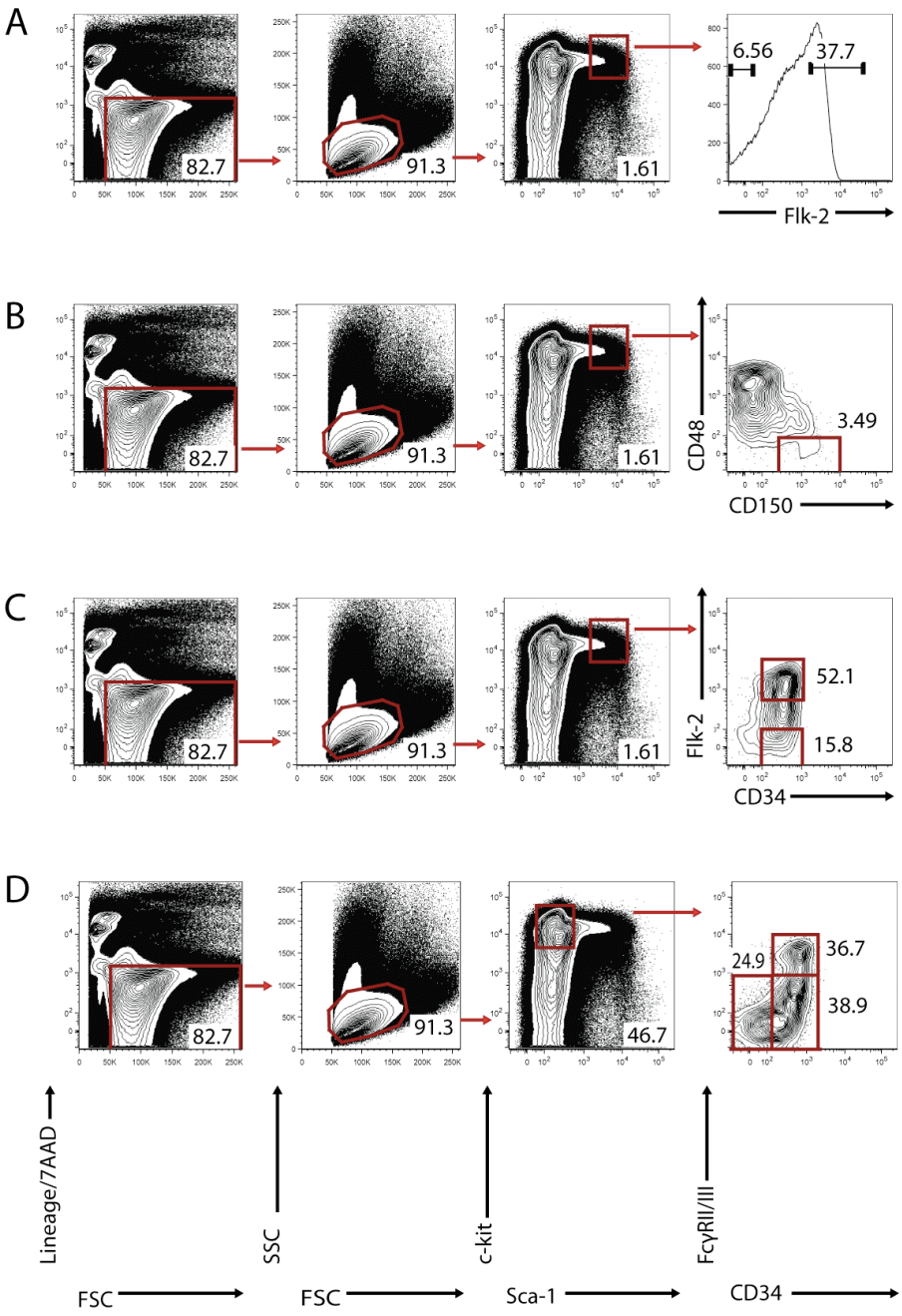
A
82.7
91.3
1.61
6.56
37.7
Flk-2
B
82.7
91.3
1.61
CD48
3.49
CD150
C
82.7
91.3
1.61
Flk-2
52.1
15.8
CD34
D
82.7
91.3
46.7
24.9
36.7
38.9
Lineage/7AAD
FSC
SSC
FSC
c-kit
Sca-1
FcγRII/III
CD34

Figure 3.2

Definition of the CDCP progenitor subset in the lineage negative compartment of the adult mouse BM.

Representative FACS plot showing how CDCP cells are identified in BM cells. Cells were first subject to a sub-optimal lineage depletion. Isolation of these cells was carried out according to Flk-2^{+} and c-kit^{int} expression and was further defined by the presence of MCSF-R and the absence of IL-7Rα expression.

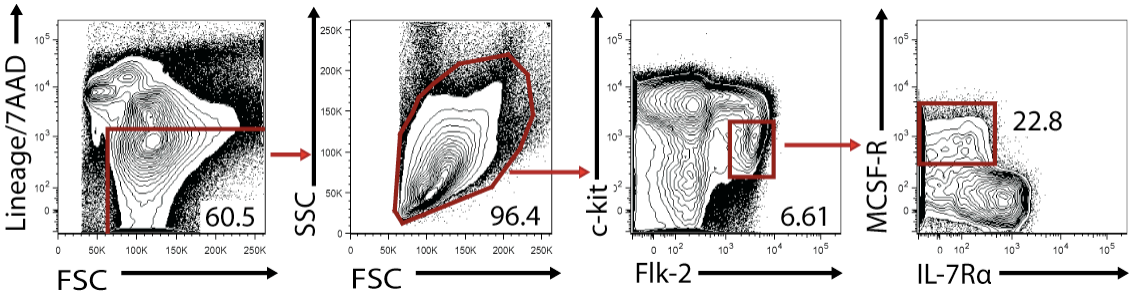
Lineage/7AAD
FSC
60.5
SSC
FSC
96.4
c-kit
Flk-2
6.61
MCSF-R
IL-7Rα
22.8

Based on the 'classical' hierarchical scheme of haematopoiesis which segregates lymphoid and myeloid development (Akashi et al., 2000), the counterpart to the CMP population in the lymphoid lineage is the CLP. This progenitor population was originally defined by Kondo and co-workers as LIN^- IL-7Rα^+ c-kit^{int} Sca-1^{int} and constituted 0.02% of total BM cells (Kondo et al., 1997). When we applied this definition to BM cells, we found that whilst c-kit and Sca-1 levels were predominantly intermediate, a small frequency of LIN^- IL-7Rα^+ cells expressed high levels of c-kit and Sca-1 and also there was a noticeable contamination of Sca-1^{hi} c-kit^- cells in this pool (Figure 3.3B). After gating on only the intermediate levels of c-kit and Sca-1, a high frequency of cells were positive for Flk-2 expression (Figure 3.3B). Based on this observation, we used a refined definition to isolate a $CLP^{Flk\text{-}2+}$ population defined as LIN^- IL-7Rα^+ Flk-2^+ which expressed mainly intermediate levels of c-kit and Sca-1 and lacked the contaminating Sca-1^{hi} c-kit^- expressing cells (Figure 3.3C). This definition has since been used by other groups to identify the CLP population (Karsunky et al., 2008). An overlay of the expression of c-kit and Sca-1 from both the original CLP and the $CLP^{Flk\text{-}2}$ populations is shown in Figure 3.3D. This reflects how the $CLP^{Flk\text{-}2}$ definition is a true subset of the original CLP. Therefore, we used the $CLP^{Flk\text{-}2}$ definition in all experiments throughout the study.

Figure 3.3

Defining the CLP population in the adult BM.

A Flow cytometry staining of the LSK fraction of the BM. This gate is used as a reference in 3.3B and C in order to compare LSK cells in different populations.

B Representative FACS plot illustrating the original definition of the CLP as LIN^- IL-7Rα^+. This gating strategy identifies various c-kit and Sca-1 levels as opposed to specific intermediate levels of c-kit and Sca-1, which define the true CLP population. Nearly all LIN^- IL-7Rα^+ c-kit^{int} Sca-1^{int} are positive for Flk-2 expression.

C Representative FACS plot of the $CLP^{Flk\text{-}2}$ population whereby cells are isolated according to IL-7Rα and Flk-2 co-expression in the LIN^- compartment of the BM. This definition identifies cells which express predominantly intermediate levels of c-kit and Sca-1 expression.

D Flow cytometry staining overlay of the c-kit and Sca-1 levels of the originally defined CLP population (red) and the $CLP^{flk\text{-}2+}$ population (blue) illustrating that the $CLP^{Flk\text{-}2}$ subset specifically identifies cells which express intermediate levels of c-kit and Sca-1.

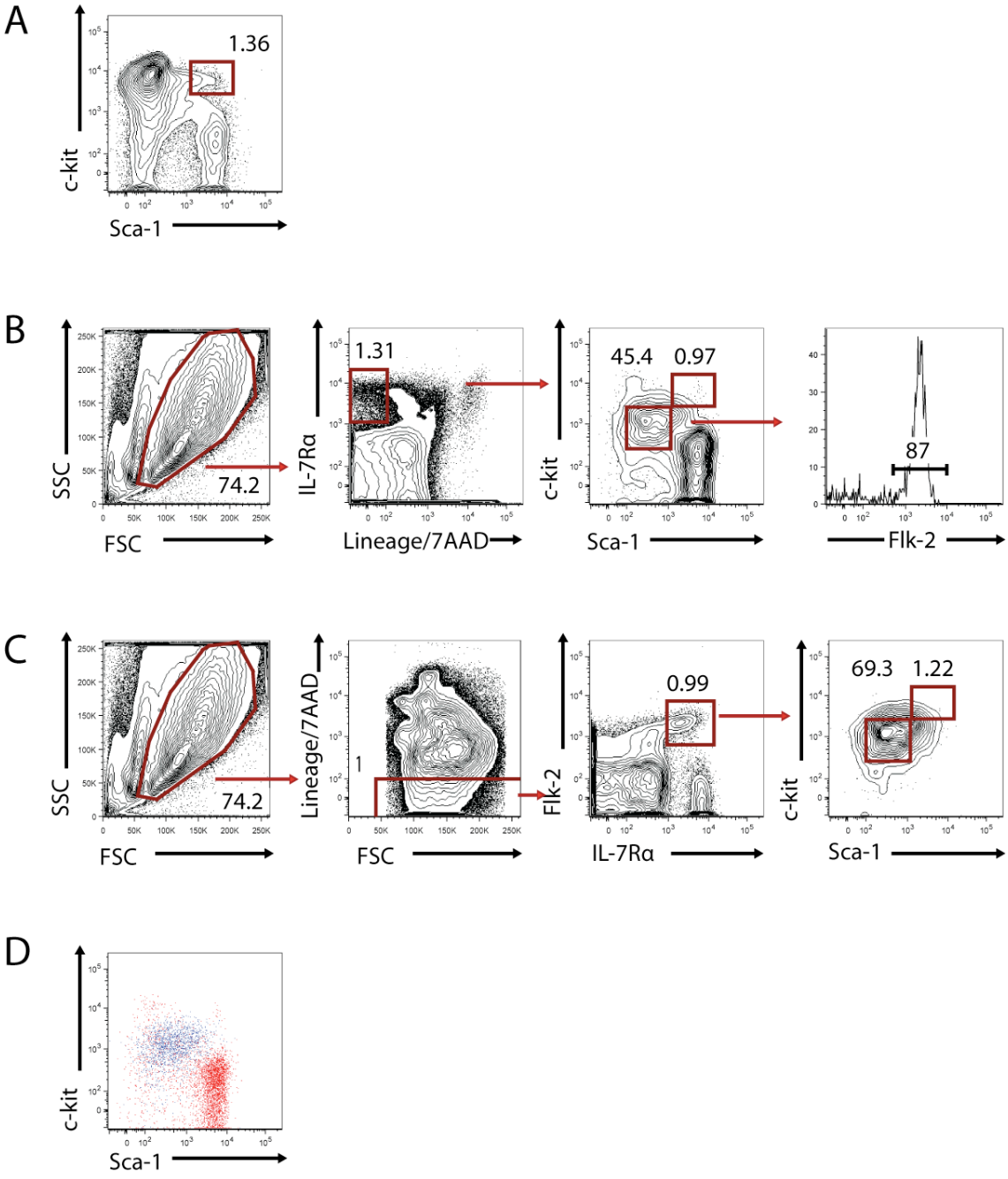
A
1.36
c-kit
Sca-1
B
SSC
FSC
74.2
1.31
IL-7Rα
Lineage/7AAD
45.4
0.97
c-kit
Sca-1
87
Flk-2
C
SSC
FSC
74.2
Lineage/7AAD
FSC
1
Flk-2
IL-7Rα
0.99
69.3
1.22
c-kit
Sca-1
D
c-kit
Sca-1

Another subset of cells in the lymphoid lineage which phenotypically resemble LMPPs is the ELP population. As previously explained, this population was originally isolated by insertion of GFP into the *Rag1* locus (Igarishi et al., 2002) and was defined as LSK Flk-2^{+} CD27^{+} Rag1^{GFP+}. These cells share the same phenotype as LMPPs except that ELPs are positive for reporter expression in the *Rag1*^{GFP} model. We aimed to create and identify an 'ELP analogue' and explore its developmental potential. Instead of inserting GFP into the *Rag1* locus, *Rag1*$^{wt/Cre}$ *x Rosa26*$^{wt/eYFP}$ mice were produced in our laboratory. In this reporter model, a Cre recombinase was inserted into the *Rag1* locus which was expressed upon activation of *Rag1*. This protein subsequently excised a transcriptional stop sequence upstream of an eYFP reporter on the constitutively active *Rosa26* locus, thereby driving eYFP expression in these cells (Figure 3.4B). In order to obtain this genotype, mice which were homozygous for Cre on the *Rag1* locus were bred with mice that were homozygous for eYFP on the *Rosa26* locus (Figure 3.4A). One advantage of this model over the *Rag1*^{GFP} model is that all cells which express *Rag1*-driven Cre remain permanently marked by eYFP. We aimed to ensure we had correctly identified an 'ELP analogue' by examining the phenotype, frequency, number and function of this population. Based on the fact that all mature B- and T-cells critically depend on *Rag1* and hence would be positive for expression of eYFP, we first analysed these populations in the spleen.

Figure 3.4

The Rag1$^{wt/Cre}$ x Rosa26$^{wt/eYFP}$ reporter model.

A Generation of *Rag1$^{wt/Cre}$ x Rosa26$^{wt/eYFP}$* reporter mice. Mice which were homozygous for Cre insertion in the *Rag1* locus were crossed to a homozygous *R26R^{eYFP}* strain. This generated a mouse which was heterozygous for Cre recombinase on the *Rag1* locus and heterozygous for the fluorescent reporter on the *Rosa26* locus.

B Diagram of Cre-mediated reporter expression. Cre-recombinase expressed under the *Rag1* promoter excises the loxP flanked stop sequence inserted into the *Rosa26* locus, driving expression of eYFP permanently in all cells.

A

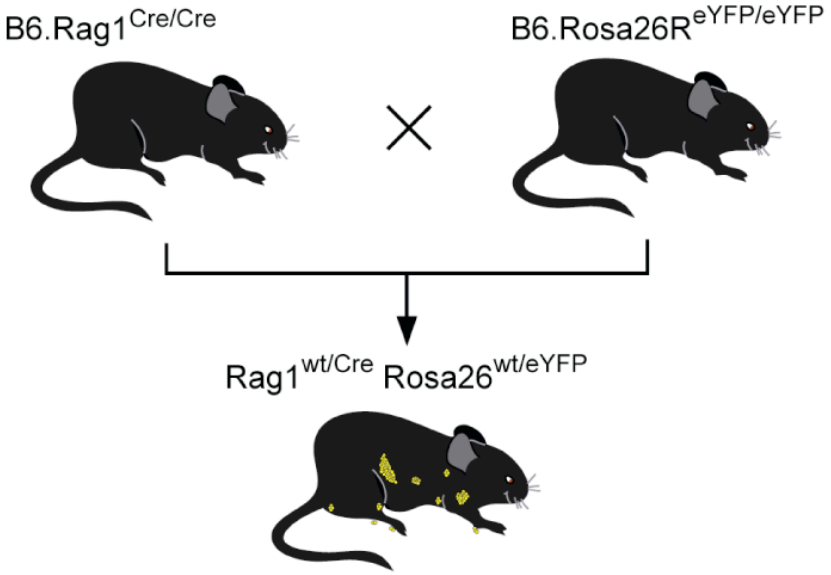
B6.Rag1Cre/Cre
B6.Rosa26ReYFP/eYFP
Rag1wt/Cre Rosa26wt/eYFP

B

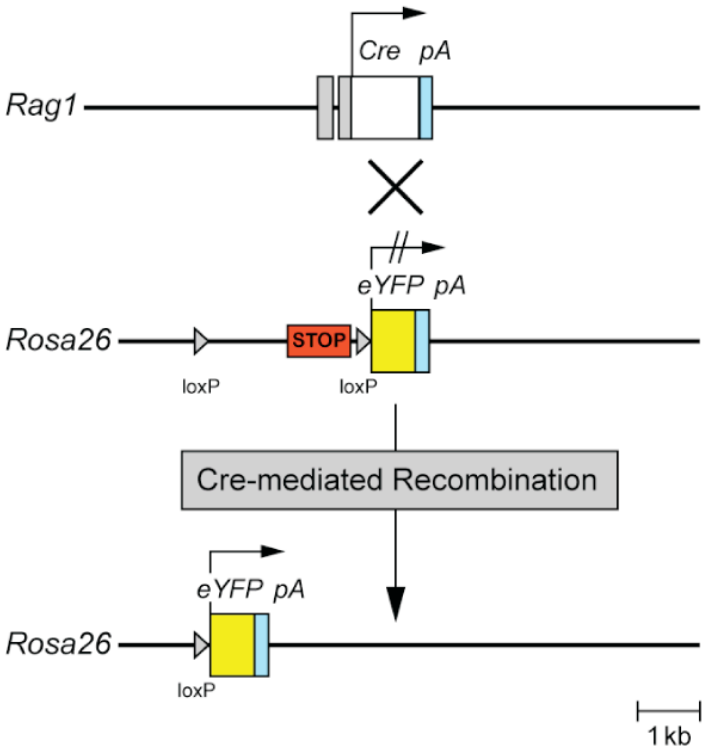
Cre pA
Rag1
eYFP pA
Rosa26
STOP
loxP
loxP
Cre-mediated Recombination
eYFP pA
Rosa26
loxP
1 kb

3.3 Analysis of mature haematopoietic splenic subsets in *Rag1* reporter mice

In order to characterise the *Rag1*$^{wt/Cre}$ *x Rosa26*$^{wt/eYFP}$ reporter model with respect to expression in the periphery, splenic lymphoid subsets were analysed for eYFP expression. All splenic B- and T-cells were virtually 100% positive for eYFP expression (Figure 3.5A). Early developmental stages of splenic B-cells were identified as CD19^{+} IgM^{+} IgD^{-}, of which 97.78 ± 0.34% were eYFP^{+}. Transitional B-cells, defined as CD19^{+} IgM^{+} IgD^{+}, were 98.47 ± 0.16% eYFP^{+} and CD19^{+} IgM^{lo} IgD^{+} B-cells containing both fully differentiated mature B-cells and re-circulating B-cells were 98.90 ± 0.19% eYFP^{+}. Both CD4 and CD8 αβ T-cells were labelled eYFP^{+} (CD4^{+} T-cells: 99.64 ± 0.068%; CD8^{+} T-cells: 99.58 ± 0.07%). The γδ T-cell population was 96.72 ± 0.26% positive for eYFP expression (see Figure 3.5A). NK T-cells as defined by cell surface expression of TCRαβ, NK1.1 and CD49b were 96.05 ± 0.70% positive for eYFP, a value comparable to that of CD4, CD8 and γδ T-cells. In contrast, NK-cells, which were identified as NK1.1^{+}, CD49b^{+} (See Figure 3.7A) showed only 29.27 ± 1.56% eYFP expression (Figure 3.5A).

Figure 3.5

EYFP expression in splenic cell populations of Rag1$^{wt/Cre}$ x Rosa26$^{wt/eYFP}$ mice.

A Bar chart representing the relative frequency of eYFP expressing cells in splenic lymphocytes. B-cell (CD19^{+}), T-cell, NK- and NK T-cell populations were analysed from at least eight individual mice in at least three independent experiments on animals aged six to eight weeks of age. Values represent mean ± S.E.M.

B Bar chart representing the relative frequency of eYFP expressing cells in myelo-erythroid subsets of the spleen. At least eight individual mice were analysed in at least three independent experiments on mice aged six to eight weeks of age. Values represent mean ± S.E.M.

C Bar chart representing the relative frequency of eYFP expressing cells in cDCs and pDCs of the spleen, without (w/o) or with (w) collagenase digestion. The decrease in the frequency of CD8^{-} DCs which were eYFP^{+} after collagenase treatment was significant. Six individual mice were analysed. Values are mean ± S.E.M.

A

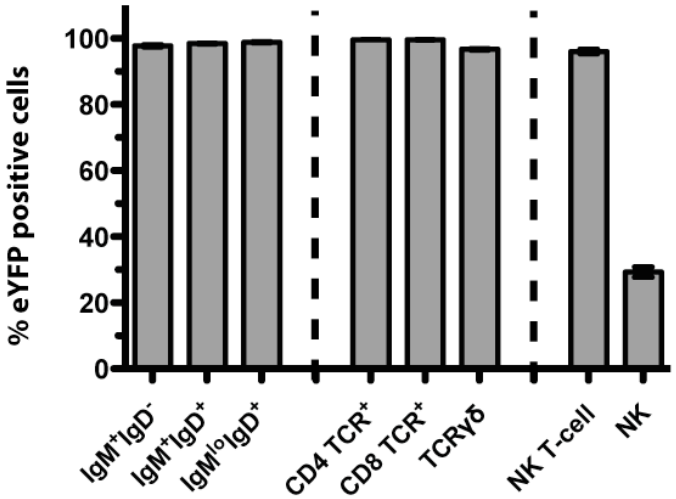
% eYFP positive cells
100
80
60
40
20
0
IgM+IgD-
IgM+IgD+
IgMloIgD+
CD4 TCR+
CD8 TCR+
TCRγδ
NK T-cell
NK

B

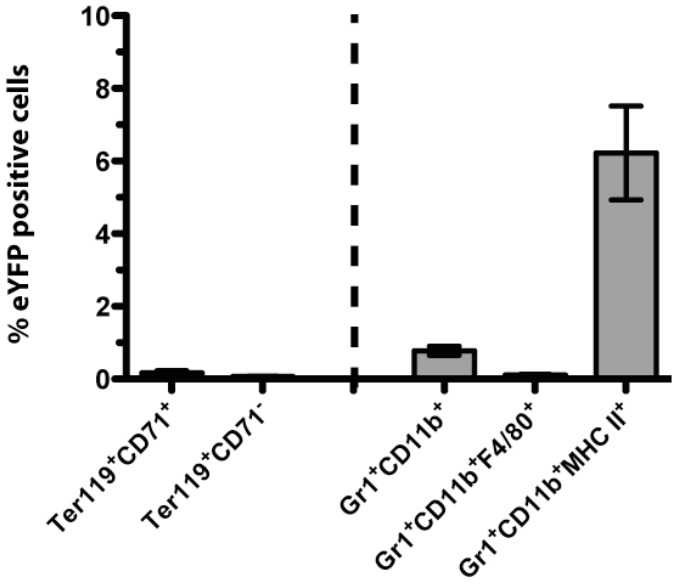
% eYFP positive cells
10
8
6
4
2
0
Ter119+CD71+
Ter119+CD71-
Gr1+CD11b+
Gr1+CD11b+F4/80+
Gr1+CD11b+MHC II+

C

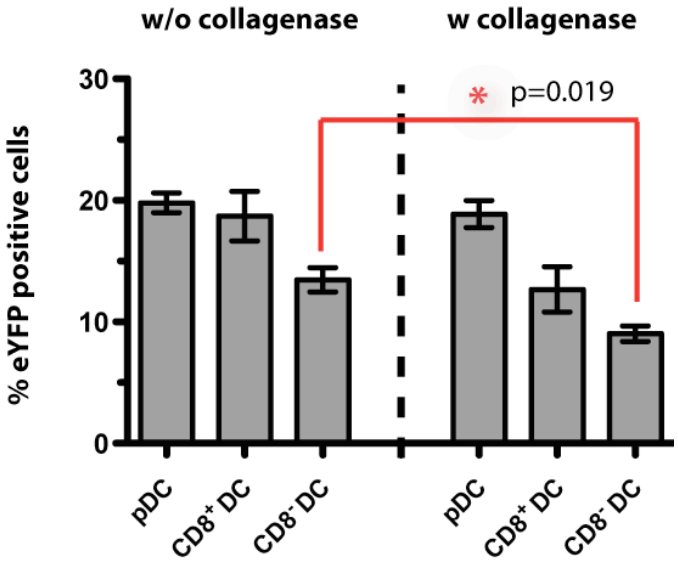
w/o collagenase
w collagenase
% eYFP positive cells
30
20
10
0
* p=0.019
pDC
CD8+ DC
CD8- DC
pDC
CD8+ DC
CD8- DC

We next extended our studies to erythroid and myeloid subsets of the spleen in *Rag1*$^{wt/Cre}$ *x Rosa26*$^{wt/eYFP}$ mice. Splenic erythroid precursors were identified as Ter119^{+} CD71^{+} (normoblasts) and Ter119^{+} CD71^{-} (reticulocytes). In both of these populations it was clear that eYFP expression was virtually absent (see Figure 3.5B and 3.6A). Similarly to erythroid cells, myeloid cells also expressed minimal eYFP expression. Splenic macrophage/monocytes and neutrophils were identified by Gr1^{+} CD11b^{+} and only 0.70 ± 0.13% of cells were positive for eYFP expression, which was reduced to 0.10 ± 0.02% when the macrophage marker F4/80 was included in the staining (Figure 3.5B). However, in Gr1^{+} CD11b^{+} myeloid cells expressing high levels of MHC class II, the frequency of eYFP expression was 6.22 ± 1.29% (Figure 3.5B and 3.6B), which may represent activated macrophages capable of phagocytosing eYFP^{+} cells. Intermediate and low levels of eYFP were also observed in this subset of cells (Figure 3.6B) and this could represent degradation of eYFP fluorescence in the lysosomal compartment of the macrophage.

PDCs and cDCs were assessed for eYFP expression with and without collagenase treatment (Figure 3.5C). PDCs were identified as PDCA-1^{+}, B220^{+}, CD11c^{+} and MHC class II^{int}, whilst DCs were classified as 'myeloid-derived' (CD11c^{+}, MHC class II^{+}, CD8α^{-}) or 'lymphoid-derived' (CD11c^{+}, MHC class II^{+}, CD8α^{+}). As shown by Figure 3.5C, prior to collagenase digestion 19.9 ± 1.11% of pDCs expressed eYFP, whilst lymphoid-derived DCs were 18.7 ± 2.04% positive for eYFP expression, with a slightly lower expression in myeloid-derived DCs (13.47 ± 1.00%).

After collagenase digestion, the relative frequency of eYFP^{+} pDCs remained similar. However, there was an increase in the relative frequency of eYFP^{+} cells in the CD11c^{+} MHC class II^{+} subset of DCs from 0.88% to 1.97% after exposure to collagenase treatment (Figure 3.7B and C). In contrast, the relative frequency of eYFP expression in

lymphoid-derived DCs decreased from 18.70 ± 2.04% to 12.67 ± 1.87%, whilst the relative frequency of eYFP expression in myeloid-derived DCs decreased from 13.47 ± 1.0% to 9.03 ± 0.64% (Figure 3.5C). This suggested that collagenase treatment was needed to remove all DCs from the spleen, and that DCs which were removed were largely negative for eYFP.

The results of lineage mapping in the spleen showed that all mature T- and B-cells were marked by eYFP, which was expected as these cells expressed *Rag1* at least twice throughout their development. There was no evidence for significant expression of eYFP in any mature myelo-erythroid populations, suggesting in the first instance that the $Rag1^{wt/Cre}$ *x* $Rosa26^{wt/eYFP}$ reporter model could be used to monitor lymphoid development. NK, pDC and DC populations were only partially marked by eYFP, suggesting that development of these mature populations could have derived from alternate lineages as well as the lymphoid lineage. In order to investigate these observations further, we next looked at eYFP expression in the BM.

Figure 3.6

Frequency of splenic erythroid and myeloid populations expressing eYFP in Rag1$^{wt/Cre}$ x Rosa26$^{wt/eYFP}$ mice.

A Representative FACS plot illustrating the virtual absence of cells expressing eYFP in splenic erythroid populations. The erythroid compartment was sub-divided into normoblasts (Ter119^{+} CD71^{+}) and reticulocytes (Ter119^{+} CD71^{-}) in mice aged six to eight weeks of age.

B Representative FACS plot illustrating the lack of eYFP expressing cells in MHC class II^{-} myeloid cells, but a significant frequency of cells expressing eYFP in the MHC class II^{+} subset. Cells were first identified by Gr1 and CD11b and further characterised by MHC class II expression in mice aged six to eight weeks of age.

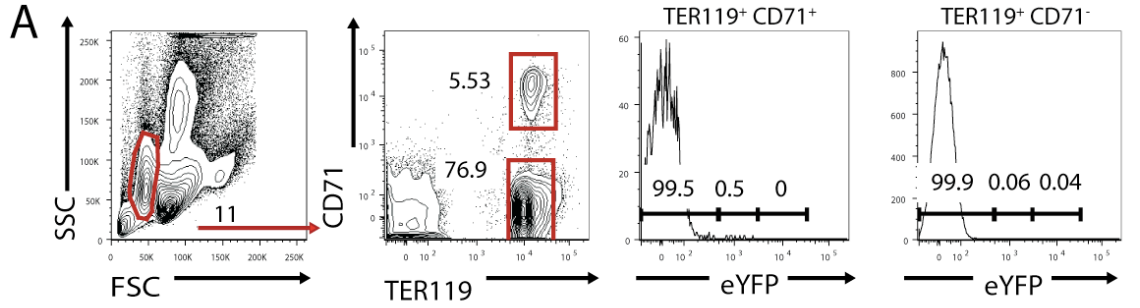
A
SSC
FSC
11
CD71
TER119
5.53
76.9
TER119+ CD71+
99.5 0.5 0
eYFP
TER119+ CD71-
99.9 0.06 0.04
eYFP

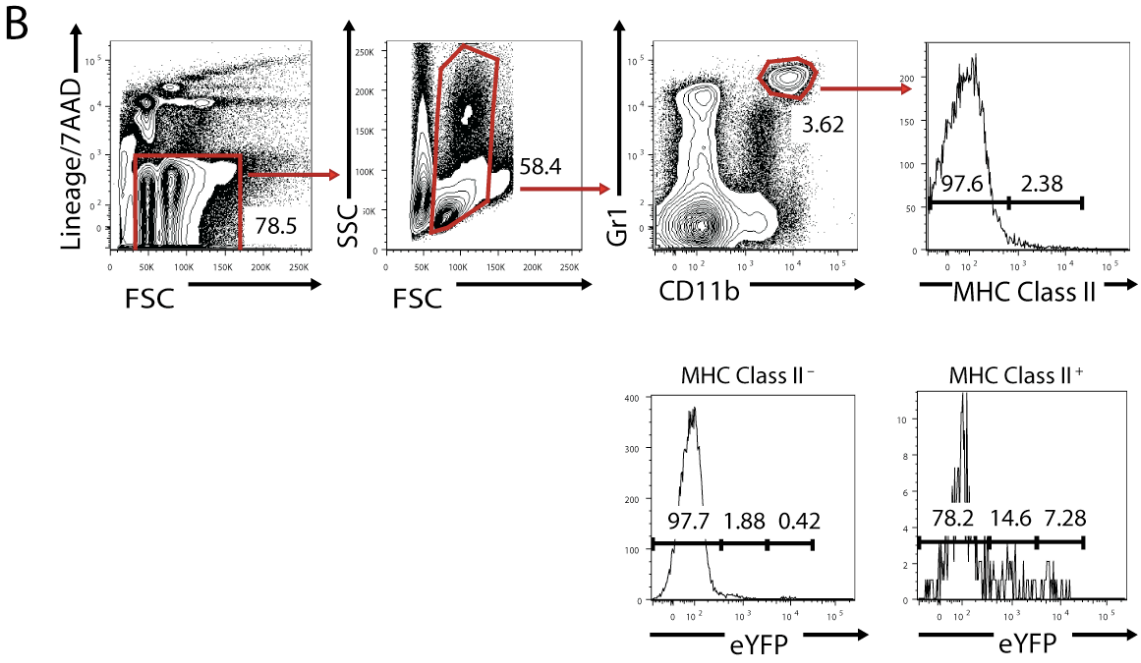
B
Lineage/7AAD
FSC
78.5
SSC
FSC
58.4
Gr1
CD11b
3.62
MHC Class II
97.6
2.38
MHC Class II-
97.7 1.88 0.42
eYFP
MHC Class II+
78.2 14.6 7.28
eYFP

Figure 3.7

Frequency of splenic NK and DC populations expressing eYFP in Rag1$^{wt/Cre}$ x Rosa26$^{wt/eYFP}$ mice.

A Representative FACS plot illustrating the relative frequency of splenic NK-cells expressing eYFP. NK-cells were defined by NK1.1 and CD49b and then analysed for eYFP expression. Both eYFP^{+} and eYFP^{-} cells were evident.

B Representative FACS plot illustrating the relative frequency of lymphoid and myeloid-derived DCs without collagenase treatment. DCs were identified by CD11c and MHC class II and then divided into either lymphoid-derived (CD8α^{+}) or myeloid-derived (CD8α^{-}) cells and analysed for eYFP expression. The lymphoid-derived DCs had a higher frequency of eYFP expressing cells than the myeloid-derived DC subset.

C Representative FACS plot illustrating the relative frequency of collagenase treated lymphoid (CD8α^{+}) and myeloid (CD8α^{-}) derived DC subsets. There is a clear increase in the expression of MHC class II on the DCs. The relative frequency of eYFP^{+} cells in both subsets decreased after digestion with collagenase.

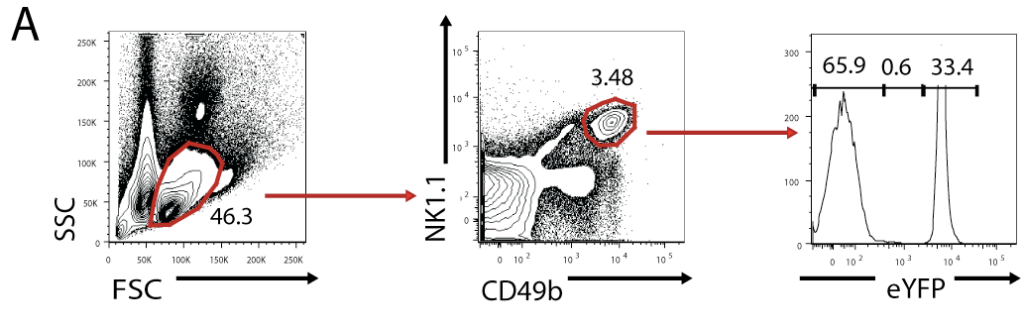
A
SSC
FSC
46.3
NK1.1
CD49b
3.48
65.9
0.6
33.4
eYFP

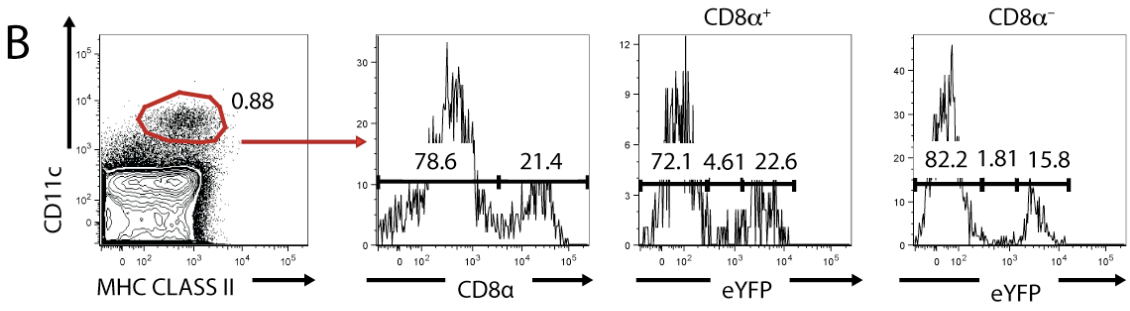
B
CD11c
MHC CLASS II
0.88
CD8α
78.6
21.4
CD8α⁺
72.1
4.61
22.6
eYFP
CD8α⁻
82.2
1.81
15.8
eYFP

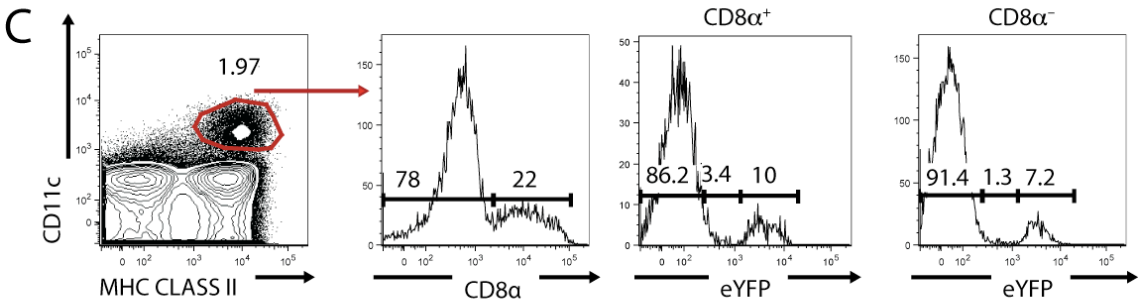
C
CD11c
MHC CLASS II
1.97
CD8α
78
22
CD8α⁺
86.2
3.4
10
eYFP
CD8α⁻
91.4
1.3
7.2
eYFP

3.4 Expression of eYFP in mature and progenitor cell populations of the BM

We first investigated myelo-erythroid populations of the BM. In the erythroid compartment of the BM, erythrocyte progenitors were defined as erythroblasts ($Ter119^{int}$ $CD71^{+}$), normoblasts ($Ter119^{+}$ $CD71^{+}$) and reticulocytes ($Ter119^{+}$ $CD71^{-}$). All three subsets showed less than 1% eYFP expression (Figure 3.8A), corresponding to the results obtained in the splenic compartment. Similar to erythrocytes, the $Gr1^{+}$ $CD11b^{+}$ myeloid population exhibited only 0.62 ± 0.09% $eYFP^{+}$ cells (Figure 3.8A) and additional characterisation of this population, utilising the macrophage marker F4/80, presented virtual absence of eYFP expression (0.01 ± 0.002%). This frequency was almost identical to that in splenic myeloid populations.

Next we explored eYFP expression in the lymphoid compartment of the BM. Immature and mature B-cells were identified according to the previous cell surface markers applied in the spleen and were almost 100% positive for eYFP (Figure 3.8B). As shown in Figure 3.9, B-cell progenitors were subdivided into pre-pro B-cells (IgM^{-}, $B220^{+}$, $CD19^{-}$, $c\text{-}kit^{int}$, $CD25^{-}$), pro B-cells (IgM^{-}, $B220^{+}$, $CD19^{+}$, $c\text{-}kit^{int}$, $CD25^{-}$) and pre B-cells (IgM^{-}, $B220^{+}$, $CD19^{+}$, $CD25^{+}$). Pre-pro B-cells exhibited 87.87 ± 1.76% eYFP expression (Figure 3.8B) which was increased after development into pro B-cells and expression of CD19 (98.8 ± 0.68%). In the pre B-cell compartment, 99.5 ± 0.7% of cells were positive for eYFP. Further observations of the pre-pro B-cell compartment revealed that the acquisition of eYFP preceded that of CD19 in the majority of cells. During maturation from pre-pro B-cells to pro B-cells, there was only a small percentage of cells which were $CD19^{+}$ and $eYFP^{-}$ (Figure 3.9A). This relationship was also clear in the pre B compartment where almost all of the cells were $CD19^{+}$ $eYFP^{+}$ (Figure 3.9B).

Figure 3.8

Expression of eYFP in mature and progenitor cell populations of the BM in Rag1$^{wt/Cre}$ x Rosa26$^{wt/eYFP}$ mice.

A Bar chart illustrating the virtual absence of eYFP expressing cells in the myelo-erythroid compartment of the BM. Six individual mice were analysed per myelo-erythroid subset in two independent experiments on mice aged six to eight weeks old. Values represent mean ± S.E.M.

B Bar chart illustrating the average frequency of eYFP expressing cells in all B-cell subsets. Six individual mice were analysed per B-cell subset in two independent experiments on mice aged six to eight weeks old. Values represent mean ± S.E.M.

C Bar chart illustrating the frequency of eYFP^{+} cells in haematopoietic progenitor compartments. Expression of eYFP was evident in the LMPP and CLP populations with minimal expression in all other progenitor subsets. At least ten individual mice were analysed per progenitor subset in at least five independent experiments on mice aged six to eight weeks of age.

A

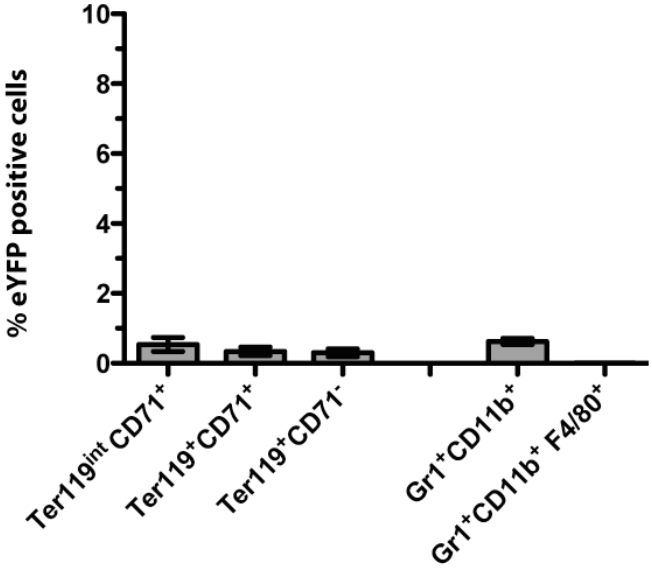
% eYFP positive cells
10
8
6
4
2
0
Ter119int CD71+
Ter119+CD71+
Ter119+CD71-
Gr1+CD11b+
Gr1+CD11b+ F4/80+

B

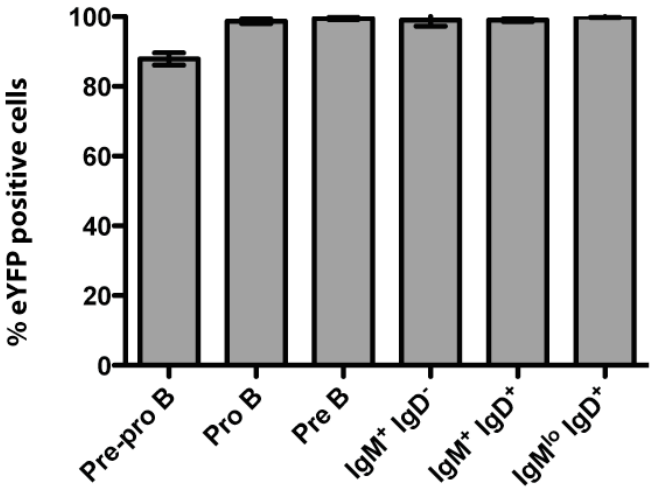
% eYFP positive cells
100
80
60
40
20
0
Pre-pro B
Pro B
Pre B
IgM+ IgD-
IgM+ IgD+
IgMlo IgD+

C

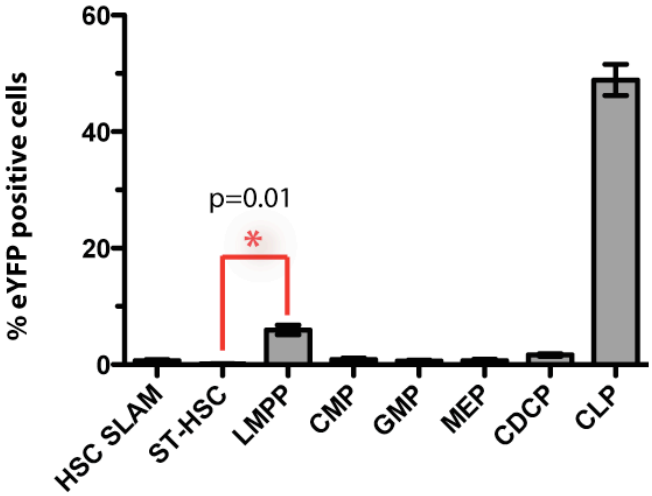
% eYFP positive cells
60
40
20
0
p=0.01
*
HSC SLAM
ST-HSC
LMPP
CMP
GMP
MEP
CDCP
CLP

Figure 3.9

EYFP expression in BM B-cell subsets of Rag1$^{wt/Cre}$ x Rosa26$^{wt/eYFP}$ mice.

A Representative FACS plot illustrating eYFP expression in the pre-pro and pro B-cell compartments of the BM. Pre-pro B-cells develop into pro B-cells by acquiring CD19 expression. This plot clearly shows that eYFP precedes the acquisition of CD19 in the majority of cells.

B Representative FACS plot illustrating eYFP expression in the pre B-cell subset of the BM. Pre B-cells have already acquired CD19 and are virtually all positive for eYFP expression. There is a minimal frequency of cells which are positive for CD19 expression but negative for eYFP expression.

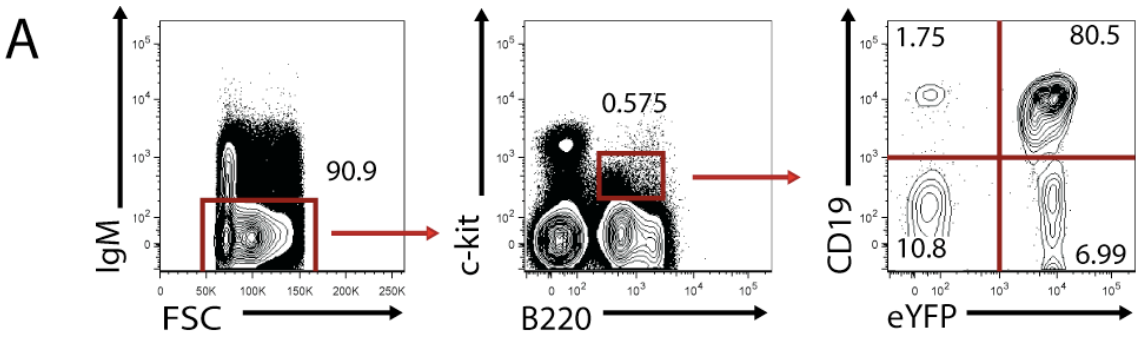
A
IgM
FSC
90.9
c-kit
B220
0.575
CD19
eYFP
1.75
80.5
10.8
6.99

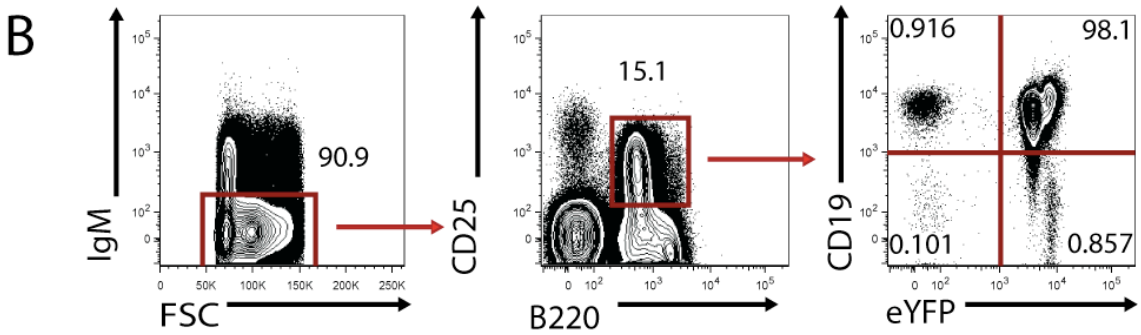
B
IgM
FSC
90.9
CD25
B220
15.1
CD19
eYFP
0.916
98.1
0.101
0.857

We next explored eYFP expression in stem cells and haematopoietic progenitors. LT-HSCs and ST-HSCs exhibited a virtual absence of eYFP expressing cells (0.11 ± 0.06% and 0.21 ± 0.16%, Figure 3.8C, Figure 3.10A and B). This proved that there was no aberrant expression of Cre recombinase in any stem cell subsets. The LMPP subpopulation however comprised 5.94 ± 0.84% $eYFP^+$ cells on average (Figure 3.8C), of which the range was between 3.5% and 9% (Figure 3.10B). These $eYFP^+$ cells represented the 'ELP analogue' population.

The 'ELP analogue' could be defined as LSK Flk-2^+ IL-7Rα^- $eYFP^+$. CD27 was not utilised in the staining as all LMPP and CLP cells are uniformly positive for this marker. Hence this population is a true subset of the LMPP pool with the additional hallmark of eYFP expression (Figure 3.11A). There was a significant increase in eYFP expression from the LMPP pool to the CLP pool indicating, at least in part, development via the ELP population.

Upon observation of the CLP population, remarkably only 48.89 ± 4.07% of CLP cells were $eYFP^+$ (Figure 3.8C). The eYFP histogram resolved an $eYFP^-$ cell population, an $eYFP^{int}$ population and an $eYFP^+$ population (Figure 3.11B). The relative frequency of $eYFP^-$ cells was almost equivalent to the relative frequency of $eYFP^+$ cells, with a small percentage (~10%) of cells residing in the $eYFP^{int}$ pool. These cells appeared to be acquiring eYFP expression, which is indicative for a developmental relationship from the $eYFP^-$ population to the $eYFP^+$ population. In addition, the segregation of eYFP expression also correlated with a minor decrease of c-kit expression in these subsets (Figure 3.11B).

Figure 3.10

EYFP expression in HSC and multipotent progenitor populations of the BM in $Rag1^{wt/Cre}$ *x* $Rosa26^{wt/eYFP}$ *mice.*

A Representative FACS plot illustrating the virtual absence of eYFP expression in the LT-HSC compartment of the BM, as defined by the SLAM definition. Due to the absence of *Rag1* expression in LT-HSCs, it is expected that these cells would be negative for eYFP expression.

B Representative FACS plot illustrating eYFP expression in the ST-HSC and LMPP populations of the BM. There was a virtual absence of eYFP expressing cells in the ST-HSC compartment, but a significant percentage of cells expressing eYFP in the LMPP pool. This figure shows that eYFP is first significantly expressed in the LMPP population, which represents the ELP subset.

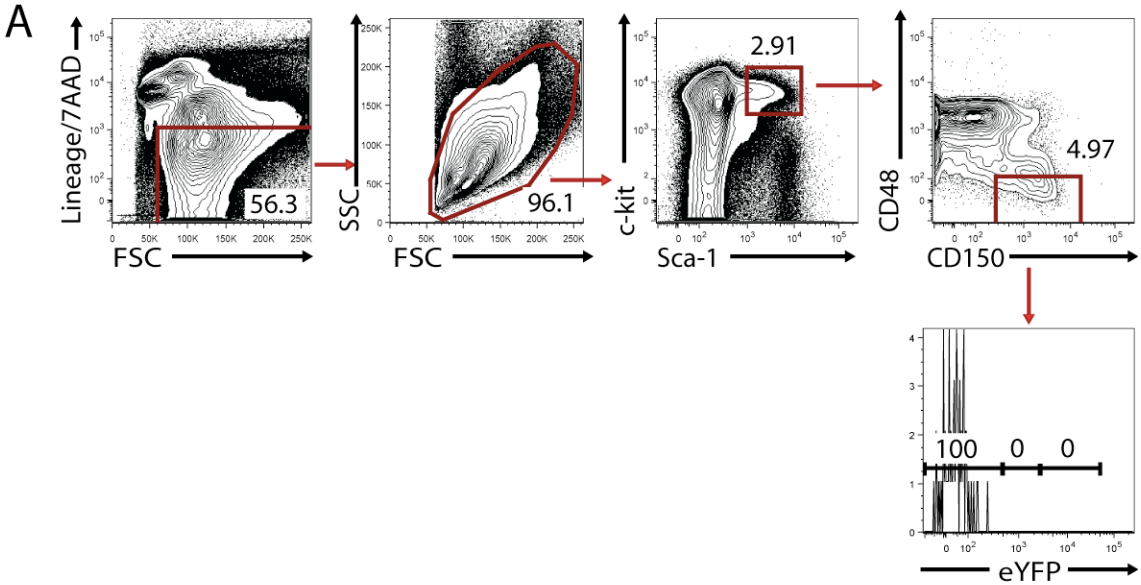
A
Lineage/7AAD
FSC
56.3
SSC
FSC
96.1
c-kit
Sca-1
2.91
CD48
CD150
4.97
100 0 0
eYFP

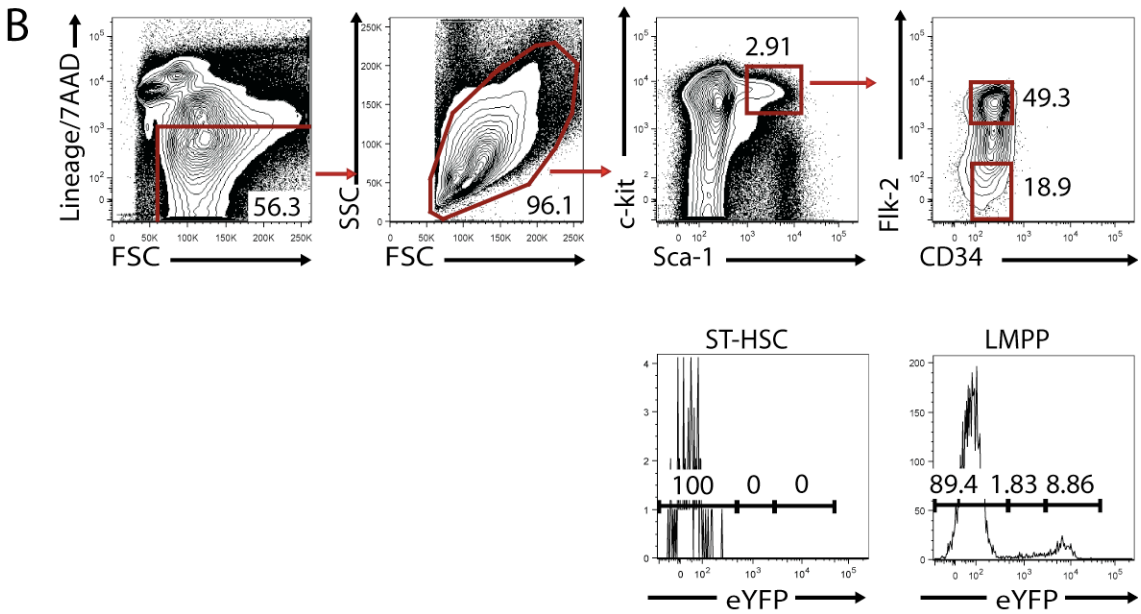
B
Lineage/7AAD
FSC
56.3
SSC
FSC
96.1
c-kit
Sca-1
2.91
Flk-2
CD34
49.3
18.9
ST-HSC
100 0 0
eYFP
LMPP
89.4 1.83 8.86
eYFP

Figure 3.11

EYFP expression in early lymphoid compartments of the BM in $Rag1^{wt/Cre}$ *x* $Rosa26^{wt/eYFP}$ *mice.*

A Representative FACS plots illustrating the isolation of an 'ELP analogue'. This cell population was defined as LSK, Flk-2^{+}, IL-7Rα^{-} and further isolated by expression of eYFP.

B Representative FACS plot illustrating expression of eYFP in the CLP subset. Cells were first identified as LIN^{-} IL-7Rα^{+} Flk-2^{+}. Further characterisation of this population revealed a divide in eYFP expression.

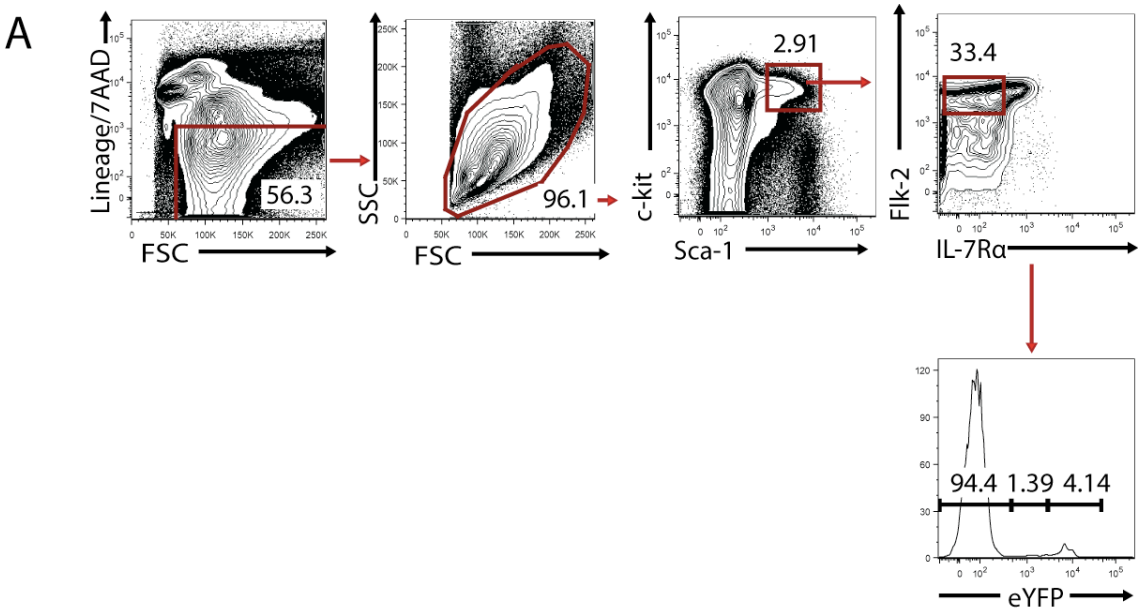
A
Lineage/7AAD
FSC
56.3
SSC
FSC
96.1
c-kit
Sca-1
2.91
Flk-2
IL-7Rα
33.4
94.4 1.39 4.14
eYFP

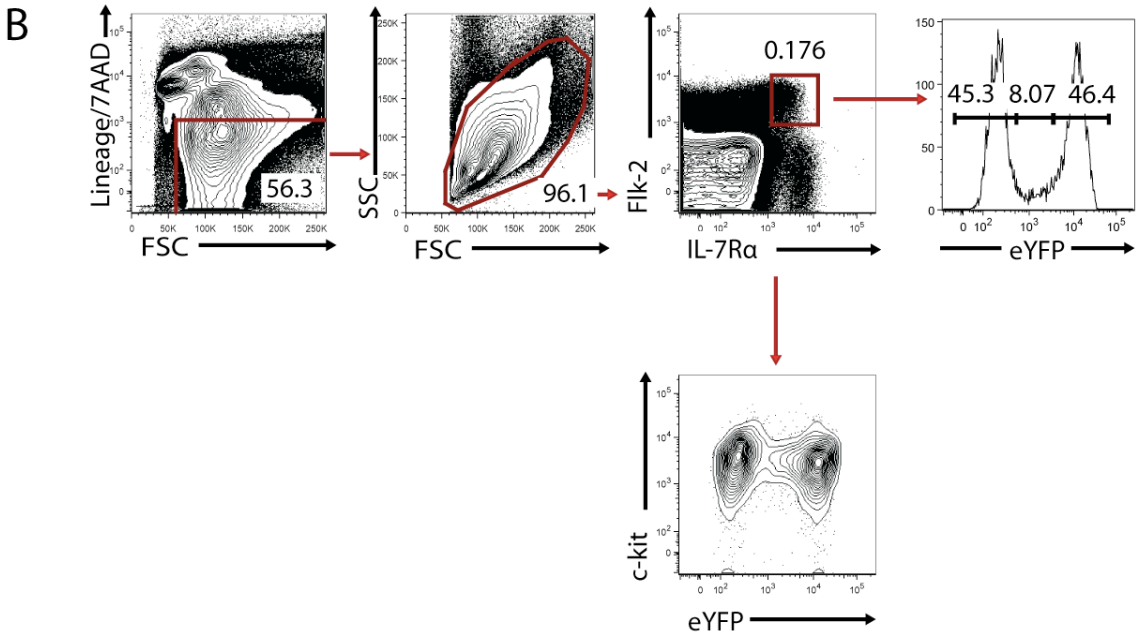
B
Lineage/7AAD
FSC
56.3
SSC
FSC
96.1
Flk-2
IL-7Rα
0.176
45.3 8.07 46.4
eYFP
c-kit
eYFP

Next we investigated eYFP expression in lineage committed subsets of early haematopoietic progenitors. The LIN^- c-kit^{hi} Sca-1^- compartment of the BM was subdivided into CMP, GMP and MEP populations (Figure 3.12A). In concordance with the absence of reporter expression in mature myeloid and erythroid cells in the periphery, all subpopulations were virtually negative for eYFP expression. Similarly, the CDCP population expressed only a minimal amount of eYFP (1.9 ± 0.24%, Figure 3.8C and 3.12B). Due to the fact that approximately 20% of pDC and DC splenic populations were $eYFP^+$, this might suggest that the CDCP may not be the only progenitor population giving rise to mature DCs. An $eYFP^+$ progenitor such as the ELP or the CLP may have given rise to a substantial frequency of DCs. Alternatively, a small frequency of CDCPs could expand preferentially at a later stage or activation of *Rag1* and subsequent expression of eYFP could have occurred after the CDCP stage in some cells.

Figure 3.12

EYFP expression in myeloid and dendritic progenitor populations of the BM in $Rag1^{wt/Cre}$ *x* $Rosa26^{wt/eYFP}$ *mice.*

A Representative FACS plot illustrating the virtual absence of eYFP expression in myeloid progenitors. Three subpopulations of LIN^- c-kit^{hi} Sca-1^- cells could be isolated based on the expression of CD34 and FcγRII/III expression. The CMP pool was identified as $CD34^+$ FcγRII/III^-, the GMP was characterised as $CD34^+$ FcγRII/III^+ and the MEP was defined as $CD34^-$ FcγRII/III^{lo}.

B Representative FACS plot illustrating the percentage of cells expressing eYFP in the CDCP population of the BM. The CDCP population was identified as LIN^- Flk-2^+ c-kit^{int} MCSF-R^+ IL-7Rα$^-$ and showed that only a minute frequency of cells were positive for eYFP expression.

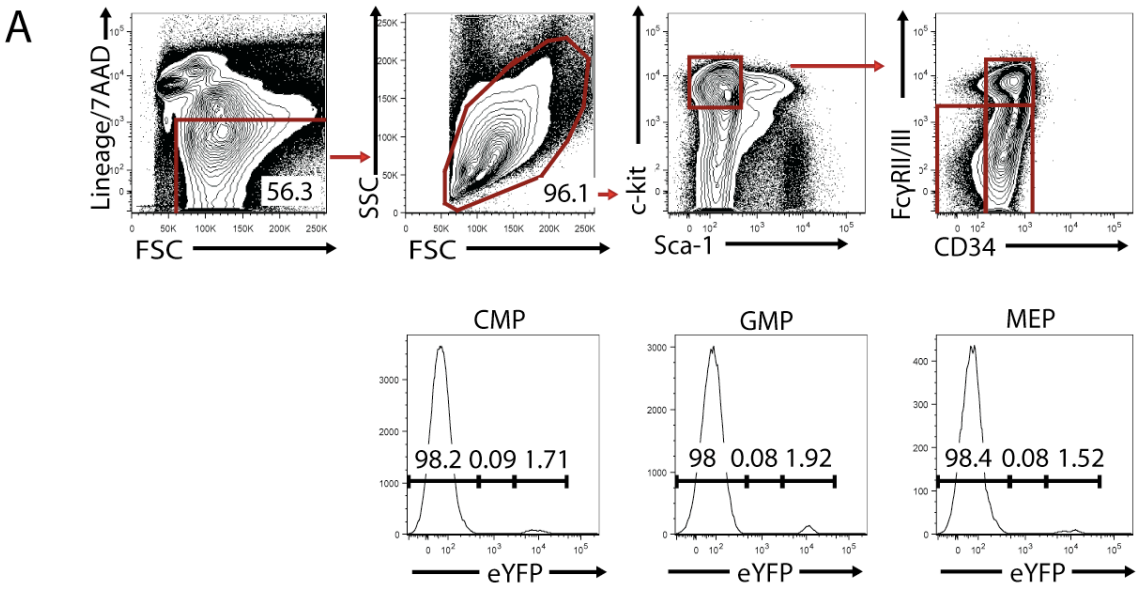
A
Lineage/7AAD
FSC
56.3
SSC
FSC
96.1
c-kit
Sca-1
FcγRII/III
CD34
CMP
98.2 0.09 1.71
eYFP
GMP
98 0.08 1.92
eYFP
MEP
98.4 0.08 1.52
eYFP

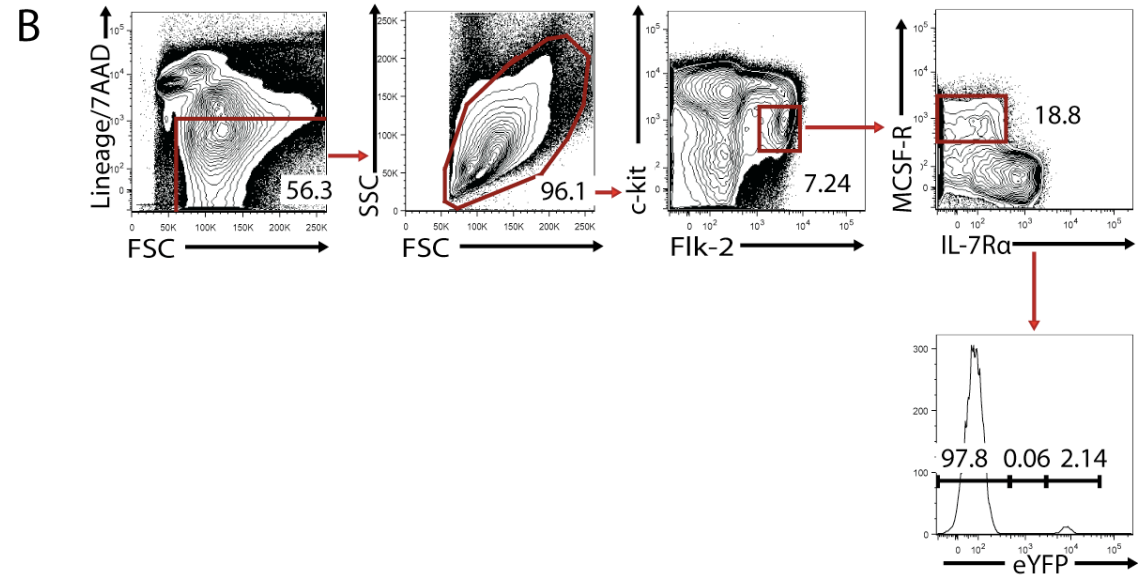
B
Lineage/7AAD
FSC
56.3
SSC
FSC
96.1
c-kit
Flk-2
7.24
MCSF-R
IL-7Rα
18.8
97.8 0.06 2.14
eYFP

3.5 Investigation of the frequency of eYFP$^+$ cells in the thymic compartment of the haematopoietic system

We next investigated eYFP expression in thymic populations of *Rag1*$^{wt/Cre}$ *x* *Rosa26*$^{wt/eYFP}$ mice. It is thought that the earliest thymocyte progenitors in the adult mouse are dependent on a continuing input of blood borne progenitors (Scollay et al., 1986), which are of BM origin. However, the identity of these progenitors is still unknown. Early T-precursor populations can form B-cells (Wu et al., 1991), NK-cells (Carlyle et al., 1998), myeloid cells (Lee et al., 2001, Balciunaite et al., 2005; Wada et al., 2008; Bell and Bhandoola, 2008) and DCs (Ardavin et al., 1993) as well as T-cells, suggesting the thymus is seeded by some form of multipotent progenitor cell. We hypothesised that mapping the expression of eYFP in the thymus and correlating this with eYFP expression observed in BM progenitor pools would indicate which populations are "thymic seeding cells". Within the thymic compartment, all subsets from ETPs to mature CD4 and CD8 populations were analysed for the expression of eYFP.

Focusing firstly on mature cells, in concordance with splenic T-cells subsets, CD4 SP and CD8 SP T-cells were almost 100% positive for eYFP expression (99.77 ± 0.02% and 99.72 ± 0.03%, Figure 3.13A). This observation could also be extended to the double positive population (99.58 ± 0.32%). However, this was not the case in early thymic populations. The ETP population was identified as LIN$^-$ c-kit^{hi} CD44$^+$ CD25$^-$ (Godfrey et al., 1992), the DN2 population as LIN$^-$ CD44$^+$ CD25$^+$, the DN3 population as LIN$^-$ CD44$^-$ CD25$^+$ and the DN4 population as LIN$^-$ CD44$^-$ CD25$^-$. As shown in Figure 3.13A, the frequency of cells in the ETP compartment expressing eYFP was 75.80 ± 3.50%, increasing to 84.70 ± 1.70% in DN2. Virtually all of the cells were eYFP$^+$ from the DN3 stage onwards. The increase in the frequency of eYFP$^+$ cells is

depicted in Figure 3.13B. Unlike the cells in the CLP pool which expressed intermediate levels of eYFP illustrating a developmental progression, there was little evidence for intermediate populations in early thymic compartments (Figure 3.13B). This suggests that ETP cells may be derived from two progenitor cell types, one which is $eYFP^{-}$ and one which is $eYFP^{+}$ as there was no evidence of $eYFP^{-}$ cells converting into $eYFP^{+}$ cells.

Figure 3.13

Expression of eYFP in thymocyte subsets in Rag1$^{wt/Cre}$ x Rosa26$^{wt/eYFP}$ mice.

A Bar chart illustrating the average frequency of cells expressing eYFP in all mature and thymocyte populations of the thymus. At least seven individual mice were analysed per subset in at least four independent experiments. Mice were analysed at four to six weeks of age. Values are mean ± S.E.M.

B Representative FACS plots illustrating the expression of eYFP in early thymic subsets. DN1-4 populations were characterised on LIN$^-$ cells by CD44 and CD25 expression and then analysed for expression of eYFP. The ETP population was defined as LIN$^-$ CD44$^+$ CD25$^-$ c-kit^{hi}.

A

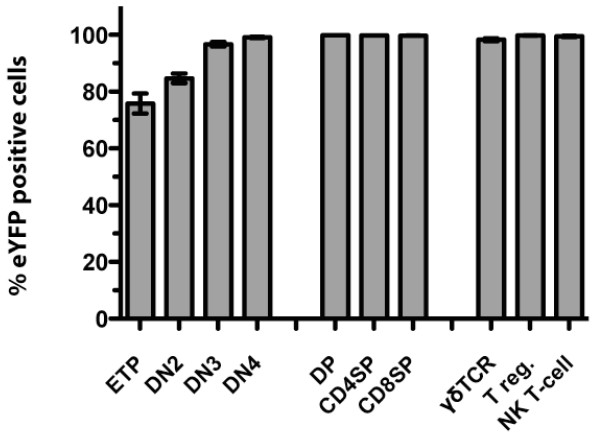
% eYFP positive cells
100
80
60
40
20
0
ETP
DN2
DN3
DN4
DP
CD4SP
CD8SP
γδTCR
T reg.
NK T-cell

B

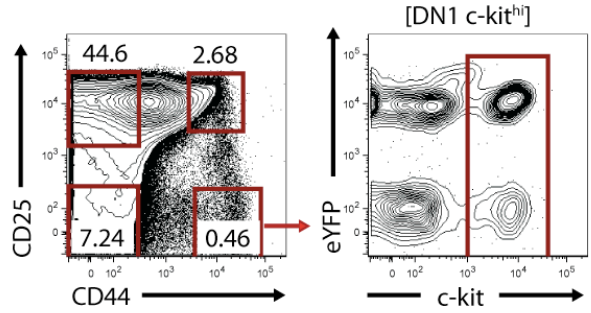
[DN1 c-kit^hi]
44.6
2.68
7.24
0.46
CD25
CD44
eYFP
c-kit

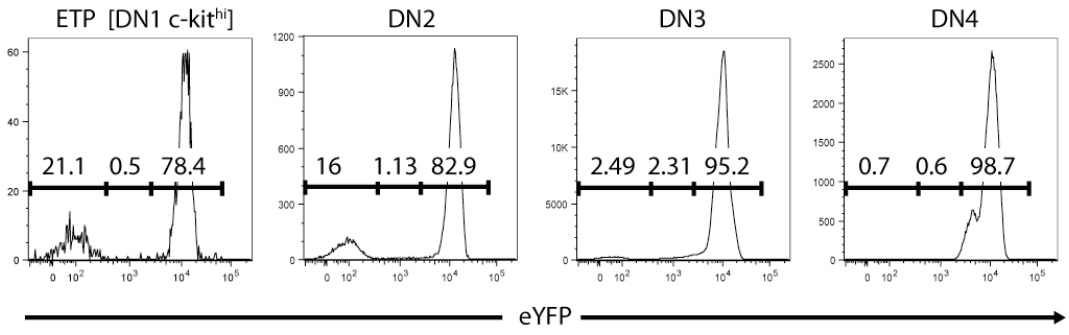
ETP [DN1 c-kit^hi]
DN2
DN3
DN4
21.1 0.5 78.4
16 1.13 82.9
2.49 2.31 95.2
0.7 0.6 98.7
eYFP

3.6 Comparison of cellularity of haematopoietic populations in *Rag1$^{wt/Cre}$ x Rosa26$^{wt/eYFP}$* mice with C57BL/6 mice

We further enumerated the absolute numbers of all haematopoietic subsets in *Rag1$^{wt/Cre}$ x Rosa26$^{wt/eYFP}$* reporter mice to exclude any potential aberration of haematopoietic development and homeostasis.

In the spleen, (Figure 3.14) the number of all myeloid, B, pDC, CD8$^+$ DC, NK, NK T-cell and αβ T-cell subsets between *Rag1$^{wt/Cre}$ x Rosa26$^{wt/eYFP}$* and C57BL/6 mice were not significantly different. However, the reticulocyte population in C57BL/6 mice amounted to 2.10 x 10^6 ± 0.71 x 10^6 whereas in *Rag1$^{wt/Cre}$ x Rosa26$^{wt/eYFP}$* mice this cell number was increased to 5.21 x 10^6 ± 0.43 x 10^6 (Figure 3.14A). In addition, there was a significant difference in the number of the splenic CD8α$^-$ DC population between the mouse strains. This difference in numbers was 1.3 fold (Figure 3.14B) with a value of 0.54 x 10^6 ± 0.06 x 10^6 in C57BL/6 mice, compared to 0.75 x 10^6 ± 0.09 x 10^6 in *Rag1$^{wt/Cre}$ x Rosa26$^{wt/eYFP}$* reporter mice; however this difference only occurred upon inclusion of collagenase to the processing of the organs. The number of CD4 TCRγδ T-cells was also different between strains. In C57BL/6 mice, the amount of cells only equated to 0.39 x 10^4 ± 0.06 x 10^4 whilst in *Rag1$^{wt/Cre}$ x Rosa26$^{wt/eYFP}$* mice, 1.45 x 10^4 ± 0.3 x 10^4 cells were present (Figure 3.14C).

Analysis of the BM (Figure 3.15) revealed that the erythroid populations had significantly different numbers between mutant and wildtype mice. The Ter119$^+$ CD71$^+$ subset amounted to 4.8 x 10^6 ± 0.53 x 10^6 in C57BL/6 mice and 10.70 x 10^6 ± 0.23 x 10^6 in *Rag1$^{wt/Cre}$ x Rosa26$^{wt/eYFP}$* mice (Figure 3.15A), whilst the Ter119$^+$ CD71$^-$ subset was 0.42 x 10^6 ± 0.07 x 10^6 in C57BL/6 and 2.52 x 10^6 ± 0.29 x 10^6 in *Rag1$^{wt/Cre}$ x Rosa26$^{wt/eYFP}$* mice (Figure 3.15A). Seeing as though the number of reticulocytes in the spleen was also lower in the C57BL/6 strain than the *Rag1$^{wt/Cre}$ x Rosa26$^{wt/eYFP}$* mice

strain, this suggests that cells may be proliferating at a higher rate in the *Rag1*$^{wt/Cre}$ *x* *Rosa26*$^{wt/eYFP}$ mice as they develop down the erythroid lineage. Unlike the erythroid compartments, the number of immature B-cells was lower in the reporter mice than in wildtype mice (Figure 3.15B). The absolute number of $CD19^+$ IgM^+ IgD^+ B-cells was $4.87 \times 10^5 \pm 0.57 \times 10^5$ in C57BL/6 mice and 50% less in *Rag1*$^{wt/Cre}$ *x* *Rosa26*$^{wt/eYFP}$ mice ($2.42 \times 10^5 \pm 0.33 \times 10^5$). The BM myeloid and NK populations showed no significant changes in numbers. Additionally, in the thymus, all the cell numbers were comparable (Figure 3.15C). Due to the fact that there were alterations in the numbers of haematopoietic populations which were both positive and negative for *Rag1*-driven expression of Cre, we deduced that these differences were not caused by toxic levels of the Cre protein. These minor discrepancies may have been due to minor variations in the background of these mice strains.

Figure 3.14

Absolute cell numbers of all splenic populations in C57BL/6 and Rag1$^{wt/Cre}$ x Rosa26$^{wt/eYFP}$ mice.

A Bar chart illustrating the absolute number of cells in all myelo-erythroid, B- and T-cell subsets of the spleen of wildtype and *Rag1*$^{wt/Cre}$ *x Rosa26*$^{wt/eYFP}$ mice, aged six to eight weeks old. The number of Ter119^{+}, CD71^{-} erythroid cells was significantly higher in the *Rag1*$^{wt/Cre}$ *x Rosa26*$^{wt/eYFP}$ strain. Analysis was carried out on at least six individual mice per subset in at least two independent experiments. Values represent mean ± S.E.M.

B Bar chart illustrating the absolute number of cells in pDC, DC, NK and NK T-cell subsets of the spleen of wildtype and *Rag1*$^{wt/Cre}$ *x Rosa26*$^{wt/eYFP}$ mice, aged six to eight weeks old. PDC and DC subset numbers were calculated with or without treatment with collagenase. There was a significant difference in the number of CD8^{-} DC between the two strains after collagenase treatment. Analysis was carried out on at least six individual mice per subset in at least two independent experiments. Values represent mean ± S.E.M.

C Bar chart illustrating the absolute number of cells in CD4^{+} and CD8^{+} γδ T-cells of the spleen of wildtype and *Rag1*$^{wt/Cre}$ *x Rosa26*$^{wt/eYFP}$ mice, aged six to eight weeks old. There was a significantly higher number of CD4 γδ T-cells in the *Rag1*$^{wt/Cre}$ *x Rosa26*$^{wt/eYFP}$ mice compared to C57BL/6 mice. Analysis was carried out on at least eight individual mice per subset in at least two independent experiments. Values represent mean ± S.E.M.

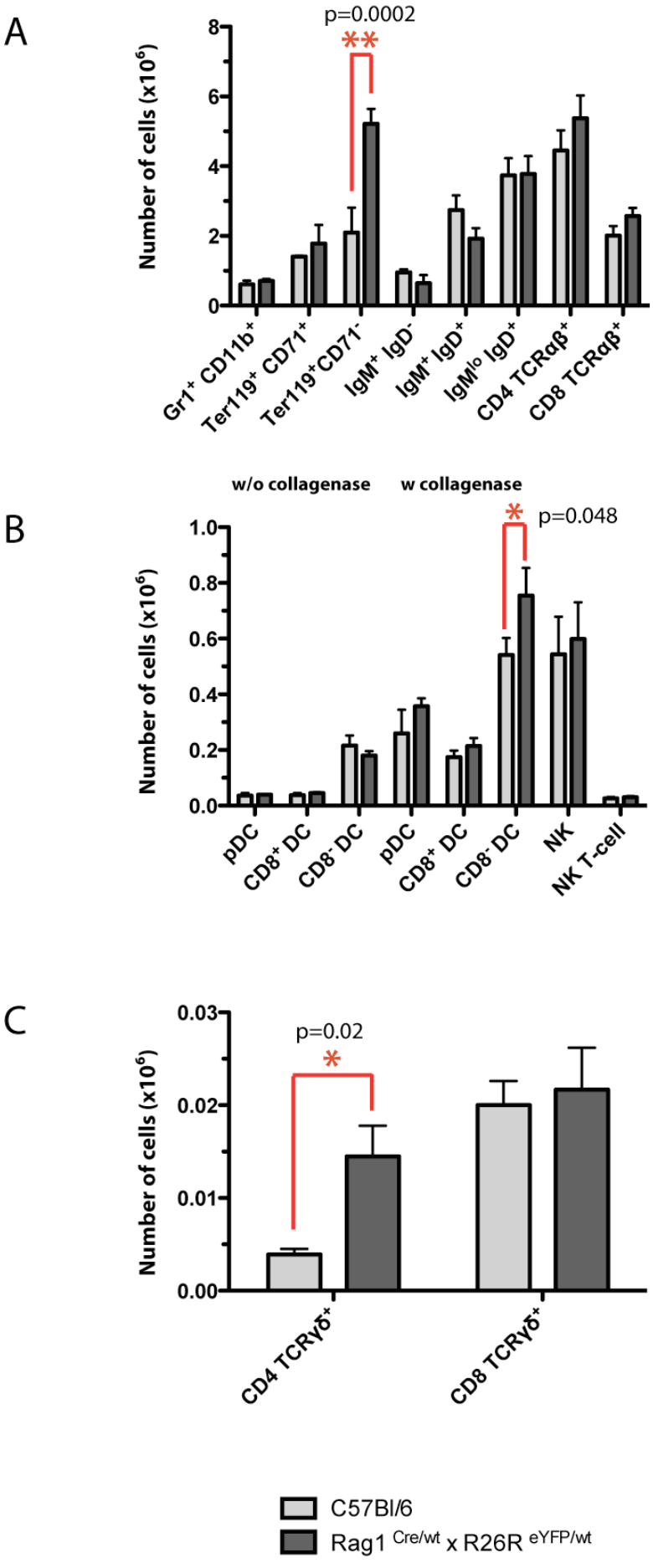
A
p=0.0002
**
Number of cells (x10⁶)
8
6
4
2
0
Gr1⁺ CD11b⁺
Ter119⁺ CD71⁺
Ter119⁺CD71⁻
IgM⁺ IgD⁻
IgM⁺ IgD⁺
IgM^lo IgD⁺
CD4 TCRαβ⁺
CD8 TCRαβ⁺
B
w/o collagenase
w collagenase
*
p=0.048
Number of cells (x10⁶)
1.0
0.8
0.6
0.4
0.2
0.0
pDC
CD8⁺ DC
CD8⁻ DC
pDC
CD8⁺ DC
CD8⁻ DC
NK
NK T-cell
C
p=0.02
*
Number of cells (x10⁶)
0.03
0.02
0.01
0.00
CD4 TCRγδ⁺
CD8 TCRγδ⁺
C57Bl/6
Rag1 Cre/wt x R26R eYFP/wt

Figure 3.15

Absolute cell numbers of BM and thymic populations in C57BL/6 and Rag1$^{wt/Cre}$ x Rosa26$^{wt/eYFP}$ mice.

A Bar chart illustrating the absolute number of myeloid and erythroid cells per femur pair in the BM of wildtype and *Rag1$^{wt/Cre}$ x Rosa26$^{wt/}$*eYFP mice, aged six to eight weeks old. Both erythroid subset numbers were significantly different between the two strains. Analysis was carried out on at least six individual mice per subset in at least two independent experiments. Values represent mean ± S.E.M.

B Bar chart illustrating the absolute number of B-cell subsets and NK-cells per femur pair in the BM of wildtype and *Rag1$^{wt/Cre}$ x Rosa26$^{wt/eYFP}$* mice, aged six to eight weeks old. All B-cell populations are positive for CD19 expression. There was a significantly higher number of transitional B-cells in wildtype mice compared to *Rag1$^{wt/Cre}$* x *Rosa26$^{wt/}$*eYFP mice. Analysis was carried out on at least six individual mice per subset in at least two independent experiments. Values represent mean ± S.E.M.

C Bar chart illustrating the absolute numbers of thymic populations of wildtype and *Rag1$^{wt/Cre}$ x Rosa26$^{wt/eYFP}$* mice, aged six to eight weeks old. All cell populations were similar in both strains. Analysis was carried out on at least six individual mice per subset in at least two independent experiments. Values represent mean ± S.E.M.

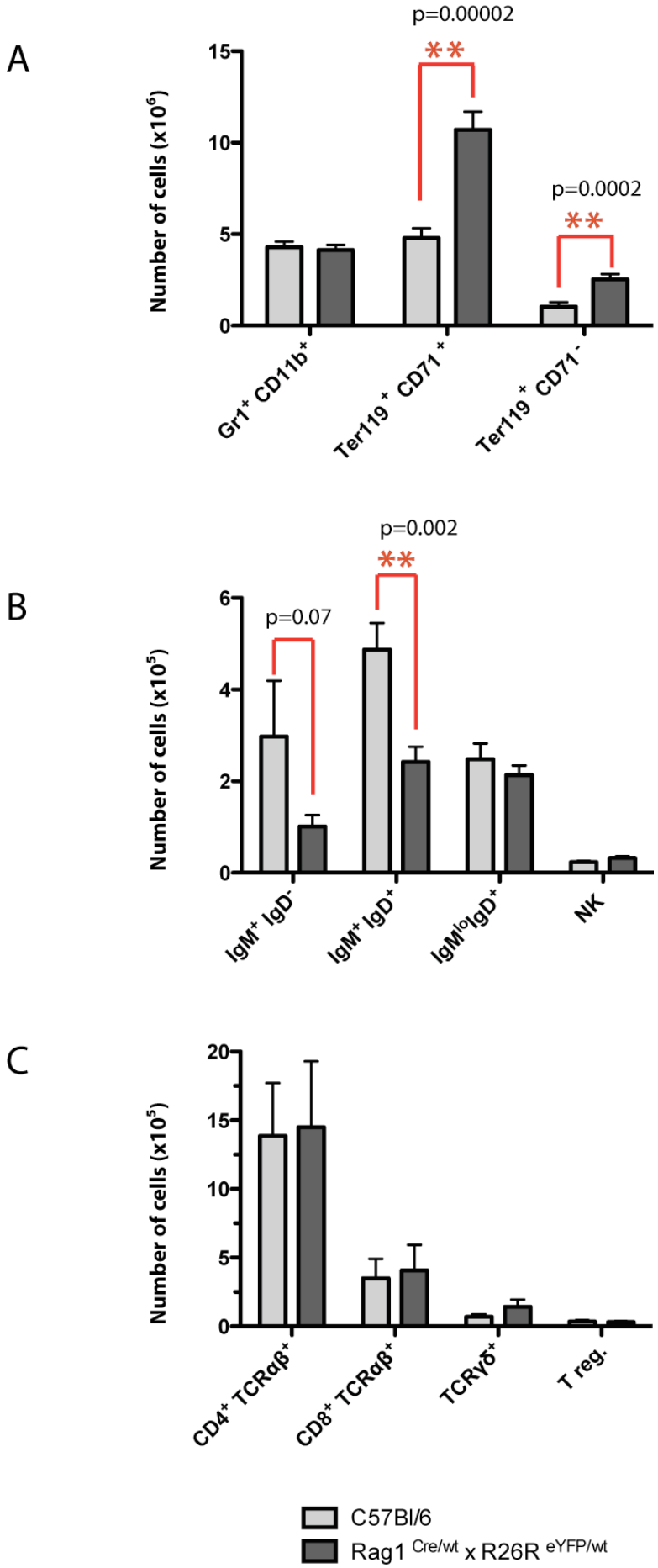
A
p=0.00002
**
p=0.0002
**
Number of cells (x10⁶)
15
10
5
0
Gr1⁺ CD11b⁺
Ter119⁺ CD71⁺
Ter119⁺ CD71⁻
B
p=0.002
**
p=0.07
Number of cells (x10⁵)
6
4
2
0
IgM⁺ IgD⁻
IgM⁺ IgD⁺
IgM^lo IgD⁺
NK
C
Number of cells (x10⁵)
20
15
10
5
0
CD4⁺ TCRαβ⁺
CD8⁺ TCRαβ⁺
TCRγδ⁺
T reg.
C57Bl/6
Rag1 Cre/wt x R26R eYFP/wt

3.7 Expression of eYFP in haematopoietic populations compared in different Cre reporter mouse strains

We next examined eYFP expression in all haematopoietic progenitor populations using different mouse strains (Figure 3.16). We compared eYFP expression in a constitutively active strain (*Rosa26*^{eYFP}), and reporter mouse strains utilising either a lymphoid specific knock-in Cre (*Rag1*$^{wt/Cre}$ *x Rosa26*$^{wt/eYFP}$*),* a lymphoid-specific transgenic Cre (*hCD2::iCre x R26R*$^{wt/eYFP}$) and a pan-haematopoietic transgenic Cre (*vav1::iCre x R26R*$^{wt/eYFP}$). A basic assumption for lineage tracing experiments is that there is constant accessibility of the reporter locus, so that chromatin modification within the locus during lymphoid development can be disregarded. We aimed to answer this by analysing the *Rosa26*^{eYFP} and *vav1::iCre x R26R*$^{wt/eYFP}$ strains. Using C57BL/6 mice as a negative control, the *Rosa26*^{eYFP} strain had virtually identical mean fluorescence intensity of eYFP in all populations, indicating that there was no change in the transcriptional and translational activity throughout differentiation. The *vav1::iCre x R26R*$^{wt/eYFP}$ reporter marked 93.4% of LT-HSCs (Figure 3.16), reflecting the fact that the *vav1* gene is turned on at the very beginning of haematopoietic development. This expression increased in ST-HSCs to 96.3% and then further to 100% by the LMPP and later stages. This was an important observation, as LMPP and CLP populations were partially negative for eYFP expression in the *Rag1*$^{wt/Cre}$ *x Rosa26*$^{wt/eYFP}$ model, but this proved that all cells downstream of HSCs had an accessible *Rosa26* locus which could undergo recombination.

We also analysed the *Rag1*$^{wt/Cre}$ *x Rosa26*$^{wt/eYFP}$ and *hCD2::iCre x R26R*$^{wt/eYFP}$ reporters to compare the onset of reporter activity during lymphoid development in the BM. Upon observation of haematopoietic progenitor populations in *Rag1*$^{wt/Cre}$ *x Rosa26*$^{wt/eYFP}$ mice, it was clear that this model provided several important advantages for the

dissection of lymphoid development. This was due to eYFP first being expressed in the ELP compartment (Figure 3.16), allowing us to visualise development from the earliest specified lymphoid pool. Lineage mapping using this reporter model revealed a segregation of eYFP in the CLP population; however the *hCD2::iCre x R26R*$^{wt/eYFP}$ reporter labelled a significantly lower frequency of CLP cells.

Figure 3.16

Expression of eYFP in all haematopoietic progenitor populations compared between different mouse strains in lineage depleted BM.

Representative histograms of all LIN^- haematopoietic progenitor populations and their frequency of eYFP expression in different mouse strains. Haematopoietic populations were identified as previously defined. C57BL/6 mice were used as a negative control and *Rosa26*^{eYFP} mice were used as a positive control for eYFP expression. Analysis of the *vav1::iCre x R26R*$^{wt/eYFP}$ strain illustrated that the *Rosa26* locus opened efficiently in all haematopoietic populations, as all subsets downstream of LT-HSCs were positive for eYFP. The *Rag1*$^{wt/Cre}$ *x Rosa26*$^{wt/eYFP}$ strain provided the best tool for investigating lymphoid development, as eYFP expression was first evident in the LMPP population. The *hCD2::iCre x R26R*$^{wt/eYFP}$ strain, which has been commonly used to observe thymocyte development, labelled only approximately 25% of CLP cells with eYFP. Analysis was carried out on at least six individual mice per subset per strain, aged six to eight weeks old, in at least three independent experiments.

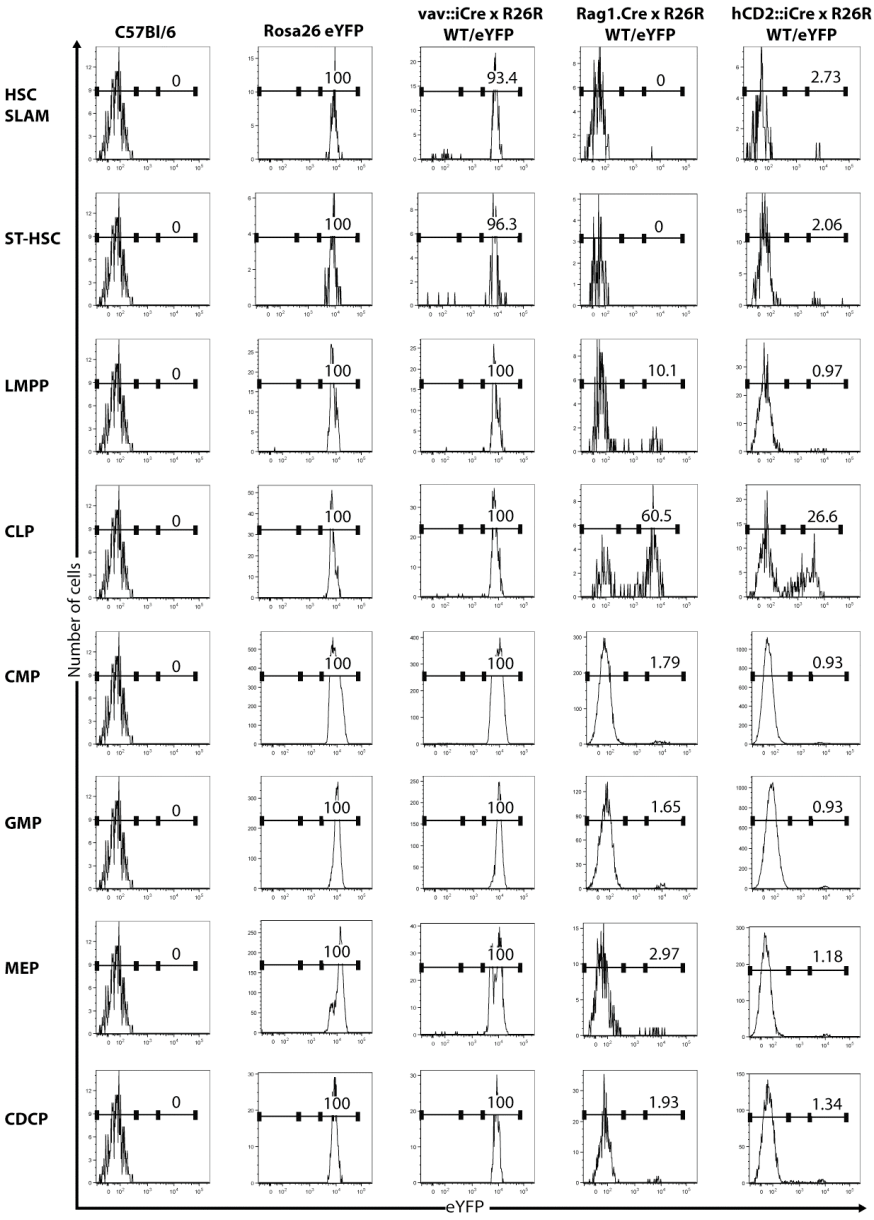
C57Bl/6
Rosa26 eYFP
vav::iCre x R26R WT/eYFP
Rag1.Cre x R26R WT/eYFP
hCD2::iCre x R26R WT/eYFP
HSC SLAM
ST-HSC
LMPP
CLP
CMP
GMP
MEP
CDCP
0
100
93.4
0
2.73
0
100
96.3
0
2.06
0
100
100
10.1
0.97
0
100
100
60.5
26.6
0
100
100
1.79
0.93
0
100
100
1.65
0.93
0
100
100
2.97
1.18
0
100
100
1.93
1.34
Number of cells
eYFP

3.8 The effect of gender and aging on haematopoiesis

After investigating intrinsic factors which could affect the expression of eYFP in BM progenitor populations, we next focused on extrinsic factors. Oestrogen is thought to exert an inhibitory effect on lymphopoiesis and it has been described that in pregnant mice, where levels of the hormone are high, early B-lineage development is suppressed (Medina et al., 1993). In terms of lymphoid progenitor cells, depletion of the LSK fraction of the BM has already been reported after oestrogen treatment (Kouro et al., 2001) which also includes the ELP population (Medina et al., 2001). Because levels of oestrogen are higher in female mice than male mice, we hypothesised that female mice would have a lower frequency and number of lymphoid progenitors than male mice. Therefore, we opted to compare the differences in pool sizes between genders. In addition, it is well established that lymphopoiesis is less efficient with age. Thymic involution and the frequency and function of pre B-cells are markedly diminished in senescent mice (Stephan et al., 1996; Stephan et al., 1998). However, very few studies on T- and B-cell progenitors combine the effect of gender and age. To address this, we analysed male and female C57BL/6 mice aged six weeks and one year old (Figure 3.17A). The frequency of cells in the LSK compartment was significantly higher in male mice (3.24 ± 0.58% of LIN^- cells) than females (1.86 ± 0.29% of LIN^- cells). However, this was not evident in the ST-HSC compartment, which exhibited a lower frequency of cells in male mice (9.81 ± 1.36% of LSK cells) than female mice (12.5 ± 0.2% of LSK cells), although this was not statistically significant. There was a noticeable difference in the frequency of cells in the LMPP population, which comprised 43.2 ± 3.05% of LSK cells in males compared to 34.1 ± 4.16% in females. In addition, the CLP population was of a statistically higher frequency of LIN^- cells in

male mice (1.95 ± 0.16%) as compared to female mice (1.43 ± 0.14%), which was also reflected in the absolute numbers (Figure 3.18B).

To combine the effect of gender with aging, progenitor populations in mice aged over one year of age were analysed. As Figure 3.17B illustrates, there was a decrease in the frequency of most compartments compared to mice aged six weeks, however there remained an overall higher frequency in cell populations of males than females. Other noticeable differences in aging alone were the size of the LSK Flk-2$^-$ CD34$^-$ pool and the IL-7Rα$^+$ Flk-2$^-$ pool. In both male and female mice, the frequency of these pools appeared to increase with age (Figure 3.17A and B). The LSK Flk-2$^-$ CD34$^-$ pool represents LT-HSCs, although the exact function of the IL-7Rα$^+$ Flk-2$^-$ compartment is unknown.

We also calculated the absolute numbers of all lymphoid progenitors per BM femur pair in male and female mice aged six weeks and one year of age. The analysis demonstrated that the absolute number of cells in males was significantly higher than females in the LMPP and CLP populations at six weeks old (Figure 3.18A and B). In contrast there was no significant difference in the number of myeloid progenitors or thymic progenitors between genders (Figure 3.18C and D). In aged mice, the number of cells in male mice was significantly higher not only in LMPP and CLP populations, but also in the LT-HSC, ST-HSC, CMP, GMP, ETP, DN2 and DN3 compartments than in females (Figure 3.19A-D). The number of LT-HSCs increased dramatically in male mice with age from $0.08 \times 10^4 \pm 0.02 \times 10^4$ at six weeks in comparison to $0.193 \times 10^4 \pm 0.03 \times 10^4$ at one year of age; however there was only a slight increase in the number of LT-HSCs in female mice ($0.03 \times 10^4 \pm 0.008 \times 10^4$ at 6 weeks and $0.04 \times 10^4 \pm 0.02 \times 10^4$ at one year of age). In comparison, the number of ST-HSC cells in male and female mice did not change noticeably with age. However, the number of CMP and GMP populations

did increase with age. This could be the reason for the observed increase in LT-HSCs, as more of these cells may have been required to differentiate into ST-HSCs and then give rise to myeloid progenitors. Alternatively, the rise in LT-HSCs could be due to an increase in self-renewing cells. The number of CMP cells increased in male mice from $4.13 \times 10^4 \pm 0.73 \times 10^4$ (Figure 3.18C) to $10.36 \times 10^4 \pm 0.83 \times 10^4$ in aged mice (Figure 3.19C), and from $1.84 \times 10^4 \pm 0.23 \times 10^4$ to $2.65 \times 10^4 \pm 0.36 \times 10^4$ in the GMP compartment. This increase in myeloid progenitor numbers was also reflected in aged female mice although the numbers were still significantly lower than that in aged male mice (Figure 3.19C). There was also a minor increase in the number of MEP cells in male and female mice with age. These results indicated an expansion of myeloid progenitors and conversely a contraction of lymphoid progenitors, but with no impact on the ST-HSC number.

In the thymus, interestingly there was a minor increase in the number of ETPs in aged male mice, but a decrease in aged female mice. The number of male ETPs increased from $0.4 \times 10^4 \pm 0.13 \times 10^4$ in mice aged six weeks (Figure 3.18B) to $0.62 \times 10^4 \pm 0.17 \times 10^4$ in mice aged one year of age (Figure 3.19B). In female mice however, the number decreased from $0.58 \times 10^4 \pm 0.2 \times 10^4$ to $0.21 \times 10^4 \pm 0.08 \times 10^4$. Given that the number of lymphoid progenitors in the BM decreased in both genders with age, it would be expected that the number of ETPs would also decrease with age. However, this was not the case in male mice. Throughout thymic development, the DN2 and DN3 populations also increased in size in male mice with age, but decreased in female mice with age. However in the DN4 population there were a higher number of cells in aged female mice ($119.29 \times 10^4 \pm 56.98 \times 10^4$; Figure 3.19D) than in male mice ($72.15 \times 10^4 \pm 25.39 \times 10^4$; Figure 3.19D), an inversion of what was observed at six weeks of age. This suggests that in aged male mice the proliferation from the DN3 to the DN4 population

was lower than the proliferation observed in aged female mice. In addition, this also suggests that the DN4 population is not suppressed by female hormones, whereas the ETP to DN3 populations may well be.

Figure 3.17

The effect of gender and aging on stem cell and lymphoid progenitor populations of lineage depleted BM.

A Representative FACS plots of ST-HSC, LMPP and CLP populations, compared between male and female C57BL/6 mice, aged six weeks old. All subpopulations illustrated a higher frequency of LIN^- cells in male mice than in female mice. Analysis was carried out on eight independent male experiments and three independent female experiments.

B Representative FACS plots of ST-HSC, LMPP and CLP populations, compared between male and female C57BL/6 mice, aged one year old. All populations had a lower relative frequency than in mice aged six weeks of age, however the frequencies were still higher in male mice than in female mice at one year of age. Analysis was carried out on six individual mice per gender from two independent experiments.


A
MALE
FEMALE
[LIN⁻]
3.3
49.1
7.41
2.07
1.8
28
12.4
1.29
c-kit
Sca-1
Flk-2
CD34
IL-7Rα
B
MALE
FEMALE
[LIN⁻]
1.74
23.1
22.4
0.90
1.38
15.2
21.6
0.47
c-kit
Sca-1
Flk-2
CD34
IL-7Rα

Figure 3.18

Absolute cell numbers of haematopoietic progenitor populations compared between male and female mice, aged six weeks of age.

A Histogram illustrating the absolute number of LT-HSC, ST-HSC and LMPP populations in the total BM of male and female C57BL/6 mice aged six weeks of age. There were a significantly higher number of LMPP cells in male mice than in female mice. Values represent mean ± S.E.M.

B Histogram illustrating the absolute number of LMPP, CLP and ETP populations in the BM and thymus of male and female C57BL/6 mice aged six weeks of age. There were a significantly higher number of LMPP and CLP cells in male mice compared to female mice. Values represent mean ± S.E.M.

C Histogram illustrating the absolute number of myeloid progenitor populations in the BM of male and female C57BL/6 mice aged six weeks of age. There was no significant difference in the number of myeloid progenitor cells between genders. Values represent mean ± S.E.M.

D Histogram illustrating the absolute number of thymocyte populations in the thymus of male and female C57BL/6 mice aged six weeks of age. There was no change in the number of DN2, DN3 or DN4 populations between male and female mice. Values represent mean ± S.E.M.

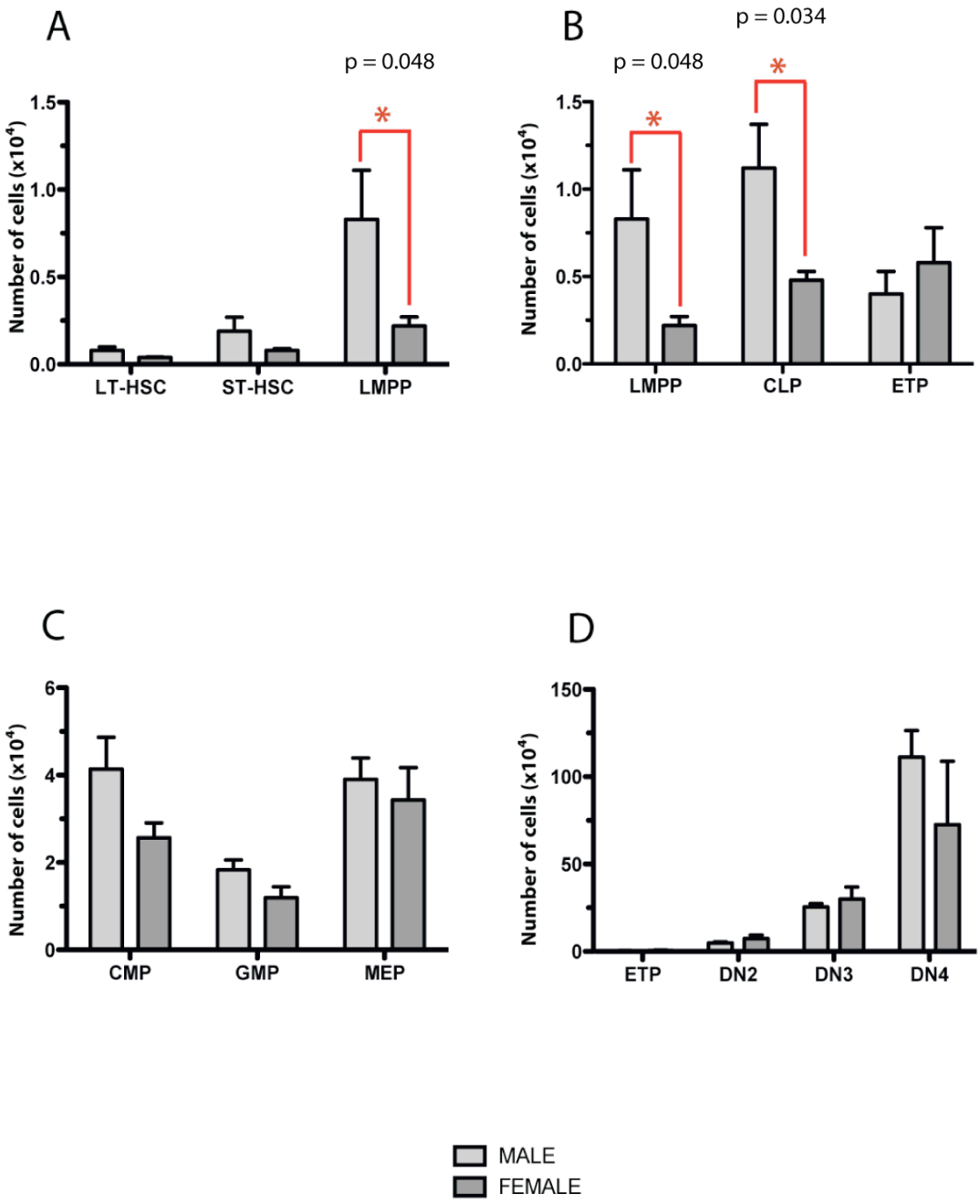
A
p = 0.048
*
Number of cells (x10⁴)
1.5
1.0
0.5
0.0
LT-HSC
ST-HSC
LMPP
B
p = 0.034
p = 0.048
*
*
Number of cells (x10⁴)
1.5
1.0
0.5
0.0
LMPP
CLP
ETP
C
Number of cells (x10⁴)
6
4
2
0
CMP
GMP
MEP
D
Number of cells (x10⁴)
150
100
50
0
ETP
DN2
DN3
DN4
MALE
FEMALE

Figure 3.19

Absolute cell numbers of haematopoietic progenitor populations compared between male and female mice, aged one year of age.

A Histogram illustrating the absolute number of LT-HSC, ST-HSC and LMPP populations in the total BM of male and female C57BL/6 mice aged one year of age. There were a significantly higher number of all subsets in male mice than in female mice after aging. Values represent mean ± S.E.M.

B Histogram illustrating the absolute number of LMPP, CLP and ETP populations in the BM and thymus of male and female C57BL/6 mice aged one year of age. There were a significantly higher number of LMPP, CLP and ETP cells in male mice compared to female mice. Values represent mean ± S.E.M.

C Histogram illustrating the absolute number of myeloid progenitor populations in the BM of male and female C57BL/6 mice aged one year of age. There were a higher number of CMP and GMP cells in males than in females in aged mice. However the number of MEPs was similar between genders. Values represent mean ± S.E.M.

D Histogram illustrating the absolute number of thymocyte populations in the thymus of male and female C57BL/6 mice aged one year of age. There a significantly higher number of ETP, DN2 and DN3 cells in aged male mice compared to aged female mice. Values represent mean ± S.E.M.

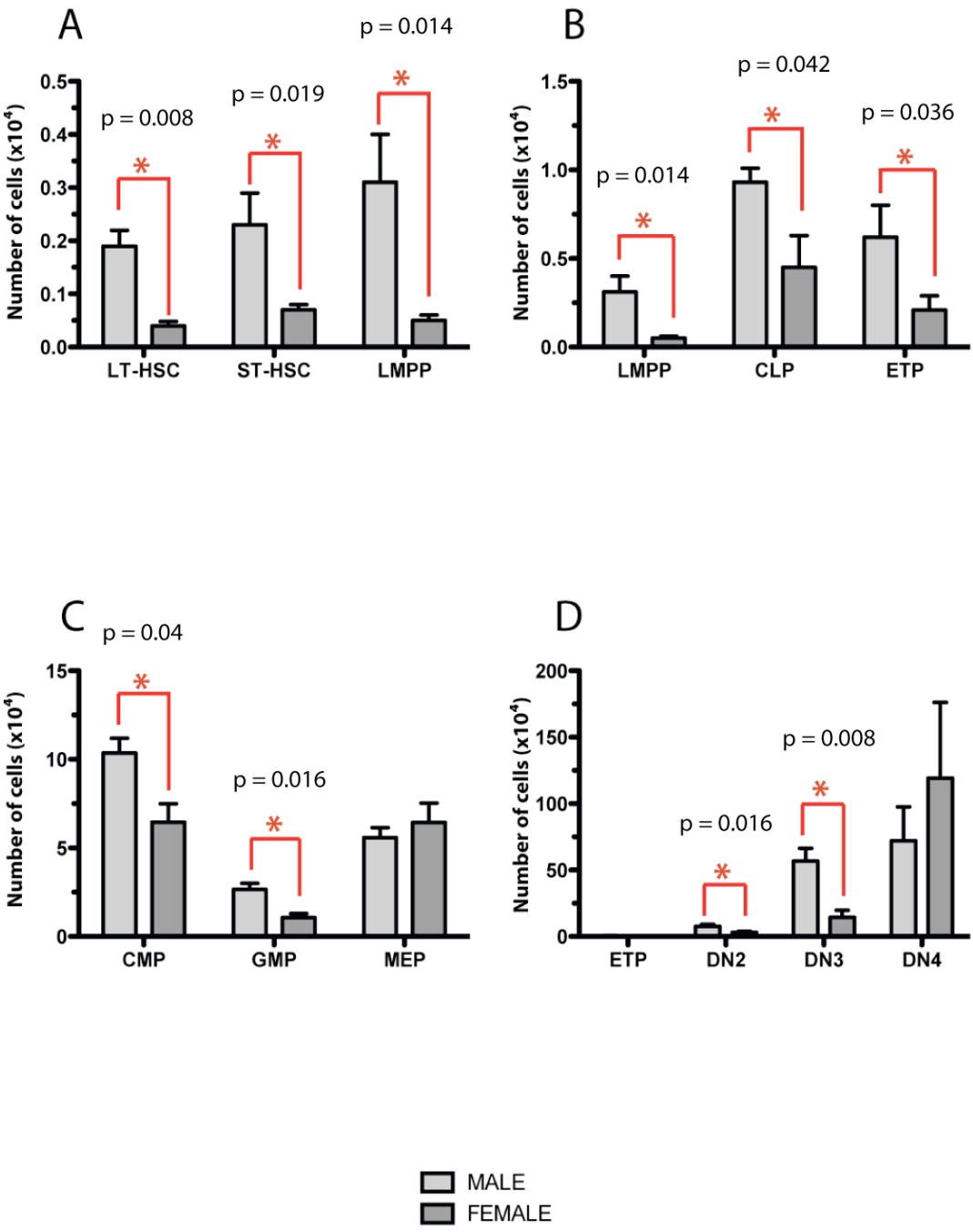
A
p = 0.008
p = 0.019
p = 0.014
Number of cells (x10⁴)
0.5
0.4
0.3
0.2
0.1
0.0
LT-HSC
ST-HSC
LMPP
B
p = 0.014
p = 0.042
p = 0.036
Number of cells (x10⁴)
1.5
1.0
0.5
0.0
LMPP
CLP
ETP
C
p = 0.04
p = 0.016
Number of cells (x10⁴)
15
10
5
0
CMP
GMP
MEP
D
p = 0.016
p = 0.008
Number of cells (x10⁴)
200
150
100
50
0
ETP
DN2
DN3
DN4
MALE
FEMALE

We also wanted to investigate whether gender and age had any effect on the $eYFP^+$ CLP, $eYFP^-$ CLP and ELP populations which were characterised using the *Rag1*$^{wt/Cre}$ *x* *Rosa26*$^{wt/eYFP}$ mice. As presented in Figure 3.20A, there was a higher frequency of $eYFP^+$ CLP cells in males (38.8%) than in females (18.5%), and a lower frequency of $eYFP^-$ CLP cells. However, the absolute number of $eYFP^-$ CLP cells was not significantly different between male and female mice (Figure 3.20B). The number of $eYFP^+$ CLP cells was significantly higher in males ($4.3 \times 10^3 \pm 0.6 \times 10^3$) than in females ($1.3 \times 10^3 \pm 0.7 \times 10^3$), possibly indicating a population which may be suppressed by oestrogen (Figure 3.20B). In addition, Figure 3.20C illustrates that the number of cells in the ELP population was also significantly higher in male mice ($0.09 \times 10^3 \pm 0.04 \times 10^3$) than female mice ($0.008 \times 10^3 \pm 0.004 \times 10^3$).

Figure 3.20

The relative frequency and number of ELP, CLP eYFP$^-$ and CLP eYFP$^+$ populations in aged male and female mice.

A Representative FACS plots of CLP cells in *Rag1$^{wt/Cre}$ x Rosa26$^{wt/eYFP}$* male and female mice aged one year old. LIN$^-$ CLP cells were analysed for the frequency of eYFP expression. Three individual mice were analysed.

B Bar chart illustrating the absolute number of CLP eYFP$^-$, CLP eYFP^{int} and CLP eYFP$^+$ populations in *Rag1$^{wt/Cre}$ x Rosa26$^{wt/eYFP}$* male and female mice, aged one year old. There were no significant differences in the number of CLP eYFP$^-$ or CLP eYFP^{int}; however male mice exhibited a significantly higher number of CLP eYFP$^+$ cells. Three individual mice were analysed. Values represent mean ± S.E.M.

C Bar chart illustrating the absolute number of cells in the ELP population utilising *Rag1$^{wt/Cre}$ x Rosa26$^{wt/eYFP}$* male and female mice aged one year old. There were a significantly higher number of ELP cells in aged male mice compared to aged female mice. Three individual mice were analysed. Values represent mean ± S.E.M.

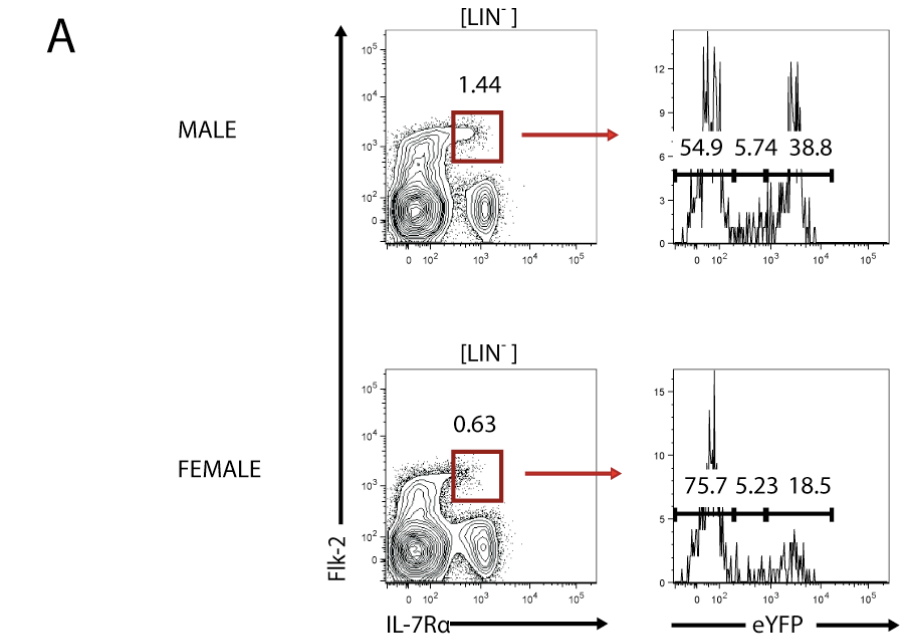
A
MALE
FEMALE
[LIN-]
1.44
54.9 5.74 38.8
0.63
75.7 5.23 18.5
Flk-2
IL-7Rα
eYFP

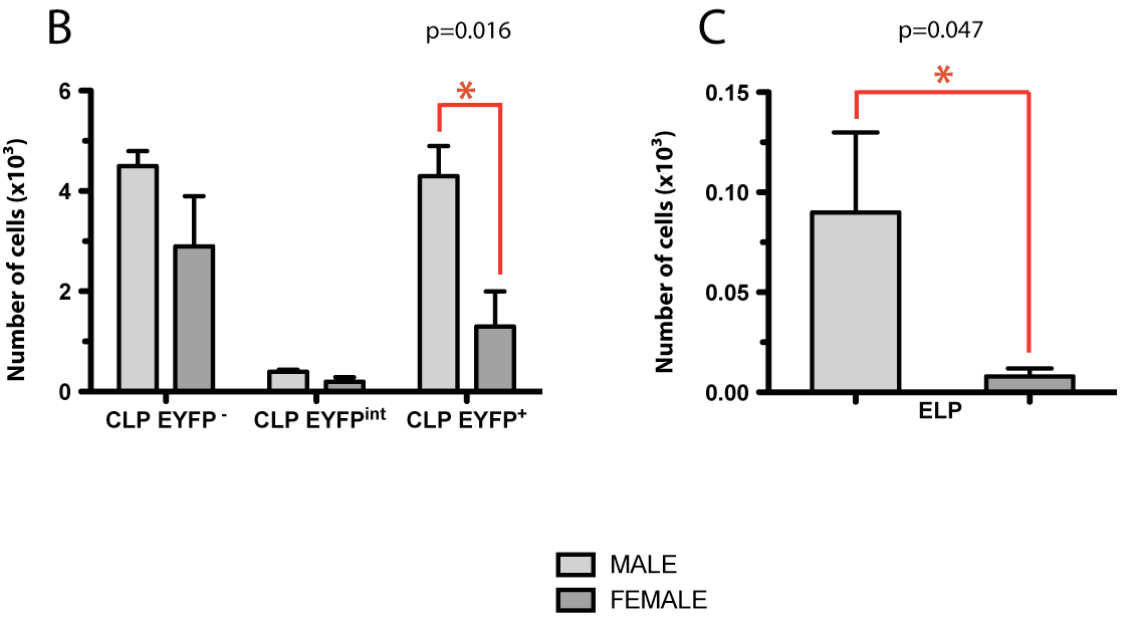
B
p=0.016
Number of cells (x10³)
CLP EYFP-
CLP EYFPint
CLP EYFP+
C
p=0.047
ELP
MALE
FEMALE

3.9 Expression of GATA-family transcription factors in haematopoietic progenitor populations

Aside from exploring which factors affected the relative size and composition of haematopoietic progenitor subsets, we also aimed to determine the gene expression of these populations. To clarify which BM progenitor cells were definitive TSCs, we analysed the expression of *Gata1 to 3* transcription factors in these populations, one set of transcription factors which have been implied in haematopoietic development. In order to assess the relative gene expression in lymphoid progenitor populations, all subsets were isolated and subject to qRT-PCR. As illustrated in Figure 3.21A, expression of *Gata1* was predominantly expressed in the MEP population, with a lower amount of expression in the GMP and CMP populations. *Gata1* expression was absent in HSC, LMPP and CLP subsets, demonstrating that *Gata1* is a transcription factor expressed exclusively in the myelo-erythroid lineage. Similarly *Gata2* was also expressed in all myelo-erythroid progenitor populations (Figure 3.21B), however the highest expression of *Gata2* was observed in LMPPs and there was a substantial amount of expression in HSCs. *Gata1* and *Gata2* expression was not assessed in thymic populations as these transcription factors are thought to be mainly involved in specification of the myelo-erythroid lineage and most cells in the thymus are already specified to the T-cell lineage. In contrast to *Gata1* and *Gata2*, the transcription factor *Gata3* was expressed mainly in the lymphoid lineage. The highest expression of *Gata3* was observed in thymic CD4 SP T-cells, with lower amounts of expression in HSCs, ETPs, DN2, DN3 and DN4 subsets. Residual expression was found in LMPPs, CLPs and CD8 SP populations (Figure 3.21C). Due to the unexpected finding of relatively high levels of *Gata3* mRNA in HSCs, but not in LMPPs and CLPs, this might suggest that the GATA-3 protein was not translated until HSCs developed into LMPPs, ELPs

and CLPs. Therefore, we next looked at the intracellular (IC) GATA-3 protein levels in lymphoid progenitor cells.

Figure 3.21

Expression of GATA1-3 transcription factors in all haematopoietic progenitor populations of the BM.

Sorted cell populations from six to eight week old C57BL/6 mice were subjected to RNA extraction, quality control and reverse transcription as described in materials and methods. 500 cell equivalent cDNA from each population was assessed in triplicates for each target gene, using the Qiagen primer/probe detection system. Arbp was used as a control to which all expression values were normalised. Values represent mean ± S.D. from at least three independent preparations of haematopoietic progenitors.

A Graph illustrating the level of expression of the transcription factor *Gata1* in all stem cell, lymphoid progenitor and myelo-erythroid progenitor populations. Expression was evident in CMP, GMP and MEP populations.

B Graph illustrating the level of expression of the transcription factor *Gata2* in all stem cell, lymphoid progenitor and myelo-erythroid progenitor populations. Expression was evident in all populations except the CLP.

C Graph illustrating the level of expression of the transcription factor *Gata3* in all stem cell, lymphoid progenitor, myelo-erythroid progenitor and thymic populations. The highest expression of *Gata3* was observed in $CD4^+$ T-cells and HSCs. There was virtually no expression in myelo-erythroid progenitor populations, but there was evidence of residual expression in LMPP, CLP and CD8 populations.

A

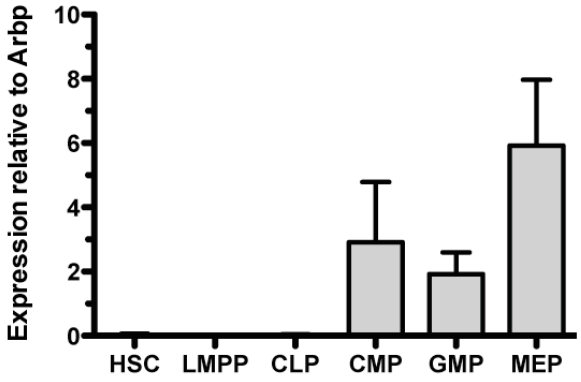
Expression relative to Arbp
10
8
6
4
2
0
HSC
LMPP
CLP
CMP
GMP
MEP

B

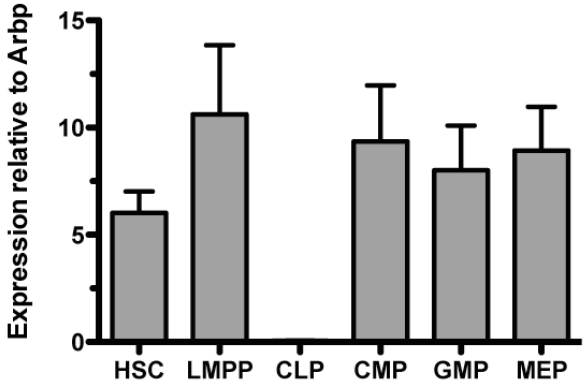
Expression relative to Arbp
15
10
5
0
HSC
LMPP
CLP
CMP
GMP
MEP

C

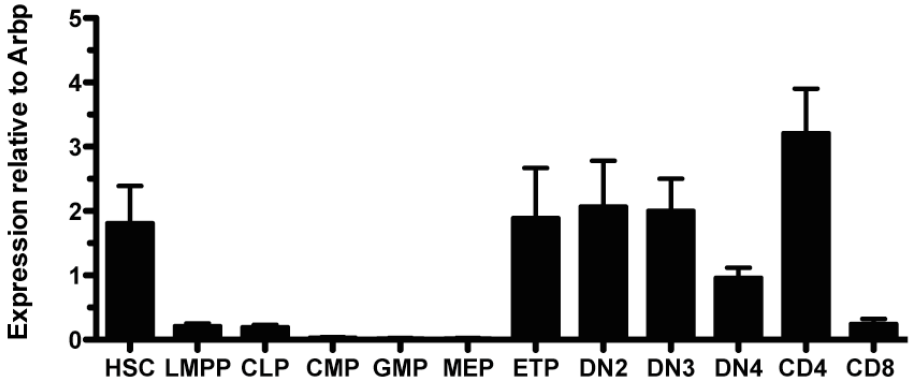
Expression relative to Arbp
5
4
3
2
1
0
HSC
LMPP
CLP
CMP
GMP
MEP
ETP
DN2
DN3
DN4
CD4
CD8

Due to high *Gata3* mRNA levels being present in BM HSCs and thymic lymphoid cells, we next set out to determine the GATA-3 protein levels in BM and thymic lymphoid progenitors. Seeing as though *Gata3* is expressed in large amounts during CD4 lineage specification (Hernandez-Hoyos et al., 2003), we first analysed GATA-3 protein levels in the thymic CD4 population and used this result as a positive control. As shown in Figure 3.22A, the $CD4^+$ TCR^{hi} population expressed high levels of the GATA-3 protein as compared to the isotype control and the $CD8^+$ TCR^{hi} population. However, there was evidence for some GATA-3 protein expression in the DP compartment. This was expected, as cells develop from the DP pool into CD4 SP cells, therefore GATA-3 would be expressed in CD4 committed DP cells. The residual presence of GATA-3 protein in the $CD8^+$ TCR^{hi} population can be explained by the fact that these cells are originating from a population of cells which had previously expressed *Gata3*, therefore it is likely that some protein will still be present inside these cells. In the DN compartments of the thymus, similar to mRNA levels, the highest expression of GATA-3 was observed in the DN2 and DN3 compartments (Figure 3.22B). GATA-3 is thought to play an important role during β-selection at the DN3 stage of development (Hendriks et al., 1999), and these results are in agreement with this model. Slightly less protein levels were present in the ETP population and the lowest expression was illustrated in the DN4 population. However, none of the populations were completely negative for GATA-3 protein expression.

We next analysed GATA-3 protein levels in BM lymphoid progenitor subsets (Figure 3.22C). The majority of evidence in the literature supports a model whereby T-cell production is initiated from ELPs or CLPs, therefore we focused our studies on these populations. Taking into consideration that lineage mapping experiments had indicated heterogeneity in the CLP population, this subset was divided into $eYFP^+$ and $eYFP^-$

populations in order to address whether the expression of GATA-3 was different. As indicated by the mRNA levels, the protein levels of GATA-3 in these populations were minor. Using GATA-3 expression as a method of identifying T-cell progenitors of the BM, this data suggests that ELP and CLPs have equal opportunity to develop into T-cells. To further address which cell populations are able to give rise to T-cells *in vivo*, functional studies of these subsets would be required.

Figure 3.22

GATA-3 intracellular protein levels in lymphoid cell populations of the BM and thymus.

A Representative FACS plot illustrating GATA-3 IC protein levels in CD4 SP, CD8 SP and DP thymocytes of *Rag1*$^{wt/Cre}$ *x Rosa26*$^{wt/eYFP}$ mice. CD4 SP and CD8 SP cells were classified as TCR^{hi} and assessed for GATA-3 protein levels. All GATA-3 levels were compared to an IgG_{2b} isotype control. Thymi were pooled and processed together. Data are representative for one from six individual experiments.

B Representative FACS plot illustrating GATA-3 IC protein levels in undepleted thymic DN1-4 populations of *Rag1*$^{wt/Cre}$ *x Rosa26*$^{wt/eYFP}$ mice. Cells were first analysed as LIN$^-$ and DN populations were identified based on CD44 and CD25 expression. The DN1 population was further characterised by c-kit expression to identify the ETP population. All GATA-3 levels were compared to an IgG_{2b} isotype control. Thymi were pooled and processed together. Data are representative for one from three experiments.

C Representative FACS plots illustrating GATA-3 IC protein levels in lineage depleted ELP and CLP BM populations of *Rag1*$^{wt/Cre}$ *x Rosa26*$^{wt/eYFP}$ mice. BM was FACS-purified into ELP, CLP eYFP$^-$ and CLP eYFP$^+$ populations (see Figure 3.11 A and B). GATA-3 protein levels were then analysed. All GATA-3 levels were compared to an IgG_{2b} isotype control. Data represent one experiment.

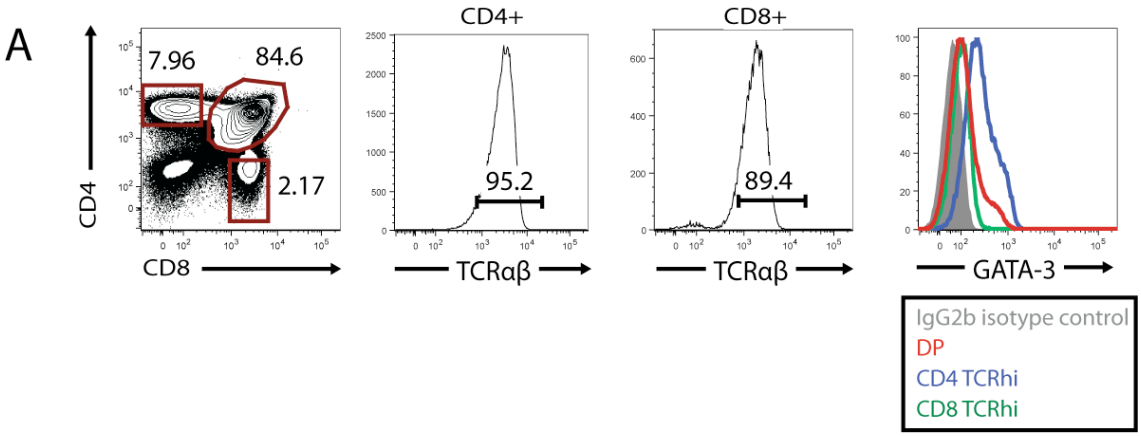
A
CD4
CD8
7.96
84.6
2.17
CD4+
95.2
TCRαβ
CD8+
89.4
TCRαβ
GATA-3
IgG2b isotype control
DP
CD4 TCRhi
CD8 TCRhi

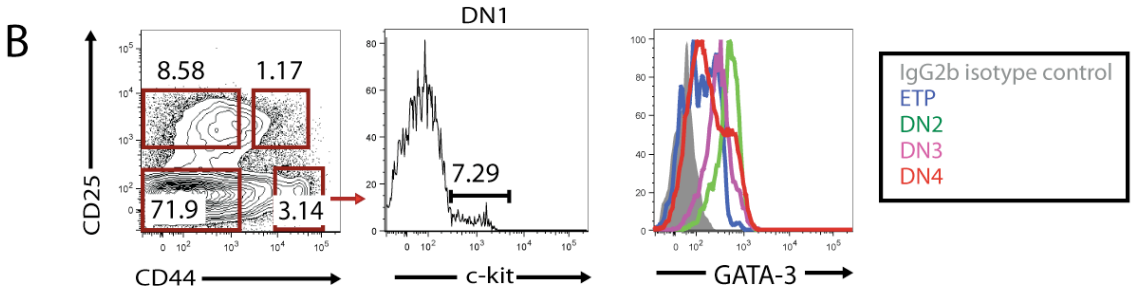
B
CD25
CD44
8.58
1.17
71.9
3.14
DN1
7.29
c-kit
GATA-3
IgG2b isotype control
ETP
DN2
DN3
DN4

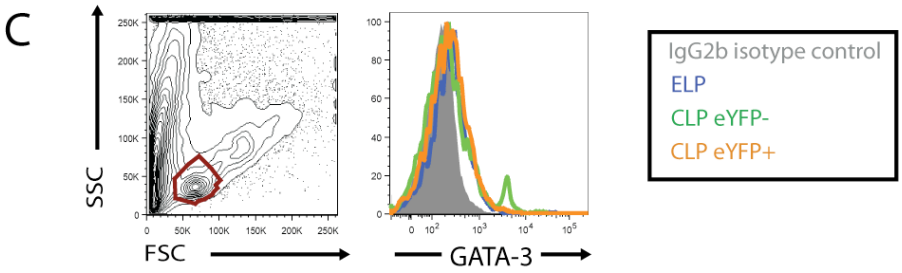
C
SSC
FSC
GATA-3
IgG2b isotype control
ELP
CLP eYFP-
CLP eYFP+

3.10 Discussion

The specific path by which lymphoid progenitors develop into mature T- and B-cells still remains unclear. It has been argued that the CLP is the main cell type giving rise to T-cells, however there has been substantial evidence arguing against this theory. The CLP population, firstly isolated and characterised by Kondo and colleagues (Kondo et al., 1997), was used to competitively reconstitute lethally irradiated Ly5.1 mice with 2×10^3 $Ly5.2^+$ CLPs and 2×10^5 $Ly5.1^+$ BM cells, resulting in only T- and B-cell reconstitution and without any myeloid reconstitution (Kondo et al., 1997). The CLP population was also reconstituted in sub-lethally irradiated *Rag2*-null mice, but still only T- and B-cells could be detected. To test for myeloid potential *in vitro*, CLPs were placed in methylcellulose culture which promotes myeloid colony formation, but myeloid colonies were not detectable from CLPs. Therefore, based on this report, it seemed in the first instance that this lymphoid-restricted progenitor was the main cell type giving rise to mature lymphocytes which was absent of any myeloid potential.

However, numerous reports have questioned the concept that the CLP is the main pre-thymic progenitor. In one of these reports (Allman et al., 2003), it was revealed that in *Ikaros* mutant mice there was a complete lack of CLPs and subsequent B-lineage development, but ongoing thymopoiesis. This suggested that the CLP population could not be the only source of thymic progenitors and may be the main progenitor for B-cells. In another study (Bell and Bhandoola, 2008), ETPs were isolated, placed on OP9 stromal cells and gave rise to cells that expressed the myeloid marker CD11b. These cells also expressed the monocyte/macrophage markers MCSF-R, F4/80 and Gr1. Upon microscopic examination, these cells also resembled cells with monocytic morphology and were capable of phagocytosis. The authors deduced that ETPs possessed myeloid potential, as well as T, NK and DC potentials and could not arise

from lymphoid restricted CLPs alone. Instead the authors suggested derivation from earlier lymphoid subsets such as ELPs or LMPPs. These findings were supported by Wada et al., (Wada et al., 2008) who cultured DN1, DN2 and DN3 cells from adult thymus on PA6 or Tst-4/DLL1 cells which support the generation of myeloid cells. They found that $CD11b^{+}$ cells were generated in these cultures, which also expressed F4/80 and which were capable of phagocytosis. On the other hand, Serwold and colleagues (Serwold et al., 2009) reported that because a lymphoid-restricted progenitor was not used as a control in these *in vitro* assays, the myeloid cells observed could have represented an artefact in the culture system. Therefore, in order to identify which cells had most thymic progenitor activity, Serwold et al. compared the kinetics of thymopoiesis between CLPs and MPPs. The results showed that seven days after transplantation, donor thymic T-lineage chimerism was evident in all mice transplanted with CLPs and peaked at day 21 when most cells were at the DP stage. In mice transplanted with MPPs however, T-lineage reconstitution was still evident at the DN stage at day 21 and continued to rise up until day 28, when DN thymocyte production was still ongoing. The authors deduced that CLPs gave rise to a single wave of thymopoiesis, whereas MPPs proliferated in the BM and generated CLPs before giving rise to thymocytes. Considering that DN production was ongoing after MPP transplantation, this data could have indicated that MPP cells proliferated more than CLPs before seeding the thymus and therefore a larger number of cells gave rise to ETPs, which could explain why this group observed DN1 production for longer. In addition, if MPP cells gave rise to CLP cells before entering the thymus, then it would be expected that the single wave of thymopoiesis, which was observed after CLP transplantation, would take place. However, this was not the case. Therefore it is possible that cells other than the CLP population can give rise to ETPs. Indeed Lai and

Kondo (Lai and Kondo, 2007) identified Flk-2^{hi} VCAM-1^{-} LMPPs which were positive for the chemokine receptor CCR9 and which exhibited similar characteristics in cell surface phenotype, gene expression patterns and differentiation potentials to ETPs.

We attempted to further clarify the source of ETPs by utilising a lineage mapping system whereby Cre recombinase expression was driven by the *Rag1* promoter. This identified an 'ELP analogue' which we hoped would mark the reported ELP population. Igarashi and colleagues (Igarashi et al., 2002) identified the ELP as approximately 3% to 5% of the LSK Flk-2^{+} $CD27^{+}$ fraction and our 'ELP analogue' marked 5.94% of LSK Flk-2^{+} cells. In $Rag1^{GFP}$ mice, GFP expression was absent in all stem cells and myelo-erythroid progenitor populations, but increased significantly in the CLP population. In comparison to our results, we observed a virtual absence of eYFP expression in cells prior to the ELP stage and in all myelo-erythroid progenitor cells also. Therefore, the $Rag1^{wt/Cre}$ *x* $Rosa26^{wt/eYFP}$ strain was able to identify an accurate 'ELP analogue' which phenotypically was identical to the ELP population. We used this reporter model to assess the relationship between lymphoid progenitor populations prior to their development into mature cells and to monitor the development of the 'ELP analogue'. Expression of eYFP was analysed in all haematopoietic lineages from HSCs through to fully functional mature cell types in BM, spleen and thymus.

In the spleen and BM, the frequency of eYFP expression in mature B- and T-cells was virtually 100%. This result was expected as B-cell receptor (BCR) and T-cell receptor (TCR) rearrangement, which are cell processes required for B- and T-cell maturation, utilise the *Rag1* and *Rag2* genes, so these cells would have passed via at least two stages of recombinase activity. In addition, NK T-cells also possess a functional TCR, explaining the complete expression of eYFP in this subset.

Splenic NK, DC and pDC cell populations exhibited similar frequencies of $eYFP^+$ cells (20–30%). This data demonstrate heterogeneity within these pools and might indicate development from more than one origin. The fraction of cells which were positive for eYFP could have originated from the ELP population or a later progenitor pool such as the CLP which had partially acquired eYFP expression. In addition, splenic NK development may have occurred via the thymus whereby more than 75% of ETPs were positive for eYFP expression. Michie et al., (Michie et al., 2000) described a bipotent T/NK progenitor in the mouse foetal thymus which was defined by NK1.1 and c-kit expression and which could efficiently generate NK-cells in foetal thymic organ culture. It is possible that a cell population similar to this one described is present in the adult mouse thymus. In addition, there have been reports that GATA-3 is important in NK-cell development. Splenic NK-cells in *Gata3*-null mice show reduced production of IFNγ (Vosshenrich et al., 2006), therefore NK-cells could develop from progenitors expressing high levels of GATA-3, such as ETPs. Furthermore, a thymic developmental pathway for the production of NK-cells was identified (Vosshenrich et al., 2006) which was characterized by GATA-3 and IL-7Rα expression, indicating a lymphoid based pathway for the development of NK-cells which may have expressed *Rag1*. Alternatively, $eYFP^+$ NK-cells may have developed from $eYFP^+$ pre-pro B-cells which were $CD19^-$ but $NK1.1^+$ and which have been shown to give rise to NK effector cells in the presence of IL-2 and IL-15 (Balciunaite et al., 2005).

The development of $eYFP^-$ NK-cells may have occurred extrathymically. Indeed extrathymic NK development has been demonstrated during the absence of *Notch1* where the earliest thymic progenitors were absent, but NK-cells still remained (Radtke et al., 1999). Also, athymic mice display an adequate number of NK-cells. Alternatively, the cells which were negative for eYFP expression may be due to either

inadequate Cre protein levels in cells expressing low levels of *Rag1*, which in turn would not permit eYFP expression from the *Rosa26* locus, or development from progenitor subsets which did not activate *Rag1*. Williams and co-workers (Williams et al., 1997) reported the differentiation of NK-cells *in vitro* from HSCs, a cell population which was negative for eYFP expression in our reporter model.

Similarly to NK-cells, both lymphoid-derived and myeloid-derived DCs only partially expressed eYFP. Considering that pDCs and cDCs are thought to arise from the CDCP progenitor, which was virtually negative for eYFP expression, development of $eYFP^+$ cells must have been due to further differentiation of the CDCP into $eYFP^+$ precursors or from alternative progenitor pools. Similar to the development of NK-cells, development of the $eYFP^+$ lymphoid-derived and myeloid-derived DCs may have occurred from $eYFP^+$ progenitors in the BM or from $eYFP^+$ intrathymic progenitors. The lymphoid-derived DCs have been considered to be related to the T-cell lineage due to their phenotype (Wu et al., 1996). Indeed, DC potentials in early thymocyte subsets have been reported by Shen et al., (Shen et al., 2003). Moreover, $eYFP^+$ pDC and cDC cells may have originated from $eYFP^+$ pre-pro B-cells, as these cells have been reported to contain $CD4^+$, $Ly6C^+$ DC precursors capable of giving rise to cDCs and pDCs (Nakano et al., 2001; Miller et al., 2002). An alternative explanation for both $eYFP^+$ and $eYFP^-$ cDC development is from the CLP or CMP progenitor pools. Manz et al., (Manz et al., 2001) compared the DC developmental potentials of BM progenitors and concluded that CLPs could give rise to $CD8\alpha^+$ and $CD8\alpha^-$ thymic DCs, whereas the CMP developed into both types of splenic cDC populations.

As expected due to lack of *Rag1* expression in the myelo-erythroid lineage, all splenic and BM myelo-erythroid cells exhibited low frequencies of $eYFP^+$ cells, except MHC class II expressing splenic myeloid cells. This subset of cells had a significantly higher

frequency of eYFP$^+$ cells compared to MHC class II negative myelo-erythroid progenitors. Due to MHC class II expression, these cells have the functional ability to act as antigen presenting cells. It is not clear whether these cells are activated macrophages which develop via the myeloid lineage or whether they represent DC 'monocyte' progenitors (Geissman et al., 2010). In any case, phagocytosed eYFP could be ingested by both DCs and macrophages causing quenching of the eYFP signal, which would explain the observed positive and intermediate levels of expression. During apoptosis of these eYFP$^+$ cells, particle internalisation would have been initiated by the interaction of specific receptors on the surface of the phagocyte with ligands on the surface of eYFP$^+$ cells. After internalisation of the particle, the phagosome would have matured by fusing with late endosomes and ultimately lysosomes to form a phagolysosome (Adrerem and Underhill, 1999).

A similar reporter model has recently been published whereby Cre recombinase was knocked into the *Rag1* locus in order to identify the ELP population, however this group used a tandem dimer red fluorescent protein (dtRFP) within the *Rosa26* locus instead of eYFP (Welner et al., 2009). This reporter model also marked over 95% of mature B- and T-cells, but no more than 3% of granulocytes, identical to our results.

In the BM, eYFP expression in all stem cells, myelo-erythroid progenitors and the CDCP population was virtually absent. However, in the LMPP compartment, expression of eYFP was significantly higher than in other progenitor populations, which suggested that the eYFP$^+$ fraction of the LSK Flk-2$^+$ LMPP pool represented ELPs. In addition, the frequency of eYFP$^+$ LMPPs was almost identical to the corresponding fraction of ELPs identified by Igarishi et al., (2002). This clearly demonstrated that the *Rag1*$^{wt/Cre}$ *x Rosa26*$^{wt/eYFP}$ model could be used to identify a similar phenotype of ELP cells with good accuracy. Furthermore, as compared to other lymphoid-specific Cre

reporter mice, the *Rag1*$^{wt/Cre}$ *x Rosa26*$^{wt/eYFP}$ model proved to be expressed significantly earlier than in the corresponding cross with *huCD2::iCre.*

One population in which there was a large frequency of eYFP^{+} cells was the CLP pool. This population exhibited an expression pattern allowing the isolation of eYFP^{-}, eYFP^{int} and eYFP^{+} cells, which could help in defining precursor-product relationships. Seeing as though the CLP is thought to be the cell population via which the ELP develops, this result was unexpected as only half of the cells expressed eYFP. This data therefore clearly demonstrated that the CLP pool is heterogeneous, with development occurring not only via the ELP, but also from an eYFP^{-} population such as LMPPs. In order to determine that we had identified two separate CLP populations, we formally excluded the possibility that the *Rosa26* locus was not accessible in the eYFP^{-} CLP population by analysing a pan haematopoietic reporter model (*vav1::iCre x Rosa26R*$^{wt/eyfp}$ mice), which exhibited complete eYFP expression in all BM progenitor populations. Furthermore, the expression of c-kit was also analysed in the eYFP^{+} and eYFP^{-} fractions of the CLP. It was found that as cells upregulated eYFP, there was a small down-modulation of c-kit levels, resembling a similar observation in a recent report (Inlay et al., 2009). Inlay et al., reported that similar to eYFP expression, the CLP compartment could be separated into a Ly6D^{+} and a Ly6D^{-} pool. The Ly6D^{-} subset expressed higher levels of c-kit than the Ly6D^{+} subset, but lower levels of IL-7Rα. In addition, the Ly6D^{-} subset retained full lymphoid potential and early thymic seeding activity whilst the Ly6D^{+} subset gave rise predominantly to B-cells. In order to compare these data to eYFP^{-} and eYFP^{+} CLPs, *in vivo* transplantation studies were performed (see Chapter 4).

Analysis in later developmental subsets illustrated that pre-pro B-cells were 87.87 ± 1.76% eYFP^{+}. This result was in agreement with *Rag1*^{GFP} mice which marked 83% of

pre-pro B-cells (Esplin et al., 2009). In addition, Rumfelt and colleagues (Rumfelt et al., 2006) reported D_HJ_H rearrangement in 88% of pre-pro B-cells and in 48% of CLP cells, a process requiring the expression of *Rag1*. This result mirrored the expression of eYFP which we observed in these populations. Therefore, the eYFP expression observed in pre-pro B-cells should indicate a direct descendent from $eYFP^+$ CLP progenitors. It has been suggested by some groups that CLPs are primarily the progenitors for B-cells (Schwarz and Bhandoola, 2004). Schwarz et al. examined the blood of adult mice to determine which progenitors in the BM could enter the circulation and give rise to T-cells. They found the presence of LSK cells, representing HSCs, LMPPs and ELPs, however no CLP cells were found in the blood. The authors concluded that CLP cells were restricted to the BM and therefore were more likely to be B-cell precursors. However, it is possible that CLPs could have changed their phenotype upon entering the circulation. In order to further investigate whether the $eYFP^+$ and $eYFP^-$ CLP populations give rise to more B-cells than T-cells, functional analysis of these progenitor populations are necessary (see Chapter 4). Another interesting observation was that cells of the B-lineage first upregulated eYFP before acquiring CD19 expression. This result indicates that cells progress from the CLP $eYFP^-$ pool into the CLP $eYFP^+$ pool before irreversibly committing to the B-cell lineage.

Investigation of the T-cell branch of the lymphoid pathway illustrated that the ETP subset was 75% positive for eYFP expression, a result similar to that of pre-pro B-cells. This result argues against the possibility that reporter negative CLPs are the main pre-thymic precursors, but is indicative of development primarily from $eYFP^+$ progenitors such as ELP and $eYFP^+$ CLPs. One recent paper which identified the CLP as the main BM-derived T-cell precursor was that by Karsunky et al., (Karsunky et al., 2008) who assessed the functional potential of Flk-2^+ CLPs and concluded that this cell

population gave rise equally to B and T-lineages. Furthermore, despite ETP cells lacking IL-7Rα mRNA expression (Allman et al., 2003), new findings from *Il7rα*^{Cre}-driven fate mapping experiments have showed that around 85% of ETP cells have a previous history of *Il7rα* expression (Schlenner et al., 2010), a result not dissimilar to the amount of eYFP expression observed in ETPs from our reporter model. Therefore, these new findings would argue that the earliest T-cell population is composed mainly from cells with a previous history of transcriptional activation of *Il7rα*, representing descendents of the CLP and to some extent the LMPP populations.

The eYFP^{-} fraction of the ETP population suggests derivation from progenitor pools such as LMPPs or eYFP^{-} CLPs. Derivation from the LMPP pool can be favoured by the fact that alternate potentials have been reported in the ETP population. Previous results have shown that ETPs retain T, B, myeloid, DC and NK potentials (King et al., 2002; Gournari et al., 2002; Martin et al., 2003; Matsuzaki et al., 1993). Considering that the CLP was reported to have no myeloid potential (Kondo et al., 1997), alternative lymphoid progenitors such as LMPPs which retain myeloid potential must be contributing to thymic development.

In order to determine the expression of transcription factors critically involved in haematopoietic development in BM progenitor populations, *Gata1-3* gene expression was analysed in early haematopoietic subsets. The results indicated that at least under homeostatic conditions, cells of the lymphoid lineage predominantly expressed *Gata3*, whereas progenitor cells derived from the myelo-erythroid lineages express only *Gata1* and *Gata2*. Since GATA-3 has important roles throughout T-cell development, it was expected that high levels of GATA-3 protein would be present in ETPs and CD4 SP T-cells. One study which clearly demonstrates the requirement for GATA-3 in CD4 SP T-cell development was that by Pai and colleagues (Pai et al., 2003). In this report,

conditional gene ablation of *Gata3* using the Cre-lox system driven by the *Lck* or *Cd4* promoter to delete *Gata3* at the DN3 stage or DP stages was carried out. This resulted in a severe reduction in the number of CD4 SP cells and suggested a vital role for GATA-3 in survival and progression of T-cell progenitors. Due to *Gata3* expression being restricted to the lymphoid lineage and *Gata1* and *Gata2* expression in the myelo-erythroid lineages, these data indicated segregated lineage development with no alternate potentials in myelo-erythroid or lymphoid cells, at least in the manner of GATA transcription factor expression.

We also considered other factors which may affect lymphoid progenitor development, such as gender and age. When comparing the number of progenitors in the BM and the thymus, it was clear that there were major differences between male and female mice. Male mice exhibited higher numbers of all BM progenitors than female mice regardless of their age. One obvious explanation is that oestrogen was exerting an inhibitory effect on the differentiation and proliferation of these populations. It has been previously reported that chronic administration of oestrogen can lead to a reduced mass of BM and thymic organs (Verthelyi et al., 1998) suggesting either that differentiation is being suppressed or that cell death is occurring in these organs. Indeed oestrogen has been shown to induce death of BM cells at the IL-7 sensitive stage (Smithson et al., 2005), which include the LMPP, ELP and CLP populations. In addition, Medina et al., (Medina et al., 2001) also reported that CLP and ELPs were depleted in oestrogen treated mice. The molecular mechanisms by which oestrogen exerts its effect are thought to be via an oestrogen receptor present on BM stromal cells (Smithson et al., 2005) or by oestrogen receptors on haematopoietic cells. However, hormone responsive elements have also been identified upstream of several cytokine encoding genes such as IL-6 (Pottratz et al., 1994). This could influence the size of haematopoietic progenitor

compartments as IL-6 has been reported to induce the proliferation and differentiation of HSCs (Peters et al., 2000) and lymphoid progenitor cells (Ma et al., 2000) *in vitro.*

We also considered the effect of aging in conjunction with gender on haematopoietic progenitor populations, a concept which has so far not been reported. We found that although there was a decrease in the absolute numbers of all BM lymphoid progenitors, there was an increase in the number of myeloid progenitors with age in both female and male mice and a rise in thymic progenitor numbers of male mice with age. Due to the fact that B-lymphopoiesis reduces with age (Min et al., 2006) it was expected that the number of lymphoid progenitors would also decrease. Our findings are consistent with evidence that the frequency and number of CLPs are reduced in aged mice (Miller et al., 2003) as was the LMPP population. The underlying reason for this decline in lymphoid progenitor numbers could be due to decreased proliferation and differentiation of these subsets. During development, haematopoietic cells rely heavily on the BM microenvironment to regulate their growth, differentiation and survival and aging may change this environment such that levels of factors involved in this development are not adequate to maintain these cell populations. Changes in the endocrine system may also be playing a role. Decreases in the amount of anterior pituitary derived growth hormone occur with age (Lamberts et al., 1997) which may in turn be having an inhibitory effect on the production of hormone responsive HSCs.

In terms of myeloid cells, there have been some reports which suggest there is an age-related decline in the function of macrophages and neutrophils, although the number of these cell types does not change with age (Chatta and Dale, 1996). Our results favour a model where BM-derived myeloid progenitors increase in number with age; however whether this is reflected in mature peripheral myeloid cells was not studied. An increase in apoptosis of myeloid progenitors later in development could be

occurring, therefore explaining the need for a higher number of cells at progenitor levels.

The finding that the number of ETPs increased in male mice with age was rather intriguing. The thymus has been reported to involute with age due to a decrease in thymic epithelial volume and adipocytic degradation of stromal cells, therefore it would seem plausible that the number of thymic progenitors would decrease with age, as observed in female mice. However, current models of thymic involution have proposed that the frequency of ETPs actually increases with age and that their absolute number does not change (Aspinall et al., 2001). Due to the fact that reports have not discriminated between male and female mice, the overall number of ETPs remained unchanged in these studies, which would correspond with our results. We observed an increase in the number of ETPs in male mice and a decrease in female mice, which if analysed together would likely result in no overall change of numbers. The reported increase in the frequency of thymic progenitors is thought to be due to inhibited maturation of thymocytes, owing to defects in the thymic microenvironment, creating a compensatory increase in early compartments (as reviewed by Min et al., 2005). Therefore, this block in maturation would explain why fewer mature T-cells are produced and exported to the periphery in aged mice (as reviewed by Linton and Dorshkind, 2004).

The results obtained so far indicated that the $Rag1^{wt/Cre}$ *x* $Rosa26^{wt/eYFP}$ reporter was phenotypically identical to the $Rag1^{GFP}$ model and therefore could be used to monitor lymphoid development from the ELP population. In addition, this reporter allowed critical dissection of lymphopoiesis due to *Rag1* expression first occurring at the ELP stage as opposed to other models where reporter expression occurred at later stages of development. Lineage mapping studies revealed that ETPs and pre-pro B-cells were

derived from both eYFP$^-$ and eYFP$^+$ progenitor populations such as the ELP, eYFP$^-$ CLP and eYFP$^+$ CLP subsets, and the size of these progenitor pools were affected by both the age and gender of mice. In order to extend these observations, transplantation experiments assessing the functional potential of each population were undertaken.

CHAPTER 4

ANALYSIS OF THE FUNCTIONAL POTENTIAL OF LYMPHOID PROGENITOR POPULATIONS *IN VIVO* AND *IN VITRO*

4.1 Introduction

To further elucidate the developmental relationships between lymphoid progenitors and examine their developmental paths, we investigated the functional potential of these populations *in vivo* and *in vitro*. One unresolved issue is the exact nature of TSCs and the isolation of corresponding populations from BM and blood (Donskoy et al., 2003). Whilst some groups argue that the CLP is the main pre-thymic progenitor (Kondo et al., 1997; Karsunky et al., 2008; Serwold et al., 2009, Schlenner et al., 2010), others have suggested a model by which LMPPs and ELPs can also contribute to thymic development (Igarashi et al., 2002; Allman et al., 2003; Balciunaite et al., 2005; Lai and Kondo, 2007; Wada et al., 2008; Bell and Bhandoola, 2008). An additional BM precursor population referred to as the "CLP-2" was also identified, however these cells appeared to be downstream progeny of CLPs, and retained limited thymic repopulating activity (Martin et al, 2003, Schwarz et al., 2007). Taking into consideration these previous reports, it remains possible that the thymus is seeded by more than one lymphoid progenitor population.

In an attempt to characterise "thymic seeding cells" ETP subsets were divided into $eGFP^{hi}$ and $eGFP^{lo}$ cells, utilising reporter mice expressing enhanced green fluorescent protein (eGFP) from the endogenous *Ccr9* locus (Benz and Bleul, 2005). Progenitors with both B- and T-cell potential were present in the $eGFP^{hi}$ fraction mirroring high levels of eGFP expression in BM LSK and CLP subsets. The authors suggested that both these BM populations were likely to be the source of "thymic seeding cells". Another study by Schwarz et al., (Schwarz et al., 2007) reported that ELP, LMPP and CLP populations could efficiently generate T-lineage cells following intravenous or intrathymic injection, but with significant different kinetics. They also reported that HSCs did not generate T-cells after intravenous transfer until eight weeks post transfer,

whereas ELP, LMPP and CLP populations gave rise to T-cells after just four weeks. Therefore, the authors concluded that upon transplantation HSCs first homed to the BM and differentiated into LMPP or CLP cells before generating thymic input and therefore are unable to directly seed the thymus. This conclusion is in agreement with earlier observations by Mori and colleagues (Mori et al., 2001) who noted that after transplantation HSCs do not seed the thymus. In these experiments granulopoiesis, which is commonly used as a read-out for HSC development, was not recorded when thymocyte subsets from reconstituted radiation chimaeras were transferred into secondary recipients. Therefore, most evidence supports a model whereby ETPs are derived from ELP, LMPP or CLP progenitor populations of the BM.

Our previous results showed that in the thymus, lineage mapping in *Rag1*$^{wt/Cre}$ *x* *Rosa26*$^{wt/eYFP}$ reporter mice labelled 75% of ETPs with eYFP. This indicates that the majority of ETPs are derived from eYFP^{+} BM progenitors such as ELP and CLP populations, whilst the eYFP^{-} subset of ETPs may be attributed to CLP eYFP^{-} or LMPP populations. To further explore this, we investigated the functional potential of ELPs and CLPs in wild type and reporter mice to determine their potential roles as committed progenitors for T- and B-cells.

4.2 Analysis of the functional potential of the 'ELP analogue' *in vivo*

We first set out to analyse the functional potential of the 'ELP analogue' in *Rag1*$^{wt/Cre}$ *x* *Rosa26*$^{wt/eYFP}$ reporter mice to ensure that, as well as being phenotypically identical to the ELP, this population also had the same functional capacity. ELPs were defined as LSK Flk-2^{+} eYFP^{+} (Figure 4.1A). After FACS isolation (Figure 4.1B) ELPs were transferred i.v. into mice deficient for *Rag2* and the common cytokine γ chain (*Rag2/Il2rg*-null). BM, spleen and thymus were analysed at three and five weeks post injection. Reconstitution of the transferred 'ELP analogue' was monitored by identifying donor-derived eYFP^{+} cells in the host mouse.

At three weeks post ELP transfer, the frequency of donor-derived eYFP^{+} cells in the BM was 0.45% (Figure 4.2A) which consisted of either NK- or B-cells. The majority of ELP-derived cells at this time point were pre B-cells (57.20%, Figure 4.2A). There was also evidence for completed B-cell development in the BM as indicated by the presence of immature B-cells (16.10%). The remainder of graft-derived cells were NK1.1^{+} cells, demonstrating that at three weeks after transfer the ELP developed mainly into B- and NK-cells. There was no evidence for eYFP^{+} cells in the thymus (Figure 4.2B), indicating that intrathymic T-cell development did not occur yet. In addition, no eYFP^{+} myeloid cells were detected. T-cells were defined by TCRαβ expression and myeloid cells (neutrophils and monocyte/macrophages) were identified as Gr1^{+}, CD11b^{+} (Lagasse and Weissman, 1996).

Figure 4.1

Analysis of the ELP population before and after FACS purification, isolated from the BM of $Rag1^{wt/Cre}$ *x* $Rosa26^{wt/eYFP}$ *mice.*

A Pre-sort of the ELP population. BM from $Rag1^{wt/Cre}$ *x* $Rosa26^{wt/eYFP}$ mice were pooled and depleted for LIN^- cells. The ELP population was isolated as LSK Flk-2^+ $eYFP^+$. Samples are representative of nine individual cell sorts.

B Post-sort of the ELP population after isolation using the FACS Aria II. The ELP population was sorted to over 95% purity.

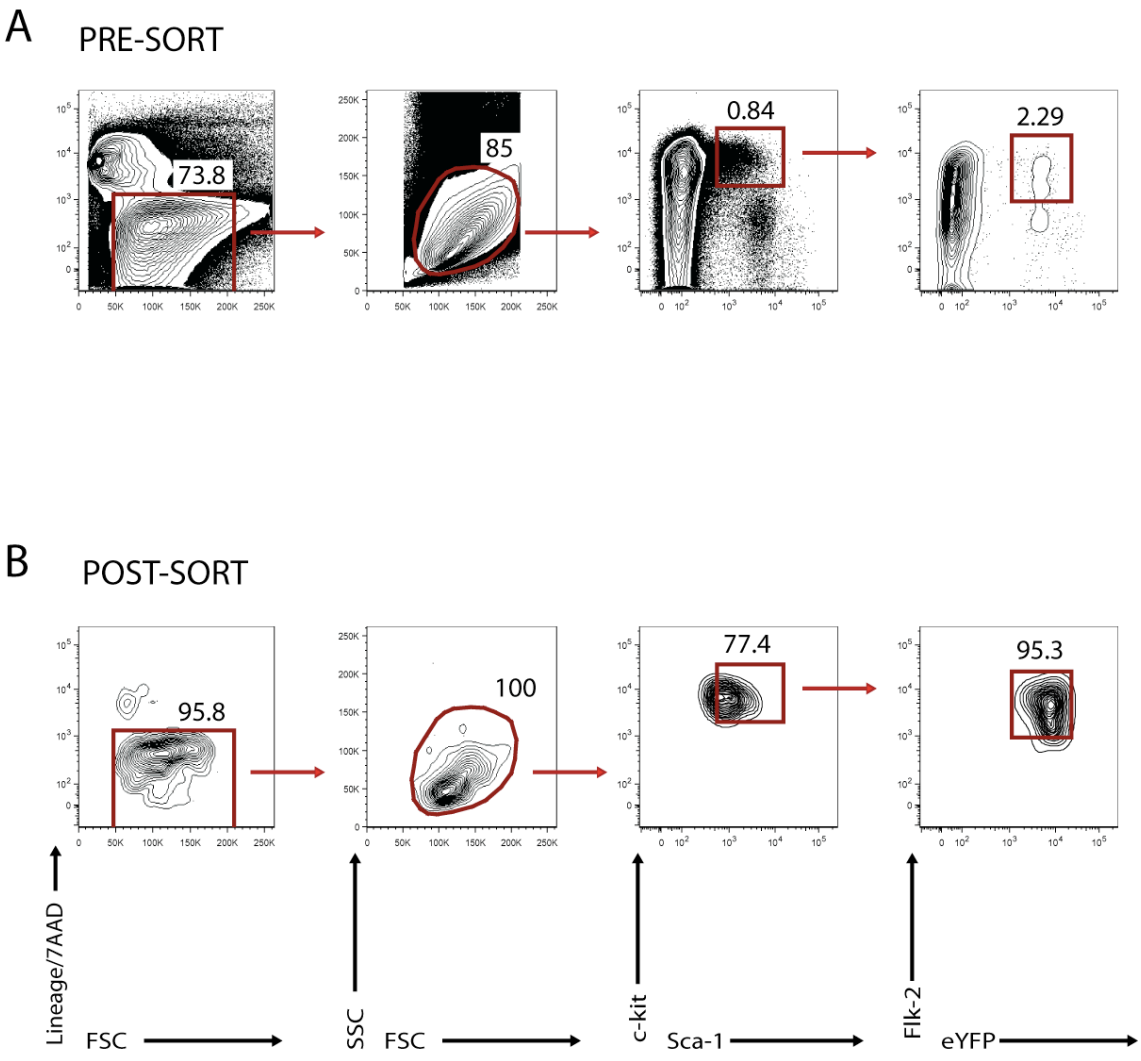
A
PRE-SORT
73.8
85
0.84
2.29
B
POST-SORT
95.8
100
77.4
95.3
Lineage/7AAD
FSC
SSC
FSC
c-kit
Sca-1
Flk-2
eYFP

Figure 4.2

Reconstitution potential of the ELP population in the BM and thymus of Rag2/Il2rg-null mice at three weeks post transfer.

A Representative FACS plot illustrating reconstitution of the ELP population in the BM of *Rag2/Il2rg*-null mice. 10^3 $eYFP^+$ ELPs from four to six week old $Rag1^{wt/Cre}$ *x* $Rosa26^{wt/eYFP}$ mice were injected i.v. into sub-lethally irradiated (3 Gray) *Rag2/Il2rg*-null mice. Reconstitution was measured by the expression of eYFP. Staining is representative for one experiment.

B Representative FACS plot illustrating reconstitution of the ELP population in the thymus of *Rag2/Il2rg*-null mice. 10^3 $eYFP^+$ ELPs from four to six week old $Rag1^{wt/Cre}$ *x* $Rosa26^{wt/eYFP}$ mice were injected i.v. into sub-lethally irradiated (3 Gray) *Rag2/Il2rg*-null mice. Compared to the control wildtype mouse (PBS injected), eYFP expression was virtually absent in the thymus. Staining is representative for one experiment.

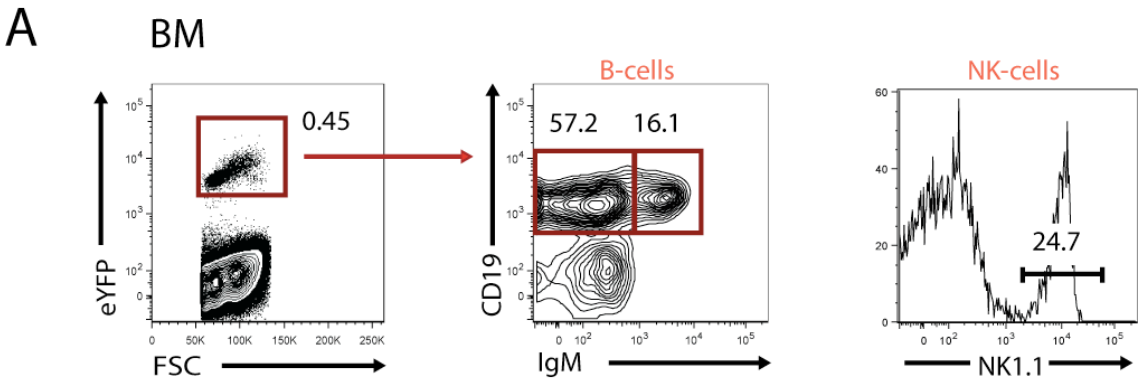
A
BM
0.45
eYFP
FSC
B-cells
57.2
16.1
CD19
IgM
NK-cells
24.7
NK1.1

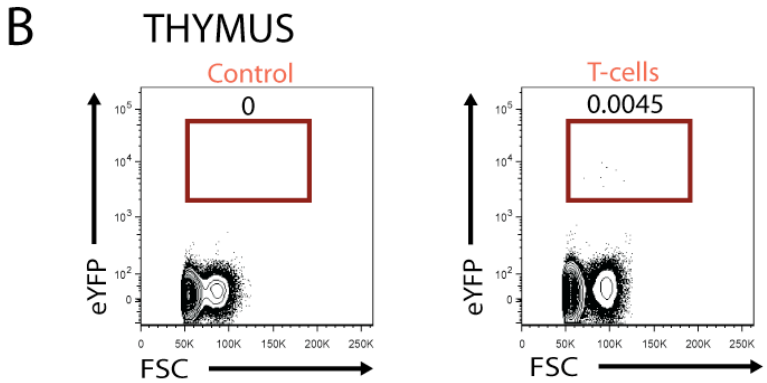
B
THYMUS
Control
0
eYFP
FSC
T-cells
0.0045
eYFP
FSC

Figure 4.3

Reconstitution potential of the ELP population in the spleen of Rag2/Il2rg-null mice at three weeks post transfer.

Representative FACS plot illustrating splenic reconstitution of the ELP three weeks post injection into *Rag2/Il2rg*-null mice. 10^3 $eYFP^+$ ELPs from four to six week old $Rag1^{wt/Cre}$ *x* $Rosa26^{wt/eYFP}$ mice were injected i.v. into sub-lethally irradiated (3 Gray) *Rag2/Il2rg*-null mice. Donor-derived cells were identified by eYFP expression. Staining is representative for one experiment.

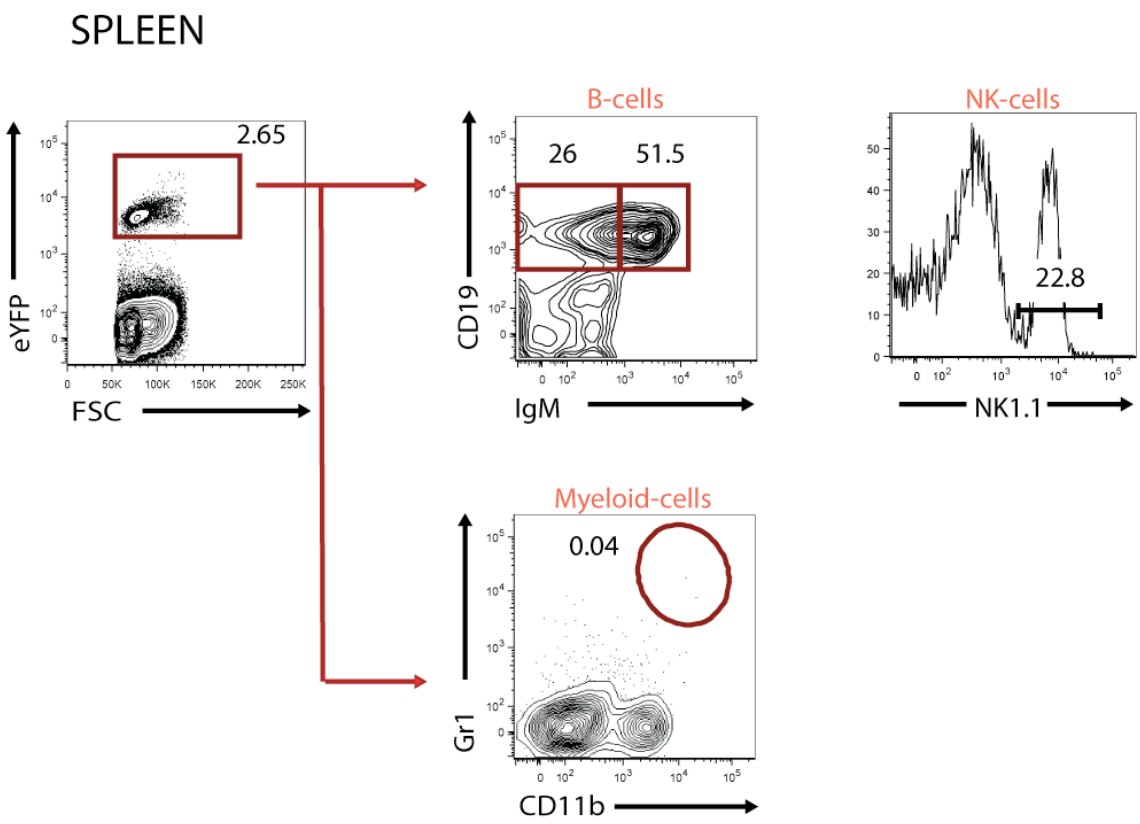
SPLEEN
2.65
eYFP
FSC
B-cells
26
51.5
CD19
IgM
NK-cells
22.8
NK1.1
Myeloid-cells
0.04
Gr1
CD11b

Reconstitution restricted to NK and B-cells by ELPs was also evident in the spleen after three weeks post transfer (Figure 4.3). The frequency of ELP-derived splenic NK-cells was 22.80% (Figure 4.3). Splenic $CD19^+$ IgM^+ B-cells, encompassing immature and transitional B-cells, accounted for 51.50% of donor-derived cells and the remainder (26.00%) were mature B-cells. However, there was no evidence for significant $eYFP^+$ splenic myeloid or T-cells. These data demonstrated that B- and NK-cell reconstitution from the ELP was evident after three weeks, in accordance with the observations of Igarashi and colleagues (Igarashi et al., 2002), which used ELPs derived from *Rag1*^{GFP} mice in their experiments.

We next extended our analysis and included later time points after transplantation to assess the lymphoid potential of ELPs after transfer into *Rag2/Il2rg*-null recipients. Five weeks post transplantation, B-, NK- and T-cell reconstitution was evident. In the BM, the vast majority of $CD19^+$ cells were IgM^+ immature B-cells (26.45 ± 12.82; Figure 4.4A), with only 15.22 ± 6.25% of $CD19^+$ cells in the pre B-cell compartment, suggesting a single wave of donor-derived B-cell development. NK-cells (21.01 ± 10.22%) were still present in the BM, but no myeloid reconstitution was detectable (data not shown).

At this time point, T-cell reconstitution was observed in the thymus (77.33 ± 8.74%; Figure 4.4B). A single wave of donor-derived T-cells had proceeded past the DN stages of development at five weeks post transfer and donor-derived cells gave rise to DP cells (27.94 ± 18.19%) CD4 SP (58.33 ± 16.66%) and CD8 SP (11.15 ± 1.4%) cells. The frequency of $eYFP^+$ thymic cells expressing TCRαβ was also analysed. 5.31 ± 3.4% of $eYFP^+$ cells expressed low levels of TCRαβ, identifying those cells as developing thymocytes, 26.03 ± 11.41% of $eYFP^+$ cells were $TCR\alpha\beta^{int}$ which were characterised as DP T-cells and 69.17 ± 15.02% of cells were TCR^{hi} which represented CD4 SP and

CD8 SP cell populations. Therefore, reconstitution of the ELP via DN1-4 stages must have taken place between three and five weeks post transfer; a finding in agreement with previously reported results (Igarashi et al., 2002).

In the spleen, ELP-derived cells were composed of T, B, NK and to a minor extent myeloid cells (Figure 4.5). T-cells were identified by TCRαβ and further characterised by CD4 and CD8 antigens, indicative of mature cells exported from the thymus. During maturation of BM-derived immature B-cells in the spleen, IgM is downregulated on the surface of cells and IgD is upregulated. Therefore, at five weeks post transfer, splenic B-cells which are characterised as $CD19^{+}$ and IgM^{lo} were likely to be mature cells which expressed IgD on their surface. Only a small frequency of $eYFP^{+}$ cells were $CD19^{+}$ IgM^{lo} whilst the majority of reconstituted B-cells were $CD19^{+}$ IgM^{+} representing either immature B-cells ($CD19^{+}$ IgM^{+} IgD^{-}) or immature B-cells in the transition to becoming mature cells ($CD19^{+}$ IgM^{+} IgD^{+}). There was a significant decrease in the frequency of $eYFP^{+}$ splenic NK-cells at five weeks compared to at three weeks post transfer. Since only reconstituted NK and B-cells were observed in the spleen at three weeks, the high frequency of NK-cells at this time point was plausibly only caused by the low abundance of peripheral lymphoid cells. On the other hand, the high frequency of splenic NK-cells at three weeks post transfer could have indicated abundant reconstitution of NK-cells, which may have altered at five weeks post transfer. The decrease in the frequency of splenic NK-cells from three to five weeks may have been caused by cell death or migration of NK-cells from the spleen to alternate secondary organs such as lymph nodes. In addition, the frequency of reconstituted splenic myeloid cells was very low (0.44 ± 0.26%), suggesting that the injected ELP cells had minimal myeloid potential *in vivo,* an observation also reported by Igarashi and colleagues (Igarashi et al., 2002).

The transplantation of ELP cells into alymphoid mice proved that this population contained T-, NK- and B-cell potential, in agreement with Igarashi et al (Igarashi et al., 2002). Donor-derived NK- and B-cell reconstitution was present in the BM and spleen at three and five weeks post transfer, however T-cell reconstitution was not evident in the thymus and spleen until five weeks post transfer. In addition, minimal myeloid potential was observed in the ELP population. These results show that the 'ELP analogue' was functionally as well as phenotypically identical to the originally described ELP population.

Figure 4.4

Reconstitution potential of the ELP population in the BM and thymus at five weeks post transfer in Rag2/Il2rg-null mice.

A Representative FACS plot illustrating ELP reconstitution of the BM five weeks post injection into *Rag2/Il2rg*-null mice. 10^3 $eYFP^+$ ELPs from four to six week old $Rag1^{wt/Cre}$ *x* $Rosa26^{wt/eYFP}$ mice were injected i.v. into sub-lethally irradiated recipients. Donor-derived cells were detected by expression of eYFP and further analysed for B-cell and NK-cell populations. Staining is representative for two experiments with two to three mice per group.

B Representative FACS plot illustrating ELP reconstitution of the thymus five weeks post injection of the cells into *Rag2/Il2rg*-null mice. 10^3 $eYFP^+$ ELPs from four to six week old $Rag1^{wt/Cre}$ *x* $Rosa26^{wt/eYFP}$ mice were injected i.v. into sub-lethally irradiated recipients. Donor-derived cells were detected by expression of eYFP and further analysed for CD4 and CD8 antigens. Staining is representative for two experiments with two to three mice per group.

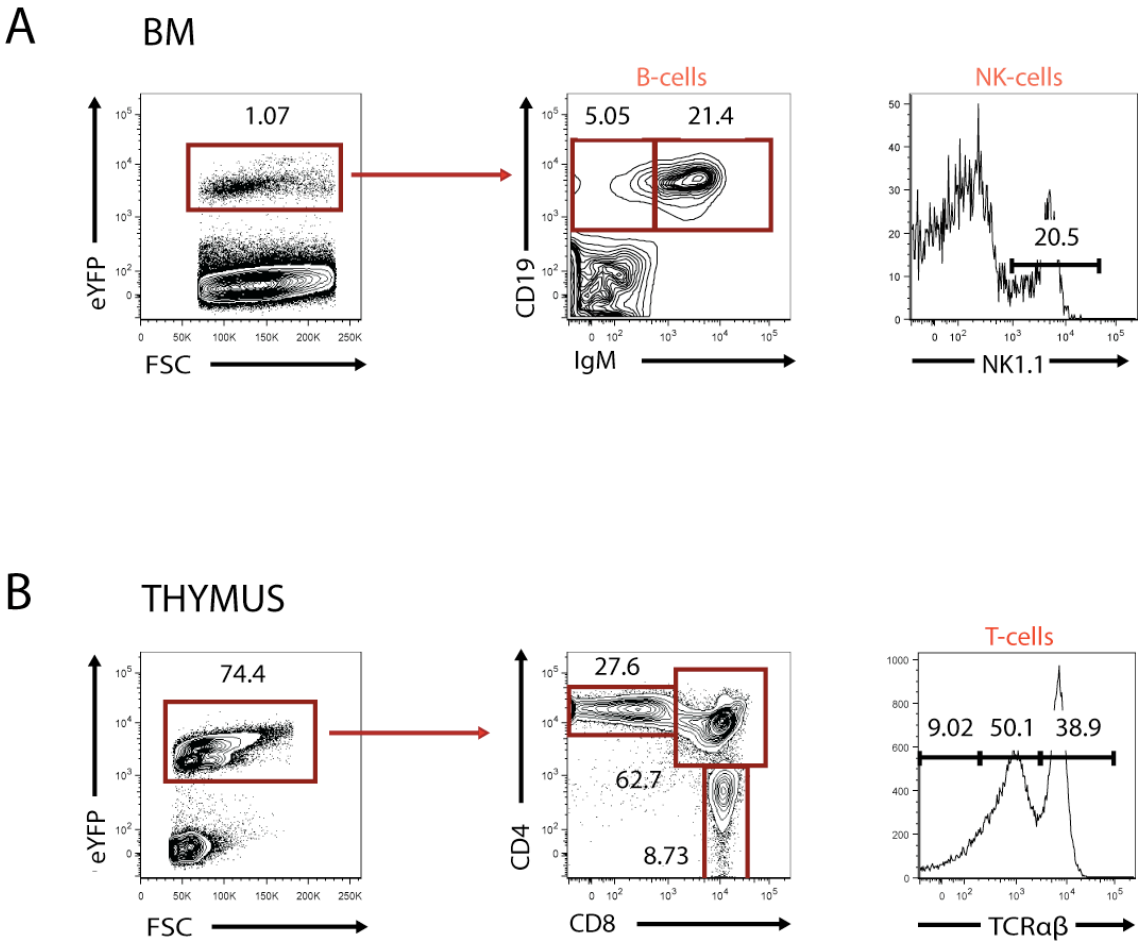
A
BM
1.07
eYFP
FSC
B-cells
5.05
21.4
CD19
IgM
NK-cells
20.5
NK1.1
B
THYMUS
74.4
eYFP
FSC
27.6
62.7
8.73
CD4
CD8
T-cells
9.02
50.1
38.9
TCRαβ

Figure 4.5

Reconstitution potential of the ELP population in the spleen at five weeks post transfer in Rag2/Il2rg-null mice.

Representative FACS plot illustrating ELP reconstitution in the spleen five weeks post injection into *Rag2/Il2rg*-null mice. 10^3 $eYFP^+$ ELPs from four to six week old $Rag1^{wt/Cre}$ x $Rosa26^{wt/eYFP}$ mice were injected i.v. into sub-lethally irradiated recipients. Staining is representative for two experiments with two to three mice per group.

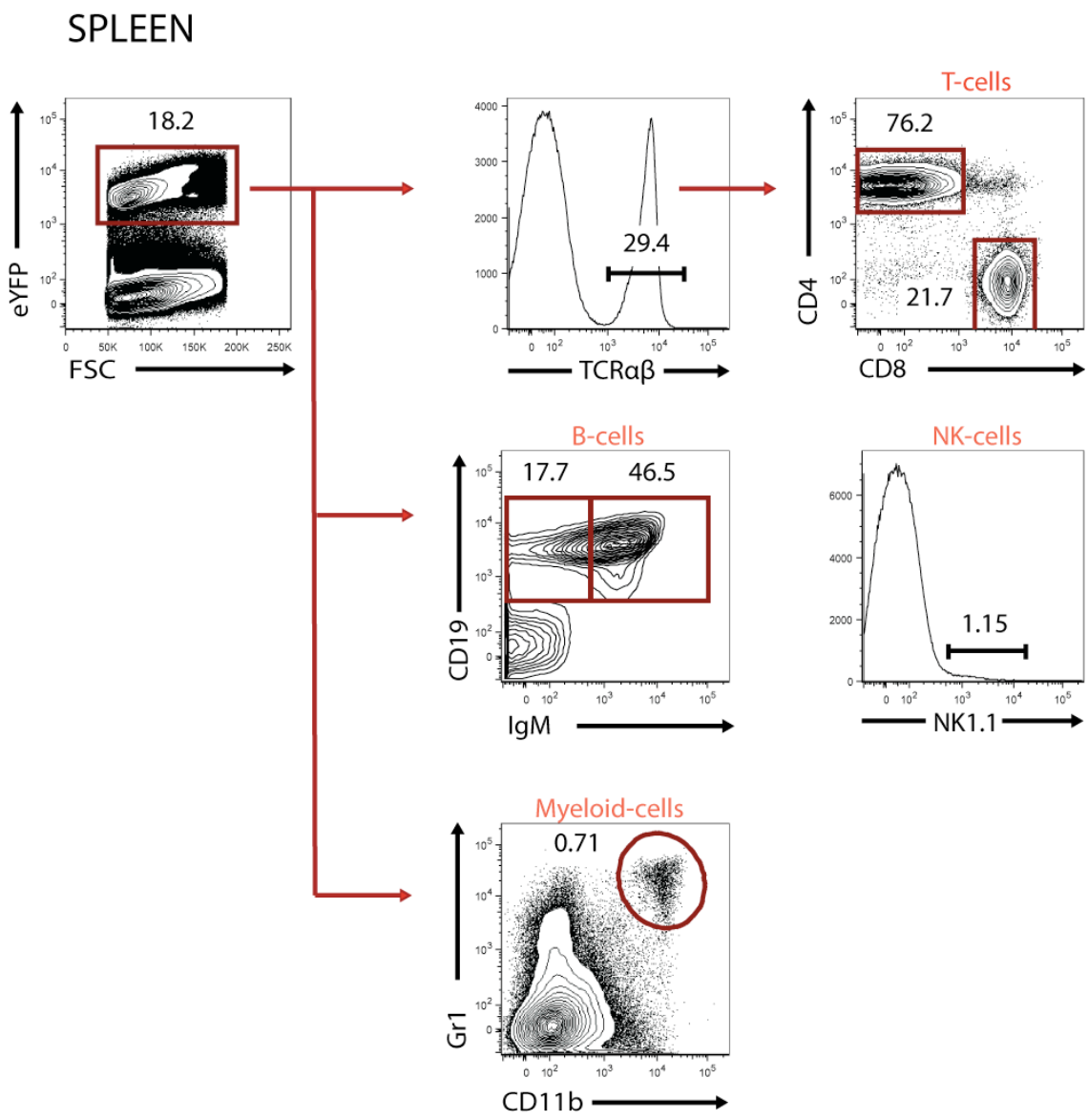
SPLEEN
18.2
eYFP
FSC
29.4
TCRαβ
T-cells
76.2
21.7
CD4
CD8
B-cells
17.7
46.5
CD19
IgM
NK-cells
1.15
NK1.1
Myeloid-cells
0.71
Gr1
CD11b

4.3 Analysis of the functional potential of the CLP population *in vivo*

We next investigated the developmental potential of the CLP population in relation to the 'ELP analogue'. In addition to previous reports indicating that the CLP population may be the main precursor for B-cells (Allman et al., 2003; Schwarz et al., 2004) but not T-cells (Wada et al., 2008; Bell and Bhandoola, 2008) there have also been studies suggesting myeloid potential in the CLP fraction (Balciunaite et al., 2005; Rumfelt et al., 2006; Mebius et al., 2001). Balciunaite and colleagues reported that one in ten CLP cells *in vitro* developed into macrophages (Balciunaite et al., 2005). Similarly, Rumfelt et al., (Rumfelt et al., 2006) found that CLP cells placed on a S17 stromal cell layer supplemented with SCF, Flk-2 ligand and IL-7 cytokines also produced a significant number of myeloid colonies. These CLP cells also expressed high mRNA levels of *Csfr1*, a gene expressed in the myeloid lineage. Furthermore, the phenotypical counterpart of the adult CLP in the foetal liver has been shown to give rise to macrophages *in vitro* (Mebius et al., 2001). Therefore, we aimed to compare the developmental potential of the CLP population to the 'ELP analogue' and assess any possible myeloid potential of the CLP *in vivo*. To do this, LIN^- IL-$7R\alpha^+$ Flk-2^+ cells were isolated from B6 CD45.1-congenic mice (Figure 4.6) and injected into sub-lethally irradiated *Rag2/Il2rg*-null mice. Reconstitution by CLPs was monitored by identifying donor-derived $CD45.1^+$ cells in the host mouse.

At two weeks post transfer, the CLP population had reconstituted the BM, spleen and thymus and developed into B-, T- and NK-cells (Table 4). In the BM, donor-derived reconstitution was confined mainly to NK-cells, with some reconstitution into pre B and immature B-cells, but minimal reconstitution into myeloid cells. The low frequency of pre B-cells but the higher frequency of immature B-cells in the BM might indicate that an early wave of donor-derived B-cells had already developed. The very low frequency

of myeloid reconstitution in the BM after two weeks indicated that the CLP had minimal myeloid potential.

In the spleen at two weeks post transfer, donor-derived immature and mature B-cell reconstitution was abundant in frequency and this was accompanied by some NK-cell reconstitution. The small frequency of donor-derived splenic NK-cells indicated that the majority of these cells were still confined to the BM. In addition, there was a virtual absence of reconstitution into splenic T- or myeloid cells.

In the thymus at two weeks, reconstitution of donor-derived cells were predominantly at the DN stage, with a low frequency of CD4 SP and CD8 SP cells. This result differed from that of the 'ELP analogue', where T-cell reconstitution was not observed until after three weeks post transfer. There was also evidence for thymic NK-cells, which could have been due to re-circulation of NK-cells or NK-cell development in the thymus.

Figure 4.6

Analysis of BM CLP preparations before and after FACS purification, isolated from the BM of B6/J CD45.1 mice.

A Analysis of the CLP population before FACS purification. The CLP population was isolated according to the definition LIN^- IL-7Rα^+ Flk-2^+.

B Analysis of the CLP population after FACS purification. The CLP population was sorted to over 95% purity.

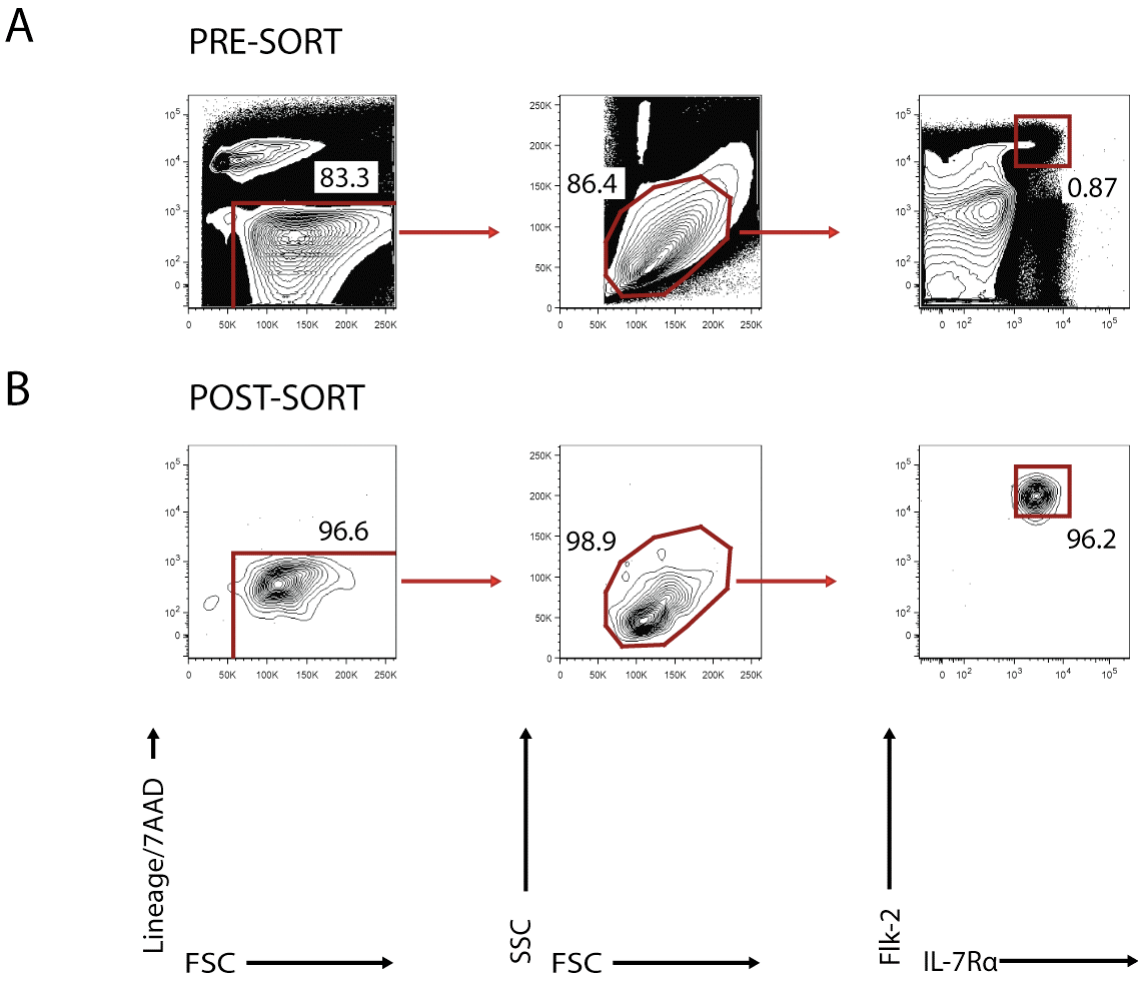
A
PRE-SORT
83.3
86.4
0.87
B
POST-SORT
96.6
98.9
96.2
Lineage/7AAD
FSC
SSC
FSC
Flk-2
IL-7Rα

Three weeks post transfer in the BM, the frequency of pre B-cells and immature B-cells was virtually negative, suggesting CLP-derived B-cells had completed development in this organ, had exited the BM and entered the periphery. Near completion of B-cell maturation was also observed in the spleen where the majority of reconstituted B-cells were mature. There was a minor increase in the frequency of reconstituted BM myeloid cells, although there was no evidence for abundant myeloid reconstitution in the spleen, indicating that the cells in the BM had not yet entered the spleen or that the small frequency of observed myeloid cells was an artefact. The frequency of $CD45.1^{+}$ BM and splenic NK-cells showed no dramatic change compared to two weeks post transfer, however the relative contribution of transferred cells to the BM and spleen also did not change drastically.

In the thymus, there was a minor fall in the frequency of reconstituted NK-cells from 11.49 ± 4.23% at two weeks to 6.04 ± 3.18% at three weeks. T-cell reconstitution in the thymus was still restricted to the DN compartment, the same as at two weeks post transfer, which explained why there was a lack of reconstituted splenic T-cells. This result also mirrored what was observed in the thymus after reconstitution of the 'ELP analogue'.

At four weeks post transfer, the relative frequency of reconstituted B- and myeloid cells in the BM had increased, however this could have been due to the major decrease in the frequency of donor-derived NK-cells present in the BM at this time point. Alternatively, this could also have indicated that a second wave of B-cell development was occurring which was related to a developmental heterogeneity within the CLP pool and different rates of differentiation and proliferation. The relative frequency of reconstituted BM myeloid cells had increased substantially, from 2.08 ± 0.24% at three weeks to 17.38 ± 7.90% at four weeks. Since the frequency of CLP-derived myeloid cells remained low

in the spleen, this suggested that the observed increase in the BM was due the lack of alternate cell types. The percentage of donor-derived NK-cells in the BM and thymus had decreased at this time point; however there was no evidence for a higher level of NK-cells in the spleen, suggesting that the cells may have died. In the thymus however, there was now evidence for reconstituted DP, CD4 SP and CD8 SP T-cells and low level T-cell reconstitution was also observed in the spleen (11.06 ± 16.3%).

In comparison to the 'ELP analogue' at three weeks post transfer, the CLP population had virtually completed B-cell development in the BM. In addition, CLP-derived splenic immature and mature B-cells were also present; suggesting that BM-derived immature B-cells had seeded the spleen and continued maturation. However at this time point, the 'ELP analogue' was still progressing via B-cell development in the BM, as indicated by the abundance of pre B-cells. This indicated that both the ELP and CLP populations could give rise to B-cells as previously reported (Kondo et al., 1997; Igarashi et al., 2002) but that the CLP was at a developmentally later stage than the ELP. Both cell types were also able to give rise to NK and T-cells. However, the CLP population was able to reconstitute thymic progenitor cells at the DN stage after two and three weeks, but this was not observed until five weeks post transfer with the 'ELP analogue', suggesting that longer time is required for ELP cells to generate T-cells than CLPs. This could be due to ELP cells remaining for longer in the circulation before entering the thymus than CLP cells, or ELP cells may first home to the BM and continue lymphoid development prior to migration to the thymus. With regards to myeloid development, the ELP population was virtually absent of any significant myeloid potential *in vivo*, but myeloid potential was detected in the BM of CLP-derived cell transfers. However, this increase in myeloid reconstitution may have been due to

the lack of alternate cell types in the BM at four weeks post transfer and therefore may not represent a significant myeloid reconstitution.

Table 4

Reconstitution potential of the CLP population at two, three and four weeks after injection into Rag2/Il2rg-null mice.

Table illustrating the reconstitution frequency of CD45.1^{+} CLP cells in *Rag2/Il2rg*-null mice at two, three and four weeks post injection. 2 x 10^{3} CD45.1^{+} CLPs from four to six week old B6/J CD45.1 mice were injected i.v. into sub-lethally irradiated recipients. Donor-derived progeny was measured in the BM (orange), thymus (green) and spleen (blue) by gating on CD45.1^{+} cells. One experiment was performed. The number of recipients per time point is shown in the table.

	Percentage of donor derived cells (CD45.1$^+$)							
	2 Weeks			3 Weeks		4 Weeks		
	Recipient 1	Recipient 2	Recipient 3	Recipient 1	Recipient 2	Recipient 1	Recipient 2	Recipient 3
Bone Marrow								
Pre B	0.00	2.35	1.63	0.93	0.97	38.20	47.30	37.20
Immature B	12.50	5.29	15.90	2.54	1.53	6.54	10.20	4.83
NK cells	96.00	72.80	97.90	73.90	88.50	7.24	13.20	19.60
Myeloid	0.43	0.87	0.44	2.32	1.84	32.00	15.10	5.03
Thymus								
DN	74.70	54.90	96.80	100.00	99.30	0.47	44.90	1.05
DP	4.98	0.20	0.65	0.00	0.00	94.50	8.51	81.00
CD4SP	12.10	27.50	0.65	0.00	0.00	2.95	12.20	7.82
CD8SP	1.53	9.17	1.30	0.00	0.00	1.15	13.90	5.77
NK	16.90	3.61	14.40	9.21	2.86	0.05	2.81	0.11
Spleen								
Immature B	76.20	68.00	85.20	33.80	33.60	1.37	7.12	0.31
Mature B	16.40	11.70	8.29	64.90	64.00	96.10	87.80	58.70
NK	3.49	6.70	3.08	2.17	1.89	3.45	2.08	1.42
Myeloid	0.38	0.60	0.17	0.21	0.10	0.05	0.08	0.04
T	0.09	0.06	0.34	0.08	0.07	0.19	3.19	29.80

4.4 Analysing the functional potential of the ELP, CLP eYFP$^-$ and CLP eYFP$^+$ pools *in vivo*

Analysis of eYFP expression in *Rag1*$^{wt/Cre}$ *x Rosa26*$^{wt/eYFP}$ mice, reported in chapter 3, demonstrated that the CLP could be subdivided into two pools, identified by the lack or presence of reporter expression. These data had also demonstrated that the majority of pre B-cells and ETPs were derived from eYFP$^+$ progenitors. In addition, functional data of the CLP had indicated that there may have been two waves of B-cell development. Therefore, the next step was to isolate the ELP, CLP eYFP$^-$ and CLP eYFP$^+$ populations and compare these cell types with respect to their B- and T-cell potential.

Using *Rag1*$^{wt/Cre}$ *x Rosa26*$^{wt/eYFP}$ mice, the ELP population - isolated as previously described (Figure 4.1) - and CLP populations were isolated (Figure 4.7). All populations were transplanted into *Rag2/Il2rg*-null mice and the developmental potential of these cell populations were analysed at five weeks post transfer in the spleen.

Splenic B-cell reconstitution was measured by CD19 expression and T-cell reconstitution was assessed by expression of TCRαβ. The mean frequency of splenic eYFP$^+$ cells expressing CD19 was similar between the ELP, CLP eYFP$^-$ and CLP eYFP$^+$ subsets (Figure 4.8A). The same could also be observed in the frequency of eYFP$^+$ cells expressing TCRαβ in the spleen (Figure 4.8B). However, when absolute numbers of CD19$^+$ donor-derived cells were compared between the three cell populations, there were significant differences.

The ELP and CLP eYFP$^+$ pools reconstituted significantly higher numbers of splenic CD19$^+$ cells compared to the CLP eYFP$^-$ pool (Figure 4.9A). The number of ELP-derived cells which had reconstituted into splenic B-cells was 87.60 x 10^4 ± 49.05 x 10^4 whilst CLP eYFP$^+$ cells generated 49.12 x 10^4 ± 37.59 x 10^4 B-cells. However, the CLP eYFP$^-$ population only reconstituted 13.21 x 10^4 ± 10.53 x 10^4 splenic B-cells,

which was over five fold lower than the average number of reconstituted ELP splenic B-cells and over three fold lower than the number of CLP eYFP$^+$-derived B-cells. The number of ELP-derived splenic B-cells was in the range of 53 x 10^4 to 79 x 10^4, however there appeared to be one outlier where the number of reconstituted splenic B-cells was 159.19 x 10^4 cells. Similarly, transfer of the CLP eYFP$^+$ subset gave rise to numbers of splenic B-cells within the range of 43 x 10^4 to 93 x 10^4, however there was also one outlier which gave rise to only 2.80 x 10^4 B-cells. The range of splenic B-cells reconstituted by the CLP eYFP$^-$ population however were much lower and mostly in the range of 6 x 10^4 to 11 x 10^4 with one outlier reconstituting 31 x 10^4 cells, but this value was still lower than the range of B-cells reconstituted by the other cell types. Therefore, it appeared that the ELP and CLP eYFP$^+$ populations were giving rise to significantly higher numbers of splenic B-cells than the CLP eYFP$^-$ population. This indicated that either the ELP and CLP eYFP$^+$ subsets were more favourable candidates for pre B-cells than the CLP eYFP$^-$ population, or other factors such as migration and differentiation were influencing B-cell reconstitution from the CLP eYFP$^-$ subset. However, due to all three cell types being injected into the same host, which had been irradiated with 3 Gray, all cell populations appeared to have equal opportunity to develop in the BM and migrate to the thymus and spleen. On the other hand, it was not clear whether all CLP eYFP$^-$ cells had undergone full development into eYFP$^+$ progenitors or whether cells which had acquired eYFP were able to seed the spleen efficiently. Therefore, in order to address the issue of development, *in vitro* studies of CLP eYFP$^-$-derived B-cell development were devised (see next study). The *in vivo* data indicated that all three cell populations could develop into B-cells but with distinct different efficiency: ELP and CLP eYFP$^+$ populations generated more splenic B-cells than the CLP eYFP$^-$ population.

Therefore, there were clearly functional differences between the eYFP$^-$ and eYFP$^+$ CLP populations, suggesting that these pools harbour different potential.

Regarding T-cell development, there were no significant differences between all three cell populations (Figure 4.9B). The ELP population gave rise to 52.08 x 10^4 ± 26.47 x 10^4 splenic T-cells on average whereas the CLP eYFP$^+$ reconstituted 28.72 x 10^4 ± 33.41 x 10^4 splenic T-cells and the CLP eYFP$^-$ pool on average gave rise to 29.62 x 10^4 ± 40.09 x 10^4 cells. The difference between the mean number of ELP-derived splenic T-cells compared to the other two populations was only 1.8 fold. However, the range of reconstituted T-cells was quite different. ELP-derived splenic T-cell numbers ranged from 62 x 10^4 to 66 x 10^4, with one outlier of a value of 12 x 10^4. In contrast the number of CLP eYFP$^+$-derived splenic T-cells ranged from 0.12 to 19 x 10^4 cells with one outlier of 77.94 x 10^4 cells and the number of CLP eYFP$^-$-derived cells ranged from 0.02 to 47 x 10^4 cells with an outlier of 92 x 10^4 cells. These data indicated that all populations possessed T-cell potential however, outliers excluded, the ELP population appeared to have the highest and most consistent splenic T-cell reconstitution. Interestingly, splenic T-cell reconstitution was virtually absent in some mice. This suggests that, due to the altered thymic microenvironment in *Rag2/Il2rg*-null mice and the lack of progenitor cells constantly seeding the thymus; upon transplantation some cells were unable to efficiently enter the thymus and develop into T-cells.

Figure 4.7

Analysis of CLP eYFP$^-$ and CLP eYFP$^+$ preparations isolated from BM of Rag1$^{wt/Cre}$ x Rosa26$^{wt/eYFP}$ mice before and after FACS purification.

A Analysis of CLP populations before FACS purification. The CLP populations were isolated as LIN$^-$ IL-7Rα$^+$ Flk-2$^+$ eYFP$^-$ or LIN$^-$ IL-7Rα$^+$ Flk-2$^+$ eYFP$^+$.

B Post-sort of the CLP eYFP$^-$ population. The CLP eYFP$^-$ population was sorted to over 95% purity.

C Post-sort of the CLP eYFP$^+$ population. The CLP eYFP$^+$ population was sorted to over 95% purity.

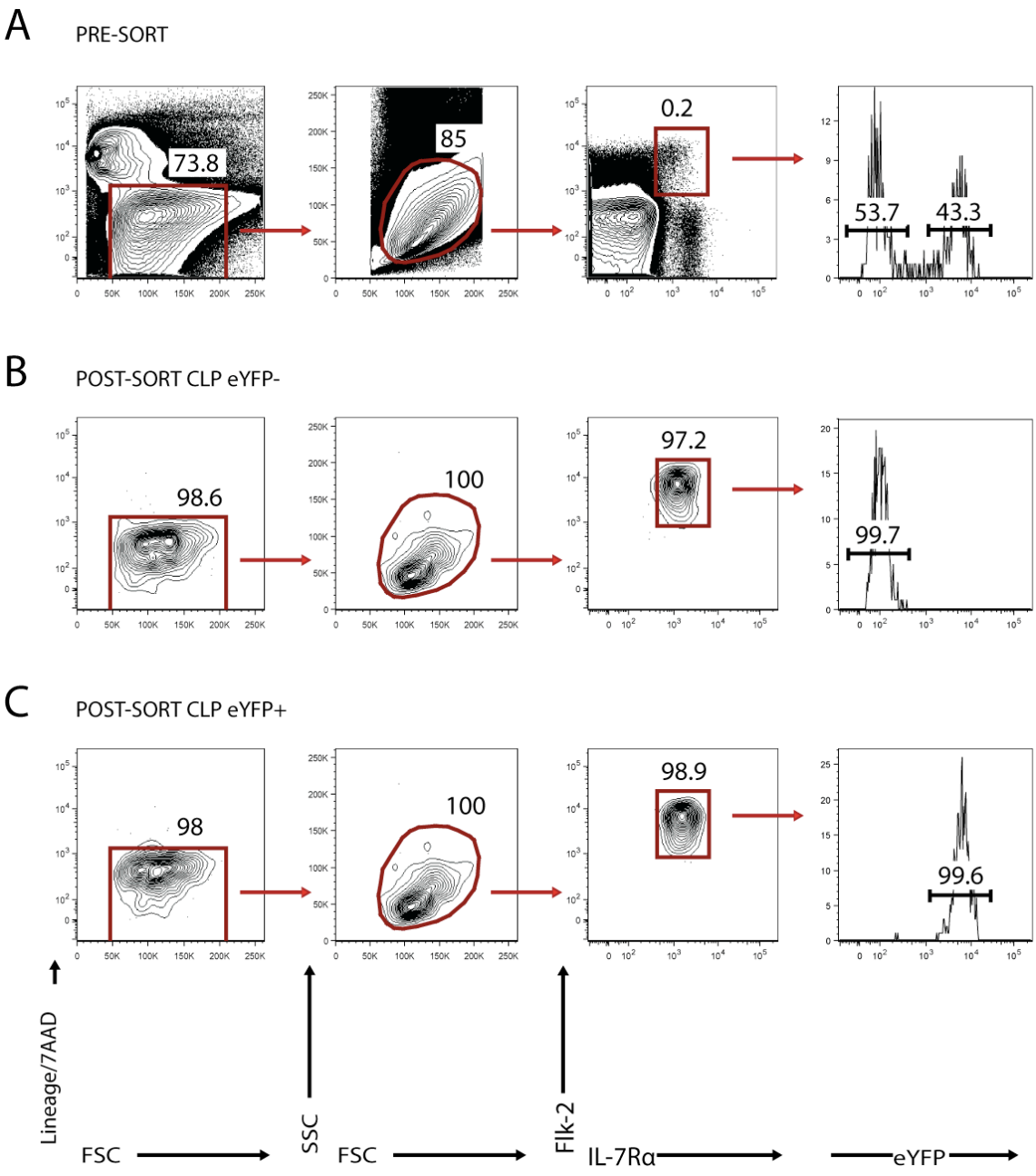
A
PRE-SORT
73.8
85
0.2
53.7
43.3
B
POST-SORT CLP eYFP-
98.6
100
97.2
99.7
C
POST-SORT CLP eYFP+
98
100
98.9
99.6
Lineage/7AAD
FSC
SSC
FSC
Flk-2
IL-7Rα
eYFP

Figure 4.8

Frequency of splenic B- and T-cell reconstitution of ELP, CLP eYFP$^-$ and CLP eYFP$^+$ populations five weeks post transfer in Rag2/Il2rg-null mice.

A Graph illustrating splenic B-cell reconstitution frequencies of the ELP, CLP eYFP$^-$ and CLP eYFP$^+$ populations, measured as the percentage of donor-derived CD19$^+$ cells. 2 x 10^3 CLP eYFP$^-$, 2 x 10^3 CLP eYFP$^+$ or 10^3 ELPs from four to six week old *Rag1$^{wt/Cre}$ x Rosa26$^{wt/eYFP}$* mice were injected i.v. into sub-lethally irradiated recipients. Mice were analysed for splenic B-cell reconstitution five weeks post transfer. Results are depicted individually and as an average. Results are representative of two experiments with two to three mice per group.

B Graph illustrating splenic T-cell reconstitution frequencies of the ELP, CLP eYFP$^-$ and CLP eYFP$^+$ populations, measured as the percentage of donor-derived TCRαβ$^+$ cells. 2 x 10^3 CLP eYFP$^-$, 2 x 10^3 CLP eYFP$^+$ or 10^3 ELPs from four to six week old *Rag1$^{wt/Cre}$ x Rosa26$^{wt/eYFP}$* mice were injected i.v. into sub-lethally recipients. Mice were analysed for splenic T-cell reconstitution five weeks post transfer. Results are depicted individually and as an average. Results are representative of two experiments with two to three mice per group.

A

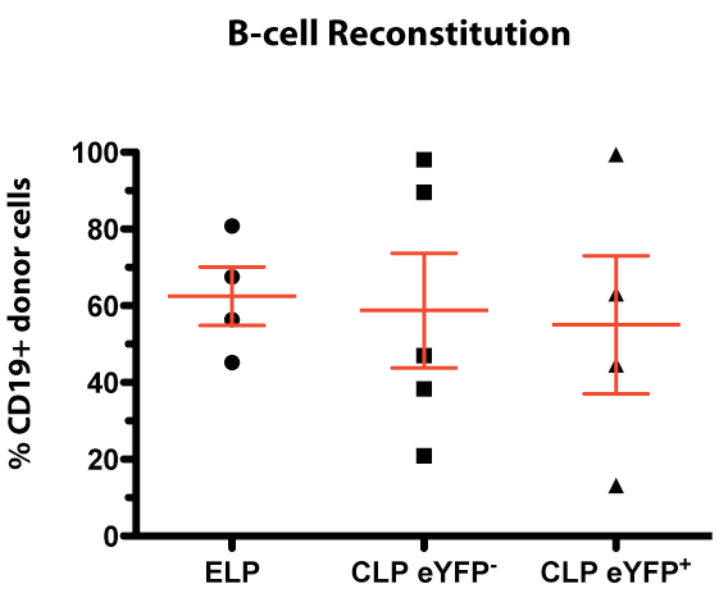
B-cell Reconstitution
% CD19+ donor cells
100
80
60
40
20
0
ELP
CLP eYFP-
CLP eYFP+

B

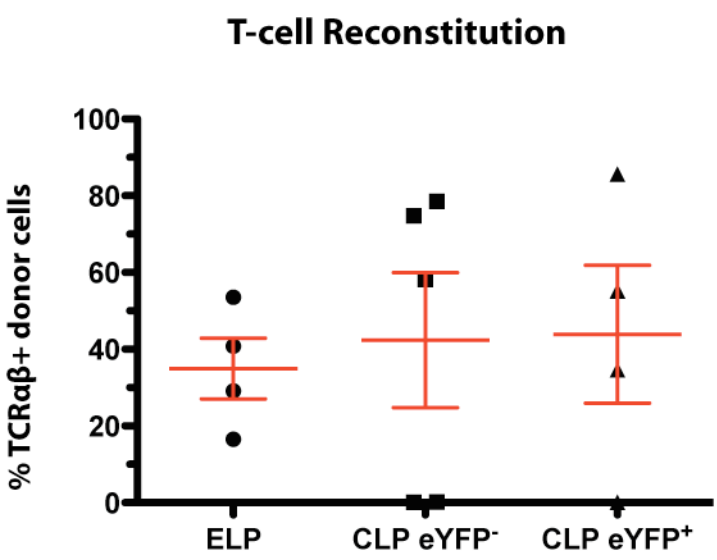
T-cell Reconstitution
% TCRαβ+ donor cells
100
80
60
40
20
0
ELP
CLP eYFP-
CLP eYFP+

Figure 4.9

Absolute numbers of splenic B and T-cell reconstitution compared between ELP, CLP eYFP$^-$ and CLP eYFP$^+$ populations five weeks post transfer into Rag2/Il2rg-null mice.

A Graph illustrating splenic B-cell reconstitution numbers of the ELP, CLP eYFP$^-$ and CLP eYFP$^+$ populations. 2 x 10^3 CLP eYFP$^-$ and 2 x 10^3 CLP eYFP$^+$ or 10^3 ELPs from four to six week old *Rag1$^{wt/Cre}$ x Rosa26$^{wt/eYFP}$* mice were injected i.v. into sub-lethally irradiated recipients. Mice were analysed for splenic B-cell reconstitution five weeks post transfer. Results are depicted individually and as an average. Results are representative of two experiments with two to three mice per group.

B Graph illustrating splenic T-cell reconstitution numbers of the ELP, CLP eYFP$^-$ and CLP eYFP$^+$ populations. 2 x 10^3 CLP eYFP$^-$, 2 x 10^3 CLP eYFP$^+$ or 10^3 ELPs from four to six week old *Rag1$^{wt/Cre}$ x Rosa26$^{wt/eYFP}$* mice were injected i.v. into sub-lethally irradiated recipients. Mice were analysed for splenic T-cell reconstitution five weeks post transfer. Results are depicted individually and as an average. Results are representative of two experiments with two to three mice per group.

A

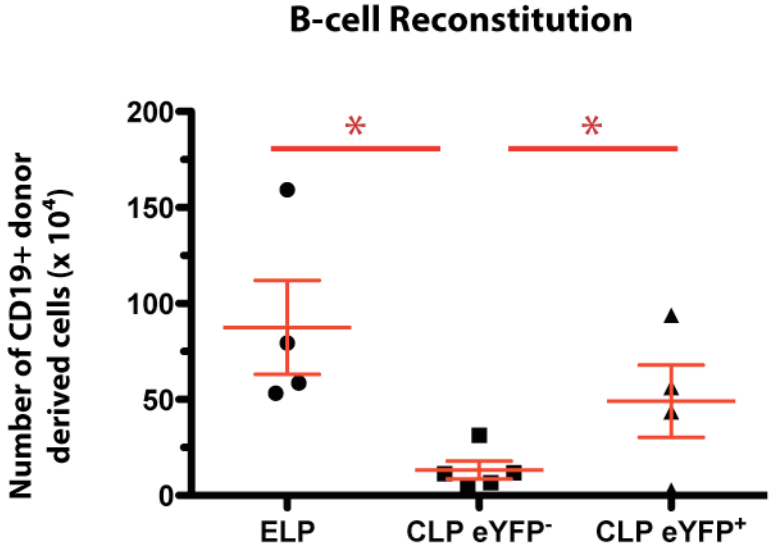
B-cell Reconstitution
Number of CD19+ donor derived cells (x 10⁴)
200
150
100
50
0
*
*
ELP
CLP eYFP⁻
CLP eYFP⁺

B

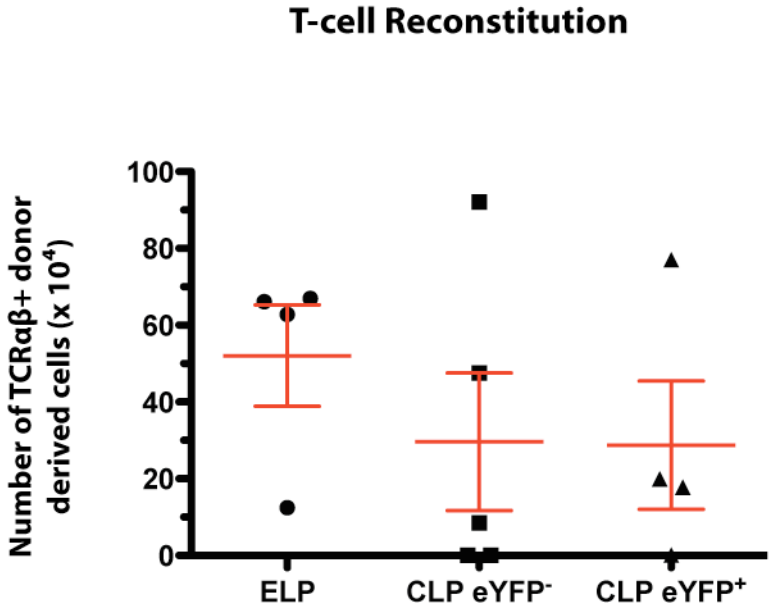
T-cell Reconstitution
Number of TCRαβ+ donor derived cells (x 10⁴)
100
80
60
40
20
0
ELP
CLP eYFP⁻
CLP eYFP⁺

4.5 B-cell developmental potential of ELP, CLP eYFP$^-$ and CLP eYFP$^+$ pools *in vitro*

In order to investigate whether all CLP eYFP$^-$ cells could acquire eYFP during development into B-cells and to assess the rate of kinetics by which B-cells were generated, all three cell populations were sorted from *Rag1*$^{wt/Cre}$ *x Rosa26*$^{wt/eYFP}$ mice and placed on OP9 stromal cells in the presence of IL-7, Flk-2 ligand and SCF (see materials and methods) and analysed after three, five and ten days in culture. Cells expressing CD19 were considered as terminally-committed B-cell progenitors, since *Cd19* is the target gene of the master regulator of B-lineage commitment *Pax5* (reviewed by Maier and Hagman, 2002).

We first examined the generation of B-committed cells from the ELP population. CD19 upregulation on ELP cells was not evident until day ten in culture (Figure 4.10A). Next, we investigated the ability of CLP eYFP$^-$ cells to give rise to B-cells (Figure 4.10B). In the CLP eYFP$^-$ cultures, both eYFP and CD19 expression were measured. These cells upregulated eYFP after just three days in culture and their frequency increased at five and ten days, where the majority of cells had acquired eYFP. CD19 upregulation however was not observed until day ten in this population and interestingly, the frequency of CD19 positive cells was lower than the frequency of cells which had upregulated eYFP$^+$. This indicated that cells had to first upregulate eYFP before committing to the B-cell lineage, a result which was also observed during lineage mapping in the pre-pro B-cell compartment (chapter 3). A representative FACS plot of this developmental relationship, illustrating that only a minute frequency of cells which were CD19$^+$ had not acquired eYFP expression is presented in Figure 4.11A. Both the ELP and the CLP eYFP$^-$ pools exhibited similar frequencies of CD19 expression by day ten, indicating that these two cell pools developed into B-cells *in vitro* with similar

kinetics. In contrast, low level CD19 expression was evident in the CLP eYFP$^+$ pool after just three days and by ten days virtually all cells expressed CD19, to a higher extent than what was observed in ELP or CLP eYFP$^-$ pools (Figure 4.10C). This indicated that the CLP eYFP$^+$ pool was at a later stage of B-lineage development than the other subsets.

We next assessed the number of cells generated throughout the time course from each subset. All three populations exhibited comparable numbers of cells in culture at three and five days, however at day ten significant differences were observed (Figure 4.11B). The number of CLP eYFP$^+$ cells increased over a 100 fold from day five (2 x 10^4 cells) to day ten (4.2 x 10^6 cells), whereas the number of ELP cells increased from 3 x 10^4 cells at day five to 4 x 10^5 cells at day ten, a difference of only 13 fold. In contrast to both the CLP eYFP$^-$ and ELP subsets, the number of CLP eYFP$^-$ cells exhibited only a marginal increase. 1.7 x 10^4 cells were present in culture at day five and this value increased only 3 fold to 5.6 x 10^4 cells at day ten. This observation suggests that the CLP eYFP$^+$ pool proliferated more than the ELP or CLP eYFP$^-$ subsets between day five and day ten in culture, with the CLP eYFP$^-$ exhibiting only minimal proliferation. These results also indicate a 75 fold difference between the number of CLP eYFP$^+$ and CLP eYFP$^-$ cells at day ten, providing evidence that the CLP population is heterogeneous in response to stimuli during *in vitro* culture. In addition, similar to the results obtained *in vivo*, the CLP eYFP$^+$ pool was the first subset to give rise to B-cells; whereas the ELP and CLP eYFP$^-$ pools both exhibited similar kinetics of differentiation, suggestive for a closely related developmental stage. The CLP eYFP$^+$ and ELP pools were proliferating more during B-cell development *in vitro* than the CLP eYFP$^-$ pool and this may have been the reason for the low number of reconstituted splenic B-cells observed *in vivo*. In addition, all CLP eYFP$^-$ cells expressed eYFP

during B-cell development *in vitro*, therefore the lower number of reconstituted B-cells derived from this population *in vivo* could not be attributed to an impaired differentiation into $eYFP^+$ progenitors.

Figure 4.10

Analysis of the B-cell potential of ELP, CLP eYFP$^-$ and CLP eYFP$^+$ populations in vitro.

A Representative FACS plot showing the upregulation of CD19 on ELP cells, isolated from the BM of *Rag1$^{wt/Cre}$ x Rosa26$^{wt/eYFP}$* mice and placed on sub-confluent OP9 stromal cells. B-cell development was analysed after three, five and ten days in culture. Results are representative for three independent experiments.

B Representative FACS plot showing the upregulation of eYFP and CD19 on CLP eYFP$^-$ cells, isolated from the BM of *Rag1$^{wt/Cre}$ x Rosa26$^{wt/eYFP}$* mice and placed on sub-confluent OP9 stromal cells. B-cell development was analysed after three, five and ten days in culture. Results are representative for three independent experiments.

C Representative FACS plot showing the upregulation of CD19 on CLP eYFP$^+$ cells, isolated from the BM of *Rag1$^{wt/Cre}$ x Rosa26$^{wt/eYFP}$* mice and placed on sub-confluent OP9 stromal cells. B-cell development was analysed after three, five and ten days in culture. Results are representative for three independent experiments.

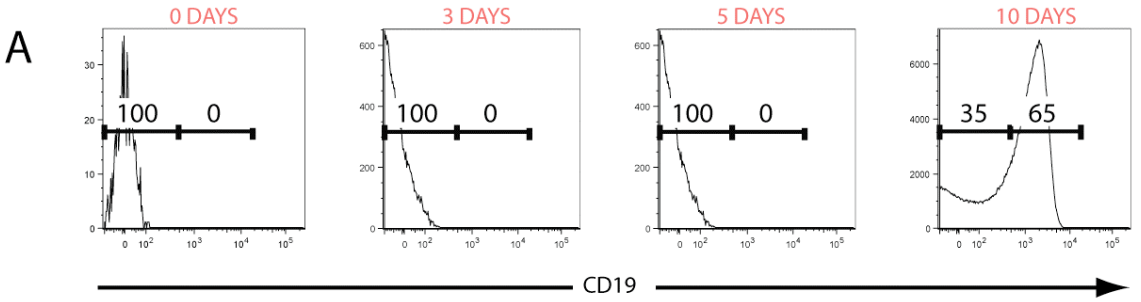
A
0 DAYS
3 DAYS
5 DAYS
10 DAYS
100 0
100 0
100 0
35 65
CD19

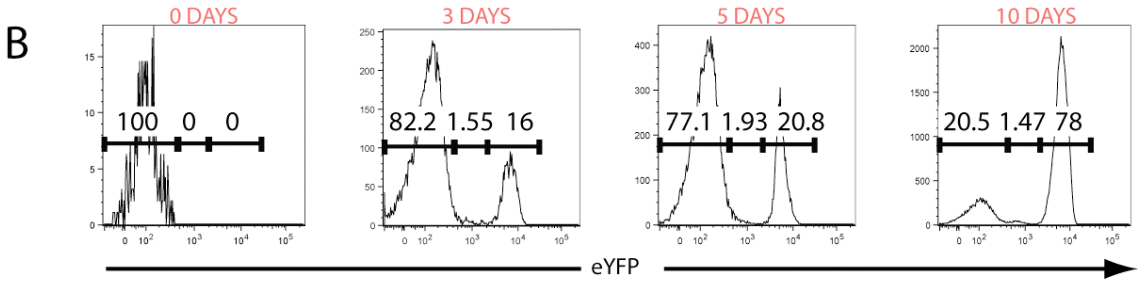
B
0 DAYS
3 DAYS
5 DAYS
10 DAYS
100 0 0
82.2 1.55 16
77.1 1.93 20.8
20.5 1.47 78
eYFP

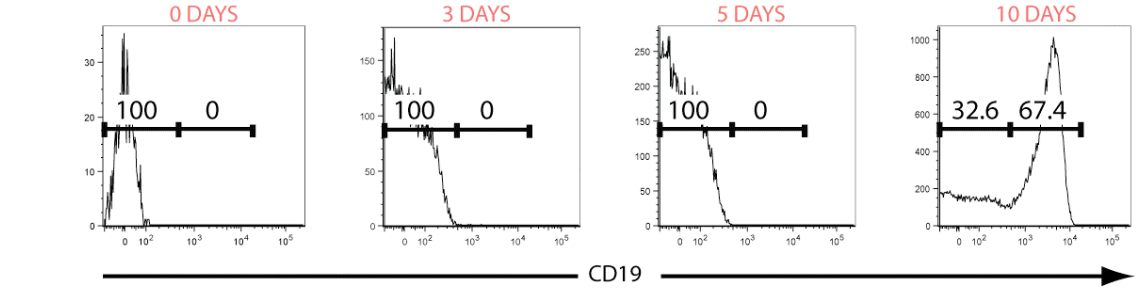
0 DAYS
3 DAYS
5 DAYS
10 DAYS
100 0
100 0
100 0
32.6 67.4
CD19

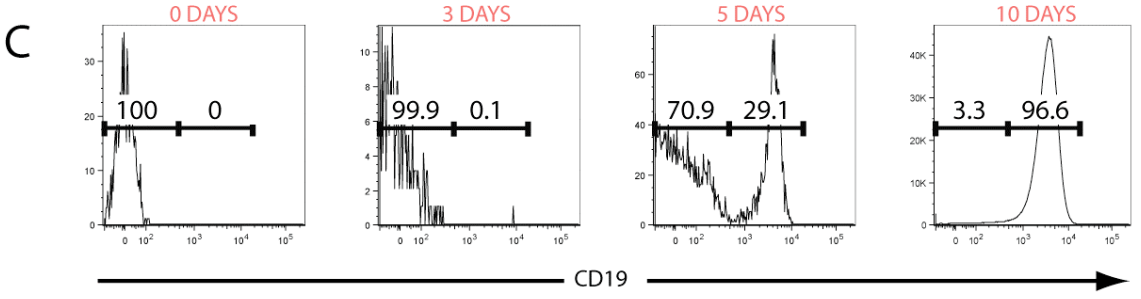
C
0 DAYS
3 DAYS
5 DAYS
10 DAYS
100 0
99.9 0.1
70.9 29.1
3.3 96.6
CD19

Figure 4.11

Sequence of B-cell development in lymphoid progenitors obtained from Rag1$^{wt/Cre}$ x Rosa26$^{wt/eYFP}$ reporter mice in vitro.

A Representative FACS plot illustrating CD19 expression in the CLP eYFP^{-} population after ten days in culture. Cells were co-incubated on GFP^{+} OP9 stromal cells and kinetics of B-cell differentiation were assessed. Stroma cells were excluded from the analysis by gating on GFP^{-} cells. Sample is representative for three independent experiments.

B Graph illustrating the absolute number of ELP, CLP eYFP^{-} and CLP eYFP^{+} cells in culture over time. Time in days is plotted against a logarithmic scale of the number of cells. Results are representative for three independent experiments.

A

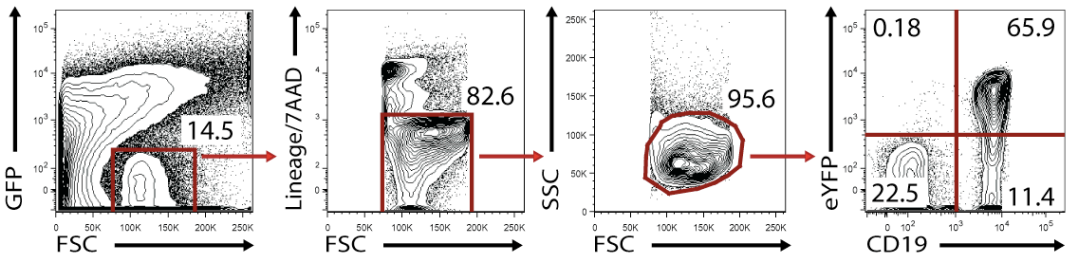
GFP
FSC
14.5
Lineage/7AAD
FSC
82.6
SSC
FSC
95.6
eYFP
CD19
0.18
65.9
22.5
11.4

B

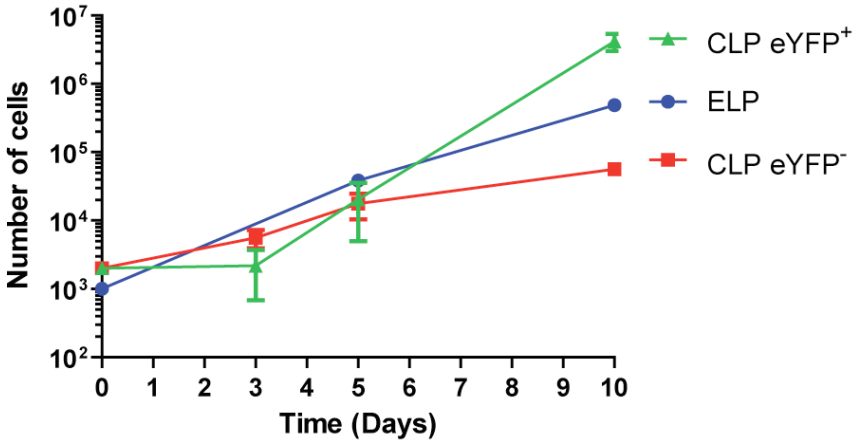
Number of cells
Time (Days)
CLP eYFP+
ELP
CLP eYFP-

4.6 Discussion

Currently there are conflicting views in the literature regarding which BM-derived progenitors enter the circulation and seed the thymus, thereby giving rise to ETPs. Whilst some authors favour a model with the CLP representing the main lymphoid restricted progenitor pool which develops into ETPs, others have suggested that LMPPs and ELPs are more likely to be pre-thymic progenitors due to their similar phenotype and functional potential. We attempted to address this question by assessing the functional potential of the ELP and CLP populations. Utilising a novel lineage tracing reporter model whereby *Rag1* expression would result in permanently marking all cells and their products by eYFP, we were able to identify an 'ELP analogue' population and dissect the CLP population into $eYFP^{+}$ and $eYFP^{-}$ subsets. We compared the functional potential of these populations *in vivo* and *in vitro* in order to determine potential precursor-product relationships and further elucidate lymphoid progenitor pathways.

We first compared the functional potential of the 'ELP analogue' with the published results for the original ELP by transfer into alymphoid recipients. We opted to use *Rag2/Il2rg*-null mice as hosts since this strain allows good engraftment of developing lymphoid progenitors and a superior read-out for non-lymphoid potential of transferred material (Colucci et al., 1999). The *Rag2* gene is indispensable for the somatic rearrangement of B- and T-cell receptor gene segments during B- and T-cell development and the common cytokine receptor γ chain is a functional subunit of the receptors for IL-2, IL-4, IL-7, IL-9 and IL-15 and is required for the development of B-, T- and NK-cells (Di Santo et al., 1995). Therefore, mice deficient in both these genes lack mature B-, T- and NK-cells and have a reduced number of lymphoid progenitor cells, which limits competition for developmental niches following transfer of ELP or CLP populations.

Reconstitution analysis revealed that the 'ELP analogue' gave rise to NK-, B- and T-cells, corresponding to what was found by Igarashi and colleagues (Igarashi et al., 2002). NK and B-cells were present in the BM and spleen at three and five weeks post transfer but T-cells were not evident in the thymus and spleen until five weeks post transfer. Furthermore, we did not observe any significant reconstitution of myeloid lineages in our experiments, in agreement with published results (Igarashi et al., 2002). Based on this, we concluded that the 'ELP analogue' was functionally and phenotypically largely identical to the ELP.

We next compared the cellular reconstitution of the 'ELP analogue' to the CLP and also assessed the CLP population for putative myeloid potential. We found that the CLP population exhibited T-, B- and NK-cell reconstitution in agreement with its original description (Kondo et al., 1997) and similar to the observed reconstitution of the 'ELP analogue'. However, both B- and T-cell reconstitution occurred earlier in recipients reconstituted with CLP cells compared to mice transplanted with the 'ELP analogue'. This suggested that the CLP was at a developmentally later stage than the ELP analogue, which seems to be arguably in favour for a hierarchical model of progenitor development. In addition, we observed the presence of donor-derived myeloid cells at four weeks post CLP transfer, which is conflicting with the findings of Kondo et al (Kondo et al., 1997). This myeloid potential of the CLP may have been due to a lack of alternate cell types in the BM at later time points and a subsequent increase in the percentage of donor-derived myeloid cells. In this context it is of importance that myelopoiesis in general is relatively rapid compared to lymphopoiesis. In transplantation experiments, the CMP population develops into myeloid cells after just six days (Akashi et al., 2000) and the LMPP population after just one week (Adolfsson et al., 2001). We injected CLP cells into *Rag2/Il2rg*-null mice, which lack all mature

lymphoid cells, but retain all myeloid cells. Therefore, graft-derived differentiation in this strain would be competing with endogenous myelopoiesis. Due to CLP-derived myelopoiesis not appearing until four weeks after transplantation in our experiments, it is unlikely that the CLP possessed significant myeloid reconstitution. Furthermore, because the 'ELP analogue' appeared to be at an earlier stage of development than the CLP, indicating that it may be a direct precursor of the CLP pool, and lacked any myeloid potential *in vivo*, it is unlikely that the CLP population retained myeloid potential. However, because there was some evidence for myeloid reconstitution, we cannot completely rule out the fact that the CLP contains minimal myeloid potential which is only observed after the production of all other cells.

To investigate the lymphoid potential of the CLP population more rigorously, we dissected the CLP based on reporter expression in *Rag1*$^{wt/Cre}$ *x Rosa26*$^{wt/eYFP}$ mice and analysed their functional potential *in vivo* and *in vitro*. We found that *in vivo*, the CLP eYFP^{+} and the ELP generated similar numbers of splenic B-cells, which were significantly higher than the number of donor-derived splenic B-cells generated from the CLP eYFP^{-} pool. This suggested that ELP and CLP eYFP^{+} subsets harbour a stronger constitutive potential to generate B-cells *in vivo*. This result is remarkably similar to more recent observations (Inlay et al., 2008), reporting that Ly6D^{+} CLPs predominantly gave rise to B-cells *in vivo*, as we observed with eYFP^{+} CLPs, indicating that both Ly6D and eYFP markers could be used to separate functional different subsets of CLPs. Alternatively, the low number of splenic B-cells generated from CLP eYFP^{-} cells could indicate that only a small fraction of this population *in vivo* develops into B-cells. Furthermore, the CLP eYFP^{-} population might not have proliferated as extensively during B-cell development than the CLP eYFP^{+} and ELP pools, or migrated and seeded the BM and spleen as efficiently.

To gain further information as to the kinetics of B-lineage differentiation between the three subsets, we also analysed their B-cell potential *in vitro*. The results indicated that the CLP eYFP$^+$ pool gave rise to B-cells with faster kinetics than either the CLP eYFP$^-$ or ELP pools, indicating that the CLP eYFP$^+$ subset was at a later developmental stage than the ELP and CLP eYFP$^-$ subsets and possibly already primed for B-lineage commitment. Månsson et al., (Månsson et al., 2010) also reported heterogeneity within the CLP using *Rag1*^{GFP} mice which were crossed to mice expressing human CD25 under the control of the mouse *λ5* promoter. They divided the CLP into GFP^{lo} and GFP^{hi} cells and reported that GFP^{hi} CLPs generated CD19$^+$ cells already after 2.25 days in culture, whereas the GFP^{lo} cells took 6.25 days to upregulate CD19. This group also reported a significant upregulation of *Pax5* and *Ebf1* in the GFP^{hi} cells as compared to the GFP^{lo} cells, both genes indicative of B-cell development. This report suggests that the CLP eYFP$^+$ pool is already specified to the B-lineage due to the expression of B-lineage genes. In addition, in our hands, the ELP and CLP YFP$^-$ pools appeared to be at a similar stage of lymphoid development due to B-cell commitment occurring at day ten in both cell populations.

The number of CLP eYFP$^+$ cells in culture also rapidly increased throughout the time course, as did the ELP population, but not to the extent of the CLP eYFP$^+$ population. In contrast there was no major increase in the number of CLP eYFP$^-$ cells. This suggested that the CLP eYFP$^+$ and ELP fractions proliferated more during B-cell development than the CLP eYFP$^-$ pool and may have been the reason for the observed higher number of splenic B-cells reconstituted *in vivo*. The *in vitro* data also showed that eYFP$^-$ CLP cells first upregulated eYFP before committing to the B-cell lineage, indicative of a precursor-product relationship between the CLP eYFP$^-$ and CLP eYFP$^+$ pools. Due to all cells of the ELP population already expressing eYFP, this pool might develop

directly into the CLP eYFP$^+$ pool (see proposed model of B-lineage development). In agreement with Schwarz and Bhandoola (Schwarz and Bhandoola, 2004) and Allman and colleagues (Allman et al., 2003), these results suggest that CLP eYFP$^+$ cells represent the main B-cell precursors, which is also in accordance with our results showing that pre-pro B-cells *ex vivo* were derived predominantly from eYFP$^+$ precursors. Similar to our data, a recent report (Welner et al., 2009) demonstrated that in *Rag1*$^{wt/Cre}$ *x Rosa26* $^{wt/tdRFP}$ reporter mice, only 50% of the CLP compartment was marked. The same group found that the CLP RFP$^+$ cohort *in vitro* proliferated to a higher extent and gave rise to CD19$^+$ B-cells prior to the CLP RFP$^-$ population.

The *in vivo* and *in vitro* data combined indicated that ELP and CLP eYFP$^+$ populations were able to give rise to a higher number of B-cells both *in vitro* and *in vivo* than the CLP eYFP$^-$ pool. In addition they suggest the CLP eYFP$^+$ subset was at a later stage of lymphoid development than both the ELP and CLP eYFP$^-$ pools. Taking into consideration that the CLP pool could also be divided based on the expression of Ly6D (Inlay et al., 2009), we proposed that both eYFP and Ly6D markers could be utilised to illustrate the development from lymphoid progenitors into pre-pro B-cells. Therefore, we analysed the expression of both eYFP and Ly6D on CLP cells, but found that expression of the two markers did not correlate (see proposed model of B-lineage development). Nevertheless, both markers could be used to signify development down the B-lineage pathway.

Proposed model of B-lineage development

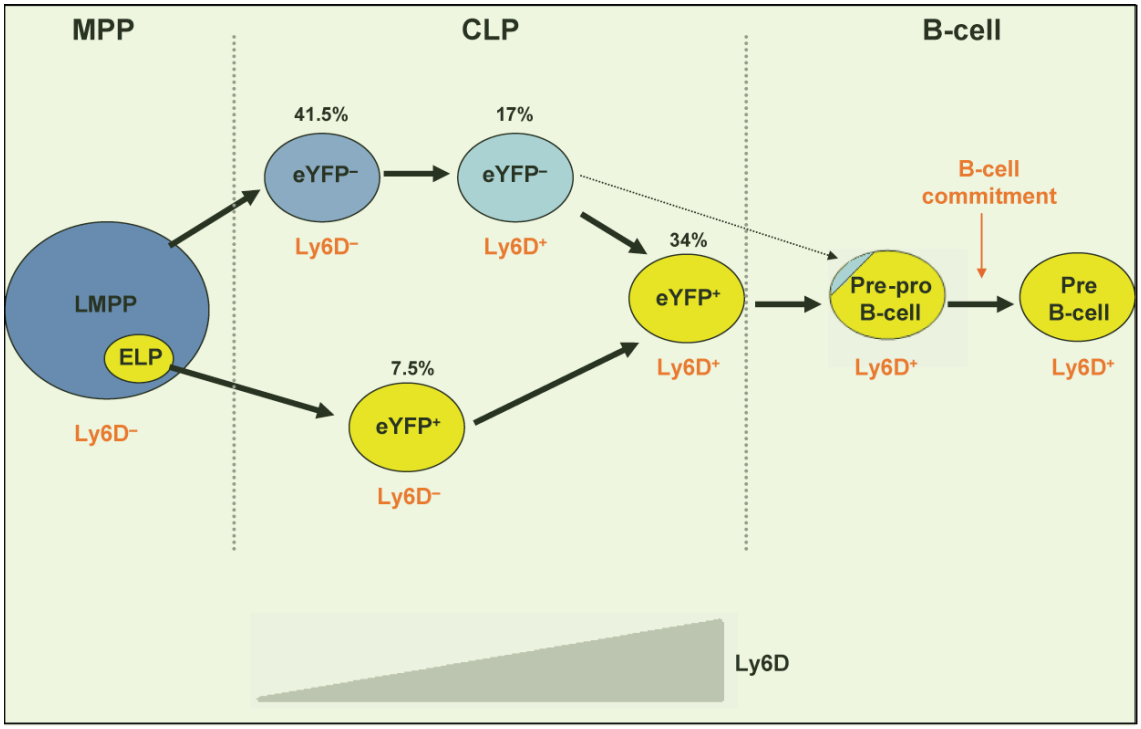

We also compared all three populations with respect to T-cell development. Unlike B-cell differentiation *in vivo,* the number of reconstituted splenic T-cells was similar between the three subsets. Therefore, this indicated that a similar number of T-cells had been produced in the thymus and exported to the spleen from each subset, showing that all three populations had T-cell potential. This result is in good agreement with our observation that *Gata3* mRNA levels in all three populations were identical and therefore no genetic preference for T-cell development was obvious.

However, we cannot completely rule out the fact that the three cell populations - ELP, CLP eYFP^{-} and CLP eYFP^{+} - may not have migrated and seeded the organs with the same efficiency, despite functional potential being assessed under the same conditions. This might explain the low number of reconstituted splenic B-cells generated from the

CLP eYFP$^-$ fraction, compared to the CLP eYFP$^+$ and ELP subsets. One possible explanation for these observations – apart from the aforementioned – could be the presence of non - T/B-cell potential such as NK and DC potential in the CLP eYFP$^-$ pool.

Regarding the relevant contributions of all three entities to thymopoiesis, our lineage mapping data suggests that ETPs were derived predominantly from eYFP$^+$ progenitor cells. Despite that, upon transfer into alymphoid recipients *in vivo,* all ELP, CLP eYFP$^-$ and CLP eYFP$^+$ populations could give rise to ETPs (see proposed model of lymphoid development below). Similar to B-lineage development, we also based T-cell development on Ly6D expression. Based on the fact that ETPs expressed only low levels of Ly6D (Inlay et al., 2009), we proposed that only Ly6D$^-$ progenitors could produce ETPs. In addition, due to ELPs being a subpopulation of the LMPP, this population may also contain T-cell potential.

Proposed model of lymphoid development

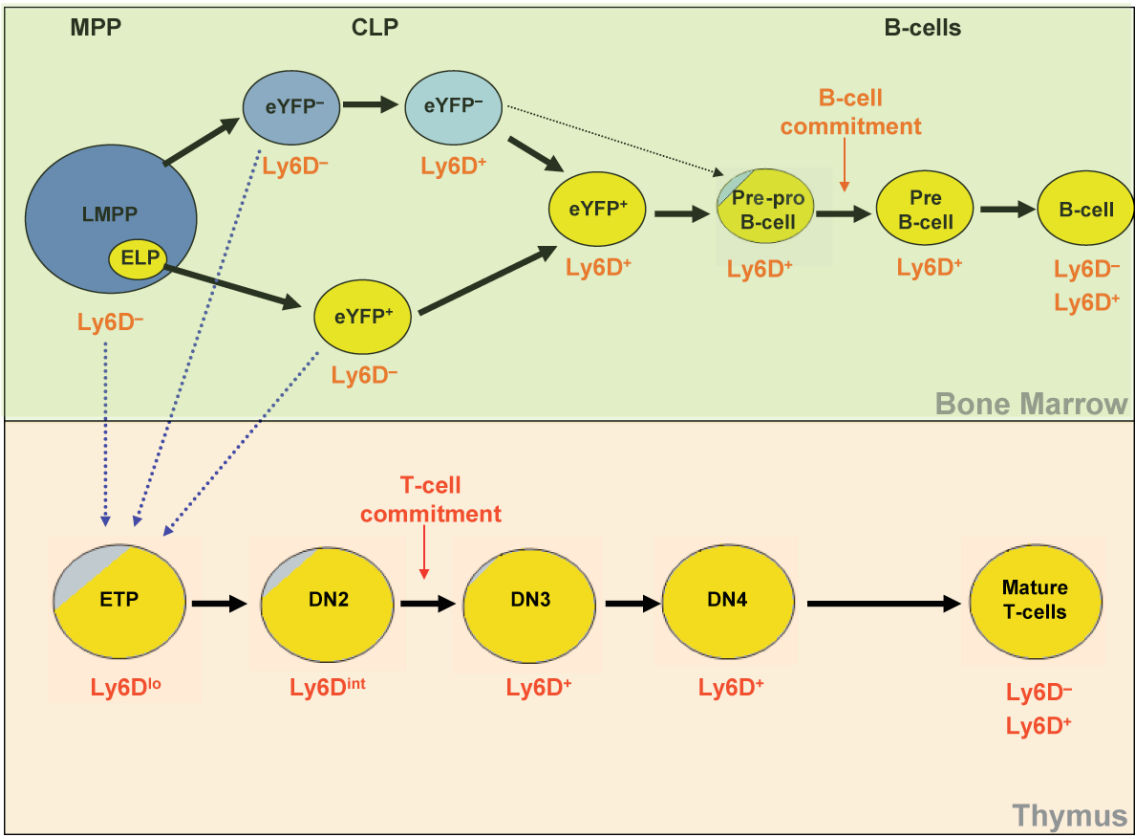

During the last three decades, several models of haematopoiesis have been proposed. The 'classical model' of haematopoiesis was proposed just after the finding that T-, B- and myeloid cells were all derived from HSCs (Abramson et al., 1977) and suggested a dichotomy between the myelo-erythroid and lymphoid lineages. However, this assumption was based on microscopic observations and a limited number of experimental findings.

In 1983, the stochastic model of haematopoiesis was introduced in which lineage determination is completely random (Ogawa et al., 1983), a model which is evidently at odds with observations that multipotent progenitors become gradually more restricted

towards a particular lineage by expressing lineage specific transcription factors and by responding to lineage promoting cytokines.

The sequential restriction model (Brown et al., 1985) suggested a defined sequence whereby if progenitor cells were exposed to various inducers of differentiation they would undergo development down a particular pathway. However, progenitor cells which did not encounter any signal for differentiation down that lineage would continue on to the next sequence of development. A cell could first make erythroid, then myeloid, B- and finally T-cells. This model does not sufficiently explain the existence of LMPP cells which can generate lymphoid and myeloid cells, but not erythroid cells.

In 2001, the myeloid-based model of haematopoiesis (Katsura et al., 2001) was proposed. This model postulated that HSCs first diverged into a common myelo/lymphoid progenitor which then generated myelo/T- and myelo/B- progenitors capable of giving rise to B-, T- and myeloid cells. There is evidence that this sequence of events occurs in human haematopoiesis (Doulatov et al,, 2010) and in the foetal liver of mice (Lu et al., 2002). Unfortunately this model seems to be in conflict with the presence of the CLP population (Kondo et al., 1997) and later the ELP (Igarashi et al., 2002) and LMPP (Adolfsson et al., 2005) populations since these cell types can produce both T- and B-cells with a gradual decrease in their myeloid potential. Although the LMPP population contains both lymphoid and myeloid potential and could be viewed as the common myelo/lymphoid progenitor proposed by Katsura et al., the ELP is a subpopulation of the LMPP and contains no detectable myeloid potential *in vivo* (Igarashi et al., 2002 and our data), suggesting that lymphoid progenitors lose myeloid potential and gradually become restricted to the lymphoid lineage. In addition, the detectable myeloid potential in the ETP (Wada et al., 2008; Bell and Bhandoola, 2008)

which also supports the model of Katsura et al. can be explained by the fact that the LMPP cells probably migrate to the thymus and form ETPs.

A modified version of the classical model of haematopoiesis was proposed in 2005 by Adolfsson and colleagues (Adolfsson et al., 2005) which incorporated the LMPP population and in 2007 by Ye and Graf (Ye and Graf, 2007), incorporating both the ELP and LMPP populations. Our model supports a similar scheme of development, but with the refinement of a subdivision of the CLP. We propose that the $eYFP^+$ CLP is likely to be the main pool for B-cell development. Both the ELP and CLP $eYFP^–$ populations must develop into the CLP $eYFP^+$ pool before committing to the B-cell lineage. However, all ELP, CLP $eYFP^–$ and CLP $eYFP^+$ populations can give rise to ETPs and further develop into T-cells. In addition, because the ELP is a subpopulation of the LMPP, this population is also potentially a pre-thymic progenitor. It has to be stressed that our proposed model represents a scheme of lymphoid development under homeostatic conditions. Under conditions resulting in significant alterations in the generation and/or turnover of specific subsets, as observed in acute or chronic infection, the pathways of cellular differentiation may exhibit a considerable degree of plasticity.

CHAPTER 5

THE EFFECT OF AN ACUTE INFLAMMATORY RESPONSE ON THE COMPOSITION OF HAEMATOPOIETIC PROGENITOR COMPARTMENTS

5.1 Introduction

We next investigated the effects of inflammation on the composition of haematopoietic progenitor compartments and tried to define the molecular mechanism involved in the process. Previous models of bacterial-induced inflammation have reported decreased output of both BM myelopoiesis and lymphopoiesis and phenotypic changes in stem and progenitor compartments. A bacterial model of infection using *Staphylococcus aureus* (Scumpia et al., 2010) resulted in an expansion of the LSK compartment. To define the mechanism involved in this expansion, mice deficient for components of the TLR4 signalling pathway were analysed. *Myd88*-null, *Trif*-null or *Myd88*/*Trif* -null mice were infected, however there was no change in the increased frequency and number of LSK cells. This indicated that TLR signalling was not required in response to *Staphylococcus aureus* infection. This group additionally investigated the effect of polymicrobial sepsis induced by cecal ligation puncture on haematopoietic progenitor cells. They observed a tripling in the number of LSK cells and a subsequent increase in the frequency of ST-HSCs and LT-HSCs, which was also not altered in *Myd88*-null mice, or during blockade of TNFα, IL-1, IL-6 and IFNα inflammatory cytokines. A decrease in the number of BM B-cells and upstream CLP cells was also reported which was due in part to TLR4 signalling as *Myd88*-null mice displayed a delay in pre B-cell depletion. This indicated that the TLR4 pathway was partially responsible for the reduction in B-cells during infection, but did not alter the phenotype of earlier haematopoietic subsets. A decrease in the number of myeloid progenitor cells was also observed. However a previous report (Delano et al., 2007) suggests that this may be due to myeloid progenitor cells being exported to the periphery.

In a bacterial infection model using *E. coli* (Zhang et al., 2008), the same expansion of the LSK compartment was observed and there was an increase in the number of LSK

cells incorporating 5-bromo-2'-deoxyuridine (BrdU) after infection, indicating that these cells had a higher proliferation rate than control cells. In contrast, there was a decrease in the LIN$^-$ c-kit^{hi} Sca-1$^-$ compartment. *In vitro* culture of LIN$^-$ c-kit^{hi} Sca-1$^-$ cells with plasma of *E. coli* infected mice resulted in a significant increase in the number of LSK cells, and the authors suggested that the reason for the expansion observed in the LSK compartment may have been due to LIN$^-$ c-kit^{hi} Sca-1$^-$ cells inverting their phenotype. The same could also be observed after culture with LPS, TNFα, IL-6 and IFNγ. After placing the 'inverted' cells in semi-solid medium, which supports the growth of CFU-granulocyte/erythrocyte/macrophage/megakaryocyte (CFU-GEMM), there was increased CFU-GM activity. Therefore there appeared to always be a decrease in the number of LIN$^-$ c-kit^{hi} Sca-1$^-$ cells during bacterial infection, representing myeloid progenitors during homeostatic conditions, and a subsequent increase in the frequency and number of LSK cells, which appeared to retain myeloid potential. However, bacterial-induced inflammatory changes in haematopoietic progenitor compartments could not be attributed to any specific mechanism.

In order to determine this, we created a model of acute inflammation by injecting a sub-lethal dose of endotoxin from *Salmonella minnesota* into C57BL/6 mice. LPS is present in the outer membrane of all gram negative bacteria and is the component by which host cells recognise bacteria (reviewed by Freudenberg and Galanos, 1990), therefore we opted to use pure LPS to elicit an inflammatory response. One advantage of using LPS as opposed to the complete bacterium is that signalling mechanisms and their impact on innate immune responses have been extensively investigated.

The interaction of LPS with cells of the innate immune system leads to the release of endogenous cytokines, which initiates inflammatory responses essential for antibacterial defence (Beutler et al., 2003). The release of high concentrations of these cytokines

however can cause toxic shock (Karima et al., 1999). Some of these symptoms include fever, nausea, leukopenia, thrombocytopenia and organ failure (Morrison et al., 1979). Due to the discovery that C3H/HeJ mice were non-responsive to LPS, owing to a mutation in the *Tlr4* gene, TLR4 has been recognised as the signalling protein by which LPS activates cells (Poltorak et al., 1998). LPS consists of three parts; a lipid A, a core oligosaccharide and an O side chain. It is lipid A which binds to TLR4 and causes inflammatory effects. TLR4, predominantly expressed on macrophages and DCs, recognises LPS (Hoshino et al., 1999) with the aid of CD14, MD-2 and LPS-binding protein (LBP; Shimazu et al., 1999), and signals via the MyD88 or TRIF pathways, subsequently activating NFκB and inducing the production of TNFα. The primary source of TNFα is macrophages (Rosenstreich et al., 1980) and this cytokine is the primary mediator of the lethal action of endotoxin (Beutler et al., 1985). During this inflammatory process, TNFα may be inducing changes in the proliferation and differentiation of haematopoietic progenitors. One report showed that TNFα could inhibit the proliferation of HSCs *in vitro* (Zhang et al., 1995). However, TNFα has also been suggested to cause proliferation of HSCs (Rezzoug et al., 2008). Rezzoug and colleagues found that TNFα increased the proliferation and differentiation of HSCs into multipotent progenitors *in vitro* and inhibited the apoptosis of HSCs *in vivo*. Therefore, the effect of TNFα on haematopoietic progenitor cells during inflammation remains unclear.

The effects of LPS on haematopoietic progenitor cells have been studied by some groups (Scumpia et al., 2010; Welner et al., 2009). Scumpia and colleagues found that injection of 5μg LPS into mice caused a transient increase in the frequency of LSK populations which began at 18 hours post injection and lasted 72 hours. The authors deduced that this was due to an increase in LT-HSC and ST-HSC compartments. This

expansion was also observed in *Ifnαr*-null mice indicating that IFNα was not the only cytokine responsible, however the exact mechanism was not studied. Therefore, we aimed to investigate the effects of LPS on all haematopoietic progenitor populations, as well as mature cells in the circulation and determine the cause of inflammation-induced changes.

5.2 Analysis of the body temperature and circulating RBC and WBC number of C57BL/6 mice during LPS challenge

Since high amounts of LPS causes endotoxic shock which results in death, we studied the effect of a sub-lethal dose of LPS. One symptom of septic shock is a change in body temperature, therefore to compare the lower concentration of LPS used in our studies, we monitored this parameter. As Figure 5.1A shows, there were no major differences in the temperature of LPS injected mice in comparison to control mice. We next looked at the number of circulating red and white blood cells during LPS challenge. There were also no major differences in the number of circulating RBCs in mice injected with LPS compared to control mice (Figure 5.1B). In contrast, there were clear differences in the number of circulating granulocytes and lymphocytes (Figure 5.2). These numbers were also different between male and female mice.

As illustrated in Figure 5.2A, there was a mobilisation of granulocytes into the circulation in male mice 3.5 hours post LPS injection. The number of granulocytes in the peripheral blood increased significantly from $1.68 \pm 0.16 \times 10^9$/l at control levels to $7.98 \pm 1.17 \times 10^9$/l after 3.5 hours. In female mice however, this was not evident until after seven hours, where an increase from $1.68 \pm 0.16 \times 10^9$/l at control levels to $11.3 \pm 1.61 \times 10^9$/l could be observed. This indicated a delay in the increase of circulating granulocytes in response to LPS in females compared to male mice. In both genders, the number of granulocytes increased continually until 12 hours post injection, when both female number ($11.45 \pm 1.92 \times 10^9$/l) and male number ($15.33 \pm 2.45 \times 10^9$/l) reached their maximum. Granulocyte numbers had returned to steady state levels by 48 hours in female mice ($1.83 \pm 1.79 \times 10^9$/l), whereas it took until 72 hours for numbers in male mice ($2.83 \pm 1.8 \times 10^9$/l) to reach homeostatic levels. This observation indicated that neutrophils were being mobilised into the circulation in both male and female mice, but

male mice were more efficient in mobilising granulocytes and in reaching a higher number in peripheral blood.

We next observed the effect of LPS on circulating lymphocytes. In male and female mice, there was a significant decrease in the number of lymphocytes immediately after LPS challenge (Figure 5.2B). The number of lymphocytes in male mice had decreased from 11.46 ± 0.39 x 10^9/l at control levels to 4.62 ± 0.34 x 10^9/l after just 3.5 hours, whilst female numbers declined from 10 ± 2.12 x 10^9/l at control levels to 1.9 ± 0.4 x 10^9/l. The number of lymphocytes in female mice had returned to homeostatic levels by 72 hours (11.43 ± 1.25 x 10^9/l), but more time was required in male mice.

We also analysed the number of circulating monocytes (Figure 5.2C) and observed only minor changes between LPS injected and control mice. A significant decrease in the number of monocytes was observed in male and female mice at 3.5 hours post LPS injection and there was a significant increase in the number of monocytes at 48 hours post injection in male mice, however at all other time points there were no significant differences.

Figure 5.1

Body temperature and number of circulating RBCs in C57BL/6 mice injected with LPS as compared to control mice.

A Graph illustrating the effect of a sub-lethal dose of LPS on the body temperature of C57BL/6 mice, aged eight weeks of age. Control mice were injected with double distilled water. Data are representative of three independent experiments, using 24 mice per group. Values represent mean ± S.E.M.

B Graph illustrating the effect of a sub-lethal dose of LPS challenge on the circulating RBC number of C57BL/6 mice, aged eight weeks of age. Control mice were injected with double distilled water. The number of circulating RBCs did not enter outside of the physiological range during LPS challenge, therefore no anaemia was observed. Data are representative of four independent experiments, using one to six mice per group. Values represent mean ± S.E.M.

A

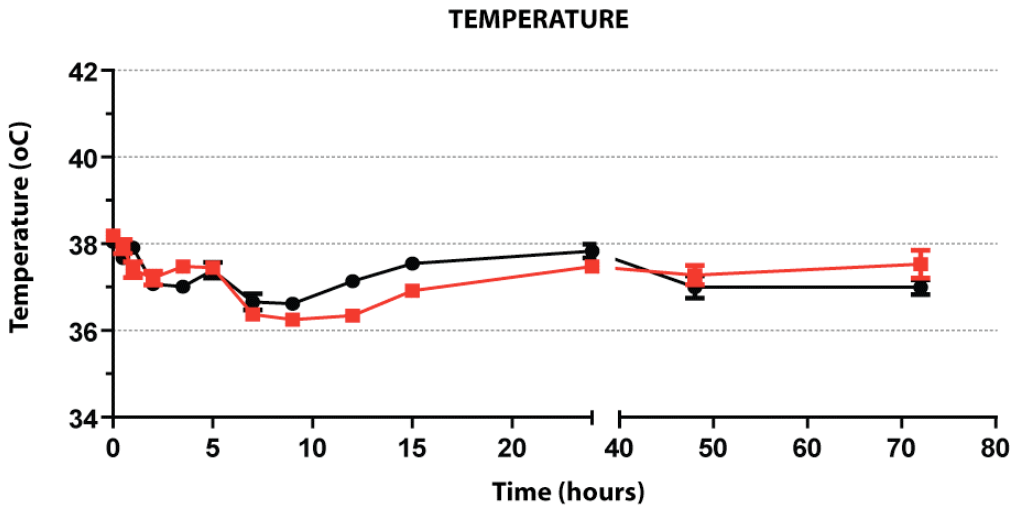
TEMPERATURE
Temperature (oC)
42
40
38
36
34
0
5
10
15
20
40
50
60
70
80
Time (hours)

B

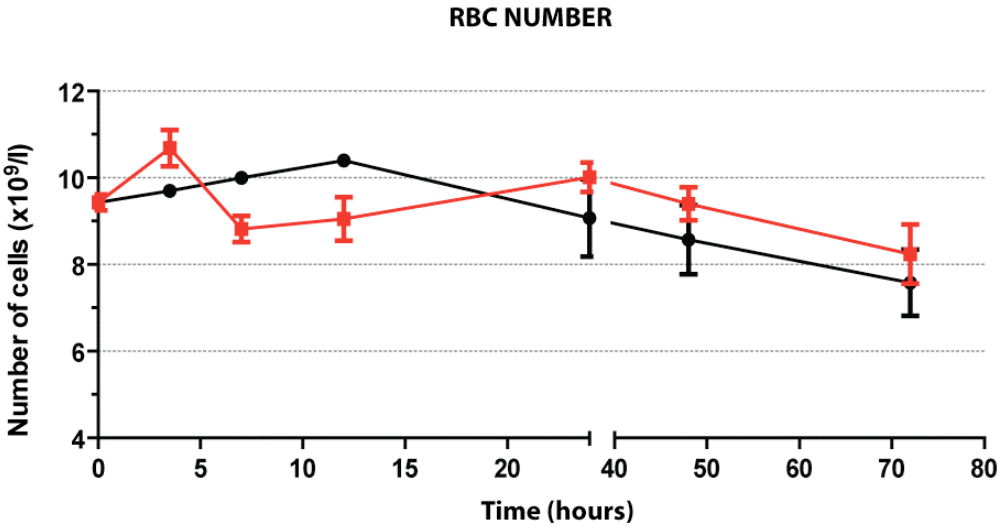
RBC NUMBER
Number of cells (x10^9/l)
12
10
8
6
4
0
5
10
15
20
40
50
60
70
80
Time (hours)

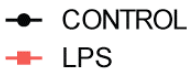
CONTROL
LPS

Figure 5.2

Number of circulating granulocytes, lymphocytes and monocytes compared between LPS injected and control C57BL/6 mice.

A Graph illustrating the number of circulating granulocytes in male (red line) and female (blue line) mice aged eight weeks of age, after LPS challenge. Control mice were injected with double distilled water (black line). Data represents results from two independent male experiments and one independent female experiment, using three to five mice per time point. Significance was calculated using the Student's T-test ($p < 0.05$). Values represent mean ± S.E.M.

B Graph illustrating the number of circulating lymphocytes in male (red line) and female mice (blue line) aged eight weeks of age, after LPS challenge. Control mice were injected with double distilled water (black line). Data represents results from two independent male experiments and one independent female experiment, using three to five mice per time point. Significance was calculated using the Student's T-test ($p < 0.05$). Values represent mean ± S.E.M.

C Graph illustrating the number of circulating monocytes in male (red line) and female mice (blue line) aged eight weeks of age, after LPS challenge. Control mice were injected with double distilled water (black line). Data represents results from two independent male experiments and one independent female experiment, using three to five mice per time point. Significance was calculated using the Student's T-test ($p < 0.05$). Values represent mean ± S.E.M.

A

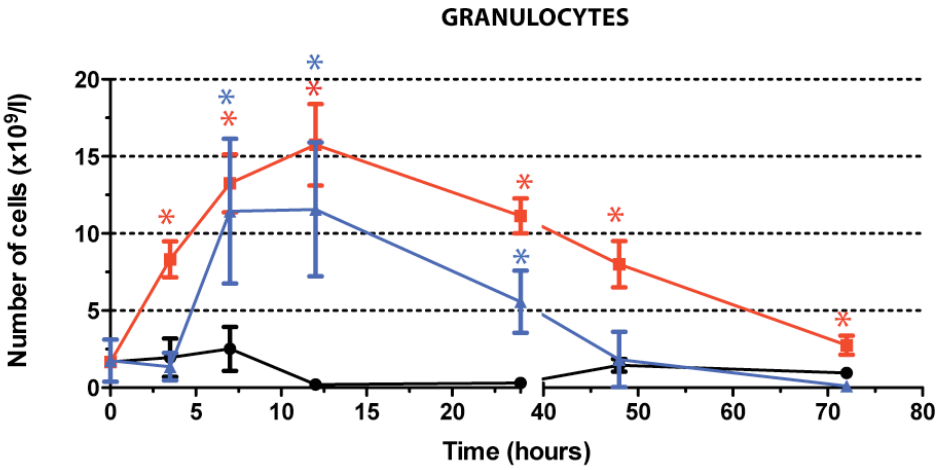
GRANULOCYTES
Number of cells (x10⁹/l)
Time (hours)

B

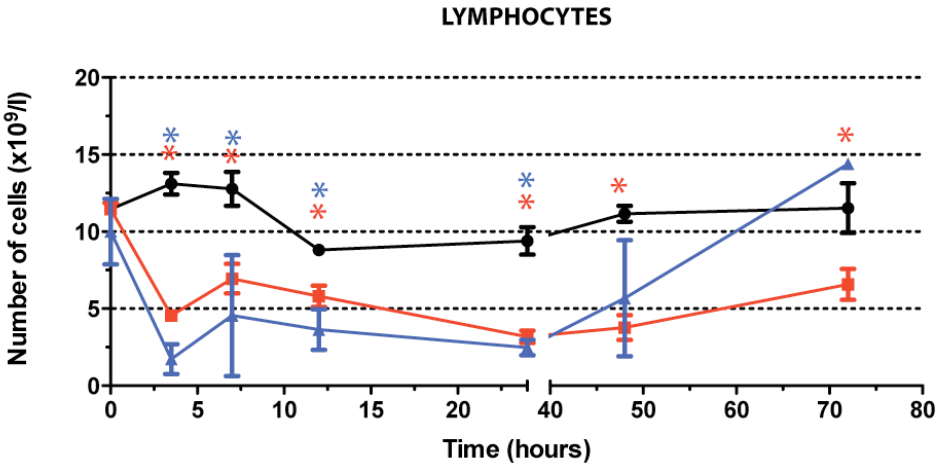
LYMPHOCYTES
Number of cells (x10⁹/l)
Time (hours)

C

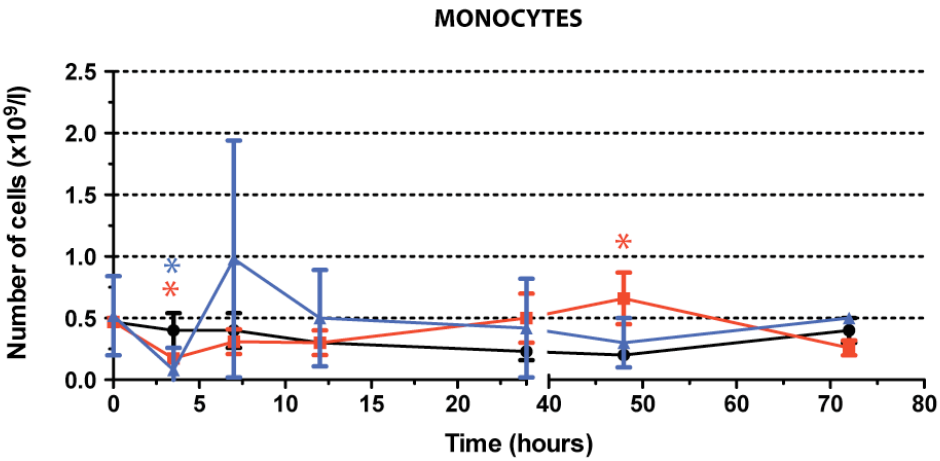
MONOCYTES
Number of cells (x10⁹/l)
Time (hours)

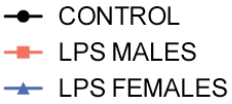
CONTROL
LPS MALES
LPS FEMALES

5.3 The effects of LPS challenge on the frequency of mature myeloid and B-cells in the BM

Based on the observations that there were an increased number of circulating granulocytes and a decrease in the number of circulating lymphocytes, we investigated whether the changes in these numbers could be due to alterations in the output of BM cells. In the following all numbers for BM cells are given per femur pair. We found that the total number of BM cells was reduced significantly throughout the time course (Figure 5.3). At 12 hours post LPS injection, there was a significant decrease in the number of cells from $3.4 \times 10^7 \pm 0.19 \times 10^7$ to $2.1 \times 10^7 \pm 0.2 \times 10^7$. This number remained low at 24 hours but had returned to homeostatic levels by 72 hours. Therefore, this indicated that cells from the BM may have been exported to the periphery between 12 and 24 hours post LPS challenge.

We next explored whether these cells may have been BM neutrophils and monocytes ($Gr1^+$ $CD11b^+$; Figure 5.4). At 12 hours post LPS there was a decline in the frequency of $Gr1^+$ $CD11b^+$ cells compared to control mice and this decreased even further at 24 hours post LPS. At 72 hours however, the frequency returned to control levels. We also analysed BM $Gr1^+$ $CD11b^+$ cells at 120 hours post LPS to see if there was a compensatory increase in the frequency of myeloid cells after the total BM number had recovered. We found that this was indeed the case and the frequency of $Gr1^+$ $CD11b^+$ cells had increased almost three fold between 72 and 120 hours. Therefore, the reduced number of total BM cells at 12 and 24 hours post LPS reflected the export of BM neutrophils and monocytes into the circulation. In addition, in order to 'refill' the myeloid compartment, it seemed that there was a compensatory increase in the production of mature myeloid cells once the inflammation-induced effects of LPS

challenge had been cleared. This could have been due to increased production of mature cells from BM progenitors.

Next, we observed the frequency of BM B-cells, which were identified by CD19 expression (Figure 5.5). After 12 hours post LPS, there was no significant change in the frequency of cells compared to control mice, however at 24 hours an increase in the frequency of these cells was observed. This may have been due to B-cell progenitors developing into mature cells, or it could have been due to circulating B-cells homing to the BM during LPS challenge, which would be one explanation for the reduced number of these cells in the blood. In contrast, at 72 and 120 hours post LPS there was a virtual depletion of BM B-cells. This suggested that lymphopoiesis had stalled and might indicate the depletion of upstream progenitors.

Figure 5.3

Reduction in the total number of BM cells after LPS challenge in C57BL/6 mice.

Graph illustrating the total number of BM cells per femur pair at 0, 12, 24 and 72 hours post LPS challenge in C57BL/6 mice, aged eight weeks of age. For the control, C57BL/6 mice were injected with double distilled water. Ten mice were analysed (five male and five female) per time point from three independent experiments. Significance was calculated using the Student's T-test ($p < 0.05$). Values represent mean ± S.E.M.

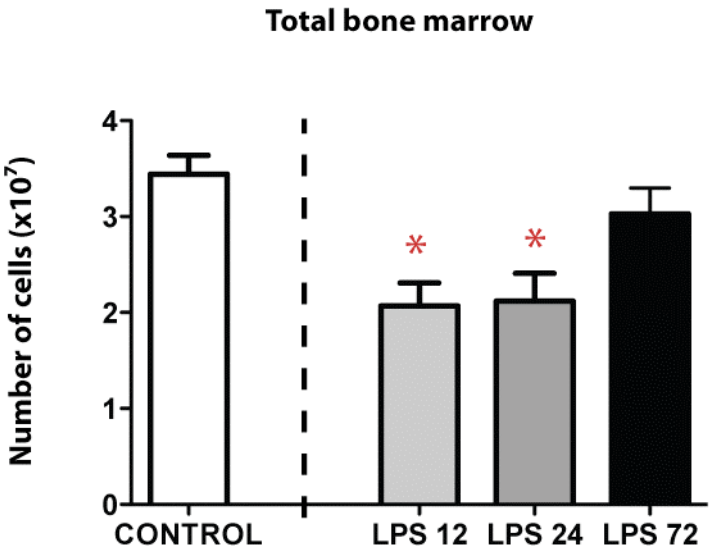
Total bone marrow
Number of cells (x10^7)
4
3
2
1
0
*
*
CONTROL
LPS 12
LPS 24
LPS 72

Figure 5.4

Frequency of BM neutrophils and monocytes during LPS challenge in C57BL/6 mice.

Representative FACS plots illustrating the frequency of BM neutrophils and monocytes at 0, 12, 24, 72 and 120 hours post LPS challenge in C57BL/6 mice, aged eight weeks of age. Myeloid cells were identified by combined expression of Gr1 and CD11b. In all histograms, $NK1.1^{+}$, $CD3\varepsilon^{+}$ and $7AAD^{+}$ cells were electronically excluded from analysis. For the control, C57BL/6 mice were injected with double distilled water. Samples are representative of one experiment using five mice per time point.

CONTROL

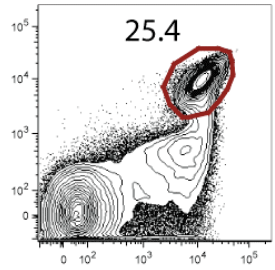

12 HOURS POST LPS

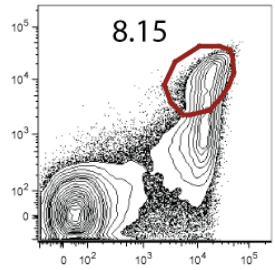

24 HOURS POST LPS

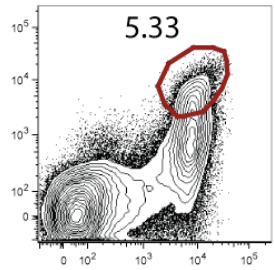

72 HOURS POST LPS

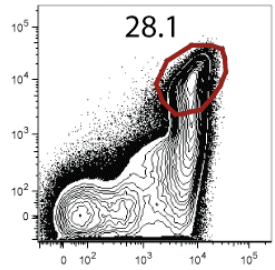

120 HOURS POST LPS

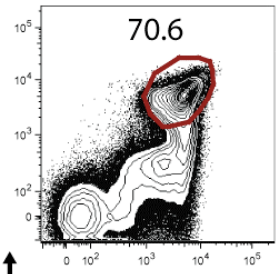

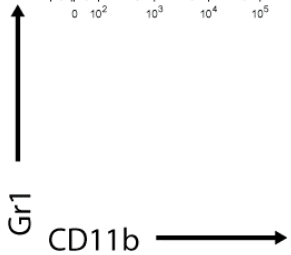

Figure 5.5

Frequency of BM B-cells during LPS challenge in C57BL/6 mice.

Representative FACs plots illustrating the frequency of BM B-cells at 0, 12, 24, 72 and 120 hours post LPS challenge in C57BL/6 mice, aged eight weeks of age. For the control, C57BL/6 mice were injected with double distilled water. In all histograms, $NK1.1^+$, $CD3\varepsilon^+$ and $7AAD^+$ cells were electronically excluded from analysis. Samples are representative of one experiment using five mice per time point.

CONTROL

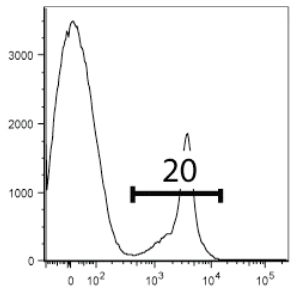

12 HOURS POST LPS

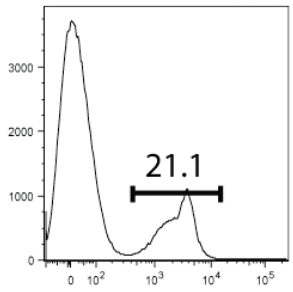

24 HOURS POST LPS

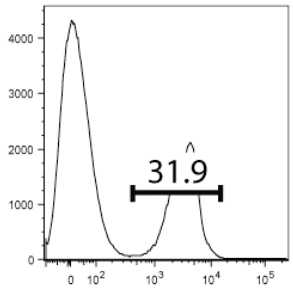

72 HOURS POST LPS

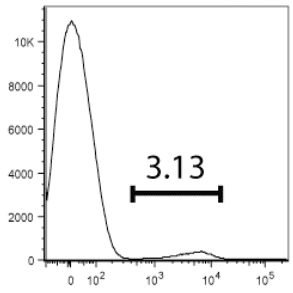

120 HOURS POST LPS

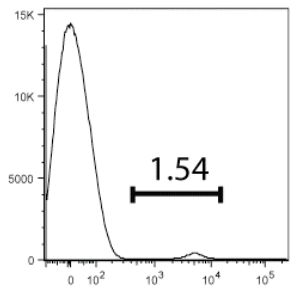

CD19 →

5.4 Analysis of the number of haematopoietic progenitor cells during LPS challenge

We had observed a virtual depletion of BM B-cells 72 hours after LPS challenge, therefore we investigated whether this was due to an absence of upstream lymphoid progenitor cells. All BM progenitor cells are identified as LIN^-. We found that there was a decline in the total number of LIN^- cells 12 and 24 hours post LPS injection (Figure 5.6A). A significant decrease in the number of LIN^- cells occurred after 12 hours (from $3.94 \times 10^5 \pm 0.49 \times 10^5$ to $2.58 \times 10^5 \pm 0.32 \times 10^5$) and more severely at 24 hours post injection ($1.24 \times 10^5 \pm 0.13 \times 10^5$), which had returned to steady state levels by 72 hours ($2.97 \times 10^5 \pm 0.48 \times 10^5$). Therefore, during 12 and 24 hours post LPS, there was a decrease in the number of progenitor cells. Due to a reported expansion of the LSK compartment and a decrease in the number of LIN^- c-kit^{hi} Sca-1^- cells in other models of inflammation (Belyaev et al., 2010; Singh et al., 2008; Zhang et al., 2008), we analysed the number of cells in these populations throughout the time course. The number and frequency of LSK cells, representing during homeostatic levels stem cells and multipotent progenitors, increased significantly at 12, 24 and 72 hours post LPS injection (Figure 5.6B), in agreement with other published data. At 12 hours, the cell number increased 1.3 fold, from $2.13 \times 10^4 \pm 0.25 \times 10^4$ at control levels to $2.94 \times 10^4 \pm 0.33 \times 10^4$. The number of cells further increased at 24 hours ($3.05 \times 10^4 \pm 0.5 \times 10^4$) and 72 hours ($4.99 \times 10^4 \pm 0.94 \times 10^4$). In contrast to an expansion in the LSK compartment, there was a major decrease in the number of LIN^- c-kit^{hi} Sca-1^- cells (Figure 5.6C), a compartment composed of myelo-erythroid progenitors during homeostatic levels. In control mice, the number of cells equated to $10.48 \times 10^4 \pm 1.29 \times 10^4$ and this declined significantly to $1.96 \times 10^4 \pm 0.52 \times 10^4$ at 12 hours. Similar numbers were observed at 24 hours ($2.16 \times 10^4 \pm 0.46 \times 10^4$) and the

cell number began to return to steady state levels by 72 hours ($9.91 \times 10^4 \pm 2.1 \times 10^4$). Therefore, as suggested by Zhang and colleagues (Zhang et al., 2008), the increase in the number of LSK cells could have been due to a conversion of LIN^- c-kit^{hi} $Sca\text{-}1^-$ cells into LSK cells. On observation of the frequency of cells in these compartments, there was an increase in the frequency of LSK cells and a subsequent decrease in the frequency of LIN^- c-kit^{hi} $Sca\text{-}1^-$ cells, which appeared to upregulate Sca-1 on their surface (Figure 5.7).

Figure 5.6

Absolute number of LIN$^-$, LSK and LIN$^-$c-kit^{hi} Sca-1$^-$ cells during LPS challenge in C57BL/6 mice.

A Graph illustrating the number of LIN$^-$ cells per femur pair in the BM at 0, 12, 24 and 72 hours post LPS challenge of C57BL/6 mice, aged eight weeks of age. Control C57BL/6 mice were injected with double distilled water. Ten mice were analysed (five male and five female) per time point from three independent experiments. Significance was calculated using the Student's T-test ($p < 0.05$). Values represent mean ± S.E.M.

B Graph illustrating the number of LSK cells per femur pair in the BM at 0, 12, 24 and 72 hours post LPS challenge of C57BL/6 mice, aged eight weeks of age. Control C57BL/6 mice were injected with double distilled water. Ten mice were analysed (five male and five female) per time point from three independent experiments. Significance was calculated using the Student's T-test ($p < 0.05$). Values represent mean ± S.E.M.

C Graph illustrating the number of LIN$^-$ c-kit^{hi} Sca-1$^-$ cells per femur pair in the BM at 0, 12, 24 and 72 hours post LPS challenge of C57BL/6 mice, aged eight weeks of age. Control C57BL/6 mice were injected with double distilled water. Ten mice were analysed (five male and five female) per time point from three independent experiments. Significance was calculated using the Student's T-test ($p < 0.05$). Values represent mean ± S.E.M.

A

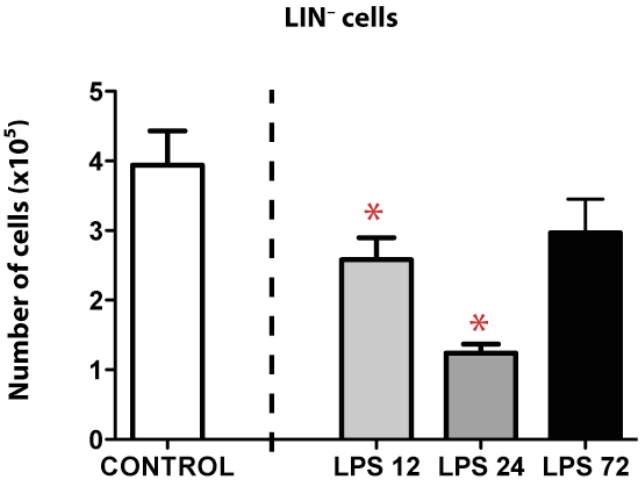
LIN⁻ cells
Number of cells (x10⁵)
5
4
3
2
1
0
*
*
CONTROL
LPS 12
LPS 24
LPS 72

B

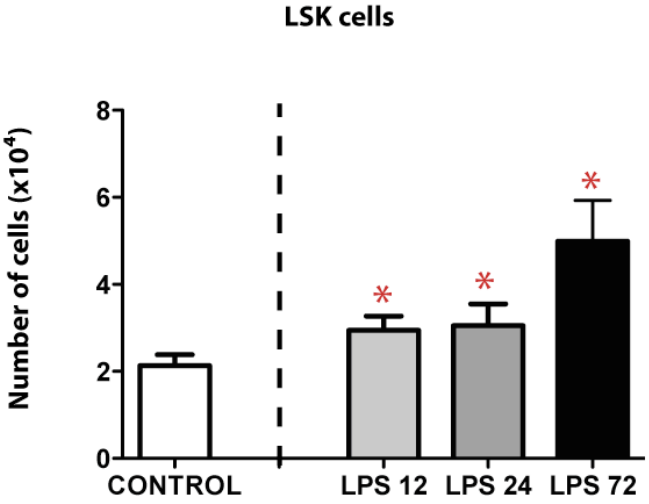
LSK cells
Number of cells (x10⁴)
8
6
4
2
0
*
*
*
CONTROL
LPS 12
LPS 24
LPS 72

C

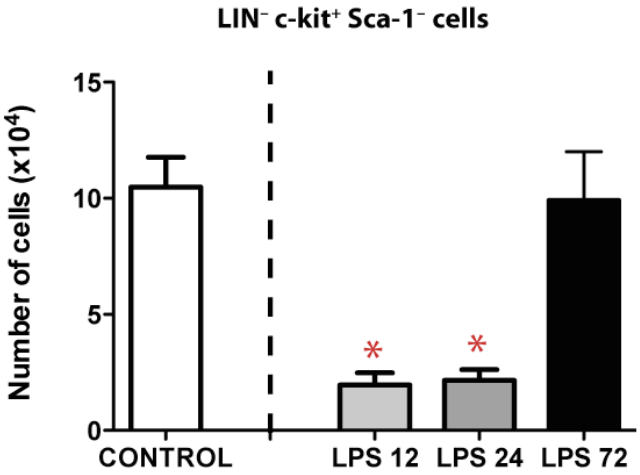
LIN⁻ c-kit⁺ Sca-1⁻ cells
Number of cells (x10⁴)
15
10
5
0
*
*
CONTROL
LPS 12
LPS 24
LPS 72

5.5 Composition of haematopoietic progenitor compartments during LPS challenge

We next investigated the composition of LSK cells during LPS challenge and also analysed the CLP population. The frequency and number of LSK $CD34^+$ $Flk\text{-}2^-$ cells, representing ST-HSCs during homeostatic conditions, were increased significantly at 12, 24 and 72 hours post LPS challenge (Figure 5.7 and 5.8A). The number of cells in this compartment increased from $0.27 \times 10^4 \pm 0.03 \times 10^4$ in control mice to $1.17 \times 10^4 \pm 0.16 \times 10^4$ at 12 hours post LPS injection. This number remained constant at 24 hours ($1.18 \times 10^4 \pm 0.2 \times 10^4$) and starting declining at 72 hours ($0.8 \times 10^4 \pm 0.15 \times 10^4$). The observed increase in frequency and number could have occurred for more than one reason; a higher number of ST-HSCs were needed during LPS challenge, CD34 was upregulated on LSK cells, or that CMP and GMP cells, which were $CD34^+$ and usually resided in the LIN^- c-kit^{hi} $Sca\text{-}1^-$ compartment, had upregulated Sca-1 on their surface and were also identified by these surface markers. In marked contrast, LSK $CD34^+$ $Flk\text{-}2^+$ progenitors, which would represent LMPPs during homeostatic conditions, decreased in frequency and number at 12 and 24 hours (Figure 5.7 and Figure 5.8B). The number of cells declined significantly from $0.94 \times 10^4 \pm 0.13 \times 10^4$ in control mice to $0.29 \times 10^4 \pm 0.06 \times 10^4$ at 12 hours post LPS. This number remained low at 24 hours ($0.32 \times 10^4 \pm 0.09 \times 10^4$) and increased significantly at 72 hours ($1.73 \times 10^4 \pm 0.34 \times 10^4$). This number of LMPP cells at 72 hours was also significantly higher than the control, indicating a major production of LMPPs from ST-HSCs at this time point. By 72 hours, cells in the LSK gate which were $CD34^+$ and $Flk\text{-}2^-$ were likely representing true ST-HSCs because the frequency of LIN^- c-kit^{hi} $Sca\text{-}1^-$ cells had returned to homeostatic levels (Figure 5.7), indicating that any cells which had upregulated Sca-1 on their surface during LPS challenge, had lost the expression of this marker. Therefore,

it is conceivable that ST-HSCs could have differentiated into LMPP cells at 72 hours post LPS and induced an increase in the frequency and number of this population. Reasons for this increase may have been the need to compensate for the loss LMPPs during LPS challenge, which would subsequently lead to an increased production of both mature myeloid and lymphoid cells. This reactive mechanism would explain the observed increase in the frequency of mature myeloid cells at 120 hours post LPS challenge. Alternatively, because LMPPs contain cells primed to undergo development down the lymphoid lineage, their decrease in frequency and number could be the cause for the cessation of lymphopoiesis.

To further investigate lymphopoiesis, the CLP population, which is thought to be downstream of the LMPP population and a precursor for B-cells (Allman et al., 2003, Schwarz and Bhandoola, 2004), was also analysed. 12 and 24 hours post LPS injection, there was a virtual depletion of the CLP population, both in terms of frequency and number (Figure 5.7 and Figure 5.8C). The number of CLP cells decreased significantly from $0.32 \times 10^4 \pm 0.06 \times 10^4$ in control mice to $0.03 \times 10^4 \pm 0.02 \times 10^4$ after 12 hours. This number also remained low at 24 hours ($0.04 \times 10^4 \pm 0.01 \times 10^4$) but increased at 72 hours ($0.2 \times 10^4 \pm 0.06 \times 10^4$). Because there was a major increase in the number of LMPP cells at 72 hours post LPS, and an increase in the number of CLP cells also at this time point, this indicated that differentiation from the LMPP pool into the CLP had taken place. In addition, because CLP cells were virtually absent during LPS challenge, this could be one reason for the observed depletion of BM B-cells at 72 hours. On the other hand, the frequency of BM B-cells remained constant at 12 hours after LPS injection and increased at 24 hours post LPS, which could have been due to CLP cells rapidly differentiating into mature lymphocytes at the onset of LPS challenge. There was also a reduction in the level of Flk-2 expression on both LMPP and CLP cells at 12

and 24 hours compared to the control (Figure 5.7) and a decrease in the level of IL-7Rα expression on CLP cells. This indicated that there may have been a lack of production of cytokines promoting differentiation and proliferation of lymphoid progenitor cells, in order to inhibit lymphopoiesis.

Figure 5.7

Frequency of haematopoietic progenitor compartments during LPS challenge in the BM of C57BL/6 mice.

FACS plots illustrating the frequency of haematopoietic progenitor populations during LPS challenge in the BM of C57BL/6 mice, aged eight weeks of age. Control mice were injected with double distilled water. Mice were analysed at 0, 12, 24 and 72 hour time points and assessed for their expression of cell surface markers. Data is representative of one from three independent experiments using at least four mice per time point per group.

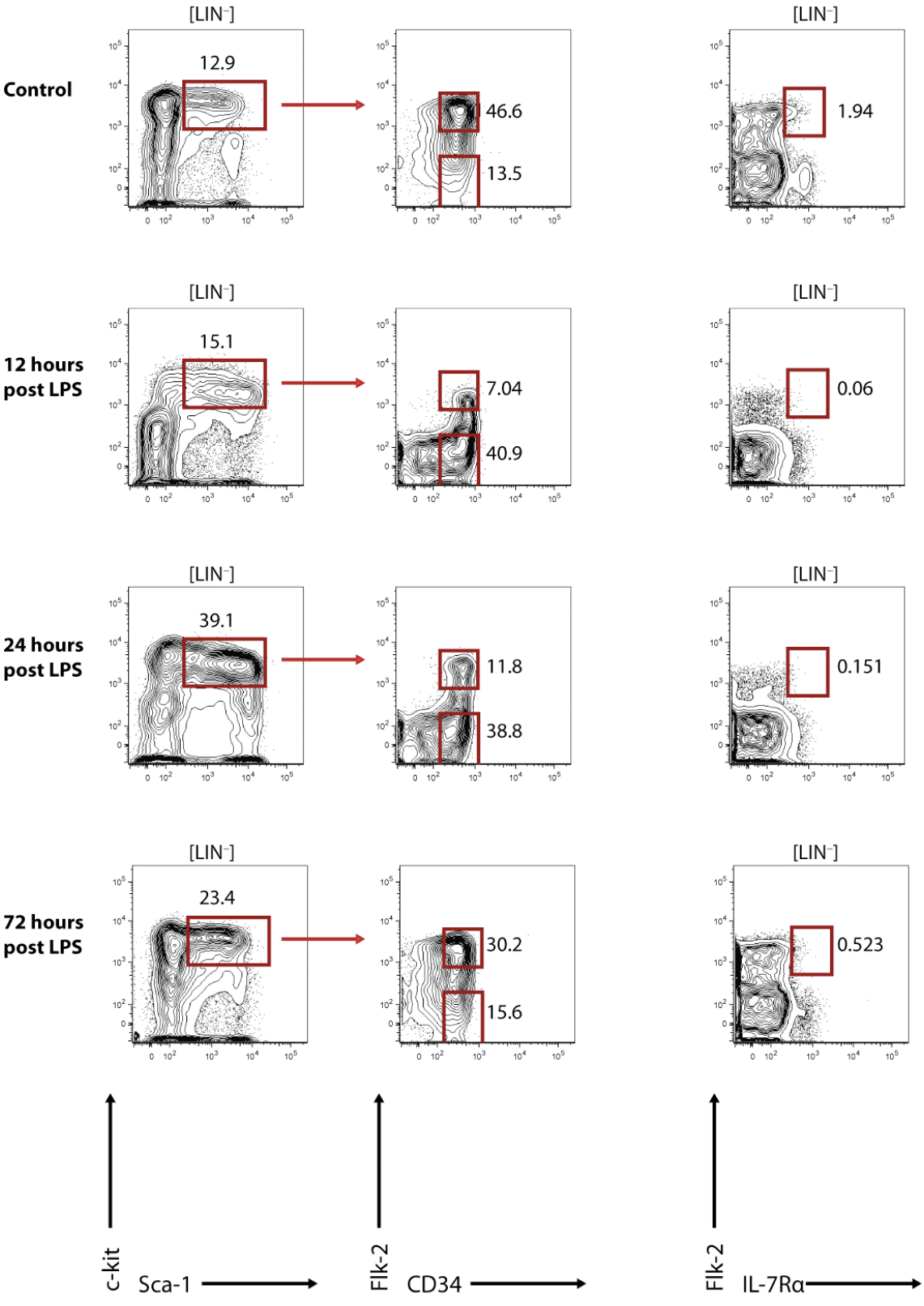
Control
12 hours post LPS
24 hours post LPS
72 hours post LPS
[LIN-]
12.9
46.6
13.5
1.94
15.1
7.04
40.9
0.06
39.1
11.8
38.8
0.151
23.4
30.2
15.6
0.523
c-kit
Sca-1
Flk-2
CD34
Flk-2
IL-7Rα

Figure 5.8

Absolute number of progenitor cells in BM of LPS challenged C57BL/6 mice.

A Graph illustrating the number of LSK $CD34^+$ $Flk\text{-}2^-$ cells per femur pair at 0, 12, 24 and 72 hours post LPS challenge in C57BL/6 mice, aged eight weeks of age. Control mice were injected with double distilled water. Ten mice were analysed (five male and five female) per time point from three independent experiments. Significance was calculated using the Student's T-test ($p < 0.05$). Values represent mean ± S.E.M.

B Graph illustrating the number of LSK $CD34^+$ $Flk\text{-}2^+$ cells per femur pair at 0, 12, 24 and 72 hours post LPS challenge in C57BL/6 mice, aged eight weeks of age. Control mice were injected with double distilled water. Ten mice were analysed (five male and five female) per time point from three independent experiments. Significance was calculated using the Student's T-test ($p < 0.05$). Values represent mean ± S.E.M.

C Bar graph illustrating the number of LIN^- IL-$7R\alpha^+$ $Flk\text{-}2^+$ cells per femur pair at 0, 12, 24 and 72 hours post LPS challenge in C57BL/6 mice, aged eight weeks of age. Control mice were injected with double distilled water. Ten mice were analysed (five male and five female) per time point from three independent experiments. Significance was calculated using the Student's T-test ($p < 0.05$). Values represent mean ± S.E.M.

A

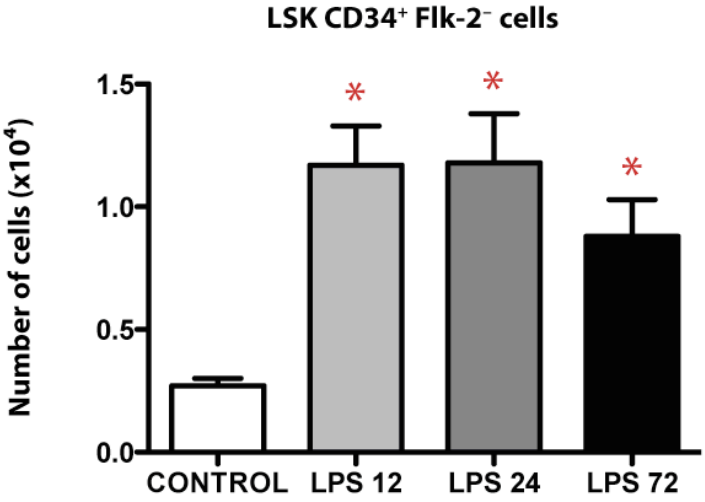
LSK CD34⁺ Flk-2⁻ cells
Number of cells (x10⁴)
1.5
1.0
0.5
0.0
*
*
*
CONTROL
LPS 12
LPS 24
LPS 72

B

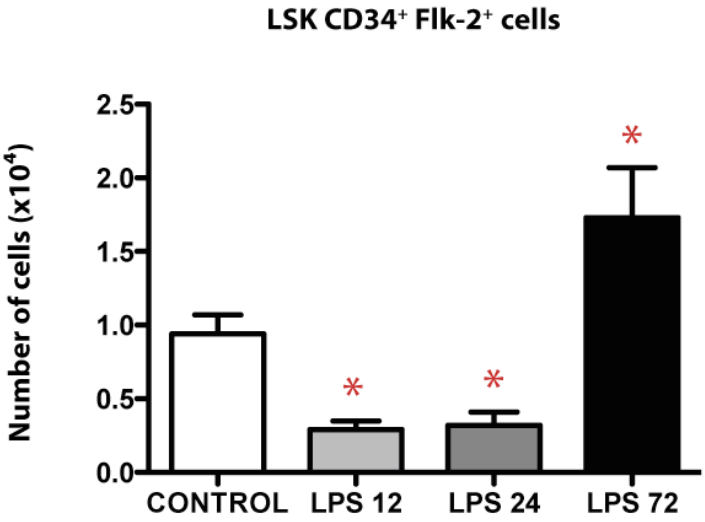
LSK CD34⁺ Flk-2⁺ cells
Number of cells (x10⁴)
2.5
2.0
1.5
1.0
0.5
0.0
*
*
*
CONTROL
LPS 12
LPS 24
LPS 72

C

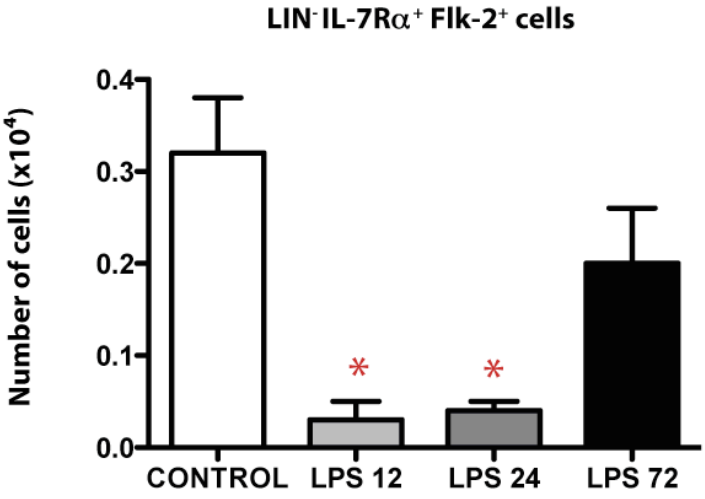
LIN⁻ IL-7Rα⁺ Flk-2⁺ cells
Number of cells (x10⁴)
0.4
0.3
0.2
0.1
0.0
*
*
CONTROL
LPS 12
LPS 24
LPS 72

5.6 The number of LT-HSCs remains constant throughout LPS challenge

After observing a decrease in the frequency and number of LMPP and CLP populations and an increase in the number of LSK CD34^{+} Flk-2^{-} cells during LPS challenge, we next attempted to further define the cause of expansion of LSK cells. To address whether the increase in LSK numbers was due to amplification of LT-HSCs during LPS challenge, we analysed the absolute cell number of LSK CD150^{+} CD48^{-} cells (Figure 5.9). Previous studies have reported that dormant LT-HSCs can be activated *in vivo* by inflammatory cytokines. Baldridge and colleagues (Baldridge et al., 2010) found that during chronic infection with *Mycobacterium avium*, LT-HSCs proliferated extensively as shown by the incorporation of BrdU. These LT-HSCs also lost some regenerative function and showed impaired engraftment after transplantation into irradiated recipients. These changes were due to IFNγ, as LT-HSCs removed from *Ifng*-deficient mice had a lower proliferative rate. Other reports have shown that IFNα can also induce the proliferation of LT-HSCs (Sato et al., 2009; Essers et al., 2009). However, most importantly, Scumpia and co-workers found that there was a significant increase in the number of LT-HSCs after polymicrobial sepsis, induced by cecal ligation puncture and also LPS injection (Scumpia et al., 2010). In contrast to this data, we found no significant differences in the number of these cells throughout the study. Due to an observed increase in the LSK CD34^{+} Flk-2^{-} compartment during LPS challenge, which represents ST-HSCs during steady state conditions and which are the immediate downstream progeny of LT-HSCs, the increase in the frequency and number of these cells was likely not due to a requirement for surplus ST-HSCs, as there was no evidence for an increased number of upstream LT-HSCs. The increase in the number of LSK

$CD34^+$ $Flk\text{-}2^-$ cells therefore could have been due to upregulation of Sca-1 on myeloid progenitors and $CD34^+$ CMP and GMP populations residing in the LSK compartment.

Figure 5.9

Absolute number of LT-HSCs during LPS challenge in C57BL/6 mice.

Graph illustrating the number of LSK $CD150^{+}$ $CD48^{-}$ cells per femur pair at 0, 12, 24 and 72 hours post LPS challenge in C57BL/6 mice, aged eight weeks of age. LT-HSC number showed no significant change throughout the study. Control mice were injected with distilled water. Ten mice were analysed (five male and five female) per time point from three independent experiments. Significance was calculated using the Student's T-test ($p < 0.05$). Values represent mean ± S.E.M.

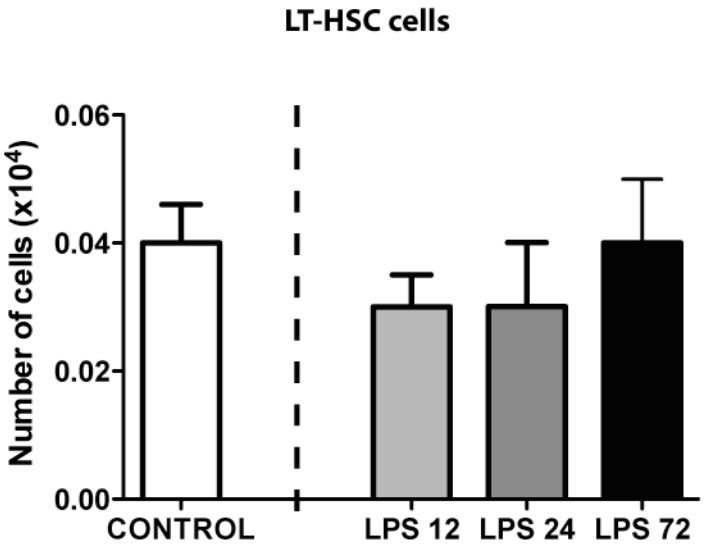
LT-HSC cells
Number of cells (x10⁴)
0.06
0.04
0.02
0.00
CONTROL
LPS 12
LPS 24
LPS 72

5.7 Phenotypic changes in myeloid progenitors during LPS challenge

One explanation for the increase in the frequency and number of LSK cells was that myeloid progenitors from the LIN^- c-kit^{hi} $Sca\text{-}1^-$ fraction may have upregulated Sca-1. Due to the lack of LIN^- c-kit^{hi} $Sca\text{-}1^-$ cells during LPS challenge, we were not able to study conventional CMPs, GMPs and MEPs. Therefore, we used the FcγRII/III antigen as a marker of GM development (Akashi et al., 2000) in all cells which were LIN^- c-kit^{hi}. As illustrated in Figure 5.10; 12, 24 and 72 hours post LPS challenge, there was still detectable FcγRII/III expression in LIN^- c-kit^{hi} cells, indicating the presence of GM progenitors. Although the frequency (Figure 5.10) and number (see Figure 5.11) of FcγRII/III^+ cells was reduced 12 and 24 hours post LPS challenge on LIN^- c-kit^{hi} cells, the presence of FcγRII/III expressing progenitors remained throughout the study. This proved that CMP and GMP populations were present in the LSK compartment of the BM, indicating that Sca-1 must have been upregulated on these cells. In addition, the presence of CMP and GMP populations indicated that myelopoiesis was still ongoing. This may have been occurring in order to refill mature myeloid cell pools of the BM, which had been depleted due to export of these cells into the circulation.

Figure 5.10

Frequency of LIN$^-$ c-kit^{hi} cells expressing FcγRII/III during LPS challenge in C57BL/6 mice.

FACS plots illustrating the presence of FcγRII/III expression on LIN$^-$ c-kit^{hi} cells. C57BL/6 mice aged eight weeks of age were analysed at 0, 12, 24 and 72 hours post LPS challenge. Control mice were injected with distilled water. Data is representative of one from three independent experiments using at least four mice per time point per group.

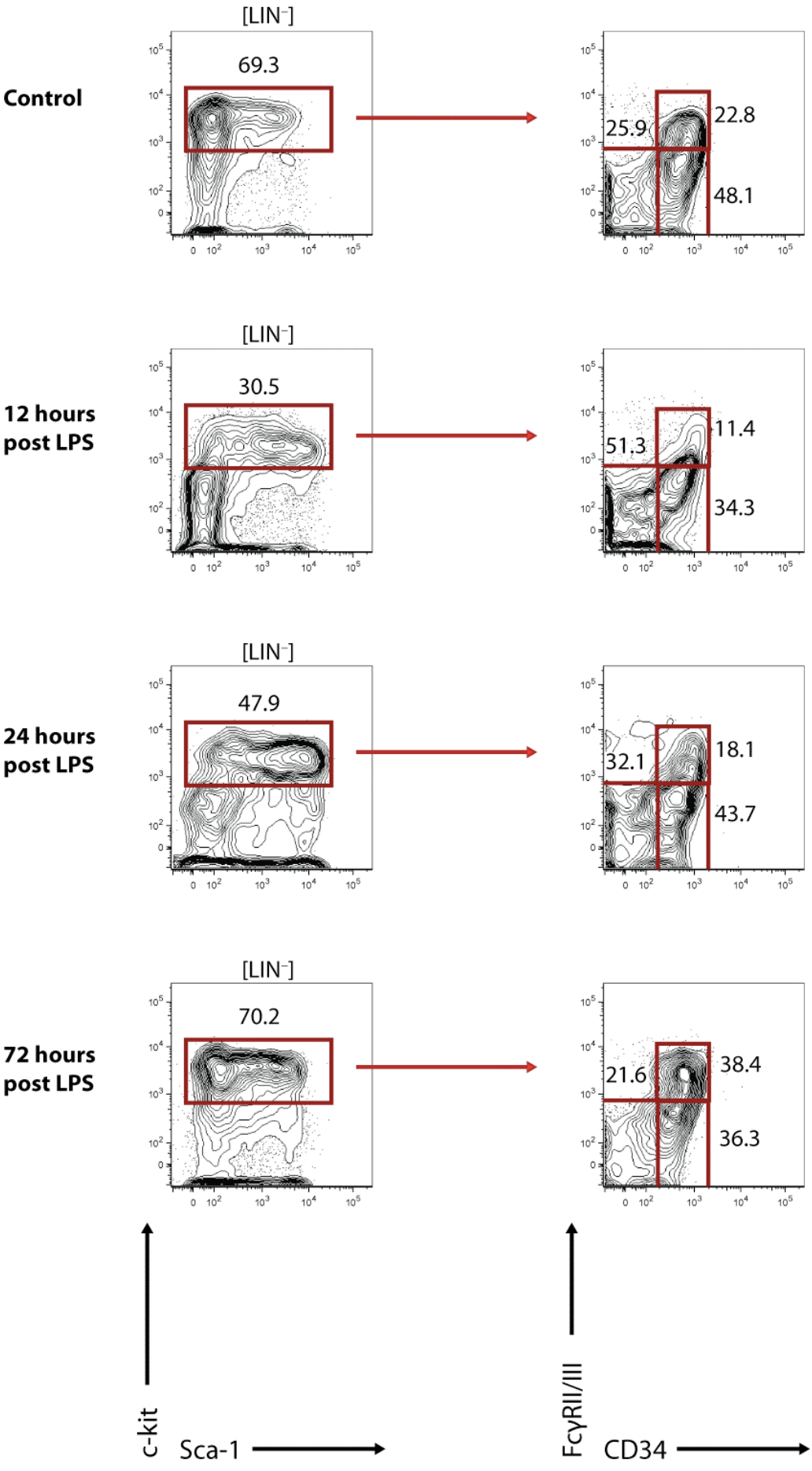
Control
[LIN⁻]
69.3
25.9
22.8
48.1
12 hours post LPS
[LIN⁻]
30.5
51.3
11.4
34.3
24 hours post LPS
[LIN⁻]
47.9
32.1
18.1
43.7
72 hours post LPS
[LIN⁻]
70.2
21.6
38.4
36.3
c-kit
Sca-1
FcγRII/III
CD34

Figure 5.11

Absolute number of LIN$^-$ c-kit^{hi} FcγRII/III$^+$ cells during LPS challenge.

Graph illustrating the number of LIN$^-$ c-kit^{hi} FcγRII/III$^+$ cells per femur pair at 0, 12, 24 and 72 hours post LPS challenge in C57BL/6 mice, aged eight weeks of age. Ten mice were analysed (five male and five female) per time point from three independent experiments. Significance was calculated using the Student's T-test ($p < 0.05$). Values represent mean ± S.E.M.

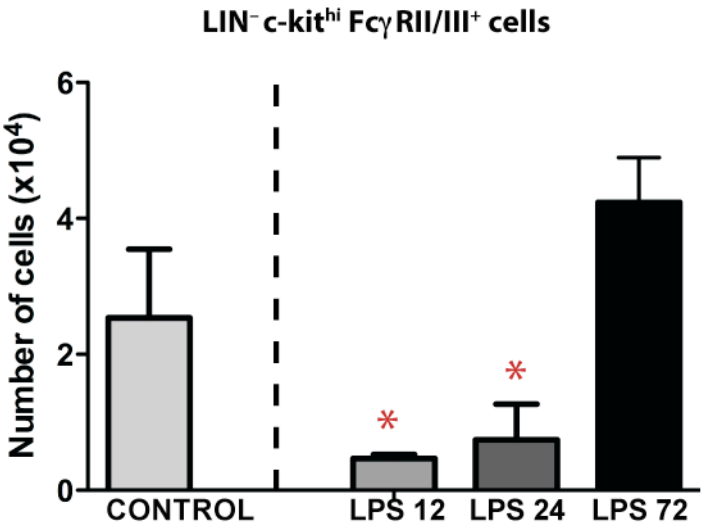
LIN⁻ c-kit^hi FcγRII/III⁺ cells
Number of cells (x10^4)
6
4
2
0
*
*
CONTROL
LPS 12
LPS 24
LPS 72

5.8 Analysis of haematopoietic progenitor cells utilising the *Rag1$^{wt/Cre}$ x Rosa26$^{wt/eYFP}$* reporter during LPS challenge

We next investigated LPS challenge in *Rag1$^{wt/Cre}$ x Rosa26$^{wt/eYFP}$* mice. This reporter model allows us to track the fate of cells by virtue of eYFP expression on cells which have passed via the ELP stage of development and expressed *Rag1*. We initially utilised this model in order to analyse the effect of LPS challenge on the ELP population. As expected due to a loss of LMPP and CLP cells, ELP cells were also absent at 12 hours post LPS (Figure 5.12). However there was some evidence for recovery at 24 hours and a substantial increase in the frequency of ELP cells at 72 hours, identical to what was observed in the LMPP population.

Next we used the *Rag1$^{wt/Cre}$ x Rosa26$^{wt/eYFP}$* to address whether eYFP^{+} lymphoid progenitor cells had been re-directed to the myeloid lineage during LPS challenge. This was based on results that there was a lack of lymphoid progenitor cells during LPS challenge and a cessation of lymphopoiesis, but the presence of FcγRII/III^{+} GMP and CMP populations. There have been previous reports suggesting that overexpression of cytokines and transcription factors in culture can re-direct lymphoid progenitors into the myeloid lineage. It has already been shown that CLPs from mice transgenic for human IL-2Rβ can be re-directed to the myeloid lineage after stimulation by human IL-2β *in vitro* (Kondo et al, 2000). The authors suggested that IL-2 receptor signalling was promoting the development of GM lineage cells from lymphoid committed cells and this revealed that lymphoid precursors retained a certain amount of developmental plasticity. However, under physiological conditions, CLPs do not express the IL-2Rβ chain and so this observed developmental plasticity may not occur *in vivo.* Furthermore, Iwasaki-Arai et al., (Iwasaki-Arai et al., 2003) reported that CLPs isolated from mice ubiquitously expressing the human GM-CSF receptor (hGM-CSFR) could be

instructed by hGM-CSF *in vitro* to develop into granulocytes, monocytes and DCs. The authors suggested that because CLP cells do not express GM-CSFR under physiological conditions and expression of this receptor is restricted to the myeloid lineage, lymphoid progenitor cells become restricted in their fate because of downregulation of receptors which respond to cytokines promoting myeloid differentiation. Indeed this may have been occurring after administration of LPS, but instead of downregulation of myeloid receptors on lymphoid cells, downregulation of receptors promoting lymphoid differentiation, such as Flk-2 and IL-7Rα, and upregulation of myeloid lineage promoting receptors may have occurred.

In addition to cytokine receptor expression, it has also been reported that enforced expression of transcription factors required for GM and MegE development, in lymphoid progenitor cells, can also cause re-direction of cells from the lymphoid to the MegE and GM lineages. Iwasaki et al., showed that enforced expression of GATA-1 could induce the differentiation of CLPs into the MegE lineage (Iwasaki et al., 2003). In addition, Xie et al (Xie et al., 2004) reported that BM and splenic B-cells could be reprogrammed into Mac-1^{+} cells after enforced expression of C/EBPα, a transcription factor required for myeloid development. These studies suggest that lineage specification of haematopoietic progenitors is governed by a variety of intrinsic and extrinsic factors, however reports of lineage re-direction induced by cytokines *in vivo* has not been well addressed.

Access to $Rag1^{wt/Cre}$ *x* $Rosa26^{wt/eYFP}$ reporter mice enabled us to assess any potential developmental plasticity of the CLP population during LPS challenge directly. EYFP expression in $Rag1^{wt/Cre}$ *x* $Rosa26^{wt/eYFP}$ mice is confined to lymphoid progenitor cells only and is absent in all stem cells and myeloid progenitors. Therefore, any expression of eYFP in myeloid cells would indicate that ELPs or CLPs had been re-directed into

myeloid progenitors and these cells had then matured into fully functional myeloid cells. We analysed mature neutrophils and monocytes in the BM (Figure 5.13) starting at 12 hours and up to five days after LPS challenge. There was no evidence for significant eYFP expression at any time point. To completely rule out eYFP expression in the myeloid compartment, we also analysed these cells in the spleen to ensure that cells had not already exited the BM by 12 hours post injection. As shown in Figure 5.14, there was no significant increase in expression of eYFP on splenic myeloid cells at any time point, indicating that re-direction of lymphoid progenitor cells into the myeloid lineage had not occurred. Therefore, the decrease in the frequency and number of CLP cells during LPS challenge was due to either apoptosis of these cells or rapid development of these cells into mature lymphocytes immediately after LPS administration.

Figure 5.12

Frequency of ELP cells in the BM during LPS challenge in Rag1$^{wt/Cre}$ x Rosa26$^{wt/eYFP}$ mice.

FACS plots illustrating the loss of ELP cells during LPS challenge in *Rag1$^{wt/Cre}$ x Rosa26$^{wt/eYFP}$* mice aged eight to ten weeks of age. Mice were analysed at 0, 12, 24, 72 and 120 hours post LPS challenge. Control mice were injected with double distilled water. Ten mice were analysed (five male and five female) per time point from two independent experiments.

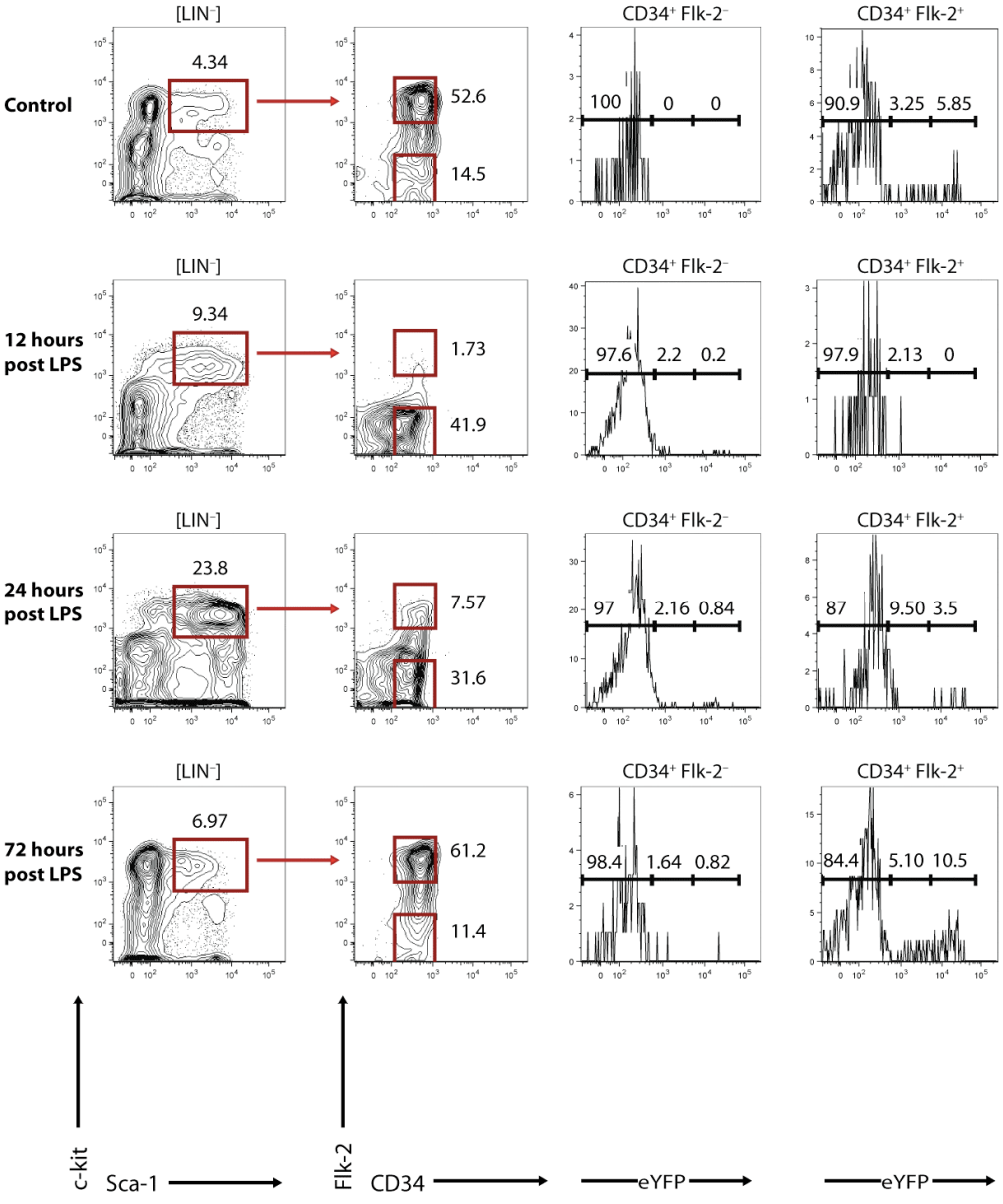
[LIN⁻]
CD34⁺ Flk-2⁻
CD34⁺ Flk-2⁺
Control
4.34
52.6
14.5
100
0
0
90.9
3.25
5.85
12 hours post LPS
9.34
1.73
41.9
97.6
2.2
0.2
97.9
2.13
0
24 hours post LPS
23.8
7.57
31.6
97
2.16
0.84
87
9.50
3.5
72 hours post LPS
6.97
61.2
11.4
98.4
1.64
0.82
84.4
5.10
10.5
c-kit
Sca-1
Flk-2
CD34
eYFP
eYFP

Figure 5.13

Frequency of BM myeloid cells expressing eYFP in Rag1$^{wt/Cre}$ x Rosa26$^{wt/eYFP}$ mice during LPS challenge.

FACS plots illustrating the lack of eYFP expression in mature myeloid cells of *Rag1$^{wt/Cre}$ x Rosa26$^{wt/eYFP}$* mice aged eight to ten weeks of age. BM myeloid cells were analysed at 0, 12, 24, 72 and 120 hours post LPS challenge. Myeloid cells were identified by combined expression of Gr1 and CD11b. In all histograms NK1.1^{+}, CD3ε^{+}, 7AAD^{+} cells were excluded from the analysis. Ten mice were analysed (five male and five female) per time point from two independent experiments.

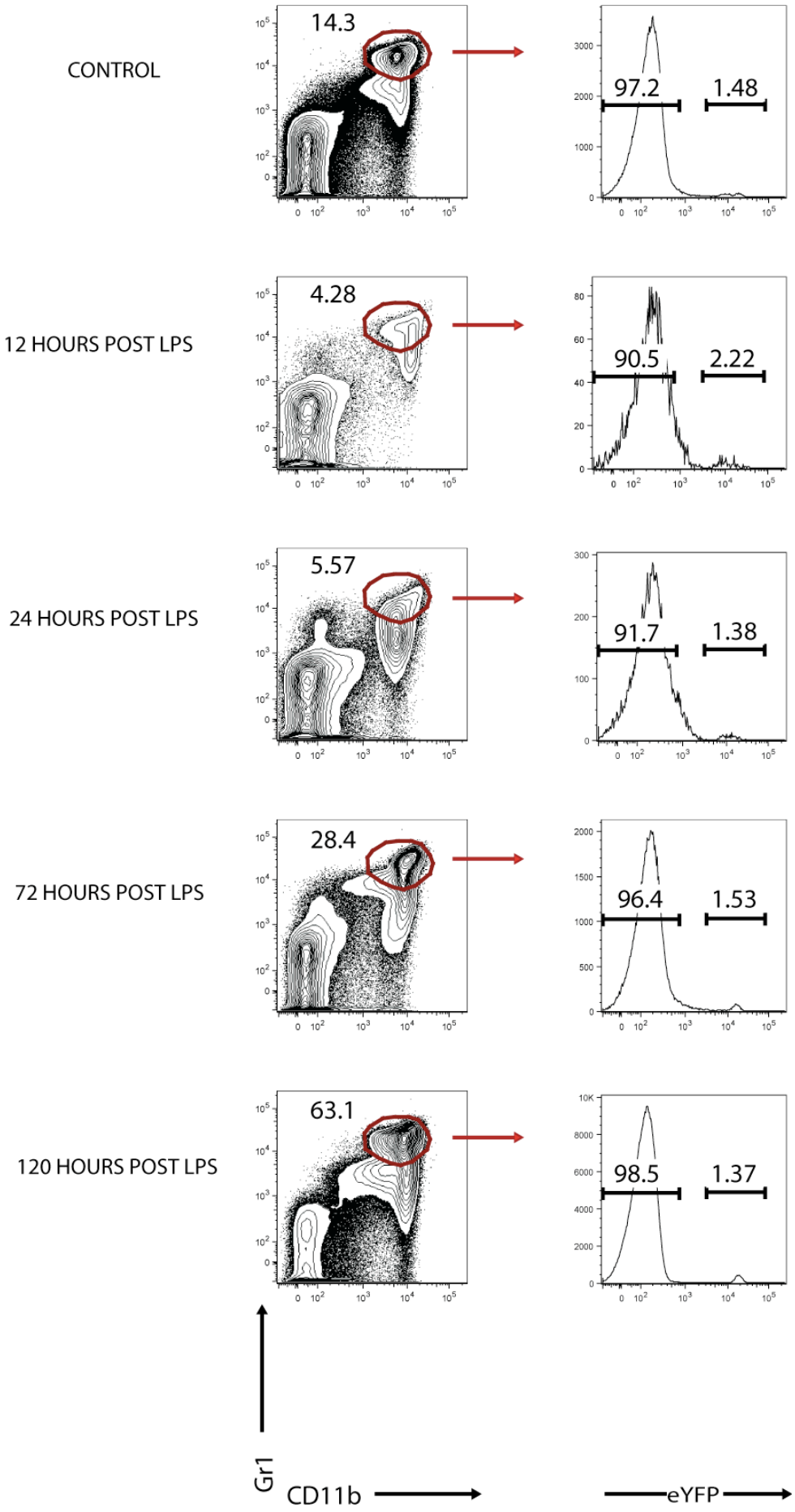
CONTROL
14.3
97.2
1.48
12 HOURS POST LPS
4.28
90.5
2.22
24 HOURS POST LPS
5.57
91.7
1.38
72 HOURS POST LPS
28.4
96.4
1.53
120 HOURS POST LPS
63.1
98.5
1.37
Gr1
CD11b
eYFP

Figure 5.14

Frequency of splenic myeloid cells expressing eYFP in Rag1$^{wt/Cre}$ x Rosa26$^{wt/Cre}$ mice during LPS challenge.

FACS plots illustrating the lack of eYFP expression in splenic myeloid cells of *Rag1$^{wt/Cre}$ x Rosa26$^{wt/eYFP}$* mice aged eight to ten weeks of age. Splenic myeloid cells were analysed at 0, 12, 24, 72 and 120 hours post LPS challenge. Cells were identified as NK1.1^{-} CD3ε^{-} 7AAD^{-} and then analysed for Gr1 and CD11b expression. Ten mice were analysed (five male and five female) per time point from two independent experiments.

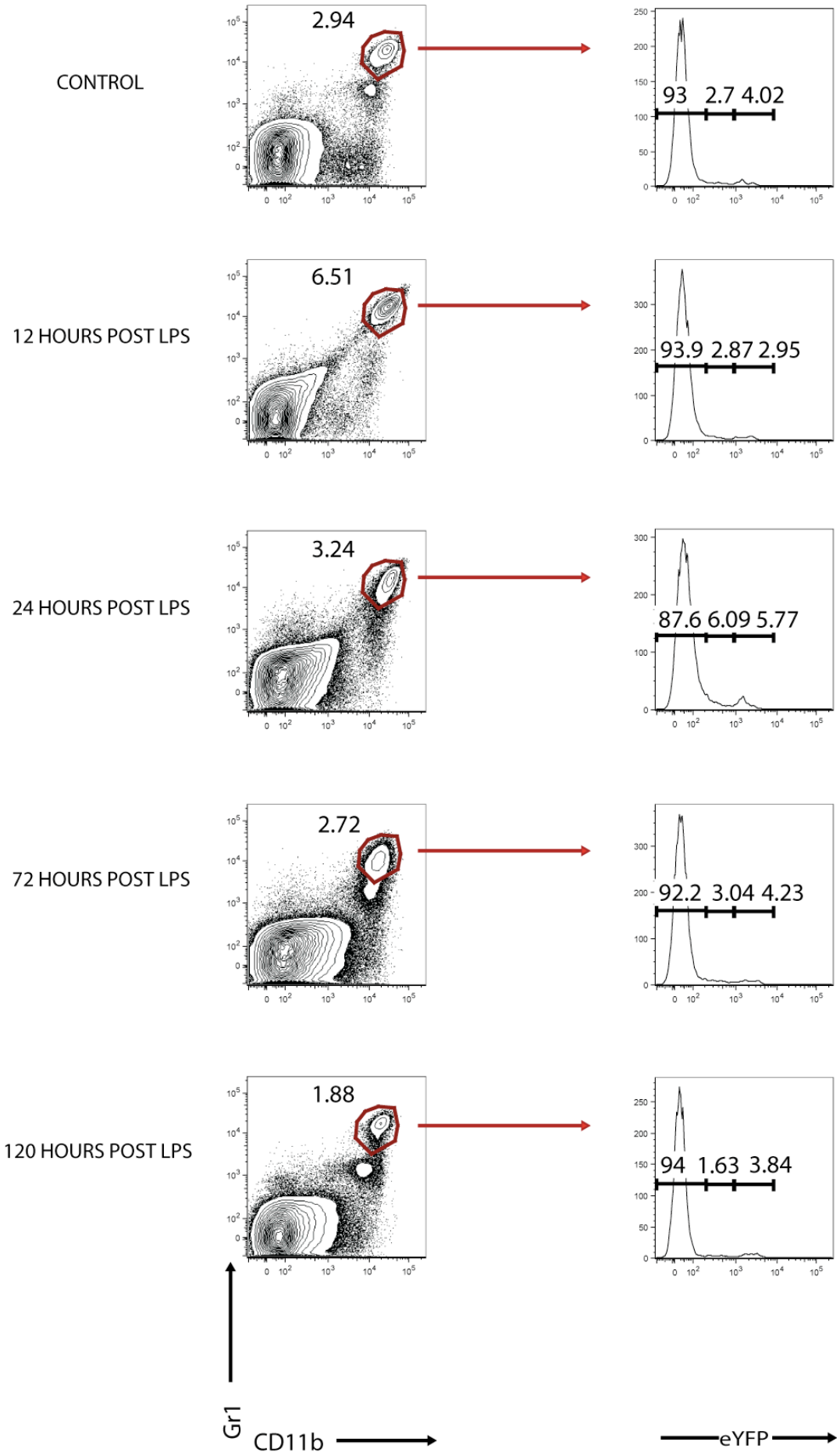
CONTROL
2.94
93 2.7 4.02
12 HOURS POST LPS
6.51
93.9 2.87 2.95
24 HOURS POST LPS
3.24
87.6 6.09 5.77
72 HOURS POST LPS
2.72
92.2 3.04 4.23
120 HOURS POST LPS
1.88
94 1.63 3.84
Gr1
CD11b
eYFP

On initial observations LPS challenge resulted in a cessation of BM lymphopoiesis and a concomitant increase in myelopoiesis. This was reflected by an increase in the number of circulating granulocytes and a decrease in the number of circulating lymphocytes. Indeed, neutrophils have been shown to localize rapidly to the site of inflammation to elicit microbicidal activity (Burg et al., 2001). Consequently, the frequency of BM-derived neutrophils declined during LPS challenge, which was likely due to the export of these cells into the circulation. It is known that localisation of neutrophils to inflammatory sites in the circulation produces a brief neutropenia, which is resolved by migration of BM neutrophils into the circulation (Glasser et al., 1987). During LPS challenge, to compensate for the loss of BM neutrophils, there was increased production of these cells once LPS-induced inflammatory changes had cleared. However, production of these neutrophils from myeloid progenitor cells did not appear to be regulated. GMP cells which give rise to mature macrophages and granulocytes under steady state conditions (Akashi et al., 2000) could not be identified by their conventional phenotype. This appeared to be due to upregulation of Sca-1 on the surface of these cells and therefore FcγRII/III^{+} GMP cells resided in the LSK fraction of the BM. This observation was also reported by Belyaev et al (Belyaev et al., 2010) during infection of mice with malaria and they found that these cells could produce mature myeloid cells *in vitro*. Therefore, although these cells could be identified in the LSK compartment, along with stem cells and multipotent progenitors, these cells were likely still producing myeloid cells. In addition, the number of LIN^{-} c-kit^{hi} FcγRII/III^{+} cells decreased during LPS challenge, suggesting that either development of myeloid progenitor cells into mature neutrophils had occurred rapidly, such that the number of cells present in the pool was minor, or that inflammatory cytokines were exerting an inhibitory effect on the number of these cells. Indeed a contraction in the number of

myeloid progenitor cells was also reported during malaria (Belyaev et al., 2010), Vaccinia virus (VV; Singh et al., 2008), human cytomegalovirus (HCMV; Gibbons et al., 1995) and *E. coli* infection (Zhang et al., 2010).

In contrast to the production of mature myeloid cells, mature lymphocyte numbers appeared to decline. In the circulation there was an immediate decrease in the number of lymphocytes after LPS challenge. The same result was also reported by Chandra and colleagues (Chandra et al., 2008) who observed a marked decrease in the number of circulating B-cells, as well as T-cells, during endotoxemia. This suggested that lymphocytes could have been homing to organs in order to provide more space for infiltrating neutrophils; were reduced because of a lack of lymphoid progenitor cells; or the cells were dying. On analysis of the BM, the frequency of B-cells increased after 24 hours, therefore this could have been indicative of circulating B-cells migrating into the BM. However, at 72 hours post LPS challenge, there was a complete depletion of these cells. Ueda and co-workers (Ueda et al., 2004) showed that TNFα and IL-1β could substantially reduce the number of lymphocytes in the BM, therefore TNFα release from macrophages during LPS challenge could be one reason for the absence of BM B-cells. Analysis of progenitor populations also revealed that LMPP and CLP cells were depleted 12 hours post LPS challenge, which would subsequently cause a cessation of B-cell production. However, this depletion was not due to re-direction of cells from the lymphoid lineage into the myeloid lineage. Contraction of the CLP population was also evident in malaria infection (Belyaev et al., 2010), but increased during VV infection (Singh et al., 2008). This was probably due to clearance of VV predominantly by the adaptive immune system, as opposed to the innate immune response during LPS challenge. Therefore, during LPS challenge, it appeared that lymphopoiesis was halted in favour of myelopoiesis.

Analysis of the stem cell compartment revealed that the number of LT-HSC cells did not change during LPS challenge. This suggested that there was no requirement for the enhanced production of ST-HSCs and even though there was an expansion in the number of LSK $CD34^+$ $Flk\text{-}2^+$ cells, this was most likely due to the presence of $CD34^+$ myeloid progenitors within the LSK compartment. Therefore, the changes in haematopoietic progenitor cells seemed to be transient.

5.9 IFNγ and TNFα cytokines are responsible for the upregulation of Sca-1 on haematopoietic progenitor cells during LPS challenge

Next we attempted to define the potential mechanisms involved in the alteration of BM progenitor phenotype and number during LPS challenge. We focused on the cause of Sca-1 upregulation on LIN$^-$ c-kit^{hi} Sca-1$^-$ cells and hypothesised that this upregulation was due to an increase in pro-inflammatory cytokines after LPS administration. Due to TNFα being the primary mediator of the effects of LPS (Beutler et al., 1985), we investigated whether this cytokine was responsible for the modulation of Sca-1 expression. In order to address this, we analysed LPS challenge in mice which were unable to respond to TNFα (*Tnfr1*-null mice). Due to the increase in Sca-1 expression being most prominent at 12 hours post LPS, mice were analysed at this time point. As shown in Figure 5.15C, compared to LPS challenge in C57BL/6 mice at 12 hours post LPS (Figure 5.15B) there appeared to be only a subtle downregulation of Sca-1 on LSK cells. However, when we analysed Sca-1 expression more closely on LIN$^-$ c-kit^{hi} cells, there was a reduction in both the frequency (Figure 5.16C) and number (Figure 5.17C) of Sca-1$^+$ cells in *Tnfr1*-null mice compared to LPS challenge in C57BL/6 mice and a significant increase in the frequency (Figure 5.16B) and number (Figure 5.17B) of Sca-1^{int} cells. There was also a significant increase in the frequency (Figure 5.16A) and number (Figure 5.17A) of Sca-1$^-$ cells. This data indicated that TNFα was partly responsible for the upregulation of Sca-1 on LIN$^-$ c-kit^{hi} Sca-1$^-$ cells, however it was not the sole cause.

Due to previous studies reporting that IFNγ is able to induce an expansion of the LSK compartment both *in vitro* (Zhao et al., 2010) and *in vivo* (Belyaev et al., 2010) during inflammatory conditions, we next assessed the effect of IFNγ on Sca-1 expression during LPS challenge. In order to do this, we analysed the phenotype, frequency and

number of haematopoietic progenitor cells in mice lacking the IFNγ receptor 1 (*Ifngr1*-null). Our results illustrated that LSK cells in *Ifngr1*-null mice exhibited much reduced levels of Sca-1 expression such that the frequency of cells in the LSK compartment (Figure 5.15D) were now comparable to control mice (Figure 5.15A). However, the frequency of LIN^- c-kit^{hi} $Sca1^-$ cells was not fully restored to wildtype levels (Figure 5.15D). On observation of Sca-1 levels in all LIN^- c-kit^{hi} cells, there was a significant increase in the frequency (Figure 5.16A) and number (Figure 5.17A) of Sca-1^- cells. This was mirrored by a decrease in the frequency and number of Sca-1^+ cells (Figure 5.16C and 5.17C). In contrast to LPS challenge in *Tnfr1*-null mice, there was no evidence for an increase in the number of Sca-1^{int} cells and instead there was a significant decrease in the number of LIN^- c-kit^{hi} cells expressing intermediate levels of Sca-1 compared to the control (Figure 5.17B). In comparison to Sca-1 modulation in *Tnfr1*-null mice, *Ifngr1*-null mice appeared to exert a larger downregulation of Sca-1 on LSK cells both in terms of frequency (Figure 5.16) and number (Figure 5.17). Therefore, IFNγ seemed to be largely responsible for the expression of Sca-1 on LIN^- c-kit^{hi} $Sca1^-$ cells. However, the frequency and number of Sca-1^- cells in the LIN^- c-kit^{hi} fraction were not fully restored to wildtype levels in *Tnfr1*-null or *Ifngr1*-null mice.

In order to fully restore the frequency and number of LIN^- c-kit^{hi} Sca-1^- cells during LPS challenge to wildtype levels, we next investigated whether TNFα and IFNγ could be acting in synergy to upregulate Sca-1 on LIN^- c-kit^{hi} Sca-1^- cells. This assumption was based on reports which have previously shown that TNFα and IFNγ can act in synergy in other immunological processes. One study proved that TNFα and IFNγ acting together could enhance tumour cytotoxicity and activate macrophages (Esparza et al., 1987). In addition, another study investigating Sca-1 expression *in vitro* showed that

TNFα cultured alone with BM cells could not induce Sca-1, however in conjunction with IFNγ, TNFα could act synergistically to further increase the percentage of Sca-1, higher than that of IFNγ alone (Malek et al., 1989). We therefore wanted to measure the induction of Sca-1 on LIN$^-$ c-kit^{hi} Sca-1$^-$ cells in the absence of both IFNγ and TNFα signalling. To achieve this we injected neutralising anti-TNFα mAb into *Ifngr1*-null mice.

Our results demonstrated that the frequency of both the LSK and LIN$^-$ c-kit^{hi} Sca-1$^-$ compartments in these mice (Figure 5.15E) were almost identical to the control mice (Figure 5.15A). The frequency of Sca-1$^-$ cells on all LIN$^-$ c-kit^{hi} progenitors had been restored to the same level as control mice (Figure 5.16A), and this was also reflected by a subsequent decrease in the frequency of Sca-1$^+$ cells back to steady-state levels (Figure 5.16C). This result is also illustrated in Figure 5.18 which clearly shows that a major increase in Sca-1 expression was evident after injection of LPS into C57BL/6 mice. There was a minor reduction in Sca-1 upregulation in *Tnfr1*-null mice, however LPS injection in *Ifngr1*-null mice showed a major decline in Sca-1 expression. Finally we showed that ablating the effects of both IFNγ and TNFα signalling fully restored the frequency of Sca-1 to homeostatic levels. In addition, the absolute numbers of all Sca-1 levels in LIN$^-$ c-kit^{hi} cells, after ablation of TNFα and IFNγ signalling, exhibited no significant change compared to control mice (Figure 5.17). Therefore this data proved that the upregulation of Sca-1 on LIN$^-$ c-kit^{hi} Sca-1$^-$ cells was caused by IFNγ and TNFα.

Figure 5.15

Analysing the cytokines responsible for the upregulation of Sca-1 on haematopoietic progenitor cells during LPS challenge using various receptor knock out models.

FACS plots illustrating the analysis of cytokine receptor 'knock out' models in order to restore Sca-1 levels on LSK cells during LPS challenge after 12 hours. All mice analysed were aged eight to ten weeks of age. One representative experiment is shown for each mouse strain. Ten mice were analysed for each strain (five males and five females) from 15 independent experiments (three individual experiments per knock out mouse).

A Frequency of LIN^- c-kit^{hi} Sca-1^- and LSK cells in control mice injected with endotoxin-free water.

B Frequency of LIN^- c-kit^{hi} Sca-1^- and LSK cells during LPS injection into C57BL/6 mice.

C Frequency of LIN^- c-kit^{hi} Sca-1^- and LSK cells during LPS injection into *Tnfr1*-null ($TNFR1^{-/-}$) mice.

D Frequency of LIN^- c-kit^{hi} Sca-1^- and LSK cells during LPS injection into *Ifngr1*-null ($IFN\gamma R1^{-/-}$) mice.

E Frequency of LIN^- c-kit^{hi} Sca-1^- and LSK cells during LPS injection into *Ifngr1*-null ($IFN\gamma R1^{-/-}$) mice neutralised with TNFα antibody.

A

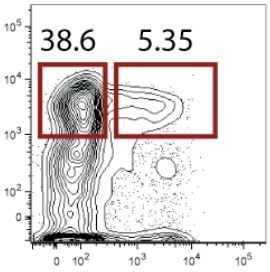

Control C57BL/6
Endotoxin free water injected

B

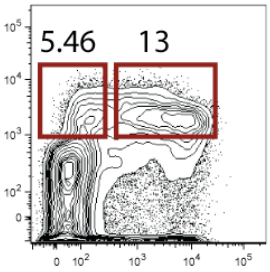

C57BL/6
LPS injected

C

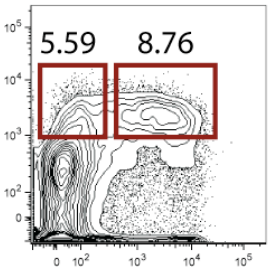

TNFR1$^{-/-}$
LPS injected

D

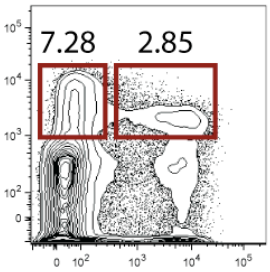

IFNγR1$^{-/-}$
LPS injected

E

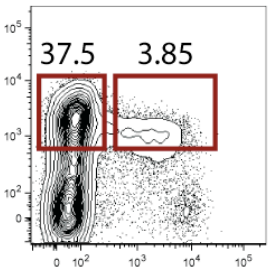

αTNF in IFNγR1$^{-/-}$
LPS injected

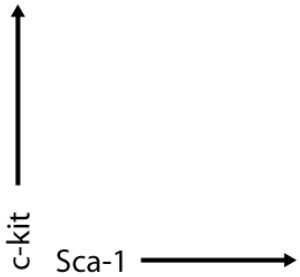

Figure 5.16

*Frequency of Sca-1 negative, intermediate and positive levels on LIN$^-$ c-kit^{hi} cells at 12 hours post LPS challenge in C57BL/6, Tnfr1-null, Ifngr1-*null *and TNFα-neutralised Ifngr1-null mice.*

A Bar chart illustrating the frequency of Sca-1$^-$ cells in LIN$^-$ c-kit^{hi} cells of C57BL/6, *Tnfr1*-null (TNFR1$^{-/-}$), *Ifngr1*-null (IFNγR1$^{-/-}$) and TNFα-neutralised *Ifngr1*-null (IFNγR1$^{-/-}$) mice 12 hours post LPS injection. Control mice were injected with distilled water. Ten mice were analysed for each mouse strain from 15 independent experiments. Significance was calculated using the Student's T-test ($p < 0.05$). Values represent mean ± S.E.M.

B Bar chart illustrating the frequency of Sca-1^{int} cells in LIN$^-$ c-kit^{hi} cells of C57BL/6, *Tnfr1*-null (TNFR1$^{-/-}$), *Ifngr1*-null (IFNγR1$^{-/-}$) and TNFα-neutralised *Ifngr1*-null (IFNγR1$^{-/-}$) mice 12 hours post LPS injection. Control mice were injected with distilled water. Ten mice were analysed for each mouse strain from 15 independent experiments. Significance was calculated using the Student's T-test ($p < 0.05$). Values represent mean ± S.E.M.

C Bar chart illustrating the frequency of Sca-1$^+$ cells in LIN$^-$ c-kit^{hi} cells of C57BL/6, *Tnfr1*-null (TNFR1$^{-/-}$), *Ifngr1*-null (IFNγR1$^{-/-}$) and TNFα-neutralised *Ifngr1*-null (IFNγR1$^{-/-}$) mice 12 hours post LPS injection. Control mice were injected with distilled water. Ten mice were analysed for each mouse strain from 15 independent experiments. Significance was calculated using the Student's T-test ($p < 0.05$). Values represent mean ± S.E.M.

A

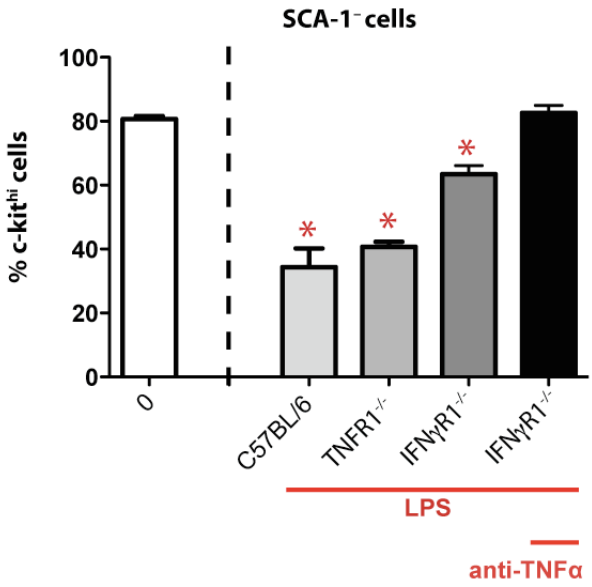
SCA-1⁻ cells
% c-kit^hi cells
100
80
60
40
20
0
0
C57BL/6
TNFR1-/-
IFNγR1-/-
IFNγR1-/-
LPS
anti-TNFα

B

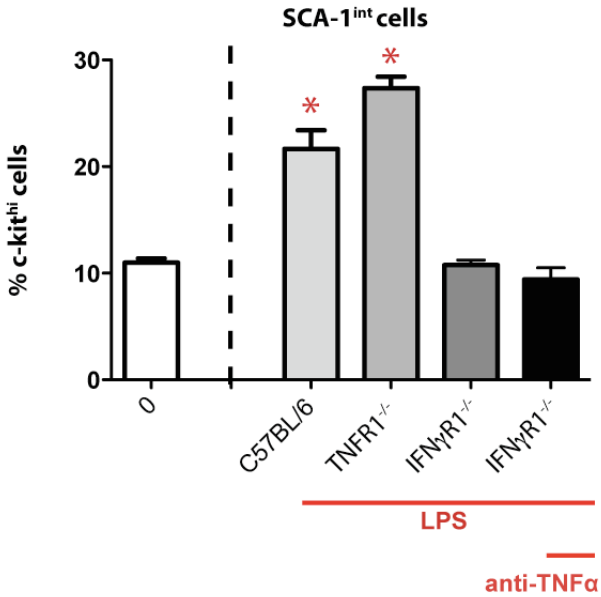
SCA-1^int cells
% c-kit^hi cells
30
20
10
0
0
C57BL/6
TNFR1-/-
IFNγR1-/-
IFNγR1-/-
LPS
anti-TNFα

C

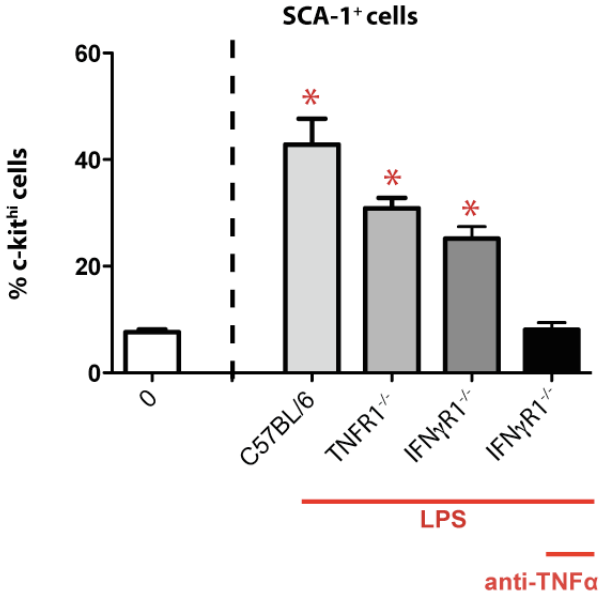
SCA-1⁺ cells
% c-kit^hi cells
60
40
20
0
0
C57BL/6
TNFR1-/-
IFNγR1-/-
IFNγR1-/-
LPS
anti-TNFα

Figure 5.17

Absolute numbers of Sca-1 negative, intermediate and positive levels on LIN$^-$ c-kit^{hi} cells at 12 hours post LPS challenge in C57BL/6, Tnfr1-null, Ifngr1-null and TNFα-neutralised Ifngr1-null mice.

A Bar chart illustrating the number of Sca-1$^-$ cells in LIN$^-$ c-kit^{hi} cells of C57BL/6, *Tnfr1*-null (TNFR1$^{-/-}$), *Ifngr1*-null (IFNγR1$^{-/-}$) and TNFα-neutralised *Ifngr1*-null (IFNγR1$^{-/-}$) mice 12 hours post LPS injection. Control mice were injected with distilled water. Ten mice were analysed for each mouse strain from 15 independent experiments. Significance was calculated using the Student's T-test ($p < 0.05$). Values represent mean ± S.E.M.

B Bar chart illustrating the number of Sca-1^{int} cells in LIN$^-$ c-kit^{hi} cells of C57BL/6, *Tnfr1*-null (TNFR1$^{-/-}$), *Ifngr1*-null (IFNγR1$^{-/-}$) and TNFα-neutralised *Ifngr1*-null (IFNγR1$^{-/-}$) mice 12 hours post LPS injection. Control mice were injected with distilled water. Ten mice were analysed for each mouse strain from 15 independent experiments. Significance was calculated using the Student's T-test ($p < 0.05$). Values represent mean ± S.E.M.

C Bar chart illustrating the number of Sca-1$^+$ cells in LIN$^-$ c-kit^{hi} cells of C57BL/6, *Tnfr1*-null (TNFR1$^{-/-}$), *Ifngr1*-null (IFNγR1$^{-/-}$) and TNFα-neutralised *Ifngr1*-null (IFNγR1$^{-/-}$) mice 12 hours post LPS injection. Control mice were injected with distilled water. Ten mice were analysed for each mouse strain from 15 independent experiments. Significance was calculated using the Student's T-test ($p < 0.05$). Values represent mean ± S.E.M.

A

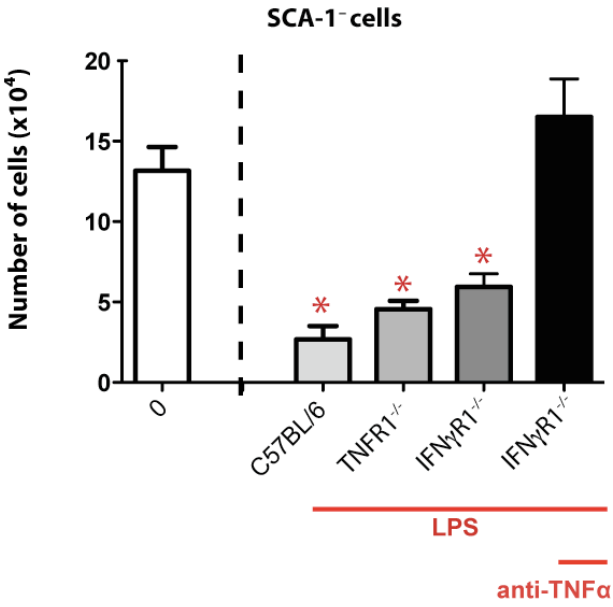
SCA-1⁻ cells
Number of cells (x10⁴)
20
15
10
5
0
0
C57BL/6
TNFR1-/-
IFNγR1-/-
IFNγR1-/-
LPS
anti-TNFα

B

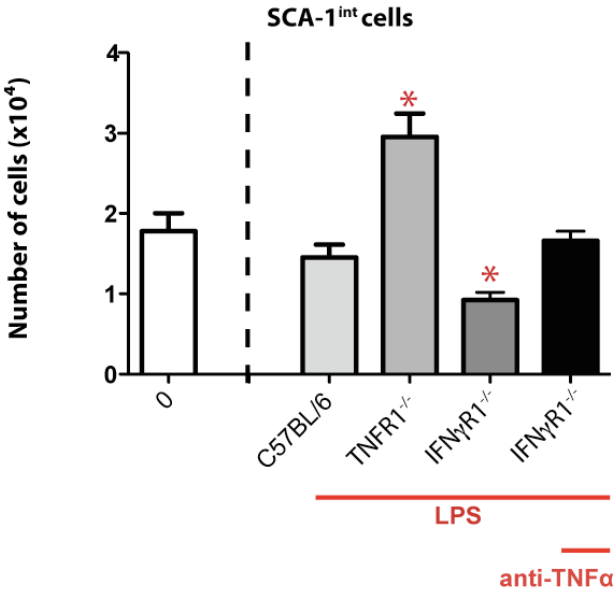
SCA-1int cells
Number of cells (x10⁴)
4
3
2
1
0
0
C57BL/6
TNFR1-/-
IFNγR1-/-
IFNγR1-/-
LPS
anti-TNFα

C

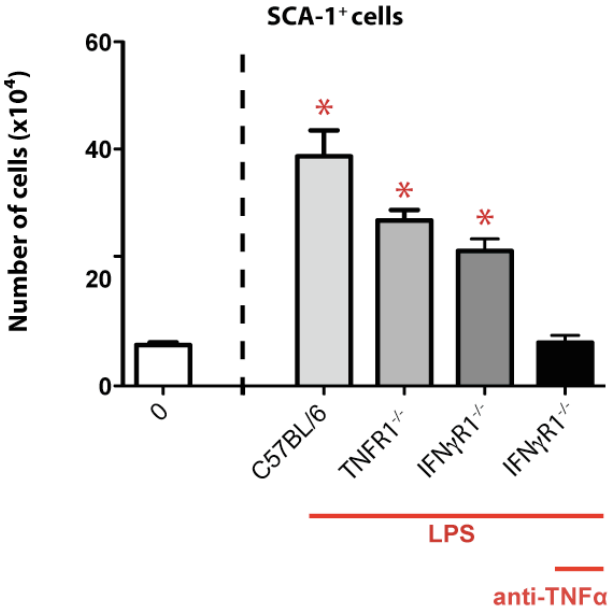
SCA-1+ cells
Number of cells (x10⁴)
60
40
20
0
0
C57BL/6
TNFR1-/-
IFNγR1-/-
IFNγR1-/-
LPS
anti-TNFα

Figure 5.18

Frequency of Sca-1 levels in LIN$^-$ c-kit^{hi} cells directly compared between different mouse strains at 12 hours post LPS challenge.

Representative histogram illustrating the Sca-1 levels of LIN$^-$ c-kit^{hi} cells after LPS challenge in different mouse strains. Sca-1 levels in control mice (dark blue line) were analysed in mice injected with distilled water. Sca-1 upregulation was observed after LPS injection in C57BL/6 mice (green line). There was only a minor reduction in Sca-1 levels after analysis of *Tnfr1*-null mice (orange line), but a major reduction of Sca-1 expression in *Ifngr1*-null mice (light blue line). However, Sca-1 levels were only fully restored once TNFα-neutralisation in *Ifngr1*-null mice was carried out (red line).

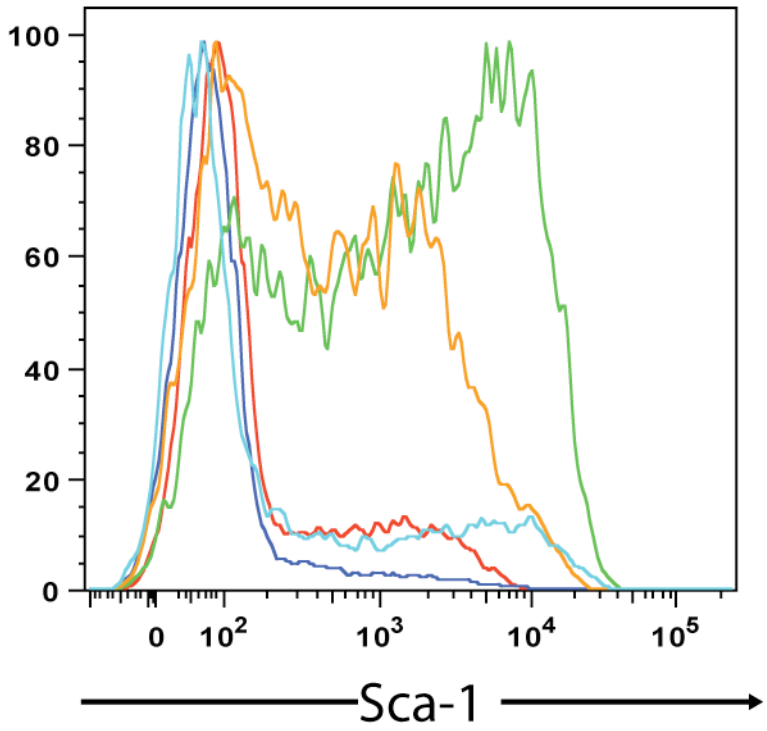

Control C57BL/6
Endotoxin free water injected

C57BL/6 LPS injected

TNFR1$^{-/-}$ LPS injected

IFNγR1$^{-/-}$ LPS injected

αTNF in IFNγR1$^{-/-}$ LPS injected

5.10 Analysis of the absolute number of haematopoietic progenitor cells in mice deficient in IFNγ and TNFα signalling

In order to assess whether the changes in ST-HSC, LMPP and CLP numbers were also due to the combined effect of TNFα and IFNγ during LPS challenge, we analysed the absolute number of these progenitor cells in *Tnfr1*-null, *Ifngr1*-null and *Ifngr1*-null mice injected with blocking anti-TNFα mAb. Due to the effects of LPS being reverted by 72 hours, we analysed progenitor cell numbers at 12 and 24 hours post LPS. As shown in Figure 5.19A, *Tnfr1*-null mice exhibited a significant increase in the number of cells with the LSK CD34$^+$ Flk-2$^-$ phenotype representing ST-HSC, CMP and GMP cell types when compared to controls. This result was indicative of only a minor decrease of Sca-1 expression on myeloid cells in *Tnfr1*-null mice. In addition, the number of LSK CD34$^+$ Flk-2$^+$ cells, representing LMPPs, and LIN$^-$ IL-7Rα$^+$ Flk-2$^+$ cells, representing CLPs, still decreased significantly after 12 and 24 hours post LPS challenge, similar to C57BL/6 LPS injected mice. Therefore, no major changes were observed in the number of ST-HSC, LMPP or CLP populations in *Tnfr1*-null mice in comparison to LPS injected C57BL/6 mice. This data suggested that TNFα signalling via TNFR1 was not responsible for the observed decline in lymphopoiesis during LPS challenge.

In LPS injected *Ifngr1*-null mice however, there was a major decrease in the absolute number of LSK CD34$^+$ Flk-2$^-$ cells (Figure 5.19B) at 12 and 24 hours compared to C57BL/6 (Figure 5.6) and *Tnfr1*-null LPS injected mice (Figure 5.19A). The number of LSK CD34$^+$ Flk-2$^-$ cells did not significantly increase at 12 hours post LPS in *Ifngr1*-null mice compared to control mice and although the increase in the number of cells at 24 hours was significant, it was minor compared to the increase observed in C57BL/6 and *Tnfr1*-null LPS injected mice. Due to the frequency of LSK cells in *Ifngr1*-null mice during LPS challenge being similar to control mice (Figure 5.15D),

this suggested that Sca-1 expression on LIN$^-$ c-kit^{hi} Sca-1$^-$ cells had been significantly downregulated. Therefore, the increase in the number of LSK CD34$^+$ Flk-2$^-$ cells observed in C57BL/6 mice may have been due in part to upregulation of Sca-1 on CD34$^+$ CMP and GMP cells caused mainly by IFNγ. In contrast, the number of LSK CD34$^+$ Flk-2$^+$ numbers did reduce, but this decrease was only significant after 24 hours post LPS (Figure 5.19B). This suggested that the reduction in the number of LMPP cells during LPS challenge was due in part to IFNγ. In addition, although LIN$^-$ IL-7Rα$^+$ Flk-2$^+$ numbers still decreased after 12 and 24 hours (Figure 5.19B), the recovery of these cells was already beginning at 24 hours. This was not observed in C57BL/6 or *Tnfr1*-null mice where the number of CLP cells at 24 hours remained low. These results indicated that IFNγ was playing a major role both in the upregulation of Sca-1 on LIN$^-$ c-kit^{hi} Sca-1$^-$ cells and in the reduction of lymphopoiesis, but that a high degree of redundancy was present in the system. We next investigated whether the cessation of lymphoid development following LPS challenge is dependent on the combined action of IFNγ and TNFα.

During previous analysis of the frequency and number of Sca-1 levels on LIN$^-$ c-kit^{hi} cells after LPS injection, both IFNγ and TNFα were responsible for restoring Sca-1 expression to wildtype levels. Therefore, we next investigated whether these two cytokines combined were also responsible for the sequestration of lymphopoiesis during LPS challenge. The number of progenitor cells in *Ifngr1*-null mice injected with antibodies specific to TNFα was calculated (Figure 5.19C). Interestingly, the number of haematopoietic progenitors was not restored to control levels. Instead, what we observed was a significant increase in the LSK CD34$^+$ Flk-2$^-$ (ST-HSC) numbers after 12 and 24 hours, a significant decrease in the LSK CD34$^+$ Flk-2$^+$ (LMPP) numbers after 12 hours and a significant decrease in the LIN$^-$ IL-7Rα$^+$ Flk-2$^+$ (CLP) numbers at 12

and 24 hours. Since the frequency and number of Sca-1 levels were fully restored to steady state levels in these mice, we assumed that ST-HSC, LMPP and CLP cells could all be identified according to their conventional phenotype. Therefore, in these mice it appeared that ablating the effects of both TNFα and IFNγ did not restore the number of lymphoid progenitors or stem cells back to control levels. This indicated that the mechanisms responsible or the level of cytokines required for the upregulation of Sca-1 on LIN^- c-kit^{hi} $Sca\text{-}1^-$ cells must be different to those leading to the transient cessation of lymphopoiesis. One obvious explanation for this observation might be the only partial neutralisation of TNFα bioactivity, resulting in ongoing TNFα signalling. A complete absence of TNFα would be required to restore lymphoid differentiation, but only partial absence of TNFα was needed to inhibit the expression of Sca-1 on LIN^- c-kit^{hi} $Sca\text{-}1^-$ cells. However, even if TNFα was not completely neutralised it would be expected that the number of progenitor cells would still mirror those observed in *Ifngr1*-null mice, where TNFα signalling was not disrupted, however this was not the case. Therefore, another explanation is that LPS may have been exerting a direct effect on TLR4 receptors present on LMPP and CLP cells (Nagai et al., 2006) which caused these cells to apoptose.

Figure 5.19

*Absolute numbers of haematopoietic progenitor subsets in Tnfr1-null, Ifngr1-*null *and TNFα-neutralised Ifngr1-null mice during LPS challenge.*

A Graph illustrating the number of LSK $CD34^+$ Flk-2^-, LSK $CD34^+$ Flk-2^+ and LIN^- IL-7Rα^+ Flk-2^+ cells per femur pair in *Tnfr1*-null ($TNFR1^{-/-}$) mice 12 and 24 hours post LPS challenge. Significance was calculated using the Student's T-test ($p < 0.05$). Ten mice were analysed per time point from three independent experiments. Values represent mean ± S.E.M.

B Graph illustrating the number of LSK $CD34^+$ Flk-2^-, LSK $CD34^+$ Flk-2^+ and LIN^- IL-7Rα^+ Flk-2^+ cells per femur pair in *Ifngr1*-null ($IFN\gamma R1^{-/-}$) mice 12 and 24 hours post LPS challenge. Significance was calculated using the Student's T-test ($p < 0.05$). Ten mice were analysed per time point from three independent experiments. Values represent mean ± S.E.M.

C Graph illustrating the number of LSK $CD34^+$ Flk-2^-, LSK $CD34^+$ Flk-2^+ and LIN^- IL-7Rα^+ Flk-2^+ cells per femur pair in TNFα-neutralised *Ifngr1*-null ($IFN\gamma R1^{-/-}$) mice 12 and 24 hours post LPS challenge. Significance was calculated using the Student's T-test ($p < 0.05$). Ten mice were analysed per time point from three independent experiments. Values represent mean ± S.E.M.

A

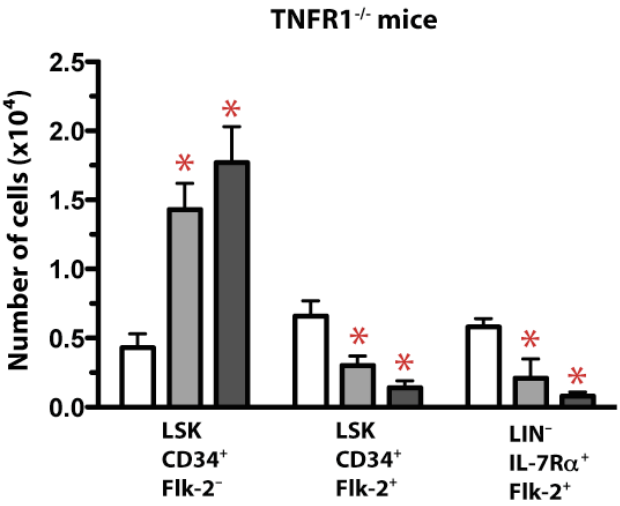
TNFR1-/- mice
Number of cells (x10⁴)
2.5
2.0
1.5
1.0
0.5
0.0
LSK CD34+ Flk-2-
LSK CD34+ Flk-2+
LIN- IL-7Rα+ Flk-2+

B

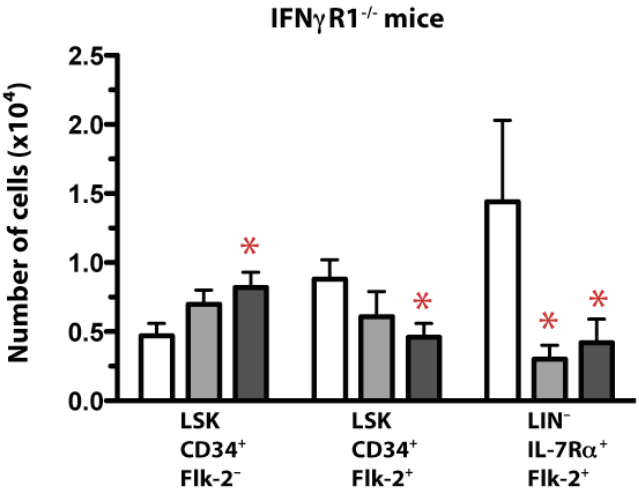
IFNγR1-/- mice
Number of cells (x10⁴)
2.5
2.0
1.5
1.0
0.5
0.0
LSK CD34+ Flk-2-
LSK CD34+ Flk-2+
LIN- IL-7Rα+ Flk-2+

C

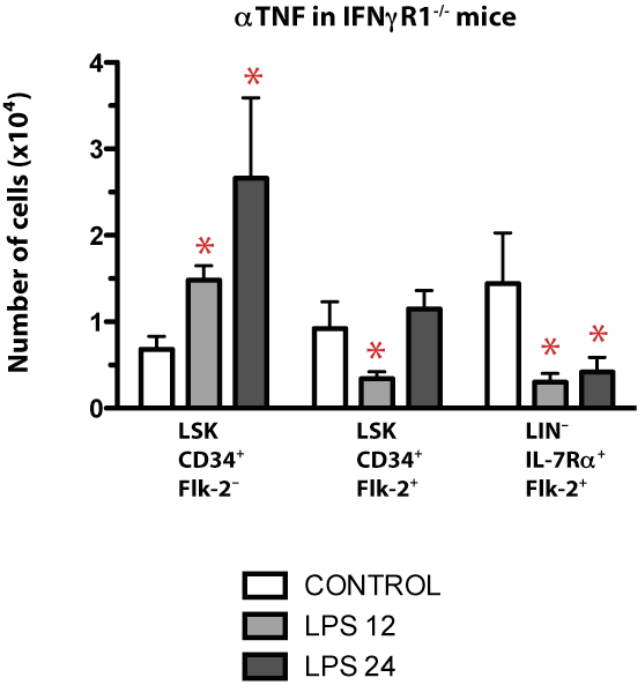
αTNF in IFNγR1-/- mice
Number of cells (x10⁴)
4
3
2
1
0
LSK CD34+ Flk-2-
LSK CD34+ Flk-2+
LIN- IL-7Rα+ Flk-2+
CONTROL
LPS 12
LPS 24

5.11 Analysis of the number of circulating white blood cells in mice deficient in IFNγ and TNFα signalling

Since the number of stem cells and progenitors was only partially rescued during LPS challenge in the absence of TNFα and IFNγ signalling, we next investigated whether the number of circulating granulocytes, lymphocytes and monocytes was changed. Coinciding with results obtained after LPS challenge in C57BL/6 mice, the number of granulocytes in both male and female mice increased significantly after LPS injection in *Tnfr1*-null mice (Figure 5.20A). Both male and female mice exhibited the highest number of granulocytes at 12 hours post LPS challenge ($9.28 \pm 3.69 \times 10^9$/l and $6.30 \pm 0.57 \times 10^9$/l). However, the number of granulocytes in male and female mice of *Tnfr1*-null mice did not reach the maximum number which was observed in C57BL/6 male ($15.33 \pm 2.45 \times 10^9$/l) and female mice ($11.3 \pm 1.61 \times 10^9$/l). The number of granulocytes in male and female mice had reduced at 24 hours ($2.62 \pm 0.39 \times 10^9$/l and $2.94 \pm 0.99 \times 10^9$/l) and this was in contrast to LPS injected C57BL/6 mice where the number of granulocytes returned to homeostatic levels at 48 hours in female and 72 hours in male mice. Therefore, this suggested that TNFα signalling was important in the recruitment of granulocytes to the site of infection and could play a role in the export of granulocytes from the BM and into the periphery.

The number of circulating lymphocytes in LPS injected *Tnfr1*-null mice (Figure 5.20B) was very similar to the number observed during LPS challenge in C57BL/6 mice. Immediately after LPS challenge, at 3.5 hours there was a steep decrease in the number of circulating lymphocytes in male mice ($4.4 \pm 0.61 \times 10^9$/l from $16.20 \pm 1.09 \times 10^9$/l) and female mice ($4.2 \pm 0.82 \times 10^9$/l from $15.47 \pm 0.89 \times 10^9$/l). Both male and female lymphocyte number remained low until 48 hours but at 72 hours there was an increase in the number of cells compared to the control. The number of cells in male mice

increased to 19.42 ± 1.38 x 10^9/l and the number of lymphocytes in female mice increased to 15.47 ± 0.89 x 10^9/l. Therefore, due to the same change in the number of lymphocytes occurring in *Tnfr1*-null mice compared to C57BL/6 mice during LPS challenge, this indicated that TNFα signalling was not playing a major role in the reduction of lymphocytes in the circulation.

The monocyte number in *Tnfr1*-null mice (Figure 5.20C) also resembled that of C57BL/6 LPS injected mice. There were only minor changes observed throughout the study, which were observed as a significant decrease in the number of monocytes in male and female mice at 3.5 hours post LPS and an increase in the number of monocytes in male and female mice at 72 hours post LPS challenge compared to control values. Therefore, in the absence of TNFα signalling, no major changes were observed in the number of circulating monocytes or lymphocytes compared to C57BL/6 LPS injected mice, but TNFα could be involved in regulating the number of circulating granulocytes.

We also looked at the number of circulating white blood cells in *Ifngr1*-null mice (Figure 5.21). Unlike in the absence of TNFα signalling, the number of granulocytes in male and female mice did not increase until 7 hours post LPS challenge (Figure 5.21A). In male mice the number of granulocytes increased further at 12 hours post LPS and the maximum amount of cells was reached (21.20 ± 5.00 x 10^9/l). This number was higher than LPS challenge in C57BL/6 and *Tnfr1*-null mice, suggesting that IFNγ may have been inhibiting the production and export of granulocytes from the BM to the periphery in male mice during LPS challenge. However in contrast, the number of granulocytes in female mice remained at a relatively constant level at 7, 12 and 24 hours post LPS (between 5.68 and 7.30 x 10^9/l cells). Therefore, this suggested that in female mice, the number of circulating granulocytes during LPS challenge was dependent on IFNγ

signalling. Therefore, these results suggested that IFNγ as well as TNFα, may also play a role in the mobilisation of granulocytes from the BM into the periphery. In addition, it appeared that the response to IFNγ and TNFα cytokines was different in male and female mice. A reduction in the number of granulocytes was observed at 72 hours in male and female mice.

The number of lymphocytes in *Ifngr1*-null mice (Figure 5.21B) during LPS challenge was similar to that observed in C57BL/6 and *Tnfr1*-null mice in that there was a significant decline in the number of cells at 3.5 hours post LPS challenge in male (2.57 ± 0.62 x 10^9/l from 7.76 ± 0.68 x 10^9/l) and female mice (2.2 ± 0.27 from 11.92 ± 0.8 x 10^9/l). Interestingly, the number of circulating lymphocytes increased in male mice at 7 hours (8.55 ± 2.78 x 10^9/l) and 12 hours (9.27 ± 1.84 x 10^9) and these values were not significantly different to those of the control. However, the number of lymphocytes declined again at 24 hours post LPS and had recovered at 72 hours. These changes were not observed in female mice where the number of lymphocytes remained low and increased only at 72 hours.

Similar to C57BL/6 and *Tnfr1*-null mice, there were no major changes observed in the number of monocytes in *Ifngr1*-null mice throughout the study (Figure 5.21C).

We next analysed the number of circulating white blood cells in TNFα-neutralised *Ifngr1*-null mice (Figure 5.22). In contrast to C57BL/6, *Tnfr1*-null mice and *Ifngr1*-null mice, the number of granulocytes peaked in male (18.8 x 10^9/l) and female mice (7.3 x 10^9/l) at 7 hours post LPS challenge (Figure 5.22A). In addition, similar to *Ifngr1*-null mice, the number of granulocytes in female mice remained lower than male mice throughout the study and ranged from 4.5 to 8.2 x 10^9/l between 7 and 72 hour time points. The number of granulocytes in male mice started to decline at 12 hours (12.25 ± 9.85 x 10^9/l) and decreased further at 24 hours (6.35 ± 1.91 x 10^9/l). However, at 12

hours post LPS in all other mouse strains, the maximum number of cells was reached. Therefore, the increase in the number of circulating granulocytes during LPS challenge seemed to be taking place over a shorter time period in the absence of TNFα and IFNγ signalling, indicating key roles for both of these cytokines in LPS-induced inflammation.

The number of lymphocytes in TNFα-neutralised *Ifngr1*-null mice (Figure 5.22B) was similar to that observed in the other mouse strains, in that the number of cells declined after LPS injection. In contrast to other mouse strains, the number of lymphocytes had not recovered by 72 hours post LPS. The number of monocytes also mirrored what was observed in the other mouse strains in that there were no major changes (Figure 5.23C). Therefore, this data indicate that TNFα and IFNγ were the key regulating elements for the mobilisation of granulocytes during LPS challenge. Although the number of white blood cells was not restored to wild type levels in any of the knock out strains during LPS challenge, mice deficient in IFNγ signalling and TNFα did recover at earlier time points in comparison to C57BL/6 injected mice.

Figure 5.20

Number of circulating granulocytes, lymphocytes and monocytes in LPS injected Tnfr1-null mice at 0, 12, 24 and 72 hour time points.

A Graph illustrating the number of circulating granulocytes in male (red line) and female mice (blue line), compared to control mice (black line). Data represents results from three independent experiments, using four mice (two male and two female) per time point. Significance was calculated using the Student's T-test ($p < 0.05$). Values represent mean ± S.E.M.

B Graph illustrating the number of circulating lymphocytes in male (red line) and female mice (blue line), compared to control mice (black line). Data represents results from three independent experiments, using four mice (two male and two female) per time point. Significance was calculated using the Student's T-test ($p < 0.05$). Values represent mean ± S.E.M.

C Graph illustrating the number of circulating monocytes in male (red line) and female mice (blue line), compared to control mice (black line). Data represents results from three independent experiments, using four mice (two male and two female) per time point. Significance was calculated using the Student's T-test ($p < 0.05$). Values represent mean ± S.E.M.

A

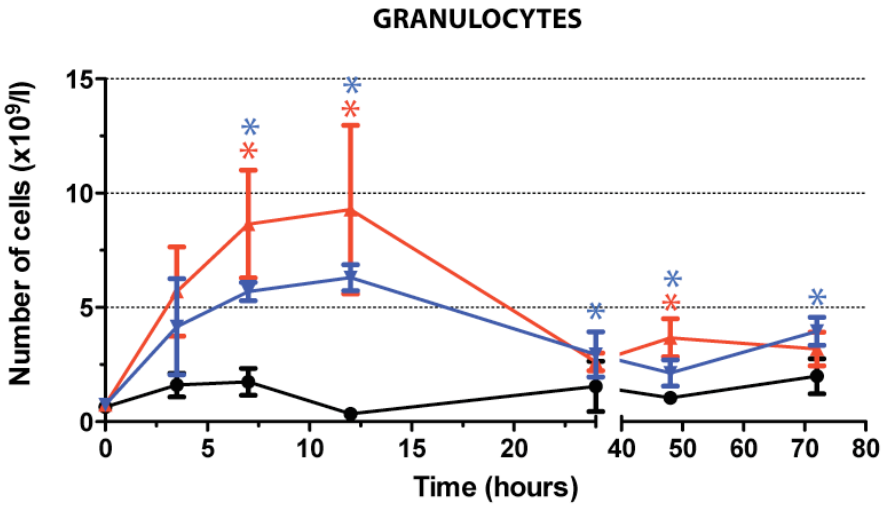
GRANULOCYTES
Number of cells (x10⁹/l)
Time (hours)

B

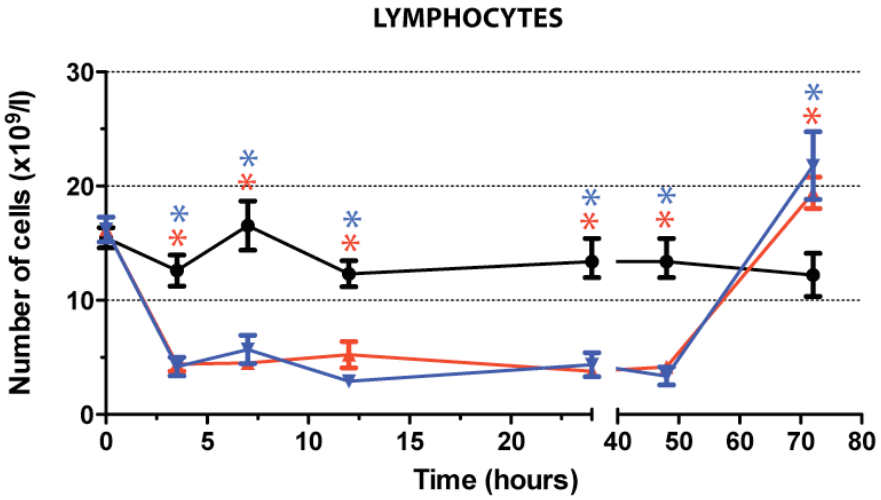
LYMPHOCYTES
Number of cells (x10⁹/l)
Time (hours)

C

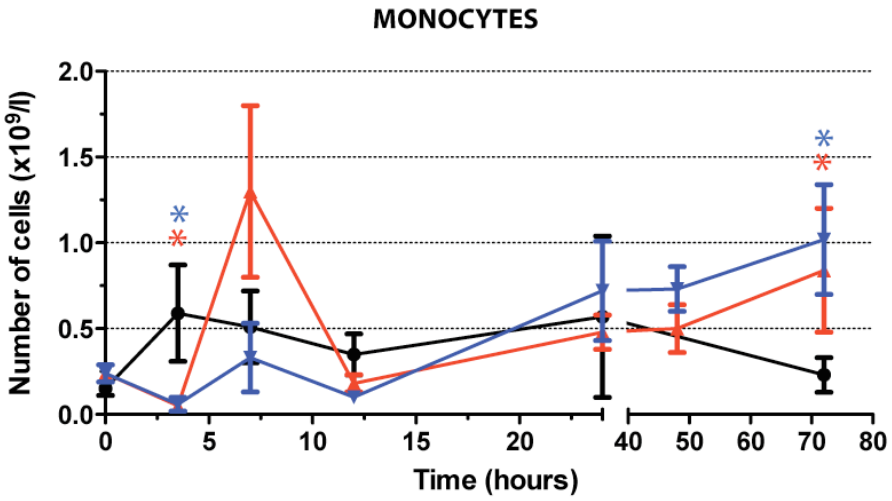
MONOCYTES
Number of cells (x10⁹/l)
Time (hours)

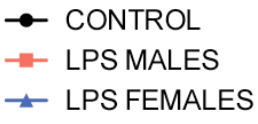
CONTROL
LPS MALES
LPS FEMALES

Figure 5.21

Number of circulating granulocytes, lymphocytes and monocytes in LPS injected Ifngr1-null mice at 0, 12, 24 and 72 hour time points.

A Graph illustrating the number of circulating granulocytes in male (red line) and female mice (blue line), compared to control mice (black line). Data represents results from three independent experiments, using four mice (two male and two female) per time point. Significance was calculated using the Student's T-test ($p < 0.05$). Values represent mean ± S.E.M.

B Graph illustrating the number of circulating lymphocytes in male (red line) and female mice (blue line), compared to control mice (black line). Data represents results from three independent experiments, using four mice (two male and two female) per time point. Significance was calculated using the Student's T-test ($p < 0.05$). Values represent mean ± S.E.M.

C Graph illustrating the number of circulating monocytes in male (red line) and female mice (blue line), compared to control mice (black line). Data represents results from three independent experiments, using four mice (two male and two female) per time point. Significance was calculated using the Student's T-test ($p < 0.05$). Values represent mean ± S.E.M.

A

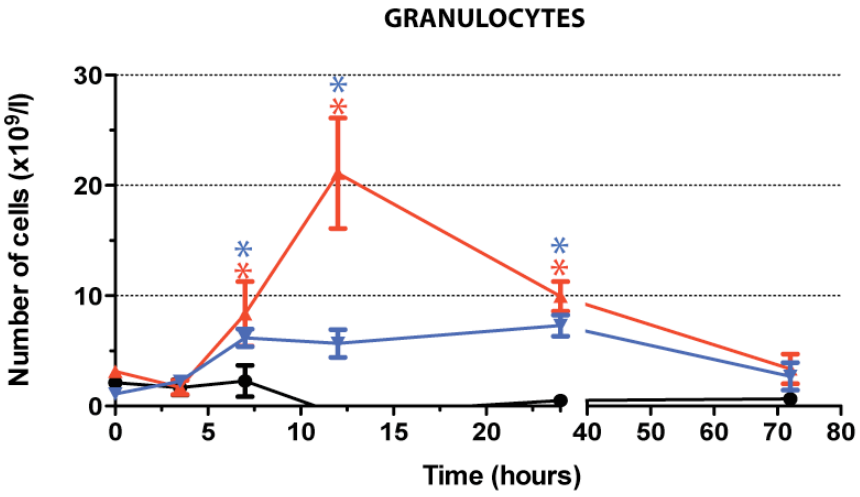
GRANULOCYTES
Number of cells (x10⁹/l)
30
20
10
0
0
5
10
15
20
40
50
60
70
80
Time (hours)

B

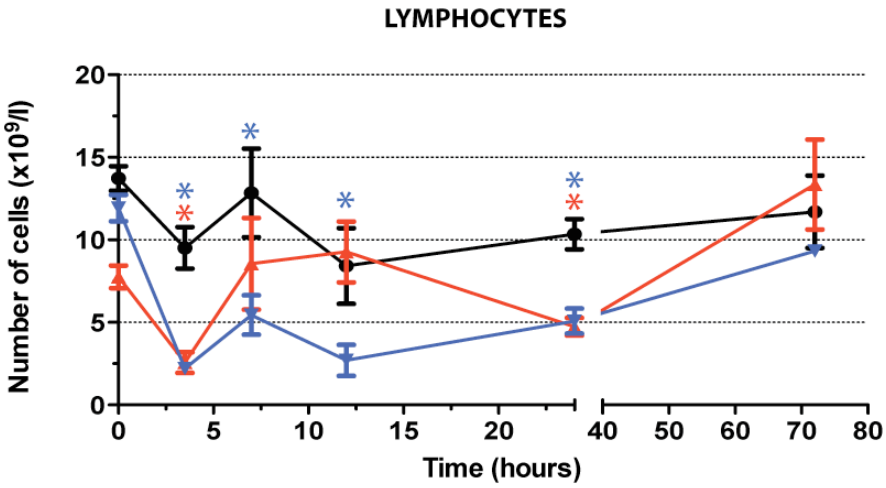
LYMPHOCYTES
Number of cells (x10⁹/l)
20
15
10
5
0
0
5
10
15
20
40
50
60
70
80
Time (hours)

C

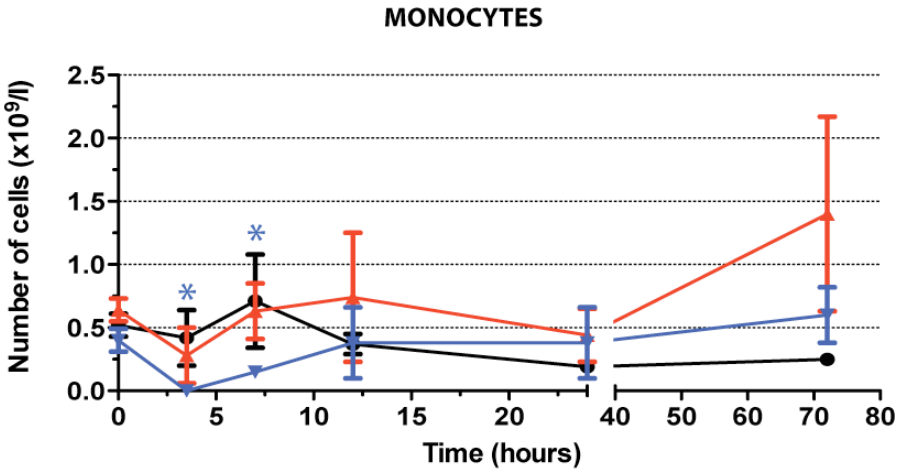
MONOCYTES
Number of cells (x10⁹/l)
2.5
2.0
1.5
1.0
0.5
0.0
0
5
10
15
20
40
50
60
70
80
Time (hours)

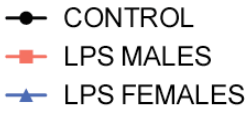
CONTROL
LPS MALES
LPS FEMALES

Figure 5.22

Number of circulating granulocytes, lymphocytes and monocytes in LPS injected TNFα-neutralised Ifngr1-null mice at 0, 12, 24 hour time points.

A Graph illustrating the number of circulating granulocytes in male (red line) and female (blue line) mice aged eight weeks of age, during steady state levels (black line) and after LPS challenge. Data represents results from three independent experiments, using one to two mice per time point. Significance was calculated using the Student's T-test ($p < 0.05$). Values represent mean ± S.E.M.

B Graph illustrating the number of circulating lymphocytes in male (red line) and female (blue line) mice aged eight weeks of age, during steady state levels (black line) and after LPS challenge. Data represents results from three independent experiments, using one to two mice per time point. Significance was calculated using the Student's T-test ($p < 0.05$). Values represent mean ± S.E.M.

C Graph illustrating the number of circulating monocytes in male (red line) and female (blue line) mice aged eight weeks of age, during steady state levels (black line) and after LPS challenge. Data represents results from three independent experiments, using one to two mice per time point. Significance was calculated using the Student's T-test ($p < 0.05$). Values represent mean ± S.E.M.

A

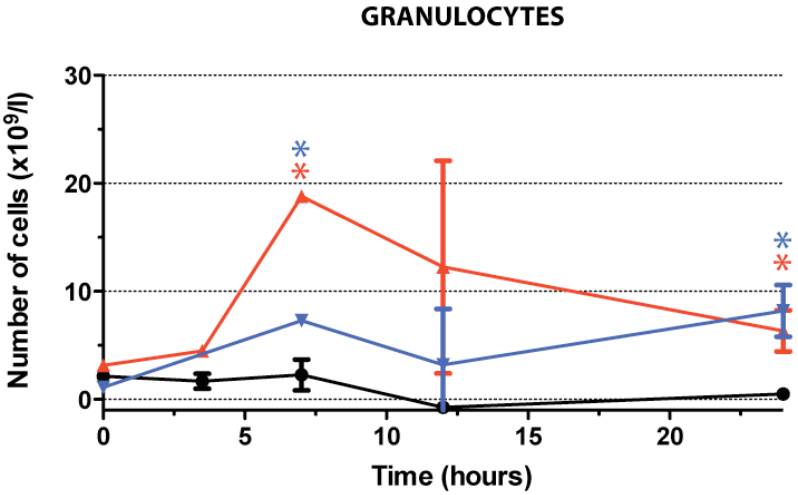
GRANULOCYTES
Number of cells (x10⁹/l)
30
20
10
0
0
5
10
15
20
Time (hours)
*
*
*
*

B

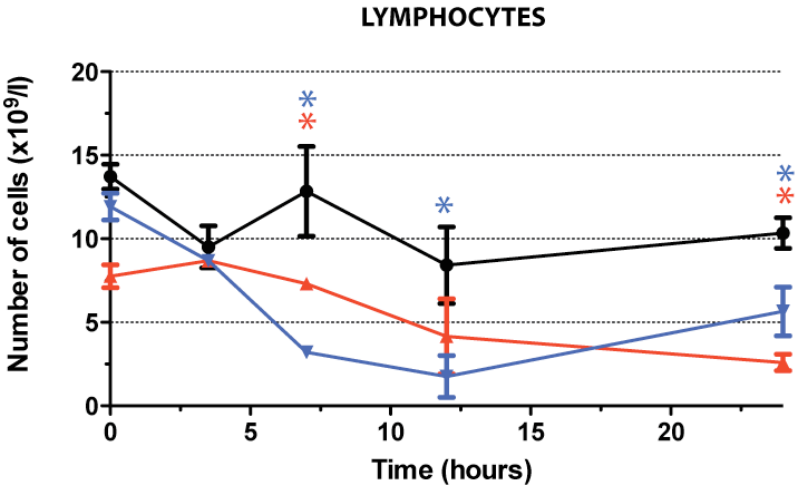
LYMPHOCYTES
Number of cells (x10⁹/l)
20
15
10
5
0
0
5
10
15
20
Time (hours)
*
*
*
*
*

C

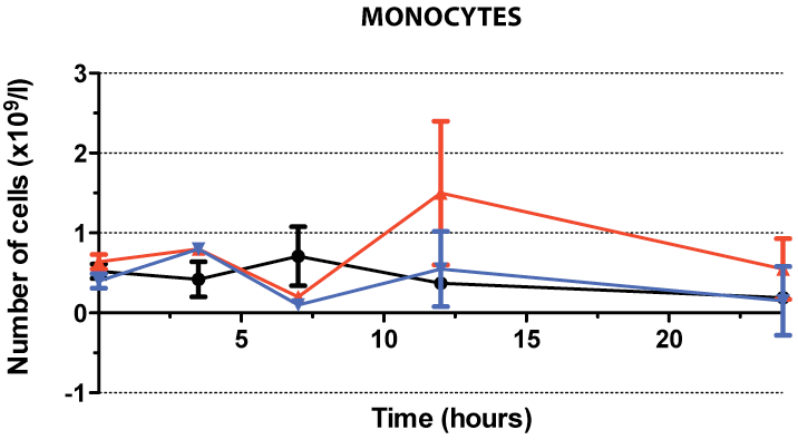
MONOCYTES
Number of cells (x10⁹/l)
3
2
1
0
-1
5
10
15
20
Time (hours)

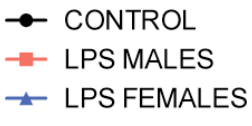
CONTROL
LPS MALES
LPS FEMALES

5.12 Serum levels of IFNγ and TNFα during LPS challenge

To further investigate why stem and progenitor cell numbers in the BM and circulating granulocyte and lymphocyte numbers were not fully restored in anti-TNFα injected *Ifngr1*-null mice and to determine when the highest amounts of IFNγ and TNFα were released during LPS challenge, we measured the serum levels of TNFα and IFNγ in the different mouse strains. The levels of IFNγ and TNFα were assessed in LPS injected C57BL/6, *Ifngr1*-null and TNFα-neutralised *Ifngr1*-null mice (Figure 5.23).

The levels of IFNγ (Figure 5.23A) in C57BL/6 control mice (26.8 ± 11.64 pg/ml) and control *Ifngr1*-null mice (12.13 ± 4.04 pg/ml) were relatively low, but levels of IFNγ were higher in control TNFα-neutralised *Ifngr1*-null mice (100.08 ± 56.33 pg/ml). This result indicated that neutralisation of TNFα caused an increase in IFNγ levels.

At 12 hours post injection, the level of IFNγ remained constant in C57BL/6 mice (22.04 ± 6.48 pg/ml) but in *Ifngr1*-null mice and TNFα-neutralised *Ifngr1*-null mice, the levels of IFNγ increased significantly to 1001.20 ± 470.14 pg/ml and 1421.06 ± 163.06 pg/ml in comparison to levels at 0 hours.

At 24 hours post LPS, the levels of IFNγ increased in C57BL/6 mice (68.69 ± 56.14 pg/ml) compared to levels at 0 and 12 hours. This coincided with a decline in total BM cellularity, export of mature myeloid cells to the periphery, and a decrease in the number of LIN^- cells, indicating that at 24 hours, IFNγ could be exerting the most severe effects. However, the levels of IFNγ decreased significantly in *Ifngr1*-null mice (74.89 ± 24.82 pg/ml). In TNFα-neutralised *Ifngr1*-null mice there was also a decrease in the level of IFNγ in the blood (991.76 ± 169.21), but not to the extent of *Ifngr1*-null mice.

The level of TNFα in all mouse strains was low in unchallenged naïve controls (Figure 5.23B). At 12 hours post injection however, the levels of TNFα increased significantly

in C57BL/6 mice (89.58 ± 12.29 pg/ml), *Ifngr1*-null mice (284.61 ± 92.27 pg/ml) and TNFα-neutralised *Ifngr1*-null mice (97.85 ± 12.37 pg/ml). The presence of TNFα in mice injected with anti-TNFα mAb might indicate that TNFα had not been completely blocked, although serum levels were reduced by 66% in comparison to *Ifngr1*-null mice. However, because only partial neutralisation occurred, this may have been one reason why lymphopoiesis was not completely restored in these mice. The level of TNFα in all strains at 24 hours were much reduced and at similar levels, but the largest decrease was observed in *Ifngr1*-null mice.

Figure 5.23

Levels of IFNγ and TNFα in C57BL/6, Ifngr1-null and TNFα-neutralised Ifngr1-null mice at 0, 12 and 24 hours post LPS injection.

A Graph illustrating the levels of IFNγ in C57BL/6, *Ifngr1*-null and TNFα-neutralised *Ifngr1*-null mice at 0, 12 and 24 hours post LPS injection. Six mice were analysed (three males and three females) per mouse strain at each time point.

B Graph illustrating the levels of TNFα in C57BL/6, *Ifngr1*-null and TNFα-neutralised *Ifngr1*-null mice at 0, 12 and 24 hours post LPS injection. Six mice were analysed (three males and three females) per mouse strain at each time point.

A

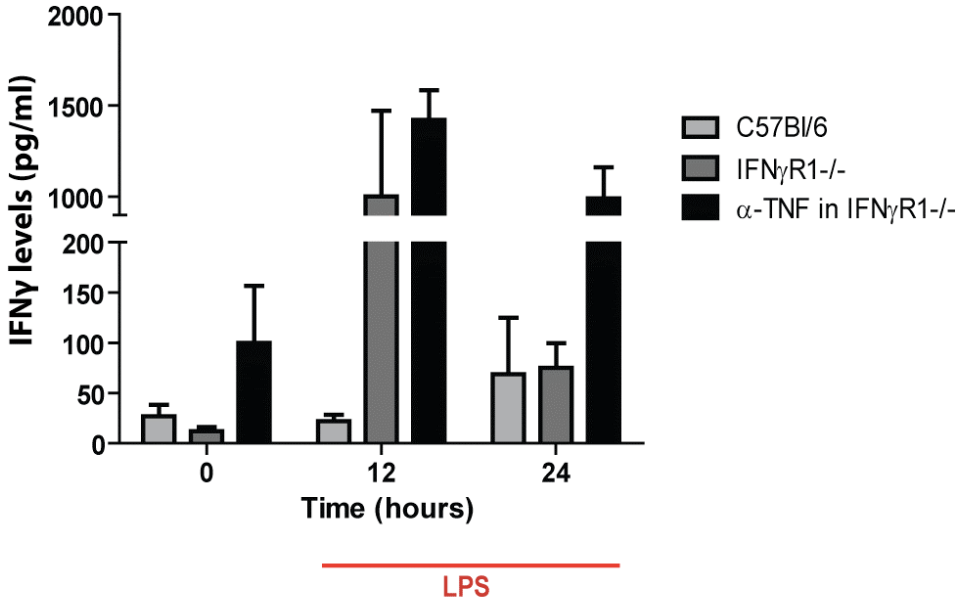
IFNγ levels (pg/ml)
2000
1500
1000
200
150
100
50
0
0
12
24
Time (hours)
LPS
C57Bl/6
IFNγR1-/-
α-TNF in IFNγR1-/-

B

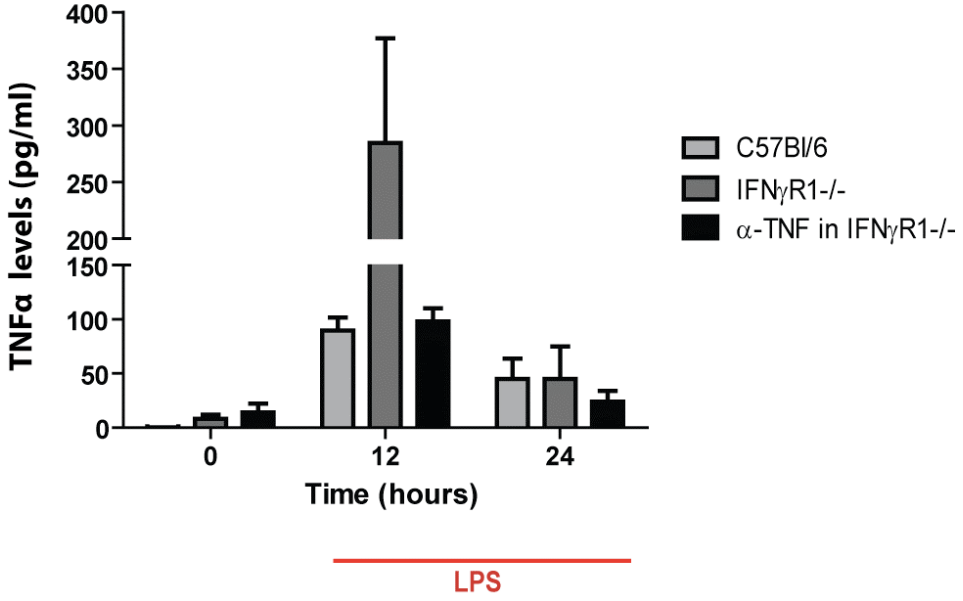
TNFα levels (pg/ml)
400
350
300
250
200
150
100
50
0
0
12
24
Time (hours)
LPS
C57Bl/6
IFNγR1-/-
α-TNF in IFNγR1-/-

5.13 Analysis of *E. coli* infection on haematopoietic progenitor compartments

We next compared the effects of LPS challenge on the phenotype of haematopoietic progenitors to bacteria-induced septicaemia, by injecting heat-inactivated *E. coli* into C57BL/6 mice. Based on the study by Freudenberg et al (2001), we calculated that the number of *E. coli* cells which was equivalent to 40µg LPS was 1.5 x 10^9 cells. However, after i.p. injection of this amount of *E. coli*, mice died after just 12 hours. Therefore, we reduced the amount of *E. coli* cells injected into C57BL/6 mice by five fold to 3 x 10^8 cells. The parameters first measured were body temperature and the circulating RBC number (Figure 5.24A and B). In marked contrast to LPS injected C57BL/6 mice, we observed a severe hypothermia after *E. coli* injection. The onset of hypothermia started after just five hours (34.79 ± 0.47^{o}C) and continued throughout the time course, reaching a minimum at 12 hours post infection (30.97 ± 1.61^{o}C). Mice started to recover from this hypothermia after 15 hours (33.27 ± 0.62^{o}C) and returned to normal body temperature by 72 hours (37.63 ± 0.15^{o}C). We next looked into the blood at the number of circulating RBCs. As shown in Figure 5.24B, there was no effect of *E. coli* on the number of circulating RBCs compared to the water injected control mice.

Figure 5.24

Body temperature and number of circulating RBCs in mice injected with E. coli, compared to LPS injected and water injected mice.

A Graph illustrating the effect of *E. coli* on the body temperature of C57BL/6 male mice, aged eight weeks of age. Mice injected with *E. coli* (green line) were compared to LPS challenged (red line) and water injected mice (black line). Data are representative of one experiment, using three male mice per group. Significance was calculated using the Student's T-test ($p < 0.05$). Values represent mean ± S.E.M.

B Graph illustrating the effect of *E. coli* on the circulating RBC number of C57BL/6 male mice, aged eight weeks of age. Mice injected with *E. coli* (green line) were compared to LPS challenged (red line) and water injected mice (black line). The number of circulating RBCs did not enter outside of the physiological range during LPS challenge or *E. coli* infection, therefore no anaemia was observed. Data are representative of one experiment, using three male mice per group. Values represent mean ± S.E.M.

A

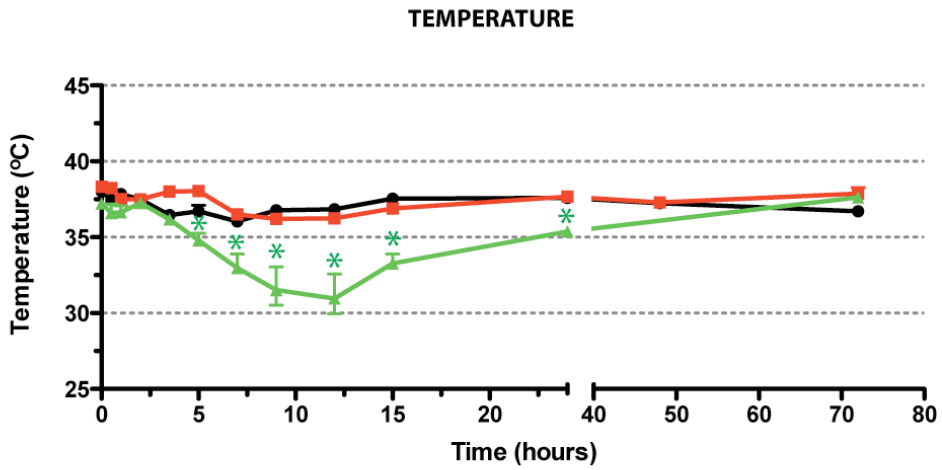
TEMPERATURE
Temperature (ºC)
45
40
35
30
25
0
5
10
15
20
40
50
60
70
80
Time (hours)
*
*
*
*
*
*

B

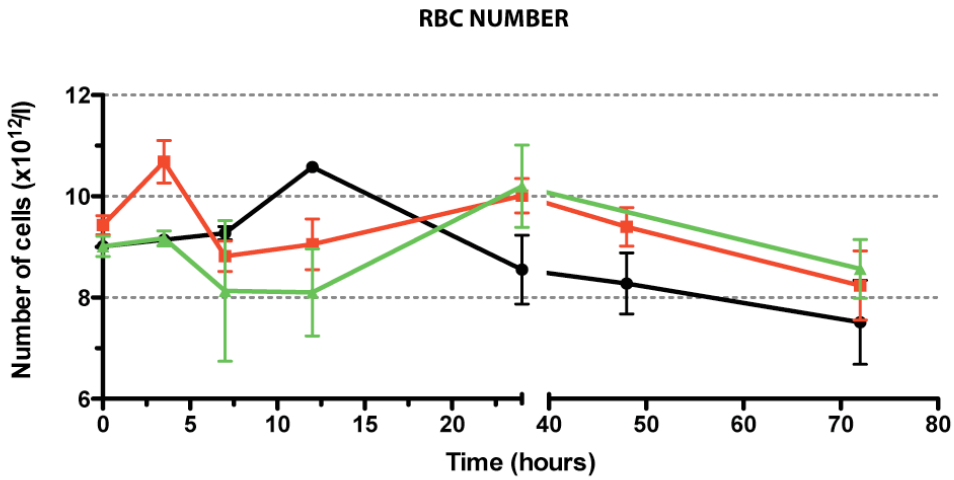
RBC NUMBER
Number of cells (x10^12/l)
12
10
8
6
0
5
10
15
20
40
50
60
70
80
Time (hours)

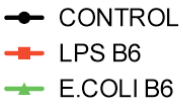
CONTROL
LPS B6
E.COLI B6

We next analysed the effect of *E. coli* infection on the composition of stem cells and progenitor cells (Figure 5.25). Similar to LPS challenge, there was an increase in the frequency of LSK cells 12 hours post *E. coli* infection, which remained after 24 hours and started returning to steady state levels by 72 hours. Subsequently, this lead to an increase in the number of LSK $CD34^{+}$ Flk-2^{-} cells (Figure 5.26A), a decrease in the frequency of LSK $CD34^{+}$ Flk-2^{+} cells (Figure 5.26B) and a virtual absence of LIN^{-} IL-7Rα^{+} Flk-2^{+} cells (Figure 5.26C). These results were identical to what was observed during injection of LPS. However, one obvious difference between *E. coli* infection and LPS challenge on haematopoietic progenitor cells was that, although the frequency of LSK cells increased after *E. coli* injection, there was little evidence for a contraction of LIN^{-} c-kit^{hi} Sca-1^{-} cells (Figure 5.25). Therefore, this indicated that expansion of the LSK compartment might have been due to an increase in the number of both LT-HSCs and ST-HSC cells. To further investigate this, we calculated the number of LT-HSCs, which are upstream of ST-HSCs and would proliferate and differentiate in response to a surplus requirement for ST-HSCs. In contrast to LPS challenge, there was a significant increase in the number of LT-HSCs (Figure 5.27), 12 and 24 hours post *E. coli* infection in comparison to the control, which had returned to steady state levels by 72 hours. This indicated that LT-HSCs and ST-HSCs populations were proliferating and differentiating rapidly during *E. coli* infection and indicated that the inflammatory response must have been more severe than with LPS challenge.

In order to further investigate this, we measured the levels of IFNγ and TNFα in the serum after *E. coli* injection and compared these values to LPS injected C57BL/6 mice, LPS injected *Ifngr1*-null mice and LPS injected TNFα-neutralised *Ifngr1*-null mice (Figure 5.28). We found that after 12 hours, the levels of IFNγ in the serum after *E. coli* infection (Figure 5.28A) in C57BL/6 mice (1967.9 ± 416.63 pg/ml) were 90 fold higher

than in LPS injected C57BL/6 mice (22.04 ± 6.48 pg/ml). The amount of IFNγ in *E. coli* infected mice at 12 hours was also higher than in LPS injected *Ifngr1*-null mice and TNFα-neutralised *Ifngr1*-null mice. The level of TNFα in the serum was also much higher during *E. coli* infection (Figure 5.28B). After 12 hours, TNFα levels in *E. coli* infected C57BL/6 mice (400.78 ± 91.86 pg/ml) were almost five fold higher than in LPS injected C57BL/6 mice (89.58 ± 12.29). The amount of TNFα in *E. coli* infected mice at 12 hours was also higher than in LPS injected *Ifngr1*-null mice and TNFα-neutralised *Ifngr1*-null mice. Therefore, these data indicate that during *E. coli* infection there was a stronger inflammatory response which was characterised by increased levels of both IFNγ and TNFα cytokines in the serum compared to LPS injected mice. Consequently, this may have been the reason that a significant increase in LT-HSC and ST-HSC cell number was observed, indicative of induced proliferation and differentiation of these subsets in order to clear the infection.

Figure 5.25

Frequency of haematopoietic progenitor compartments during E. coli infection in the BM of C57BL/6 mice.

FACS plots illustrating the frequency of haematopoietic progenitor populations during *E. coli* infection in the BM of C57BL/6 mice, aged eight weeks of age. Mice were analysed at 0, 12, 24 and 72 hour time points and assessed for their expression of cell surface markers. Data is representative of one experiment using three male mice per time point.

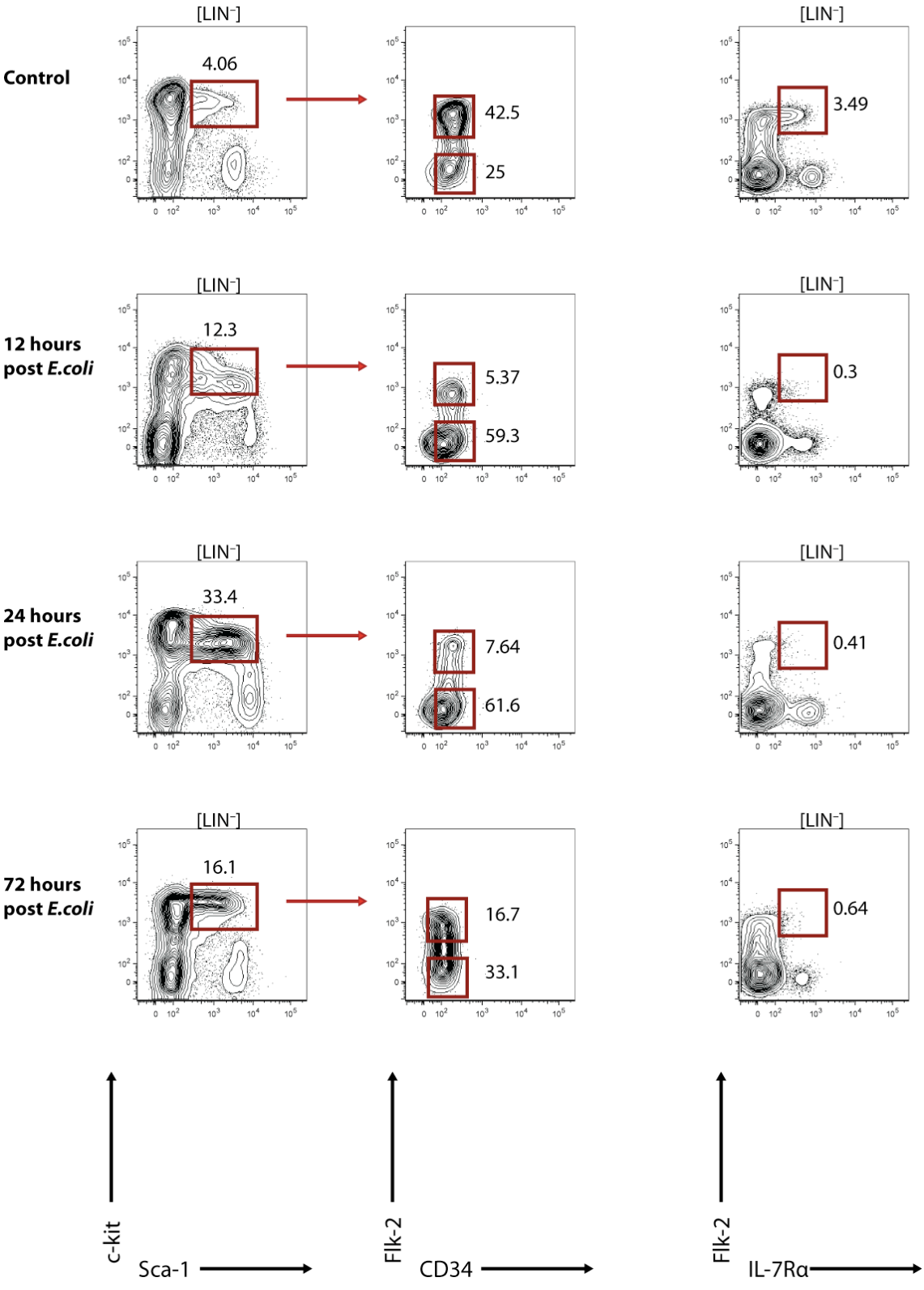
Control
12 hours post E.coli
24 hours post E.coli
72 hours post E.coli
[LIN⁻]
4.06
42.5
25
3.49
12.3
5.37
59.3
0.3
33.4
7.64
61.6
0.41
16.1
16.7
33.1
0.64
c-kit
Sca-1
Flk-2
CD34
Flk-2
IL-7Rα

Figure 5.26

Number of haematopoietic progenitor cells during E. coli infection in C57BL/6 mice.

A Graph illustrating the number of LSK $CD34^+$ Flk-2^- cells at 0, 12, 24 and 72 hours post *E. coli* infection in C57BL/6 mice, aged eight weeks of age. Data is representative of one experiment using three male mice per time point. Significance was calculated using the Student's T-test ($p < 0.05$). Values represent mean ± S.E.M.

B Graph illustrating the number of LSK $CD34^+$ Flk-2^+ cells at 0, 12, 24 and 72 hours post *E. coli* infection in C57BL/6 mice, aged eight weeks of age. Data is representative of one experiment using three male mice per time point. Significance was calculated using the Student's T-test ($p < 0.05$). Values represent mean ± S.E.M.

C Bar graph illustrating the number of LIN^- IL-7Rα^+ Flk-2^+ cells at 0, 12, 24 and 72 hours post *E. coli* infection in C57BL/6 mice, aged eight weeks of age. Data is representative of one experiment using three male mice per time point. Significance was calculated using the Student's T-test ($p < 0.05$). Values represent mean ± S.E.M.

A

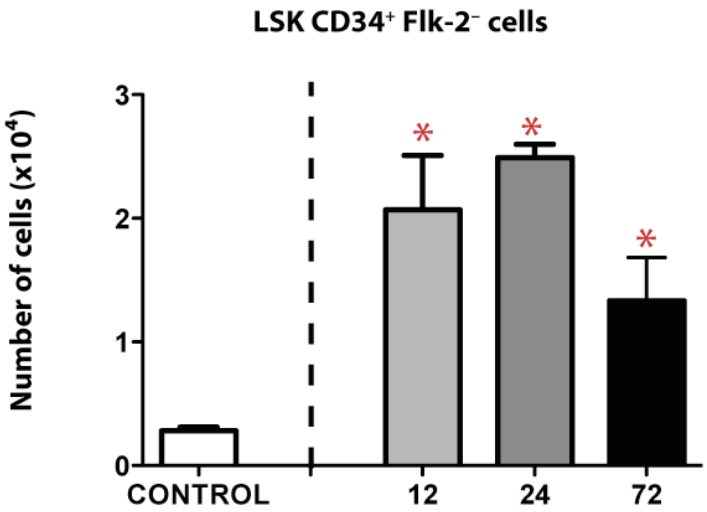
LSK CD34+ Flk-2- cells
Number of cells (x10^4)
3
2
1
0
CONTROL
12
24
72
*
*
*

B

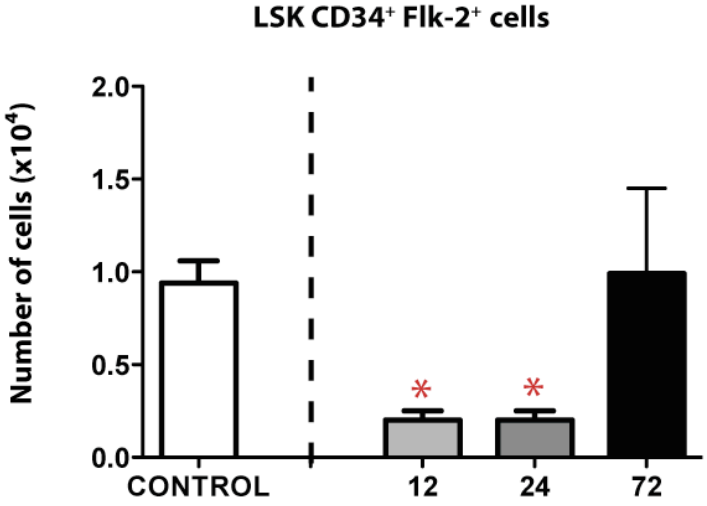
LSK CD34+ Flk-2+ cells
Number of cells (x10^4)
2.0
1.5
1.0
0.5
0.0
CONTROL
12
24
72
*
*

C

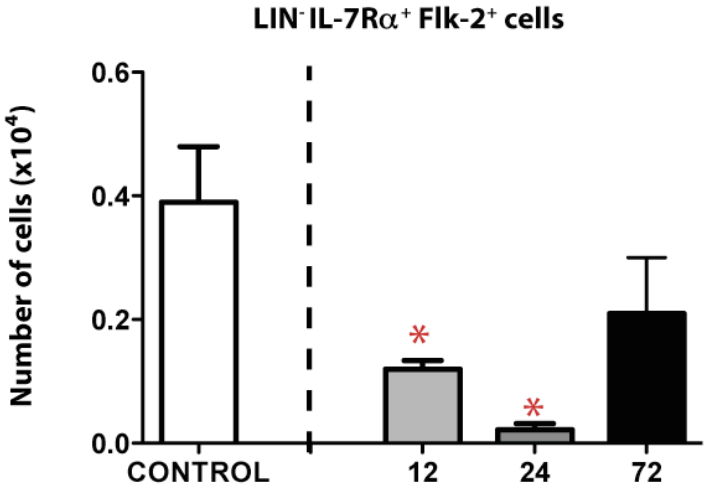
LIN- IL-7Rα+ Flk-2+ cells
Number of cells (x10^4)
0.6
0.4
0.2
0.0
CONTROL
12
24
72
*
*

Figure 5.27

Number of LT-HSCs during E. coli infection in C57BL/6 mice.

Graph illustrating the number of LSK $CD150^{+}$ $CD48^{-}$ cells at 0, 12, 24 and 72 hours post *E. coli* infection in C57BL/6 mice, aged eight weeks of age. Data is representative of one experiment using three male mice per time point. Significance was calculated using the Student's T-test ($p < 0.05$). Values represent mean ± S.E.M.

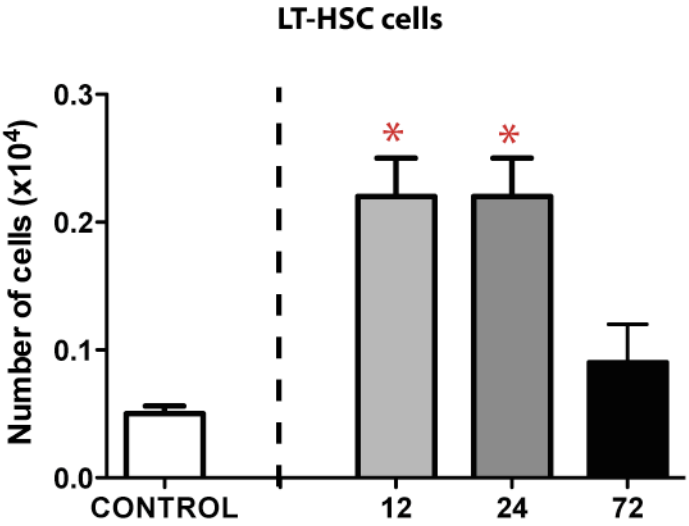
LT-HSC cells
Number of cells (x10⁴)
0.3
0.2
0.1
0.0
*
*
CONTROL
12
24
72

Figure 5.28

Serum levels of IFNγ and TNFα during E. coli infection in C57BL/6 mice.

A Graph illustrating the levels of IFNγ in C57BL/6, *Ifngr1*-null, TNFα-neutralised *Ifngr1*-null mice and *E. coli* infected mice (red bars) at 0, 12 and 24 hours post LPS injection. Six mice were analysed (three males and three females) in LPS injected mice and three male mice were analysed in *E. coli* infected mice at each time point.

B Graph illustrating the levels of TNFα in C57BL/6, *Ifngr1*-null, TNFα-neutralised *Ifngr1*-null mice and *E. coli* infected mice (red bars) at 0, 12 and 24 hours post LPS injection. Six mice were analysed (three males and three females) in LPS injected mice and three male mice were analysed in *E. coli* infected mice at each time point.

A

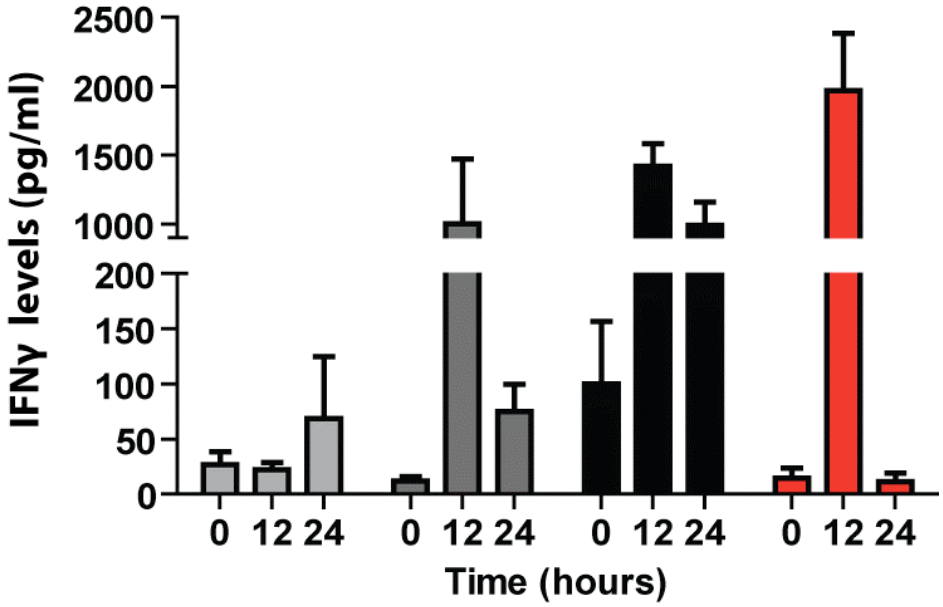
IFNγ levels (pg/ml)
2500
2000
1500
1000
200
150
100
50
0
0 12 24 0 12 24 0 12 24 0 12 24
Time (hours)

B

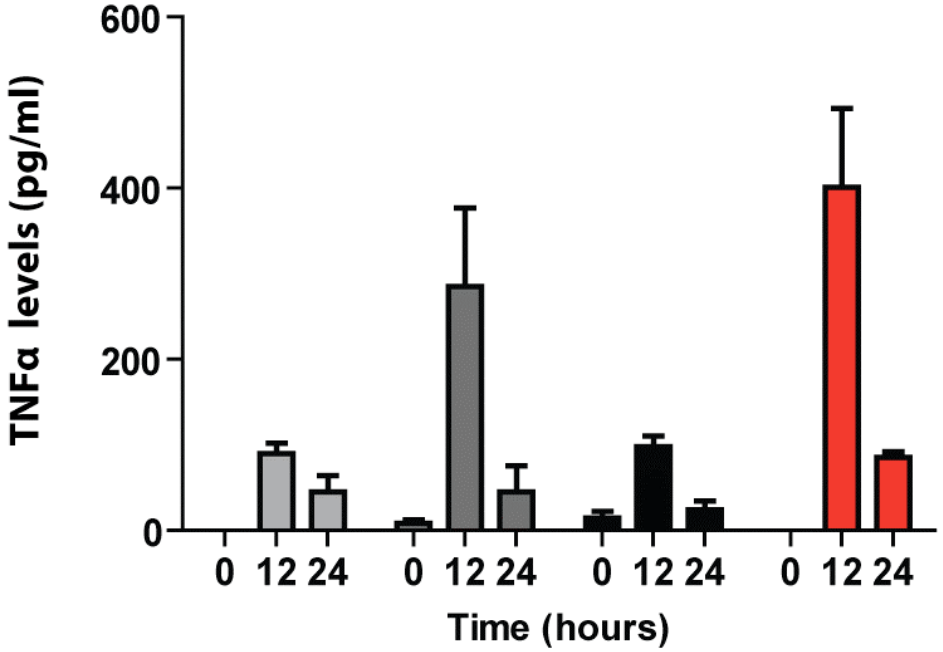
TNFα levels (pg/ml)
600
400
200
0
0 12 24 0 12 24 0 12 24 0 12 24
Time (hours)

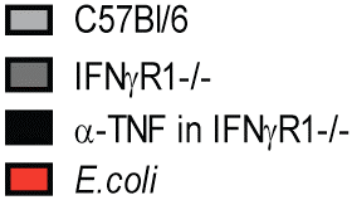
C57Bl/6
IFNγR1-/-
α-TNF in IFNγR1-/-
E.coli

5.14 Discussion

During homeostatic conditions, development of HSCs into fully functional mature cells occurs by differentiation of cells into the myelo-erythroid or lymphoid lineages. The myeloid lineage produces cells which form the innate immune response and which act at the front line of defence upon encounter of a pathogen, whilst the lymphoid lineage encompasses cells of the adaptive immune system, which are activated by innate immune cells in order to provide a stronger defence. In order for haematopoiesis to occur, HSCs must respond to extracellular cues, such as cytokines present in the BM stroma, which enables differentiation down a particular lineage. Some well studied examples of cytokines which promote lymphoid development are Flk-2 ligand and IL-7 whilst GM-CSF favours myeloid differentiation. However, during infection, pro-inflammatory cytokines such as IFNγ and TNFα are produced by innate immune cells that can also influence HSC differentiation. IFNγ is produced by NK (Kasahara et al., 1983), CD4 T_h1 and CD8 cytotoxic lymphocytes (Shtrichman and Samuel, 2001). Some publications have reported that IFNγ inhibits haematopoiesis (Raefsky et al., 1985; Zoumbos et al., 1984; Neumann et al., 1982; Selleri et al., 1996). In contrast, Brugger et al. (Brugger et al., 1993) stated that IFNγ was able to promote the expansion of peripheral blood $CD34^+$ progenitor cells by two fold in combination with SCF, IL-1, IL-3, IL-6 and erythropoietin. In addition, Caux and colleagues (Caux et al., 1992) and Yang et al., (Yang et al., 2005) reported that IFNγ was capable of stimulating early stage myelopoiesis *in vitro*. Therefore, IFNγ appears to exert both proliferative and inhibitory effects on haematopoiesis. The role of IFNγ during an acute infection was addressed in our laboratory using mouse malaria as a model (Belyaev et al., 2010). It was observed that during peak parasitaemia, there was a contraction in the frequency and number of LIN^- c-kit^{hi} $Sca\text{-}1^-$ cells, but an expansion in the LSK compartment.

Interestingly, these LSK cells also expressed the FcγRII/III antigen and cells positive for this marker were able to give rise to myeloid progeny *in vitro*. Therefore, it appeared that myeloid progenitors had upregulated Sca-1 on their surface and were now residing in the LSK compartment. Interestingly, the number of LT-HSCs remained unchanged. In addition, there was also a contraction in CLPs accompanied by a subsequent loss of pro and pre B-cells. However, a new population of LIN^{-} c-kit^{hi} IL-7Rα^{+} 'atypical' cells emerged during infection which was able to give rise to both lymphoid and myeloid progeny *in vitro,* but mainly myeloid cells *in vivo*. In addition, these 'atypical' progenitors expressed *Mpo*, a gene expressed in myelocytes and neutrophilic granulocytes and *Cebpα*, a master regulator for myelopoiesis. Therefore, although these cells expressed a functional IL-7 receptor they predominantly generated myeloid cells. These observed changes were dependent on IFNγ as during infection in *Ifngr1*-null mice, there was no observed upregulation of Sca-1 on myeloid progenitor cells, the CLP pool remained stable and there was no emergence of 'atypical progenitors'. These results indicate that myelopoiesis was favoured during malaria infection at the expense of lymphoid development.

Similar results were also reported by Zhang and co-workers who investigated the effect of *E. coli* on haematopoiesis *in vitro* (Zhang et al., 2008). This group observed an expansion of the LSK compartment after *E. coli* infection and a subsequent reduction in the LIN^{-} c-kit^{hi} Sca-1^{-} fraction. The authors concluded that LIN^{-} c-kit^{hi} Sca-1^{-} cells were inverting their phenotype and forming part of the LSK pool of cells. Although LPS, TNFα, IL-6 and IFNγ were all reported to be able to induce the conversion of LIN^{-} c-kit^{hi} Sca-1^{-} cells into LSK cells, the precise mechanism was not addressed. In summary, these results suggested that during infection, whereby the innate immune

response was required for clearance of the pathogen, lymphopoiesis was temporarily halted and myelopoiesis augmented.

Singh and colleagues (Singh et al., 2005), in addition to Belyaev and colleagues (Belyaev et al., 2010) and Zhang et al., (Zhang et al., 2008) also reported an increase in the number of LSK cells after VV infection and a decrease in the number of LIN^- c-kit^{hi} $Sca\text{-}1^-$ cells. Furthermore, $CD34^+$ cells in the LSK compartment, representing ST-HSC cells during homeostatic conditions, were primarily expanded during infection. In contrast to malaria and *E. coli* infection however, the authors observed an increase in the frequency and number of the CLP population. Whereas the increase in the CLP compartment was attributable to TLR4 signalling, as *Myd88*-null mice did not show increased CLP numbers, the observed decline in the frequency of myeloid progenitors was not changed during infection in *Myd88*-null mice. Therefore, the authors suggested that these results illustrated independent regulation of CMP and CLP compartments during VV infection. Therefore, although these studies have suggested that haematopoiesis can be 'remodelled' during infection, our understanding of the mechanisms involved are by no means complete. We aimed to further elucidate the process of haematopoiesis during inflammatory conditions by administration of LPS.

The first evidence for an innate immune response elicited by LPS was observed during analysis of circulating white blood cells. There was an observed increase in the number of circulating granulocytes and a decrease in the number of circulating lymphocytes. These circulating granulocytes would be predominantly neutrophils, which are recruited to the site of infection by chemokines and cytokines (Gomez et al., 2008). LPS is bound by a TLR4-containing complex which is present on macrophages and DCs and also on haematopoietic progenitor cells (Nagai et al, 2006). During the binding of LPS to TLR4 on macrophages, TNFα is released, which recruits neutrophils, elevates their

bactericidal capacity (Chilvers et al., 2000) and increases their life span. Furthermore, the release of TNFα is thought to act as a trigger for the upregulation of IL-8 expression. IL-8 is a central mediator of inflammation which induces the transmigration of neutrophils across endothelial barriers and to the site of infection (Baggiolini et al., 1989). Our results indicated that TNFα played a pivotal role in recruitment of granulocytes, as *Tnfr1*-null mice had a reduced number of circulating cells compared to LPS-injected C57BL/6 mice. We also found that there was a decrease in the frequency of BM-derived myeloid cells during LPS challenge, which also indicated that these cells had been exported to the periphery.

In contrast to increasing granulocyte number, there was a severe decrease in the number of circulating lymphocytes. This is in agreement with studies showing that B-cells are markedly depleted following endotoxin (Chandra et al., 2008) and sepsis challenges (Remick et al., 2000). Although it is thought that IFNγ can cause inhibition of B-cell development, as over expression of IFNγ leads to severe B-cell lineage reduction (Young et al., 1997; Grawunder et al., 1993) as well as NK–cell development deficiencies (Shimozato et al., 2002), we observed only minor increases in the number of circulating lymphocytes after LPS administration in *Ifngr1*-null mice. On the other hand, there have been some studies suggesting TNFα can have an indirect inhibitory effect on B-lineage development (Ueda et al., 2004; Sedger et al., 2002). Ueda and colleagues demonstrated that TNFα reduced the level of the chemokine CXCL12 in the BM and this coincided with lymphocyte depletion and mobilisation of B-cell progenitors into the blood; and that *Tnfα*-deficient mice showed much reduced BM lymphopenia. Our results demonstrated that TNFα alone was not the cause of lymphopenia in the circulation as LPS challenge in *Tnfr1*-null mice did not alter the circulating lymphocyte number compared to LPS-injected C67Bl/6 mice. Our data

suggests that the observed decrease in number could have been due to either homing of lymphocytes into peripheral organs, a loss of lymphoid progenitor cells or cell death. We did observe an increase in the frequency of BM B-cells at 24 hours post LPS challenge, which could have indicated some homing of circulating lymphocytes to the BM. However, these cells were completely depleted at 72 hours after injection. Similar declines in BM B-cell numbers have also been observed upon cecal ligation (Scumpia et al., 2010) and during *in vitro* LPS stimulation where LSK cells developed only into mature $Gr1^+$ $CD11b^+$ cells and not B-cells (Nagai et al., 2006). Taking into consideration that there was a vast increase in the number of granulocytes, at the expense of lymphocytes in the blood, we next looked at BM progenitor cells.

We found that there was a significant decrease in the total number of LIN^- cells, 12 and 24 hours post LPS challenge. This was attributable to the virtual depletion of LMPP, ELP and CLP cells. At 12 and 24 hours post LPS, the frequency and number of LMPP, ELP and CLP populations were markedly reduced. This in turn could have been one reason for the loss of mature lymphocyte numbers observed in the circulation. There were several possible reasons for the loss of these cells; lymphoid progenitor cells may have re-directed into an alternative lineage; pro-inflammatory cytokines may have caused inhibition of lymphopoiesis; the downregulation of cell surface markers by which lymphoid progenitors are identified; or cells may have apoptosed. This data was in contrast to the effects observed during *Mycobacterium avium* infection (Baldridge et al., 2010) and herpes virus infection (Welner et al, 2008) where the number of CLP cells increased or remained constant. These reports indicated that clearance of *Mycobacterium avium* or Herpes Virus relied on the responses of both the innate and adaptive immune systems.

We addressed whether ELP and CLP progenitor cells had been re-directed into the myeloid lineage utilising *Rag1*$^{wt/Cre}$ *x* *R26R*$^{wt/eYFP}$ mice which label lymphoid progenitors with eYFP fluorescence after activation of *Rag1* at the ELP stage of development. There have been some reports whereby re-direction of lymphoid progenitor cells into the myeloid lineage has occurred (Kondo et al., 2000; Iwasaki et al., 2000; Xie et al., 2004). However, we found that eYFP^{+} lymphoid progenitors did not re-direct into the myeloid lineage as there was no evidence for a significant increase in the expression of eYFP in BM or splenic mature myeloid cells throughout LPS challenge. However, Nagai and colleagues (Nagai et al., 2006) reported that CLPs placed in serum free culture produced CD11b^{+} Gr1^{-} CD11c^{+} DCs after administration of LPS. Therefore, it is possible that CLPs could have differentiated into DCs and exited the BM.

We also observed the effect of TNFα and IFNγ cytokines on the inhibition of lymphoid progenitor development. We found that although the frequency and number of LMPP and CLP populations were not completely restored during analysis of TNFα-neutralised *Ifngr1*-null mice, the frequency and number of cells did return to homeostatic levels in a shorter time period. However, because antibody treatment did not completely remove the cytokine from the circulation, TNFα could still have been inducing an inhibitory effect. In addition to TNFα and IFNγ, other cytokines may also have been involved in the block of lymphopoiesis. It has previously been reported that IFNα and IFNβ, which can be released from BM macrophages, have been shown to inhibit IL-7 dependent proliferation of BM cells *in vitro* (Wang et al., 1995).

During analysis of haematopoietic progenitor populations, it was clear that Flk-2 and IL-7Rα cell surface markers were downregulated during LPS challenge. This may have been due to a reduced secretion of IL-7 cytokine and Flk-2 ligand which promote

lymphoid development and an increase in cytokines promoting myeloid development, such as GM-CSF. Therefore there may not have been any physiological requirement for these markers to be present on progenitor cells.

Cell death of lymphoid progenitors could have been another reason for the virtual absence of LMPP and CLP populations. It was reported in 1995 (Maciejewski et al., 1995) that activation of Fas antigen on stem and progenitor cells could occur by both IFNγ and TNFα cytokines, which subsequently leads to transduction of a cell death signal. Therefore, because both TNFα and IFNγ cytokines levels were increased in the serum during LPS challenge, activation of Fas antigen on LMPP and CLP populations may have occurred. This may also have occurred on B-cells and myeloid progenitors, other cell populations which reduced in number after LPS challenge.

We also analysed more thoroughly the composition of the LSK compartment where LMPPs and HSCs were defined. We found that there was a significant increase in both the frequency and number of LSK cells after LPS injection, which seemed to be at the expense of LIN^- c-kit^{hi} $Sca\text{-}1^-$ cells. This same result was also reported in 2010 by Scumpia et al., who injected either LPS, induced cecal ligation and puncture to induce bacterial sepsis, or administered *Staphylococcus aureus* infection and observed a transient expansion of LSK cells. In addition, other models of inflammation including malaria (Belyaev et al., 2010), VV (Singh et al., 2005), HCMV (Gibbons et al., 1995), *Pseudonomas aeruginosa* (Rodriguez et al., 2009) and *E. coli* infection (Zhang et al., 2008) also induced LSK expansion, whilst other pathogens such as *Anaplasma phagocytophilum* (Johns et al., 2009) diminished LSK numbers. Our results indicated that myelo-erythroid progenitor cells residing in the LIN^- c-kit^{hi} $Sca\text{-}1^-$ fraction had upregulated Sca-1 on their surface. This was evident due to observed FcγRII/III expression in LIN^- c-kit^{hi} cells which included LSK cells. Consequently, there was a

significant increase in the frequency and number of LSK $CD34^+$ $Flk\text{-}2^-$ cells; which could encompass ST-HSC, CMP and GMP populations during LPS challenge. However there was also a reduction in the number of LIN^- $c\text{-}kit^{hi}$ $Fc\gamma RII/II^+$ GMP cells, similar to results obtained during malaria (Belyaev et al., 2010) and murine cytomegalovirus (MCMV; Broxmeyer et al., 2007) infection. This decrease in myeloid progenitor number may have been attributable to the direct effects of IFNγ (Murphy et al., 1986; Broxmeyer et al., 1983) and TNFα (Broxmeyer et al., 1986) seeing as though previous reports have illustrated an inhibitory effect of both these cytokines on myeloid progenitor growth. In addition, overexpression of Sca-1 has also been shown to decrease myeloid colony forming units *in vitro* (Bradfute et al., 2005).

In order to verify whether the increase in LSK $CD34^+$ $Flk\text{-}2^-$ populations was due to a surplus requirement of ST-HSCs during LPS challenge, we calculated the number of LT-HSC, as these cells feed directly into the ST-HSC pool. We deduced that there was no change in the number of LT-HSCs throughout LPS challenge. Therefore, it appeared that Sca-1 expression on LIN^- $c\text{-}kit^{hi}$ $Sca\text{-}1^-$ myeloid progenitor cells was the main reason for the increase in the LSK $CD34^+$ $Flk\text{-}2^-$ population. Due to the lack of lymphoid cells during LPS challenge, but a requirement for myelopoiesis, Sca-1 may have somehow been advantageous to the host in amplifying this process.

Sca-1 is a glycosyl phosphatidylinositol-anchored cell surface protein which is also found on mesenchymal stem cells (Baddoo et al., 2003) and has been shown to be necessary for normal HSC activity. This has been illustrated in Sca-1 knock out mice which presented defects in the short term serial transplantation of HSCs (Ito et al., 2003) and has lead to the idea that Sca-1 is important for stem cell proliferation and self-renewal. Members of the interferon family have been reported to modify the expression of Sca-1; on T-cells (Dumont et al., 1987) and B-cells (Chen et al., 2003) by

IFNγ and on LT-HSCs by IFNα (Essers et al., 2009). We determined that, although the TNFα cytokine was not completely blocked in TNFα-neutralised *Ifngr1*-null mice, the number and frequency of Sca-1 levels in LIN^- c-kit^{hi} cells were completely restored back to wildtype levels. This indicated that both IFNγ and TNFα cytokines were involved in the modulation of Sca-1 expression, but we found that the phenotype was mostly reduced in the absence of IFNγ signalling, indicating that IFNγ was exerting the most pronounced effect. Belyaev and colleagues (Belyaev et al., 2010) did report that receptors for this cytokine were present on all haematopoietic progenitor cell types and Nagai and co-workers (Nagai et al., 2006) found that LSK cells *in vitro* acquired the IFNγR in response to LPS within 24 hours, allowing these cells to respond to the cytokine. Similar results were also reported by Zhao et al, (2010). This group studied the effect of IFNγ on haematopoietic progenitor cells *in vitro* and demonstrated that addition of IFNγ to a culture containing LIN^- c-kit^{hi} Sca-1^- cells, resulted in a conversion of their phenotype to resemble LSK cells.

Because Sca-1 expression on myeloid cells was reduced completely in TNFα-neutralised *Ifngr1*-null mice, we presumed that all lymphoid progenitor cells could be identified by their classical phenotypes. Interestingly, we found that the number of ST-HSCs increased significantly 12 and 24 hours post LPS injection, the number of LMPP cells decreased at 12 hours but had recovered by 24 hours, and the number of CLP cells also reduced at 12 hours. Due to both IFNγ and to a certain extent TNFα signalling pathways been inhibited, the effects which we observed may have been due to either partial neutralisation of TNFα, an involvement from other cytokines, or LPS acting directly on haematopoietic progenitor cells. Due to the absence of IFNγ signalling during LPS challenge, it could be possible that there is redundancy between the IFNγ, IFNα and IFNβ genes and these cytokines are inhibiting lymphopoiesis.

Indeed, both IFNγ and IFNα have been shown to elicit similar function in stimulating HSCs *in vivo* during *Mycobacterium avium* infection (Baldridge et al., 2010), so they may both exert inhibitory effects on downstream progenitors.

LPS has also been reported to act directly on haematopoietic cells. Nagai and colleagues reported that TLR4 receptors were present on the surface of HSCs, all LIN^- c-kit^{hi} progenitors and to a lesser extent CLPs, which enables progenitor cells to detect infection and respond immediately. Therefore, activation of this pathway may have lead to a change in progenitor cell number. Indeed Scumpia et al, (Scumpia et al., 2010) reported that LPS-induced expansion of the LSK compartment in *vivo* was absent in TLR4 mutant *C3H/HeJ* mice and this may also be the case for LMPP and CLP reduction. In order to fully analyse whether TLR4 signalling was causing this effect, TNFα-neutralised *Ifngr1*-null mice crossed to the *C3H/HeJ* background or TLR4-deficient mice would need to be analysed.

We next compared LPS challenge to true septicaemia by infecting C57BL/6 mice with the whole *E. coli* bacterium. We initially injected mice with the amount of *E. coli* cells equivalent to the concentration of LPS used, however these mice died after just 12 hours, therefore illustrating that the full bacterium was exerting more severe inflammatory effects. Incidentally, we reduced the number of *E. coli* cells injected and found that there was a severe hypothermia throughout the time course. One possibility is that *E. coli* infection was causing vasodilation of arterial walls, which subsequently lead to a loss of heat and a decrease in body temperature. However, identical to LPS challenge, no anaemia was observed. The frequency and number of LSK $CD34^+$ Flk-2^- cells had also increased after infection which was coupled with a decrease in the frequency and number of LSK $CD34^+$ Flk-2^+ and LIN^- IL-7Rα^+ Flk-2^+ cells. The increase in the LSK $CD34^+$ Flk-2^- fraction of cells, which encompassed ST-HSC, CMP

and GMP during LPS challenge, did not appear to contain myeloid progenitors, as there was no obvious upregulation of Sca-1 on these cells. Therefore, the increase in the LSK compartment during *E. coli* may have been due to an increased requirement of ST-HSCs. To verify this, we analysed the number of LT-HSCs. In contrast to LPS challenge, we found that the number of LT-HSCs increased significantly throughout the time course. This result was identical to what was reported during polymicrobial sepsis (Scumpia et al., 2010) and during *Mycobacterium avium* infection (Baldridge et al., 2010), suggesting that the immune defence against bacteria requires an increase in LT-HSC number. This indicated that a higher proliferation and differentiation of LT-HSCs and ST-HSCs was necessary during *E. coli* infection than during LPS challenge. In order to test whether this was due to a higher level of pro-inflammatory cytokines being released from innate cells, we measured the level of IFNγ and TNFα in the serum of *E. coli* infected mice. We found that the levels of both IFNγ and TNFα in the serum of mice were significantly higher than during LPS challenge in C57BL/6 mice. Therefore, these results suggest that LPS challenge could reflect in part how the immune system responds to gram negative bacteria, however injection of the full bacterium elicited a stronger inflammatory response.

We have shown that during host recognition of LPS or *E. coli,* an innate immune response is activated, which in turn leads to the production of pro-inflammatory cytokines, namely IFNγ and TNFα. Release of these cytokines induces 'haematopoietic remodelling' whereby lymphopoiesis is transiently switched off and conversely myeloid cells are augmented. This illustrates that there is a certain degree of plasticity within the haematopoietic system such that development of cells alters in order to benefit the host, already at the level of progenitors. During this transition, IFNγ and to a lesser extent TNFα exert inhibitory effects on the size and composition of progenitor pools, limiting

the amount of mature cells which can be produced. This subsequently leads to an increased production of cells once the pathogen has been cleared. Most importantly however, is the finding that almost immediately after infection with either LPS or *E. coli*, haematopoietic progenitor cells are able to directly respond to bacteria, inducing phenotypic changes which ultimately lead to restoration of homeostasis.

CHAPTER 6

FINAL DISCUSSION

Determining the pathways of lymphoid development and factors which influence them, is of crucial importance in order to fully understand haematopoiesis and use this knowledge to increase the effectiveness of peoples' immune systems. In this study, we aimed to investigate lymphoid development from BM progenitors to mature lymphocytes in conjunction with age, gender and infection. An important issue which remains unclear during lymphoid development, at steady state levels, is the identity of BM-derived progenitors which give rise to T- and B-cells. Determining the source of "thymic seeding cells" is essential, as transplanting these cells into patients with HIV, who have a deficiency in $CD4^+$ T-cells, would enable a more efficient development of T-cells. In addition, the identification of transcription factors specifying lymphoid commitment is of importance as aberrant differentiation of these factors may be the cause of some leukaemias. Many groups have aimed to elucidate the identity of "thymic seeding cells". Results from *Ikaros* 'knock-out' mice favoured ELP and LMPP populations as pre-thymic candidates (Allman et al., 2003), whilst transplantation and *in vitro* experiments comparing the developmental potential of lymphoid progenitors in comparison to ETPs, have suggested roles for LMPP, ELP and CLP populations (Lai and Kondo, 2007; Wada et al., 2008; Bell and Bhandoola, 2008; Serwold et al., 2009). However, there has been a lack of studies whereby reporter mice have been used to map lymphoid development from early progenitors to ETPs. We attempted to address this by monitoring lineage development in *Rag1*-driven Cre reporter mice, a gene whose expression is indispensable for lymphoid development.

On analysis of $Rag1^{wt/Cre}$ *x* $Rosa26^{wt/eYFP}$ mice we found that the CLP population was heterogeneous with respect to eYFP expression, in agreement with other published data (Welner et al., 2009; Månsson et al., 2010). This indicated that the CLP population must have descended from two phenotypically different progenitor pools, an $eYFP^+$ subset

such as the ELP, and an eYFP$^-$ subset, such as the LMPP. In order to identify progenitors which give rise to ETPs and pre-pro B-cells, we analysed eYFP expression in these compartments and correlated them with expression in BM progenitor cells. Although previous expression in *Rag1*$^{wt/Cre}$ *x Rosa26*$^{wt/tdRFP}$ mice has been reported in early lymphoid compartments (Welner et al., 2009), tdRFP expression in ETP and pre-pro B-cell subsets to determine the source of T- and B-cells was not studied. Therefore, we provide new data showing that approximately 75% of ETPs express eYFP, indicating that this population is derived predominantly from ELP or eYFP$^+$ CLP subsets, with some contribution from eYFP$^-$ CLPs. These results can be correlated with those of Schlenner and colleagues (Schlenner et al., 2010) who found that the majority of ETPs had previously expressed *il7rα* transcripts throughout their development, indicative of ELP and CLP populations. In addition, although the B-lineage potential of marked and unmarked CLP populations from *Rag1*^{Cre}-reporter mice have been analysed *in vitro* (Welner et al., 2009; Månsson et al., 2010), a direct comparison of B- and T-cell potential between ELP, CLP eYFP$^-$ and CLP eYFP$^+$ populations has not been reported *in vivo* or *in vitro*. In our hands, comparative *in vivo* analysis of ELP, CLP eYFP$^-$ and CLP eYFP$^+$ populations revealed that all subsets had the potential to give rise to splenic T-cells with similar kinetics and numbers, suggesting that all three populations were potential 'thymic seeding cells'. In addition, all three populations expressed similar mRNA and protein levels of the transcription factor GATA-3, which is important for T-cell fate specification (Ting et al., 1996; Hattori et al., 1996; Hendriks et al., 1999). With regards to putative B-cell potential, similar to results obtained utilising *Rag1*^{GFP} mice (Esplin et al., 2009), we found that approximately 88% of pre-pro B-cells expressed eYFP. *In vivo* transplantation experiments revealed that CLP eYFP$^+$ and ELP populations gave rise to a higher number of splenic B-cells than the CLP eYFP$^-$ pool,

data which is so far unpublished. In addition, the CLP eYFP$^+$ pool seemed to proliferate more extensively than either the CLP eYFP$^-$ or the ELP pool *in vitro*, whereas the CLP eYFP$^-$ and ELP pools exhibited similar kinetics of B-lineage development, suggesting that these populations were upstream precursors of the CLP eYFP$^+$ pool and at similar stages of development. Interestingly, the CLP eYFP$^-$ pool first had to express eYFP before upregulation of CD19, indicative of a precursor-product relationship between the CLP eYFP$^-$ and CLP eYFP$^+$ pools. In order to fully assess the proliferative rate of the ELP, CLP eYFP$^-$ and CLP eYFP$^+$ populations, isolation of these subsets and labelling of the cells with CFSE would provide valuable information as to whether these populations are truly distinct.

Based on lineage mapping data, transplantation experiments and *in vitro* culture of lymphoid progenitor subsets, we propose an alternative model of lymphoid development, whereby cells develop from HSCs into LMPPs and ELPs which is immediately followed by a bifurcation into two developmental pathways. Based on eYFP expression, we presumed that eYFP$^-$ LMPP cells were able to give rise to eYFP$^-$ CLP cells, whilst ELP cells produced eYFP$^+$ CLPs. In addition, we also determined that that the upregulation of eYFP on CLP cells was coupled with a down regulation of c-kit expression, in agreement with Esplin and colleagues (Esplin et al., 2009). This result was also similar to what was observed by Inlay and co-workers (Inlay et al., 2009) who utilised Ly6D expression to separate the CLP population into two distinct subsets. They also found that as CLPs upregulated Ly6D, they downregulated c-kit. Therefore, we assumed that throughout B-cell development, both eYFP and Ly6D markers could be used to define heterogeneity within the CLP pool. We proposed that eYFP$^-$ and eYFP$^+$ CLP populations acquired the expression of both eYFP and Ly6D during B-cell development so that B-lineage committed CLP cells were eYFP$^+$, Ly6D$^+$.

In relation to T-cell development, because ETP cells express low levels of Ly6D (Inlay et al., 2009) we proposed that only Ly6D^{-} ELP and CLP populations could give rise to ETPs. In order to verify these statements, isolation and functional analysis of the CLP subsets, utilising both eYFP and Ly6D markers, for T- and B-cell potential may provide further insight into which cells are the main progenitors for T- as well as B-cells.

In order to further deduce the sequence of lymphoid development and to assess any potential developmental plasticity between lymphoid and myeloid lineages, we analysed haematopoiesis during acute inflammation. The phenotype and function of haematopoietic progenitor cells has been shown to be altered during malaria (Belyaev et al., 2010), VV (Singh et al., 2006), *Mycobacterium avium* (Baldridge et al., 2010) and *Staphylococcus aureus* infection (Scumpia et al., 2010). However, the effects of LPS and *E. coli* on haematopoietic progenitor cells have not been well studied. Nagai and colleagues (Nagai et al., 2006) found that CLP cells could be directed towards a DC fate during LPS challenge *in vitro* and Scumpia and colleagues (Scumpia et al., 2010) reported an increase in the frequency and number of LSK cells during LPS challenge *in vivo*, however additional phenotypic alterations and the mechanisms responsible were not elucidated. In addition, *E. coli*-induced changes on haematopoiesis have been vaguely reported by only one group (Zhang et al., 2008). We provide new data which critically addresses the effect of both LPS and *E. coli* infection on progenitor and mature cell composition *in vivo*, thereby enhancing our understanding of the haematopoietic response to these infections in every day life.

During administration of LPS and *E. coli*, we found there was a cessation of lymphopoiesis, but an augmentation of myelopoiesis. A loss of BM-derived B-cells was coupled with a virtual absence of ELP and CLP cells, further clarifying these progenitor populations as sources of pre-pro B-cells. This loss was also reflected by a reduction in

the number of circulating lymphocytes. During LPS challenge, we utilised the *Rag1*$^{wt/Cre}$ *x Rosa26*$^{wt/eYFP}$ reporter to assess any potential re-direction of lymphoid cells into the myeloid lineage. However, we found no evidence of re-direction, suggesting the loss of lymphoid cells was due to the downregulation of cell surface markers or apoptosis.

In contrast, during LPS challenge, there was an increase in myelopoiesis, as evident by the increased number of circulating granulocytes and the mobilisation of BM myeloid cells into the blood. We also observed phenotypic alterations within the myeloid progenitor compartment. LPS injected LIN$^-$ c-kit$^+$ Sca-1$^-$ CD34$^+$ myeloid cells upregulated Sca-1 on their surface, thus residing within the LSK compartment. Subsequently, this resulted in a decrease in the number of LIN$^-$ c-kit$^+$ Sca-1$^-$ cells and an increase in the number of LSK CD34$^+$ cells. Interestingly, there was no change in the number of LT-HSCs during LPS challenge. In the absence of IFNγ signalling and the neutralisation of TNFα, Sca-1 levels were restored to control levels on myeloid progenitor cells, subsequently resolving the frequency and number of LIN$^-$ c-kit^{hi} Sca-1$^-$ and LSK cells. This was evident even though TNFα was only partially neutralised. However, the frequency and number of lymphoid progenitors did not fully revert back to steady state levels, indicating that TNFα and IFNγ are not the only cytokines responsible for the loss of lymphoid progenitor cells during LPS challenge. These results are indicative for a high degree of plasticity within haematopoietic progenitor compartments during inflammation. To identify whether lymphopoiesis was not resolved due to only partial neutralisation of TNFα, it would be useful to analyse lymphoid progenitor populations during LPS challenge in *Ifngr1/Tnfr1*-null mice. This would definitively identify whether TNFα was responsible for the observed reduction in lymphoid progenitor numbers during LPS challenge.

We also compared the effects of *E. coli* infection to LPS challenge and found that although there was still a rise in the frequency and number of LSK cells, this was attributable to an increased production of LT-HSCs, as opposed to the upregulation of Sca-1 on myeloid progenitors during LPS challenge. This indicated that during an acute inflammatory response induced by LPS, homeostasis was regulated at the level of haematopoietic progenitors, whereas during a more chronic infection with *E. coli*, there was also a modulation in the stem cell compartment. We elucidated that the cytokines responsible for the observed phenotypic changes during LPS challenge and *E. coli* infection were both IFNγ and TNFα. This was reflected by an increase in the concentration of these cytokines in the serum. In addition, we found that there was a higher concentration of TNFα and IFNγ cytokines produced during *E. coli* infection than during LPS challenge, suggesting that different immunological responses were induced. Our results directly compare the haematopoietic response to LPS and *E. coli* infection, showing that a stronger immunological response was exhibited with *E. coli*. Although we did not verify the exact molecular mechanism responsible for the observed phenotypic changes in *E. coli* infection, we did determine that TNFα and IFNγ were playing vital roles in the immune response to both *E. coli* and LPS; in the modulation of haematopoietic progenitor phenotypes; in the cessation of lymphopoiesis and in the recruitment and export of granulocytes from the BM into the circulation. Our observations link the immune response directly with a transient reorganisation of developmental pathways in the progenitor compartment of the haematopoietic system and define a novel role for both TNFα and IFN-γ as key mediators for a stress-induced response of BM haematopoiesis. To assess which specific inflammatory changes were induced by LPS and which additional responses occurred after *E. coli* infection, analysing *E. coli* infection in *tlr4*-null mice would be necessary. In addition, because

LT-HSCs were increased in number during *E. coli* infection, but not during LPS challenge, isolation and cell cycle analysis of LT-HSCs during both inflammatory responses would indicate whether LT-HSCs were 'driven into cycle' during *E. coli* infection. Furthermore, the isolation and functional analysis of LSK cells for myeloid and lymphoid potential during LPS challenge and *E. coli* may provide information as to the degree of plasticity which haematopoietic progenitor cells retain during both inflammatory conditions. This could also be further elucidated by analysing the transcriptional signature of LSK cells by qRT-PCR during homeostatic conditions and after either LPS challenge or *E. coli* infection.

We also investigated the effects of age and gender on the composition of lymphoid progenitor populations and hoped to provide new insight into the causes of immunological deterioration with age, and differences between males and females. Although aging is known to reduce the number and function and mature haematopoietic cells and of HSCs, there is a lack of evidence for aging significantly inhibiting lymphoid progenitor number. In addition, aging analysed simultaneously with gender has not been reported. Our data revealed that male mice had a higher frequency and number of lymphoid progenitor populations than female mice, regardless of age. This indicated that oestrogen could have been exerting an inhibitory effect on lymphoid progenitor composition throughout the lifetime of female mice. However, our data also indicated that the number of lymphoid progenitors declined in both genders with age. Therefore, a reduction in the number of mature T- and B-cells in aged females in particular, could be attributable to an extent to a loss of lymphoid progenitor cells via oestrogen inhibition and also aging. In contrast, there were no differences in the frequency or number of myeloid progenitor cells in female mice compared to male mice at six weeks of age, suggesting that myeloid development was not affected by sex

hormones. However, the number of myeloid progenitor cells increased in both genders with age, which may have been a compensatory mechanism due to the lack of lymphopoiesis. It would be informative to measure the levels of oestrogen in young and old, male and female mice in order to identify whether the reduced lymphoid cell number in females was attributable to high levels of this hormone.

We also analysed the immune response to LPS in young male and female mice in order to assess whether the cytokines produced and the function of mature cells was different between genders. After LPS-induced inflammation, male mice produced an overall higher number of circulating granulocytes and lymphocytes compared to female mice and there was also a delay in the mobilisation of granulocytes into the circulation in female mice. Therefore, we expected that male mice would clear the infection quicker than females. However, the number of circulating granulocytes and lymphocytes returned to steady state levels at an earlier time in female mice. We determined that TNFα was partly responsible for the export of granulocytes from the BM in both male and female mice, but IFNγ also played a role in females. Therefore one reason for the female mice being able to respond to LPS challenge in a shorter time frame was likely due to the involvement of additional inflammatory cytokines. This data clearly illustrates that the immune response to LPS challenge in males and females is under alternate regulation, which may in turn be influenced by hormones. In order to determine whether alternate immunological responses in aged mice were also observed, LPS challenge in aged male and female mice could be undertaken and directly compared to the results from young mice.

Collectively our results demonstrate that precursor-product relationships between haematopoietic progenitor cells may be more complex than what has been previously proposed. The findings of markers, such as *Rag1*, which can separate lymphoid

progenitors into functionally and phenotypically distinct subsets suggests that many routes of development exist. In addition, the size of these subsets can be influenced by many extracellular factors, such as inflammation, aging and gender. In conditions whereby the lymphoid lineage is depressed, such as in aged mice or during infection, proliferation of the myeloid lineage occurs, suggesting that there is a high degree of cellular communication between the innate and adaptive immune system, even at the level of early progenitors. This communication undoubtedly leads to the production of mature cells which form an adequate immune response in order to maintain protection of the host during stressful conditions.

CHAPTER 7

REFERENCES

Abramson, S., Miller, R. G. & Phillips, R. A. (1977). The identification in adult BM of pluripotent and restricted stem cells of the myeloid and lymphoid systems. *J Exp Med* **145**, 1567-1579.

Aderem, A. & Underhill, D. M. (1999). Mechanisms of phagocytosis in macrophages. *Annu Rev Immunol* **17**, 593-623.

Adolfsson, J., Borge, O. J., Bryder, D., Theilgaard-Monch, K., Astrand-Grundstrom, I., Sitnicka, E., Sasaki, Y. & Jacobsen, S. E. (2001). Upregulation of Flt3 expression within the BM Lin(-)Sca1(+)c-kit(+) stem cell compartment is accompanied by loss of self-renewal capacity. *Immunity* **15**, 659-669.

Adolfsson, J., Mansson, R., Buza-Vidas, N. & other authors (2005). Identification of Flt3+ lympho-myeloid stem cells lacking erythro-megakaryocytic potential a revised road map for adult blood lineage commitment. *Cell* **121**, 295-306.

Akashi, K., Reya, T., Dalma-Weiszhausz, D. & Weissman, I. L. (2000). Lymphoid precursors. *Curr Opin Immunol* **12**, 144-150.

Akashi, K., Traver, D., Miyamoto, T. & Weissman, I. L. (2000). A clonogenic common myeloid progenitor that gives rise to all myeloid lineages. *Nature* **404**, 193-197.

Albright, J. W. & Albright, J. F. (1983). Age-associated impairment of murine natural killer activity. *Proc Natl Acad Sci U S A* **80**, 6371-6375.

Allman, D., Li, J. & Hardy, R. R. (1999). Commitment to the B lymphoid lineage occurs before DH-JH recombination. *J Exp Med* **189**, 735-740.

Allman, D., Sambandam, A., Kim, S., Miller, J. P., Pagan, A., Well, D., Meraz, A. & Bhandoola, A. (2003). Thymopoiesis independent of common lymphoid progenitors. *Nat Immunol* **4**, 168-174.

Ansar Ahmed, S., Penhale, W. J. & Talal, N. (1985). Sex hormones, immune responses, and autoimmune diseases. Mechanisms of sex hormone action. *Am J Pathol* **121**, 531-551.

Ardavin, C., Wu, L., Li, C. L. & Shortman, K. (1993). Thymic dendritic cells and T cells develop simultaneously in the thymus from a common precursor population. *Nature* **362**, 761-763.

Arinobu, Y., Mizuno, S., Chong, Y. & other authors (2007). Reciprocal activation of GATA-1 and PU.1 marks initial specification of hematopoietic stem cells into myeloerythroid and myelolymphoid lineages. *Cell Stem Cell* **1**, 416-427.

Artavanis-Tsakonas, S., Rand, M. D. & Lake, R. J. (1999). Notch signaling: cell fate control and signal integration in development. *Science* **284**, 770-776.

Aspinall, R. & Andrew, D. (2001). Age-associated thymic atrophy is not associated with a deficiency in the CD44(+)CD25(-)CD3(-)CD4(-)CD8(-) thymocyte population. *Cell Immunol* **212**, 150-157.

Baddoo, M., Hill, K., Wilkinson, R., Gaupp, D., Hughes, C., Kopen, G. C. & Phinney, D. G. (2003). Characterization of mesenchymal stem cells isolated from murine BM by negative selection. *J Cell Biochem* **89**, 1235-1249.

Baggiolini, M., Walz, A. & Kunkel, S. L. (1989). Neutrophil-activating peptide-1/interleukin 8, a novel cytokine that activates neutrophils. *J Clin Invest* **84**, 1045-1049.

Balciunaite, G., Ceredig, R., Massa, S. & Rolink, A. G. (2005). A B220+ CD117+ CD19- hematopoietic progenitor with potent lymphoid and myeloid developmental potential. *Eur J Immunol* **35**, 2019-2030.

Baldridge, M. T., King, K. Y., Boles, N. C., Weksberg, D. C. & Goodell, M. A. Quiescent haematopoietic stem cells are activated by IFN-gamma in response to chronic infection. *Nature* **465**, 793-797.

Baldridge, M. T., King, K. Y. & Goodell, M. A. Inflammatory signals regulate hematopoietic stem cells. *Trends Immunol*.

Bell, J. J. & Bhandoola, A. There's many a CLP on the path to B. *Blood* **115**, 2562-2563.

Bell, J. J. & Bhandoola, A. (2008). The earliest thymic progenitors for T cells possess myeloid lineage potential. *Nature* **452**, 764-767.

Belyaev, N. N., Brown, D. E., Diaz, A. I., Rae, A., Jarra, W., Thompson, J., Langhorne, J. & Potocnik, A. J. Induction of an IL7-R(+)c-Kit(hi) myelolymphoid progenitor critically dependent on IFN-gamma signaling during acute malaria. *Nat Immunol* **11**, 477-485.

Benz, C. & Bleul, C. C. (2005). A multipotent precursor in the thymus maps to the branching point of the T versus B lineage decision. *J Exp Med* **202**, 21-31.

Beutler, B., Milsark, I. W. & Cerami, A. C. (1985). Passive immunization against cachectin/tumor necrosis factor protects mice from lethal effect of endotoxin. *Science* **229**, 869-871.

Beutler, B., Hoebe, K., Du, X., Janssen, E., Georgel, P. & Tabeta, K. (2003). Lps2 and signal transduction in sepsis: at the intersection of host responses to bacteria and viruses. *Scand J Infect Dis* **35**, 563-567.

Beutler, B., Hoebe, K., Du, X. & Ulevitch, R. J. (2003). How we detect microbes and respond to them: the Toll-like receptors and their transducers. *J Leukoc Biol* **74**, 479-485.

Bhandoola, A. & Sambandam, A. (2006). From stem cell to T cell: one route or many? *Nat Rev Immunol* **6**, 117-126.

Bhandoola, A., von Boehmer, H., Petrie, H. T. & Zuniga-Pflucker, J. C. (2007). Commitment and developmental potential of extrathymic and intrathymic T cell precursors: plenty to choose from. *Immunity* **26**, 678-689.

Borge, O. J., Adolfsson, J. & Jacobsen, A. M. (1999). Lymphoid-restricted development from multipotent candidate murine stem cells: distinct and complimentary functions of the c-kit and flt3-ligands. *Blood* **94**, 3781-3790.

Borrello, M. A. & Phipps, R. P. (1996). The B/macrophage cell: an elusive link between CD5+ B lymphocytes and macrophages. *Immunol Today* **17**, 471-475.

Bradfute, S. B., Graubert, T. A. & Goodell, M. A. (2005). Roles of Sca-1 in hematopoietic stem/progenitor cell function. *Exp Hematol* **33**, 836-843.

Brown, G., Bunce, C. M. & Guy, G. R. (1985). Sequential determination of lineage potentials during haemopoiesis. *Br J Cancer* **52**, 681-686.

Broxmeyer, H. E., Lu, L., Platzer, E., Feit, C., Juliano, L. & Rubin, B. Y. (1983). Comparative analysis of the influences of human gamma, alpha and beta interferons on human multipotential (CFU-GEMM), erythroid (BFU-E) and granulocyte-macrophage (CFU-GM) progenitor cells. *J Immunol* **131**, 1300-1305.

Broxmeyer, H. E., Williams, D. E., Lu, L., Cooper, S., Anderson, S. L., Beyer, G. S., Hoffman, R. & Rubin, B. Y. (1986). The suppressive influences of human tumor necrosis factors on BM hematopoietic progenitor cells from normal donors and patients with leukemia: synergism of tumor necrosis factor and interferon-gamma. *J Immunol* **136**, 4487-4495.

Broxmeyer, H. E., Dent, A., Cooper, S. & other authors (2007). A role for natural killer T cells and CD1d molecules in counteracting suppression of hematopoiesis in mice induced by infection with murine cytomegalovirus. *Exp Hematol* **35**, 87-93.

Brugger, W., Mocklin, W., Heimfeld, S., Berenson, R. J., Mertelsmann, R. & Kanz, L. (1993). Ex vivo expansion of enriched peripheral blood CD34+ progenitor cells by stem cell factor, interleukin-1 beta (IL-1 beta), IL-6, IL-3, interferon-gamma, and erythropoietin. *Blood* **81**, 2579-2584.

Burch, J. B. (2005). Regulation of GATA gene expression during vertebrate development. *Semin Cell Dev Biol* **16**, 71-81.

Burg, N. D. & Pillinger, M. H. (2001). The neutrophil: function and regulation in innate and humoral immunity. *Clin Immunol* **99**, 7-17.

Butcher, S. K., Chahal, H., Nayak, L., Sinclair, A., Henriquez, N. V., Sapey, E., O'Mahony, D. & Lord, J. M. (2001). Senescence in innate immune responses: reduced neutrophil phagocytic capacity and CD16 expression in elderly humans. *J Leukoc Biol* **70**, 881-886.

Carlyle, J. R. & Zuniga-Pflucker, J. C. (1998). Regulation of NK1.1 expression during lineage commitment of progenitor thymocytes. *J Immunol* **161**, 6544-6551.

Caux, C., Moreau, I., Saeland, S. & Banchereau, J. (1992). Interferon-gamma enhances factor-dependent myeloid proliferation of human CD34+ hematopoietic progenitor cells. *Blood* **79**, 2628-2635.

Chandra, R., Villanueva, E., Feketova, E., Machiedo, G. W., Hasko, G., Deitch, E. A. & Spolarics, Z. (2008). Endotoxemia down-regulates BM lymphopoiesis but stimulates myelopoiesis: the effect of G6PD deficiency. *J Leukoc Biol* **83**, 1541-1550.

Chatta, G. S. & Dale, D. C. (1996). Aging and haemopoiesis. Implications for treatment with haemopoietic growth factors. *Drugs Aging* **9**, 37-47.

Chen, H. C., Frissora, F., Durbin, J. E. & Muthusamy, N. (2003). Activation induced differential regulation of stem cell antigen-1 (Ly-6A/E) expression in murine B cells. *Cell Immunol* **225**, 42-52.

Chilvers, E. R., Cadwallader, K. A., Reed, B. J., White, J. F. & Condliffe, A. M. (2000). The function and fate of neutrophils at the inflamed site: prospects for therapeutic intervention. *J R Coll Physicians Lond* **34**, 68-74.

Christensen, J. L. & Weissman, I. L. (2001). Flk-2 is a marker in hematopoietic stem cell differentiation: a simple method to isolate long-term stem cells. *Proc Natl Acad Sci U S A* **98**, 14541-14546.

Cobaleda, C., Jochum, W. & Busslinger, M. (2007). Conversion of mature B cells into T cells by dedifferentiation to uncommitted progenitors. *Nature* **449**, 473-477.

Colucci, F., Soudais, C., Rosmaraki, E., Vanes, L., Tybulewicz, V. L. & Di Santo, J. P. (1999). Dissecting NK cell development using a novel alymphoid mouse model: investigating the role of the c-abl proto-oncogene in murine NK cell differentiation. *J Immunol* **162**, 2761-2765.

de Boer, J., Williams, A., Skavdis, G. & other authors (2003). Transgenic mice with hematopoietic and lymphoid specific expression of Cre. *Eur J Immunol* **33**, 314-325.

DeKoter, R. P. & Singh, H. (2000). Regulation of B lymphocyte and macrophage development by graded expression of PU.1. *Science* **288**, 1439-1441.

Delano, M. J., Scumpia, P. O., Weinstein, J. S. & other authors (2007). MyD88-dependent expansion of an immature GR-1(+)CD11b(+) population induces T cell suppression and Th2 polarization in sepsis. *J Exp Med* **204**, 1463-1474.

Di Santo, J. P. (2006). Natural killer cell developmental pathways: a question of balance. *Annu Rev Immunol* **24**, 257-286.

Donskoy, E., Foss, D. & Goldschneider, I. (2003). Gated importation of prothymocytes by adult mouse thymus is coordinated with their periodic mobilization from BM. *J Immunol* **171**, 3568-3575.

Dorshkind, K., Montecino-Rodriguez, E. & Signer, R. A. (2009). The ageing immune system: is it ever too old to become young again? *Nat Rev Immunol* **9**, 57-62.

Doulatov, S., Notta, F., Eppert, K., Nguyen, L. T., Ohashi, P. S. & Dick, J. E. Revised map of the human progenitor hierarchy shows the origin of macrophages and dendritic cells in early lymphoid development. *Nat Immunol* **11**, 585-593.

Dumont, F. J. & Boltz, R. C. (1987). The augmentation of surface Ly-6A/E molecules in activated T cells is mediated by endogenous interferon-gamma. *J Immunol* **139**, 4088-4095.

Esparza, I., Mannel, D., Ruppel, A., Falk, W. & Krammer, P. H. (1987). Interferon gamma and lymphotoxin or tumor necrosis factor act synergistically to induce macrophage killing of tumor cells and schistosomula of Schistosoma mansoni. *J Exp Med* **166**, 589-594.

Esplin, B. L., Welner, R. S., Zhang, Q., Borghesi, L. A. & Kincade, P. W. (2009). A differentiation pathway for B1 cells in adult BM. *Proc Natl Acad Sci U S A* **106**, 5773-5778.

Essers, M. A., Offner, S., Blanco-Bose, W. E., Waibler, Z., Kalinke, U., Duchosal, M. A. & Trumpp, A. (2009). IFNalpha activates dormant haematopoietic stem cells in vivo. *Nature* **458**, 904-908.

Evans, M. J. & Kaufman, M. H. (1981). Establishment in culture of pluripotential cells from mouse embryos. *Nature* **292**, 154-156.

Fietta, A., Merlini, C., De Bernardi, P. M., Gandola, L., Piccioni, P. D. & Grassi, C. (1993). Non specific immunity in aged healthy subjects and in patients with chronic bronchitis. *Aging (Milano)* **5**, 357-361.

Forsberg, E. C., Serwold, T., Kogan, S., Weissman, I. L. & Passegue, E. (2006). New evidence supporting megakaryocyte-erythrocyte potential of flk2/flt3+ multipotent hematopoietic progenitors. *Cell* **126**, 415-426.

Foss, D. L., Donskoy, E. & Goldschneider, I. (2001). The importation of hematogenous precursors by the thymus is a gated phenomenon in normal adult mice. *J Exp Med* **193**, 365-374.

Freudenberg, M. A., Merlin, T., Gumenscheimer, M., Kalis, C., Landmann, R. & Galanos, C. (2001). Role of lipopolysaccharide susceptibility in the innate immune response to Salmonella typhimurium infection: LPS, a primary target for recognition of Gram-negative bacteria. *Microbes Infect* **3**, 1213-1222.

Freudenberg, M. A., Tchaptchet, S., Keck, S., Fejer, G., Huber, M., Schutze, N., Beutler, B. & Galanos, C. (2008). Lipopolysaccharide sensing an important factor in the innate immune response to Gram-negative bacterial infections: benefits and hazards of LPS hypersensitivity. *Immunobiology* **213**, 193-203.

Gage, F. H. (2000). Mammalian neural stem cells. *Science* **287**, 1433-1438.

Galanos, C. & Freudenberg, M. A. (1993). Bacterial endotoxins: biological properties and mechanisms of action. *Mediators Inflamm* **2**, S11-16.

Geissmann, F., Manz, M. G., Jung, S., Sieweke, M. H., Merad, M. & Ley, K. Development of monocytes, macrophages, and dendritic cells. *Science* **327**, 656-661.

Georgiades, P., Ogilvy, S., Duval, H., Licence, D. R., Charnock-Jones, D. S., Smith, S. K. & Print, C. G. (2002). VavCre transgenic mice: a tool for mutagenesis in hematopoietic and endothelial lineages. *Genesis* **34**, 251-256.

Gibbons, A. E., Price, P. & Shellam, G. R. (1995). Analysis of hematopoietic stem and progenitor cell populations in cytomegalovirus-infected mice. *Blood* **86**, 473-481.

Glasser, L. & Fiederlein, R. L. (1987). Functional differentiation of normal human neutrophils. *Blood* **69**, 937-944.

Godfrey, D. I., Zlotnik, A. & Suda, T. (1992). Phenotypic and functional characterization of c-kit expression during intrathymic T cell development. *J Immunol* **149**, 2281-2285.

Goldman, J. P., Blundell, M. P., Lopes, L., Kinnon, C., Di Santo, J. P. & Thrasher, A. J. (1998). Enhanced human cell engraftment in mice deficient in RAG2 and the common cytokine receptor gamma chain. *Br J Haematol* **103**, 335-342.

Goldschneider, I., Komschlies, K. L. & Greiner, D. L. (1986). Studies of thymocytopoiesis in rats and mice. I. Kinetics of appearance of thymocytes using a direct intrathymic adoptive transfer assay for thymocyte precursors. *J Exp Med* **163**, 1-17.

Gomez, C. R., Nomellini, V., Faunce, D. E. & Kovacs, E. J. (2008). Innate immunity and aging. *Exp Gerontol* **43**, 718-728.

Gounari, F., Aifantis, I., Martin, C., Fehling, H. J., Hoeflinger, S., Leder, P., von Boehmer, H. & Reizis, B. (2002). Tracing lymphopoiesis with the aid of a pTalpha-controlled reporter gene. *Nat Immunol* **3**, 489-496.

Grawunder, U., Melchers, F. & Rolink, A. (1993). Interferon-gamma arrests proliferation and causes apoptosis in stromal cell/interleukin-7-dependent normal murine pre-B cell lines and clones in vitro, but does not induce differentiation to surface immunoglobulin-positive B cells. *Eur J Immunol* **23**, 544-551.

Hamilton, D. L. & Abremski, K. (1984). Site-specific recombination by the bacteriophage P1 lox-Cre system. Cre-mediated synapsis of two lox sites. *J Mol Biol* **178**, 481-486.

Hardy, R. R., Li, Y. S., Allman, D., Asano, M., Gui, M. & Hayakawa, K. (2000). B-cell commitment, development and selection. *Immunol Rev* **175**, 23-32.

Harigae, H., Takahashi, S., Suwabe, N. & other authors (1998). Differential roles of GATA-1 and GATA-2 in growth and differentiation of mast cells. *Genes Cells* **3**, 39-50.

Harrison, D. E. (1983). Long-term erythropoietic repopulating ability of old, young, and fetal stem cells. *J Exp Med* **157**, 1496-1504.

Hattori, N., Kawamoto, H., Fujimoto, S., Kuno, K. & Katsura, Y. (1996). Involvement of transcription factors TCF-1 and GATA-3 in the initiation of the earliest step of T cell development in the thymus. *J Exp Med* **184**, 1137-1147.

Heinzel, K., Benz, C., Martins, V. C., Haidl, I. D. & Bleul, C. C. (2007). BM-derived hemopoietic precursors commit to the T cell lineage only after arrival in the thymic microenvironment. *J Immunol* **178**, 858-868.

Hendriks, R. W., Nawijn, M. C., Engel, J. D., van Doorninck, H., Grosveld, F. & Karis, A. (1999). Expression of the transcription factor GATA-3 is required for the development of the earliest T cell progenitors and correlates with stages of cellular proliferation in the thymus. *Eur J Immunol* **29**, 1912-1918.

Hernandez-Hoyos, G., Anderson, M. K., Wang, C., Rothenberg, E. V. & Alberola-Ila, J. (2003). GATA-3 expression is controlled by TCR signals and regulates CD4/CD8 differentiation. *Immunity* **19**, 83-94.

Hoshino, K., Takeuchi, O., Kawai, T., Sanjo, H., Ogawa, T., Takeda, Y., Takeda, K. & Akira, S. (1999). Cutting edge: Toll-like receptor 4 (TLR4)-deficient mice are hyporesponsive to lipopolysaccharide: evidence for TLR4 as the Lps gene product. *J Immunol* **162**, 3749-3752.

Hosoya, T., Maillard, I. & Engel, J. D. From the cradle to the grave: activities of GATA-3 throughout T-cell development and differentiation. *Immunol Rev* **238**, 110-125.

Huang, S., Hendriks, W., Althage, A., Hemmi, S., Bluethmann, H., Kamijo, R., Vilcek, J., Zinkernagel, R. M. & Aguet, M. (1993). Immune response in mice that lack the interferon-gamma receptor. *Science* **259**, 1742-1745.

Igarashi, H., Gregory, S. C., Yokota, T., Sakaguchi, N. & Kincade, P. W. (2002). Transcription from the RAG1 locus marks the earliest lymphocyte progenitors in BM. *Immunity* **17**, 117-130.

Inlay, M. A., Bhattacharya, D., Sahoo, D., Serwold, T., Seita, J., Karsunky, H., Plevritis, S. K., Dill, D. L. & Weissman, I. L. (2009). Ly6d marks the earliest stage of B-cell specification and identifies the branchpoint between B-cell and T-cell development. *Genes Dev* **23**, 2376-2381.

Ito, C. Y., Li, C. Y., Bernstein, A., Dick, J. E. & Stanford, W. L. (2003). Hematopoietic stem cell and progenitor defects in Sca-1/Ly-6A-null mice. *Blood* **101**, 517-523.

Iwasaki, H., Mizuno, S., Wells, R. A., Cantor, A. B., Watanabe, S. & Akashi, K. (2003). GATA-1 converts lymphoid and myelomonocytic progenitors into the megakaryocyte/erythrocyte lineages. *Immunity* **19**, 451-462.

Iwasaki-Arai, J., Iwasaki, H., Miyamoto, T., Watanabe, S. & Akashi, K. (2003). Enforced granulocyte/macrophage colony-stimulating factor signals do not support lymphopoiesis, but instruct lymphoid to myelomonocytic lineage conversion. *J Exp Med* **197**, 1311-1322.

Jiang, Z., Georgel, P., Du, X. & other authors (2005). CD14 is required for MyD88-independent LPS signaling. *Nat Immunol* **6**, 565-570.

Johns, J. L., Macnamara, K. C., Walker, N. J., Winslow, G. M. & Borjesson, D. L. (2009). Infection with Anaplasma phagocytophilum induces multilineage alterations in hematopoietic progenitor cells and peripheral blood cells. *Infect Immun* **77**, 4070-4080.

Karima, R., Matsumoto, S., Higashi, H. & Matsushima, K. (1999). The molecular pathogenesis of endotoxic shock and organ failure. *Mol Med Today* **5**, 123-132.

Karsunky, H., Inlay, M. A., Serwold, T., Bhattacharya, D. & Weissman, I. L. (2008). Flk2+ common lymphoid progenitors possess equivalent differentiation potential for the B and T lineages. *Blood* **111**, 5562-5570.

Kasahara, T., Djeu, J. Y., Dougherty, S. F. & Oppenheim, J. J. (1983). Capacity of human large granular lymphocytes (LGL) to produce multiple lymphokines: interleukin 2, interferon, and colony stimulating factor. *J Immunol* **131**, 2379-2385.

Katsura, Y. & Kawamoto, H. (2001). Stepwise lineage restriction of progenitors in lympho-myelopoiesis. *Int Rev Immunol* **20**, 1-20.

Kawai, T., Adachi, O., Ogawa, T., Takeda, K. & Akira, S. (1999). Unresponsiveness of MyD88-deficient mice to endotoxin. *Immunity* **11**, 115-122.

Kawamoto, H., Ikawa, T., Masuda, K., Wada, H. & Katsura, Y. A map for lineage restriction of progenitors during hematopoiesis: the essence of the myeloid-based model. *Immunol Rev* **238**, 23-36.

Kee, B. L. & Murre, C. (1998). Induction of early B cell factor (EBF) and multiple B lineage genes by the basic helix-loop-helix transcription factor E12. *J Exp Med* **188**, 699-713.

Kiel, M. J., Yilmaz, O. H., Iwashita, T., Terhorst, C. & Morrison, S. J. (2005). SLAM family receptors distinguish hematopoietic stem and progenitor cells and reveal endothelial niches for stem cells. *Cell* **121**, 1109-1121.

Kincade, P. W., Medina, K. L., Payne, K. J., Rossi, M. I., Tudor, K. S., Yamashita, Y. & Kouro, T. (2000). Early B-lymphocyte precursors and their regulation by sex steroids. *Immunol Rev* **175**, 128-137.

Kincade, P. W., Igarashi, H., Medina, K. L. & other authors (2002). Lymphoid lineage cells in adult murine BM diverge from those of other blood cells at an early, hormone-sensitive stage. *Semin Immunol* **14**, 385-394.

King, A. G., Kondo, M., Scherer, D. C. & Weissman, I. L. (2002). Lineage infidelity in myeloid cells with TCR gene rearrangement: a latent developmental potential of proT cells revealed by ectopic cytokine receptor signaling. *Proc Natl Acad Sci U S A* **99**, 4508-4513.

Kondo, M., Weissman, I. L. & Akashi, K. (1997). Identification of clonogenic common lymphoid progenitors in mouse BM. *Cell* **91**, 661-672.

Kondo, M., Scherer, D. C., Miyamoto, T., King, A. G., Akashi, K., Sugamura, K. & Weissman, I. L. (2000). Cell-fate conversion of lymphoid-committed progenitors by instructive actions of cytokines. *Nature* **407**, 383-386.

Kouro, T., Medina, K. L., Oritani, K. & Kincade, P. W. (2001). Characteristics of early murine B-lymphocyte precursors and their direct sensitivity to negative regulators. *Blood* **97**, 2708-2715.

Lagasse, E. & Weissman, I. L. (1996). Flow cytometric identification of murine neutrophils and monocytes. *J Immunol Methods* **197**, 139-150.

Lai, A. Y. & Kondo, M. (2006). Asymmetrical lymphoid and myeloid lineage commitment in multipotent hematopoietic progenitors. *J Exp Med* **203**, 1867-1873.

Lai, A. Y. & Kondo, M. (2007). Identification of a BM precursor of the earliest thymocytes in adult mouse. *Proc Natl Acad Sci U S A* **104**, 6311-6316.

Lamberts, S. W., van den Beld, A. W. & van der Lely, A. J. (1997). The endocrinology of aging. *Science* **278**, 419-424.

Lee, J. J., Kim, H. J., Chung, I. J., Park, M. R., Ryang, D. W. & Choi, C. (2001). Secondary myeloid/natural killer cell acute leukemia following T-cell lymphoma. *Leuk Lymphoma* **41**, 457-460.

Li, Y. S., Wasserman, R., Hayakawa, K. & Hardy, R. R. (1996). Identification of the earliest B lineage stage in mouse BM. *Immunity* **5**, 527-535.

Linton, P. J. & Dorshkind, K. (2004). Age-related changes in lymphocyte development and function. *Nat Immunol* **5**, 133-139.

Lu, L. S., Tung, J., Baumgarth, N., Herman, O., Gleimer, M. & Herzenberg, L. A. (2002). Identification of a germ-line pro-B cell subset that distinguishes the fetal/neonatal from the adult B cell development pathway. *Proc Natl Acad Sci U S A* **99**, 3007-3012.

Lu, Y. C., Yeh, W. C. & Ohashi, P. S. (2008). LPS/TLR4 signal transduction pathway. *Cytokine* **42**, 145-151.

Maciejewski, J., Selleri, C., Anderson, S. & Young, N. S. (1995). Fas antigen expression on CD34+ human marrow cells is induced by interferon gamma and tumor necrosis factor alpha and potentiates cytokine-mediated hematopoietic suppression in vitro. *Blood* **85**, 3183-3190.

Maier, H. & Hagman, J. (2002). Roles of EBF and Pax-5 in B lineage commitment and development. *Semin Immunol* **14**, 415-422.

Malek, T. R., Danis, K. M. & Codias, E. K. (1989). Tumor necrosis factor synergistically acts with IFN-gamma to regulate Ly-6A/E expression in T lymphocytes, thymocytes and BM cells. *J Immunol* **142**, 1929-1936.

Mansson, R., Zandi, S., Welinder, E., Tsapogas, P., Sakaguchi, N., Bryder, D. & Sigvardsson, M. Single-cell analysis of the common lymphoid progenitor compartment reveals functional and molecular heterogeneity. *Blood* **115**, 2601-2609.

Mansson, R., Hultquist, A., Luc, S. & other authors (2007). Molecular evidence for hierarchical transcriptional lineage priming in fetal and adult stem cells and multipotent progenitors. *Immunity* **26**, 407-419.

Mansson, R., Zandi, S., Anderson, K., Martensson, I. L., Jacobsen, S. E., Bryder, D. & Sigvardsson, M. (2008). B-lineage commitment prior to surface expression of B220 and CD19 on hematopoietic progenitor cells. *Blood* **112**, 1048-1055.

Manz, M. G., Traver, D., Akashi, K., Merad, M., Miyamoto, T., Engleman, E. G. & Weissman, I. L. (2001). Dendritic cell development from common myeloid progenitors. *Ann N Y Acad Sci* **938**, 167-173; discussion 173-164.

Martin, G. R. (1981). Isolation of a pluripotent cell line from early mouse embryos cultured in medium conditioned by teratocarcinoma stem cells. *Proc Natl Acad Sci U S A* **78**, 7634-7638.

Martin, C. H., Aifantis, I., Scimone, M. L., von Andrian, U. H., Reizis, B., von Boehmer, H. & Gounari, F. (2003). Efficient thymic immigration of B220+ lymphoid-restricted BM cells with T precursor potential. *Nat Immunol* **4**, 866-873.

Matsuzaki, Y., Gyotoku, J., Ogawa, M., Nishikawa, S., Katsura, Y., Gachelin, G. & Nakauchi, H. (1993). Characterization of c-kit positive intrathymic stem cells that are restricted to lymphoid differentiation. *J Exp Med* **178**, 1283-1292.

McElhaney, J. E. & Effros, R. B. (2009). Immunosenescence: what does it mean to health outcomes in older adults? *Curr Opin Immunol* **21**, 418-424.

Mebius, R. E., Miyamoto, T., Christensen, J., Domen, J., Cupedo, T., Weissman, I. L. & Akashi, K. (2001). The fetal liver counterpart of adult common lymphoid progenitors gives rise to all lymphoid lineages, CD45+CD4+CD3- cells, as well as macrophages. *J Immunol* **166**, 6593-6601.

Medina, K. L., Smithson, G. & Kincade, P. W. (1993). Suppression of B lymphopoiesis during normal pregnancy. *J Exp Med* **178**, 1507-1515.

Medina, K. L., Garrett, K. P., Thompson, L. F., Rossi, M. I., Payne, K. J. & Kincade, P. W. (2001). Identification of very early lymphoid precursors in BM and their regulation by estrogen. *Nat Immunol* **2**, 718-724.

Michie, A. M., Carlyle, J. R., Schmitt, T. M., Ljutic, B., Cho, S. K., Fong, Q. & Zuniga-Pflucker, J. C. (2000). Clonal characterization of a bipotent T cell and NK cell progenitor in the mouse fetal thymus. *J Immunol* **164**, 1730-1733.

Migliaccio, A. R., Rana, R. A., Sanchez, M., Lorenzini, R., Centurione, L., Bianchi, L., Vannucchi, A. M., Migliaccio, G. & Orkin, S. H. (2003). GATA-1 as a regulator of mast cell differentiation revealed by the phenotype of the GATA-1low mouse mutant. *J Exp Med* **197**, 281-296.

Miller, J. P., Izon, D., DeMuth, W., Gerstein, R., Bhandoola, A. & Allman, D. (2002). The earliest step in B lineage differentiation from common lymphoid progenitors is critically dependent upon interleukin 7. *J Exp Med* **196**, 705-711.

Miller, J. P. & Allman, D. (2003). The decline in B lymphopoiesis in aged mice reflects loss of very early B-lineage precursors. *J Immunol* **171**, 2326-2330.

Min, H., Montecino-Rodriguez, E. & Dorshkind, K. (2005). Effects of aging on early B- and T-cell development. *Immunol Rev* **205**, 7-17.

Min, H., Montecino-Rodriguez, E. & Dorshkind, K. (2006). Effects of aging on the common lymphoid progenitor to pro-B cell transition. *J Immunol* **176**, 1007-1012.

Miyamoto, T., Iwasaki, H., Reizis, B., Ye, M., Graf, T., Weissman, I. L. & Akashi, K. (2002). Myeloid or lymphoid promiscuity as a critical step in hematopoietic lineage commitment. *Dev Cell* **3**, 137-147.

Mori, S., Shortman, K. & Wu, L. (2001). Characterization of thymus-seeding precursor cells from mouse BM. *Blood* **98**, 696-704.

Morrison, D. C. & Ryan, J. L. (1979). Bacterial endotoxins and host immune responses. *Adv Immunol* **28**, 293-450.

Murphy, M., Loudon, R., Kobayashi, M. & Trinchieri, G. (1986). Gamma interferon and lymphotoxin, released by activated T cells, synergize to inhibit granulocyte/monocyte colony formation. *J Exp Med* **164**, 263-279.

Nagai, Y., Garrett, K. P., Ohta, S., Bahrun, U., Kouro, T., Akira, S., Takatsu, K. & Kincade, P. W. (2006). Toll-like receptors on hematopoietic progenitor cells stimulate innate immune system replenishment. *Immunity* **24**, 801-812.

Nakano, H., Yanagita, M. & Gunn, M. D. (2001). CD11c(+)B220(+)Gr-1(+) cells in mouse lymph nodes and spleen display characteristics of plasmacytoid dendritic cells. *J Exp Med* **194**, 1171-1178.

Nerlov, C., Querfurth, E., Kulessa, H. & Graf, T. (2000). GATA-1 interacts with the myeloid PU.1 transcription factor and represses PU.1-dependent transcription. *Blood* **95**, 2543-2551.

Neumann, H. A. & Fauser, A. A. (1982). Effect of interferon on pluripotent hemopoietic progenitors (CFU-GEMM) derived from human BM. *Exp Hematol* **10**, 587-590.

Nutt, S. L., Urbanek, P., Rolink, A. & Busslinger, M. (1997). Essential functions of Pax5 (BSAP) in pro-B cell development: difference between fetal and adult B lymphopoiesis and reduced V-to-DJ recombination at the IgH locus. *Genes Dev* **11**, 476-491.

Nutt, S. L., Heavey, B., Rolink, A. G. & Busslinger, M. (1999). Commitment to the B-lymphoid lineage depends on the transcription factor Pax5. *Nature* **401**, 556-562.

Ogawa, M., Porter, P. N. & Nakahata, T. (1983). Renewal and commitment to differentiation of hemopoietic stem cells (an interpretive review). *Blood* **61**, 823-829.

Ohneda, K. & Yamamoto, M. (2002). Roles of hematopoietic transcription factors GATA-1 and GATA-2 in the development of red blood cell lineage. *Acta Haematol* **108**, 237-245.

Onai, N., Obata-Onai, A., Schmid, M. A., Ohteki, T., Jarrossay, D. & Manz, M. G. (2007). Identification of clonogenic common Flt3+M-CSFR+ plasmacytoid and conventional dendritic cell progenitors in mouse BM. *Nat Immunol* **8**, 1207-1216.

Pai, S. Y., Truitt, M. L., Ting, C. N., Leiden, J. M., Glimcher, L. H. & Ho, I. C. (2003). Critical roles for transcription factor GATA-3 in thymocyte development. *Immunity* **19**, 863-875.

Pelayo, R., Welner, R., Perry, S. S., Huang, J., Baba, Y., Yokota, T. & Kincade, P. W. (2005). Lymphoid progenitors and primary routes to becoming cells of the immune system. *Curr Opin Immunol* **17**, 100-107.

Pevny, L., Simon, M. C., Robertson, E., Klein, W. H., Tsai, S. F., D'Agati, V., Orkin, S. H. & Costantini, F. (1991). Erythroid differentiation in chimaeric mice blocked by a targeted mutation in the gene for transcription factor GATA-1. *Nature* **349**, 257-260.

Poltorak, A., He, X., Smirnova, I. & other authors (1998). Defective LPS signaling in C3H/HeJ and C57BL/10ScCr mice: mutations in Tlr4 gene. *Science* **282**, 2085-2088.

Pottratz, S. T., Bellido, T., Mocharla, H., Crabb, D. & Manolagas, S. C. (1994). 17 beta-Estradiol inhibits expression of human interleukin-6 promoter-reporter constructs by a receptor-dependent mechanism. *J Clin Invest* **93**, 944-950.

Prockop, D. J. (1997). Marrow stromal cells as stem cells for nonhematopoietic tissues. *Science* **276**, 71-74.

Radtke, F., Wilson, A., Stark, G., Bauer, M., van Meerwijk, J., MacDonald, H. R. & Aguet, M. (1999). Deficient T cell fate specification in mice with an induced inactivation of Notch1. *Immunity* **10**, 547-558.

Raefsky, E. L., Platanias, L. C., Zoumbos, N. C. & Young, N. S. (1985). Studies of interferon as a regulator of hematopoietic cell proliferation. *J Immunol* **135**, 2507-2512.

Rekhtman, N., Radparvar, F., Evans, T. & Skoultchi, A. I. (1999). Direct interaction of hematopoietic transcription factors PU.1 and GATA-1: functional antagonism in erythroid cells. *Genes Dev* **13**, 1398-1411.

Remick, D. G., Newcomb, D. E., Bolgos, G. L. & Call, D. R. (2000). Comparison of the mortality and inflammatory response of two models of sepsis: lipopolysaccharide vs. cecal ligation and puncture. *Shock* **13**, 110-116.

Rezzoug, F., Huang, Y., Tanner, M. K., Wysoczynski, M., Schanie, C. L., Chilton, P. M., Ratajczak, M. Z., Fugier-Vivier, I. J. & Ildstad, S. T. (2008). TNF-alpha is critical to facilitate hemopoietic stem cell engraftment and function. *J Immunol* **180**, 49-57.

Rodriguez, S., Chora, A., Goumnerov, B. & other authors (2009). Dysfunctional expansion of hematopoietic stem cells and block of myeloid differentiation in lethal sepsis. *Blood* **114**, 4064-4076.

Rolink, A., ten Boekel, E., Melchers, F., Fearon, D. T., Krop, I. & Andersson, J. (1996). A subpopulation of B220+ cells in murine BM does not express CD19 and contains natural killer cell progenitors. *J Exp Med* **183**, 187-194.

Rolink, A. G., Schaniel, C., Busslinger, M., Nutt, S. L. & Melchers, F. (2000). Fidelity and infidelity in commitment to B-lymphocyte lineage development. *Immunol Rev* **175**, 104-111.

Rosenstreich, D. L. (1980). Genetics of resistance to infection. *Nature* **285**, 436-437.

Rossi, D. J., Bryder, D., Zahn, J. M., Ahlenius, H., Sonu, R., Wagers, A. J. & Weissman, I. L. (2005). Cell intrinsic alterations underlie hematopoietic stem cell aging. *Proc Natl Acad Sci U S A* **102**, 9194-9199.

Rothe, J., Lesslauer, W., Lotscher, H. & other authors (1993). Mice lacking the tumour necrosis factor receptor 1 are resistant to TNF-mediated toxicity but highly susceptible to infection by Listeria monocytogenes. *Nature* **364**, 798-802.

Rothenberg, E. V. & Taghon, T. (2005). Molecular genetics of T cell development. *Annu Rev Immunol* **23**, 601-649.

Rumfelt, L. L., Zhou, Y., Rowley, B. M., Shinton, S. A. & Hardy, R. R. (2006). Lineage specification and plasticity in CD19- early B cell precursors. *J Exp Med* **203**, 675-687.

Sato, T., Onai, N., Yoshihara, H., Arai, F., Suda, T. & Ohteki, T. (2009). Interferon regulatory factor-2 protects quiescent hematopoietic stem cells from type I interferon-dependent exhaustion. *Nat Med* **15**, 696-700.

Schlenner, S. M., Madan, V., Busch, K., Tietz, A., Laufle, C., Costa, C., Blum, C., Fehling, H. J. & Rodewald, H. R. Fate mapping reveals separate origins of T cells and myeloid lineages in the thymus. *Immunity* **32**, 426-436.

Schlenner, S. M. & Rodewald, H. R. Early T cell development and the pitfalls of potential. *Trends Immunol* **31**, 303-310.

Schwarz, B. A. & Bhandoola, A. (2004). Circulating hematopoietic progenitors with T lineage potential. *Nat Immunol* **5**, 953-960.

Schwarz, B. A. & Bhandoola, A. (2006). Trafficking from the BM to the thymus: a prerequisite for thymopoiesis. *Immunol Rev* **209**, 47-57.

Schwarz, B. A., Sambandam, A., Maillard, I., Harman, B. C., Love, P. E. & Bhandoola, A. (2007). Selective thymus settling regulated by cytokine and chemokine receptors. *J Immunol* **178**, 2008-2017.

Scollay, R., Smith, J. & Stauffer, V. (1986). Dynamics of early T cells: prothymocyte migration and proliferation in the adult mouse thymus. *Immunol Rev* **91**, 129-157.

Scumpia, P. O., Kelly-Scumpia, K. M., Delano, M. J. & other authors Cutting edge: bacterial infection induces hematopoietic stem and progenitor cell expansion in the absence of TLR signaling. *J Immunol* **184**, 2247-2251.

Sedger, L. M., Hou, S., Osvath, S. R., Glaccum, M. B., Peschon, J. J., van Rooijen, N. & Hyland, L. (2002). BM B cell apoptosis during in vivo influenza virus infection requires TNF-alpha and lymphotoxin-alpha. *J Immunol* **169**, 6193-6201.

Selleri, C., Maciejewski, J. P., Sato, T. & Young, N. S. (1996). Interferon-gamma constitutively expressed in the stromal microenvironment of human marrow cultures mediates potent hematopoietic inhibition. *Blood* **87**, 4149-4157.

Serbina, N. V. & Pamer, E. G. (2006). Monocyte emigration from BM during bacterial infection requires signals mediated by chemokine receptor CCR2. *Nat Immunol* **7**, 311-317.

Serwold, T., Ehrlich, L. I. & Weissman, I. L. (2009). Reductive isolation from BM and blood implicates common lymphoid progenitors as the major source of thymopoiesis. *Blood* **113**, 807-815.

Shahbazian, L. M., Quinton, L. J., Bagby, G. J., Nelson, S., Wang, G. & Zhang, P. (2004). Escherichia coli pneumonia enhances granulopoiesis and the mobilization of myeloid progenitor cells into the systemic circulation. *Crit Care Med* **32**, 1740-1746.

Shen, H. Q., Lu, M., Ikawa, T., Masuda, K., Ohmura, K., Minato, N., Katsura, Y. & Kawamoto, H. (2003). T/NK bipotent progenitors in the thymus retain the potential to generate dendritic cells. *J Immunol* **171**, 3401-3406.

Shimazu, R., Akashi, S., Ogata, H., Nagai, Y., Fukudome, K., Miyake, K. & Kimoto, M. (1999). MD-2, a molecule that confers lipopolysaccharide responsiveness on Toll-like receptor 4. *J Exp Med* **189**, 1777-1782.

Shimozato, O., Ortaldo, J. R., Komschlies, K. L. & Young, H. A. (2002). Impaired NK cell development in an IFN-gamma transgenic mouse: aberrantly expressed IFN-gamma enhances hematopoietic stem cell apoptosis and affects NK cell differentiation. *J Immunol* **168**, 1746-1752.

Shinkai, Y., Rathbun, G., Lam, K. P. & other authors (1992). RAG-2-deficient mice lack mature lymphocytes owing to inability to initiate V(D)J rearrangement. *Cell* **68**, 855-867.

Shortman, K., Scollay, R., Andrews, P. & Boyd, R. (1986). Development of T lymphocytes within the thymus and within thymic nurse cells. *Curr Top Microbiol Immunol* **126**, 5-18.

Shtrichman, R. & Samuel, C. E. (2001). The role of gamma interferon in antimicrobial immunity. *Curr Opin Microbiol* **4**, 251-259.

Sigvardsson, M., O'Riordan, M. & Grosschedl, R. (1997). EBF and E47 collaborate to induce expression of the endogenous immunoglobulin surrogate light chain genes. *Immunity* **7**, 25-36.

Siminovitch, L., McCulloch, E. A. & Till, J. E. (1963). The Distribution of Colony-Forming Cells among Spleen Colonies. *J Cell Physiol* **62**, 327-336.

Singh, P., Yao, Y., Weliver, A., Broxmeyer, H. E., Hong, S. C. & Chang, C. H. (2008). Vaccinia virus infection modulates the hematopoietic cell compartments in the BM. *Stem Cells* **26**, 1009-1016.

Smithson, G., Beamer, W. G., Shultz, K. L., Christianson, S. W., Shultz, L. D. & Kincade, P. W. (1994). Increased B lymphopoiesis in genetically sex steroid-deficient hypogonadal (hpg) mice. *J Exp Med* **180**, 717-720.

Smithson, G., Medina, K., Ponting, I. & Kincade, P. W. (1995). Estrogen suppresses stromal cell-dependent lymphopoiesis in culture. *J Immunol* **155**, 3409-3417.

Spangrude, G. J., Heimfeld, S. & Weissman, I. L. (1988). Purification and characterization of mouse hematopoietic stem cells. *Science* **241**, 58-62.

Srinivas, S., Watanabe, T., Lin, C. S., William, C. M., Tanabe, Y., Jessell, T. M. & Costantini, F. (2001). Cre reporter strains produced by targeted insertion of EYFP and ECFP into the ROSA26 locus. *BMC Dev Biol* **1**, 4.

Stephan, R. P., Sanders, V. M. & Witte, P. L. (1996). Stage-specific alterations in murine B lymphopoiesis with age. *Int Immunol* **8**, 509-518.

Stephan, R. P., Reilly, C. R. & Witte, P. L. (1998). Impaired ability of BM stromal cells to support B-lymphopoiesis with age. *Blood* **91**, 75-88.

Sternberg, N. & Hamilton, D. (1981). Bacteriophage P1 site-specific recombination. I. Recombination between loxP sites. *J Mol Biol* **150**, 467-486.

Thomson, J. A., Itskovitz-Eldor, J., Shapiro, S. S., Waknitz, M. A., Swiergiel, J. J., Marshall, V. S. & Jones, J. M. (1998). Embryonic stem cell lines derived from human blastocysts. *Science* **282**, 1145-1147.

Till, J. E. & Mc, C. E. (1961). A direct measurement of the radiation sensitivity of normal mouse BM cells. *Radiat Res* **14**, 213-222.

Ting, C. N., Olson, M. C., Barton, K. P. & Leiden, J. M. (1996). Transcription factor GATA-3 is required for development of the T-cell lineage. *Nature* **384**, 474-478.

Tsai, F. Y. & Orkin, S. H. (1997). Transcription factor GATA-2 is required for proliferation/survival of early hematopoietic cells and mast cell formation, but not for erythroid and myeloid terminal differentiation. *Blood* **89**, 3636-3643.

Tsou, C. L., Peters, W., Si, Y., Slaymaker, S., Aslanian, A. M., Weisberg, S. P., Mack, M. & Charo, I. F. (2007). Critical roles for CCR2 and MCP-3 in monocyte mobilization from BM and recruitment to inflammatory sites. *J Clin Invest* **117**, 902-909.

Ueda, Y., Yang, K., Foster, S. J., Kondo, M. & Kelsoe, G. (2004). Inflammation controls B lymphopoiesis by regulating chemokine CXCL12 expression. *J Exp Med* **199**, 47-58.

Verbeek, S., Izon, D., Hofhuis, F. & other authors (1995). An HMG-box-containing T-cell factor required for thymocyte differentiation. *Nature* **374**, 70-74.

Verfaillie, C. M. (2002). Adult stem cells: assessing the case for pluripotency. *Trends Cell Biol* **12**, 502-508.

Verthelyi, D. I. & Ahmed, S. A. (1998). Estrogen increases the number of plasma cells and enhances their autoantibody production in nonautoimmune C57BL/6 mice. *Cell Immunol* **189**, 125-134.

Vosshenrich, C. A., Garcia-Ojeda, M. E., Samson-Villeger, S. I. & other authors (2006). A thymic pathway of mouse natural killer cell development characterized by expression of GATA-3 and CD127. *Nat Immunol* **7**, 1217-1224.

Wada, H., Masuda, K., Satoh, R., Kakugawa, K., Ikawa, T., Katsura, Y. & Kawamoto, H. (2008). Adult T-cell progenitors retain myeloid potential. *Nature* **452**, 768-772.

Walsh, J. C., DeKoter, R. P., Lee, H. J. & other authors (2002). Cooperative and antagonistic interplay between PU.1 and GATA-2 in the specification of myeloid cell fates. *Immunity* **17**, 665-676.

Wang, J., Lin, Q., Langston, H. & Cooper, M. D. (1995). Resident BM macrophages produce type 1 interferons that can selectively inhibit interleukin-7-driven growth of B lineage cells. *Immunity* **3**, 475-484.

Welner, R. S., Pelayo, R., Nagai, Y., Garrett, K. P., Wuest, T. R., Carr, D. J., Borghesi, L. A., Farrar, M. A. & Kincade, P. W. (2008). Lymphoid precursors are directed to produce dendritic cells as a result of TLR9 ligation during herpes infection. *Blood* **112**, 3753-3761.

Welner, R. S., Esplin, B. L., Garrett, K. P., Pelayo, R., Luche, H., Fehling, H. J. & Kincade, P. W. (2009). Asynchronous RAG-1 expression during B lymphopoiesis. *J Immunol* **183**, 7768-7777.

Williams, D. A., Lemischka, I. R., Nathan, D. G. & Mulligan, R. C. (1984). Introduction of new genetic material into pluripotent haematopoietic stem cells of the mouse. *Nature* **310**, 476-480.

Williams, N. S., Moore, T. A., Schatzle, J. D., Puzanov, I. J., Sivakumar, P. V., Zlotnik, A., Bennett, M. & Kumar, V. (1997). Generation of lytic natural killer 1.1+, Ly-49- cells from multipotential murine BM progenitors in a stroma-free culture: definition of cytokine requirements and developmental intermediates. *J Exp Med* **186**, 1609-1614.

Wilson, C. A., Mrose, S. A. & Thomas, D. W. (1995). Enhanced production of B lymphocytes after castration. *Blood* **85**, 1535-1539.

Wu, L., Antica, M., Johnson, G. R., Scollay, R. & Shortman, K. (1991). Developmental potential of the earliest precursor cells from the adult mouse thymus. *J Exp Med* **174**, 1617-1627.

Wu, L., Li, C. L. & Shortman, K. (1996). Thymic dendritic cell precursors: relationship to the T lymphocyte lineage and phenotype of the dendritic cell progeny. *J Exp Med* **184**, 903-911.

Xie, H., Ye, M., Feng, R. & Graf, T. (2004). Stepwise reprogramming of B cells into macrophages. *Cell* **117**, 663-676.

Yang, L., Dybedal, I., Bryder, D., Nilsson, L., Sitnicka, E., Sasaki, Y. & Jacobsen, S. E. (2005). IFN-gamma negatively modulates self-renewal of repopulating human hemopoietic stem cells. *J Immunol* **174**, 752-757.

Ye, M. & Graf, T. (2007). Early decisions in lymphoid development. *Curr Opin Immunol* **19**, 123-128.

Yoshida, T., Ng, S. Y., Zuniga-Pflucker, J. C. & Georgopoulos, K. (2006). Early hematopoietic lineage restrictions directed by Ikaros. *Nat Immunol* **7**, 382-391.

Young, H. A., Klinman, D. M., Reynolds, D. A. & other authors (1997). BM and thymus expression of interferon-gamma results in severe B-cell lineage reduction, T-cell lineage alterations, and hematopoietic progenitor deficiencies. *Blood* **89**, 583-595.

Zeigler, F. C., Bennett, B. D., Jordan, C. T., Spencer, S. D., Baumhueter, S., Carroll, K. J., Hooley, J., Bauer, K. & Matthews, W. (1994). Cellular and molecular characterization of the role of the flk-2/flt-3 receptor tyrosine kinase in hematopoietic stem cells. *Blood* **84**, 2422-2430.

Zhang, Y., Harada, A., Bluethmann, H., Wang, J. B., Nakao, S., Mukaida, N. & Matsushima, K. (1995). Tumor necrosis factor (TNF) is a physiologic regulator of hematopoietic progenitor cells: increase of early hematopoietic progenitor cells in TNF receptor p55-deficient mice in vivo and potent inhibition of progenitor cell proliferation by TNF alpha in vitro. *Blood* **86**, 2930-2937.

Zhang, P., Behre, G., Pan, J., Iwama, A., Wara-Aswapati, N., Radomska, H. S., Auron, P. E., Tenen, D. G. & Sun, Z. (1999). Negative cross-talk between hematopoietic regulators: GATA proteins repress PU.1. *Proc Natl Acad Sci U S A* **96**, 8705-8710.

Zhang, P., Nelson, S., Bagby, G. J., Siggins, R., 2nd, Shellito, J. E. & Welsh, D. A. (2008). The lineage-c-Kit+Sca-1+ cell response to Escherichia coli bacteremia in Balb/c mice. *Stem Cells* **26**, 1778-1786.

Zhao, X., Ren, G., Liang, L., Ai, P. Z., Zheng, B., Tischfield, J. A., Shi, Y. & Shao, C. Brief report: interferon-gamma induces expansion of Lin(-)Sca-1(+)C-Kit(+) Cells. *Stem Cells* **28**, 122-126.

Zlotoff, D. A. & Bhandoola, A. Hematopoietic progenitor migration to the adult thymus. *Ann N Y Acad Sci* **1217**, 122-138.

Zon, L. I., Yamaguchi, Y., Yee, K., Albee, E. A., Kimura, A., Bennett, J. C., Orkin, S. H. & Ackerman, S. J. (1993). Expression of mRNA for the GATA-binding proteins in human eosinophils and basophils: potential role in gene transcription. *Blood* **81**, 3234-3241.

Zoumbos, N. C., Djeu, J. Y. & Young, N. S. (1984). Interferon is the suppressor of hematopoiesis generated by stimulated lymphocytes in vitro. *J Immunol* **133**, 769-774.